Errata

for compound **5.6** $^2J_{PtH}$ are 58.0 Hz and 57.6 Hz

for compound **5.7a** $^2J_{PtH}$ are 93.1 Hz and 62.0 Hz and $^1J_{PtC}$ are 802.8 Hz and 795.2 Hz

for compound **5.7b** $^2J_{PtH}$ are 92.8 Hz and 61.1 Hz and $^1J_{PtC}$ are 799.0 Hz and 773.1 Hz

for compound **5.9** $^2J_{PtH}$ is 81.0 Hz

for compound **5.10** $^2J_{PtH}$ is 80.0 Hz

for compound **5.11** $^2J_{PtH}$ is 78.4 Hz

for compound **5.12** $^2J_{PtH}$ is 76.4 Hz

for compound *fac*-**5.23** $^2J_{PtH}$ is 72.0 Hz

for compound *fac*-**5.24** $^2J_{PtH}$ are 75.6 Hz, 75.6 Hz and 52.4 Hz and $^1J_{PtC}$ are 677 Hz, 473.6 Hz and 660.8 Hz

for compound **5.18** $^2J_{PtH}$ is 70.2 Hz and $^1J_{PtC}$ is 522.7 Hz

for compound **5.17** $^2J_{PtH}$ is 75.5 Hz

for compound **5.13** $^2J_{PtH}$ is 69.7 Hz

p. 194 under "**Reaction of 5.6 with Brookhart's acid and synthesis of 5.16**" $^2J_{PtH}$ is 98.8 Hz

p. 54 under **2.3b** replace 10.1? with 10.1 and 131.? With 131.0

UNIVERSITY OF SOUTHAMPTON

FACULTY OF ENGINEERING, SCIENCE & MATHEMATICS

School of Chemistry

Synthesis of Phosphine- and Pyridine- Functionalised *N*-heterocyclic carbene complexes of Platinum Group Metals

by

Nikolaos Tsoureas

Thesis for the degree of Doctor of Philosophy

August 2005

Abstract

A new and improved method for the preparation of phosphine functionalised imidazolium salt NHC precursors with the systematic name 3-(aryl)-1-(n-diphenylphosphanyl-alkyl$_n$)-3H-imidazol-1-ium (n = 1 then alkyl = methyl; aryl = 2,4,6-Me$_3$-C$_6$H$_2$: **2.2b**, 2,6-(^{i}Pr)$_2$-C$_6$H$_3$: **2.2a**/ n = 2, alkyl = ethyl; aryl = 2,4,6-Me$_3$-C$_6$H$_2$: **2.4b**, 2,6-(^{i}Pr)$_2$-C$_6$H$_3$: **2.4a** / n = 3, alkyl = propyl; aryl = 2,4,6-Me$_3$-C$_6$H$_2$: **2.6**) has been developed. Pyridine functionalised imidazolium salts of the systematic name 3-(aryl)-1-(3-R-pyridin-2-yl)-3H-imidazol-1-ium (aryl = 2,6-(^{i}Pr)$_2$-C$_6$H$_3$, R = H: **2.8c**; aryl = 2,6-(^{i}Pr)$_2$-C$_6$H$_3$, R = Me: **2.8d**/ aryl = 3,5-(CF$_3$)$_2$-C$_6$H$_3$, R = H: **2.7**) have also been synthesised. Interaction of **2.8c** or **2.8d** with KN(SiMe$_3$)$_2$ leads to the formation of carbenes 3-(2,6-diisopropyl-phenyl)-1-(pyridin-2-yl)-2,3 dihydro-1H-imidazol-2-ylidene (**2.9c** = CN$^{(1)}$) and 3-(2,6-diisopropyl-phenyl)-1-(3-methyl-pyridin-2-yl)-2,3 dihydro-1H-imidazol-2-ylidene (**2.9d** = CN$^{(2)}$) respectively.

The phosphine functionalised imidazolium salts **2.2a**, **2.4b**, **2.4a** and **2.6** were used to generate the corresponding ylidenes by their reaction with KN(SiMe$_3$)$_2$, that were trapped with an appropriate Pd(II) metal precursor. Metal precursors of the type cis-PdLX$_2$ (L = tmed: X = Me; L = COD:X = Br) led to the isolation of complexes of the type (PC)PdX$_2$ (PC = 3-(aryl)-1-(n-diphenylphosphanyl-alkyl$_n$)-2,3 dihydro-1H-imidazol-2-ylidene (n = 1, aryl = 2,6-(^{i}Pr)$_2$-C$_6$H$_3$ (= (PC$^{(1)}$), X = Me: **3.3**; n = 2, aryl = 2,6-(^{i}Pr)$_2$-C$_6$H$_3$ (= (PC$^{(2)}$) or 2,4,6-Me$_3$-C$_6$H$_2$ (= PC$^{(2)'}$), X = Me: **3.1a** and **3.1b** respectively; n = 3, aryl = 2,4,6-Me$_3$-C$_6$H$_2$ (= PC$^{(3)}$), X = Me: **3.4**; n = 2, aryl = 2,6-(^{i}Pr)$_2$-C$_6$H$_3$ or 2,4,6-Me$_3$-C$_6$H$_2$, X = Br: **3.2a** and **3.2b** respectively). Interaction of [Pd(η^3-methallyl)Cl]$_2$ with the in situ generated PC$^{(2)}$ led to the isolation of salt [Pd(η^3-methallyl)(PC$^{(2)}$)]$^+$Cl$^-$ (**3.8b**), which undergoes salt exchange reactions with Na$^+$BAr$_4^-$ to give compounds [Pd(η^3-methallyl)(PC$^{(2)}$)]$^+$BAr$_4^-$ (Ar = 3,5-(CF$_3$)$_2$-C$_6$H$_3$: **3.8a**; Ar = Ph: **3.8c**). Interaction of ylidenes **2.9c** (CN$^{(1)}$) or **2.9d** (CN$^{(2)}$) with Pd(tmed)Me$_2$ in a 1.4:1 and 1:1 stoichiometry respectively leads to the isolation of complexes [(CN$^{(1)}$)PdMe$_2$](**3.5a**) and [(CN$^{(2)}$)PdMe$_2$](**3.5b**) respectively where the pyridine functionalised NHCs act as chelates. When **2.9c** is reacted with Pd(tmed)Me$_2$ in a 2:1 stoichiometry the C$_2$ symmetric complex [(CN$^{(1)}$)$_2$PdMe$_2$] (**3.6**) is formed in which the pyridine functionalities are not participating in the coordination sphere. Finally, [Pd(η^3-methallyl)(CN$^{(1)}$)]$^+$BPh$_4^-$ (**3.7**) is formed by interaction of [Pd(η^3-methallyl)Cl]$_2$ with 2 equivalents of **2.9c** followed by addition of Na$^+$BPh$_4^-$.

When a solution of **3.1a** in d_8-THF was heated, decomposition occurred by reductive elimination of 2-methyl-imidazolium salt. Similarly heating a solution of **3.3** in d_5-PhCl produces methane and other decomposition products. Complexes **3.1a** and **3.3** react with (CF$_3$)$_2$CHOH in d_5-py to give salts of the type [Pd(PC$^{(1)/(2)}$)Me(py)]$^+$(CF$_3$)$_2$CHO$^-$ (PC$^{(1)/(2)}$ = like above; PC$^{(1)}$: **4.1**; PC$^{(2)}$: **4.2**) where the Pd-CH$_3$ trans to the phosphine has been attacked by the acidic alcohol. When instead of (CF$_3$)$_2$CHOH as an acid [H(OEt$_2$)]$^+$[B{3,5-(CF$_3$)$_2$-C$_6$H$_3$}$_4$] $^-$ (Brookhart's acid) was used in the presence of an L donor complexes of the type [Pd(PC$^{(1)/(2)}$)MeL]$^+$BAr$_4^{F-}$ (BAr$_4^{F-}$ = [B{3,5-(CF$_3$)$_2$-C$_6$H$_3$}$_4$] $^-$; PC$^{(1)/(2)}$ = like above; PC$^{(1)}$, L = py: **4.7**; PC$^{(1)}$, L = 4-^{t}Bu-py: **4.8**; PC$^{(2)}$, L = py: **4.3**; PC$^{(2)}$, L = CH$_3$CN: **4.4**; PC$^{(2)}$, L = PhCN: **4.5**; PC$^{(2)}$, L = PMe$_3$: **4.6**) were prepared. The electrophilic attack is again stereospecific as evidenced by spectroscopic methods and happens at the Pd-CH$_3$ bond trans to the phosphine moiety of the ligand. Exposure of **3.5b** to Brookhart's acid followed by addition of pyridine forms the complex [Pd(CN$^{(1)}$)Me(py)]$^+$BAr$_4^{F-}$ (**4.9**) where the pyridine donor heterocycle occupies the position trans to the NHC moiety. Complexes **3.1a**, **3.3** and **3.5b** react with

MeI at room temperature in dichloromethane. The first two complexes give zwiterrions of the type [PdX₃{3-(2,6-diisopropyl-phenyl)-2-methyl-1-(n-diphenylphosphanyl-alkylₙ)-3*H*-imidazol-1-ium (n = 2, X = I, Cl: **4.10**; n = 1, X = I, Cl: **4.12**) and other unidentified products. On the other hand reaction of **3.5b** with MeI gives cleanly complex [(CN)$^{(1)}$PdMeI] (**4.13**) (iodide trans to NHC), that reacts further with CD₂Cl₂ to give [(CN)$^{(1)}$PdICl] (**4.14**). Dicationic complexes of the type [(PC$^{(2)}$)Pd(CH₃CN)]²⁺(X⁻)₂ (X = BF₄⁻: **4.15**; X = OTf⁻: **4.16**) are prepared by reaction of **3.2a** with 2 equivalents of AgX in acetonitrile. The thermally stable Pd(II) dimethyl complexes described above (**3.1a/b, 3.3, 3.5b** and **3.6**) show moderate catalytic activity towards Heck coupling, probably due to the reductive elimination of P, N functionalised 2-methyl-imidazolium salts. Cationic complexes **4.3, 4.4** and **4.6** do not catalyse the Heck coupling of chlorobenzene with methyl acrylate. Complex **3.8a** in the presence of Na⁺[CH(COOMe)₂]⁻ shows limited activity as catalyst for the Suzuki coupling of *p*-bromoacetophenone with PhB(OH)₂. Finally, the Heck coupling of *p*-bromoacetophenone with n-butylacrylate does not proceed using as catalyst Pd(dba)₂/**2.2a**, Pd(dba)₂/**2.3a** (**2.3a** = 3-(2,6-diisopropyl=phenyl)-1-(2-diphenylphosphanyloxide-ethyl)-3H-imidazol-1-ium) or Pd(dba)₂/**2.4a** in the presence of base.

Reaction of the *in situ* generated PC$^{(2)}$, **2.9c** or **2.9d** with 0.5 equivalents of [Pt(μ-SMe₂)₂Me₂]₂ gives complexes [Pt(PC$^{(2)}$)Me₂] (**5.6**), [Pt(CN$^{(1)}$)Me₂] (**5.7a**) and [Pt(CN$^{(2)}$)Me₂] (**5.7b**) respectively. **5.7b** reacts slowly with dichloromethane at room temperature to give complex [Pt(CN$^{(2)}$)MeCl] (**5.8**). Reaction of **5.7a/b** with Brookhart's acid followed by addition of a L donor gives complexes of the type [Pt(CN$^{(1)/(2)}$)MeL]⁺BAr₄$^{F-}$ (CN$^{(1)}$ or CN$^{(2)}$, L = py: **5.9** and **5.10** respectively; CN$^{(1)}$, L = 2-F-py: **5.11**; CN$^{(1)}$, L = 2,6-F₂-py: **5.12**; CN$^{(1)}$, L = Et₂O: **5.13**) where the electrophilic attack happens at the Pt-Me bond *trans* to the NHC moiety. Exchange between Et₂O and H₂O was found to happen in complex **5.13**. Complex **5.6** reacts with Brookhart's acid in the presence of pyridine in a way analogous to complex **3.1a**, thus giving complex [Pt(PC$^{(2)}$)Me(py)]⁺BAr₄$^{F-}$ (**5.16**). The novel platinum complexes **5.6** and **5.7a** react with CF₃COOH in CD₂CL₂ to give complexes [Pt((PC$^{(2)}$)Me(COOCF₃)] (**5.17**) and [Pt(CN$^{(1)}$)Me(COOCF₃)] (**5.18**) respectively, where the triflic anion occupies the site *trans* to the phosphine (**5.17**) or the site *trans* to the NHC (**5.18**). If complex **5.7a** is reacted with an excess of CF₃COOH complex [Pt(CN$^{(1)}$)(COOCF₃)₂] (**5.19**) is formed. Reaction of **5.7a** with H⁺[OH{B(C₆F5)₃}]⁻ gives complex [Pt(CN$^{(1)}$)(OH{B(C₆F5)₃}Me] (**5.22**), where the Pt-Me *trans* to the NHC moiety has been cleaved. Reaction of complexes **5.7a** and **5.6** with MeI in CD₂Cl₂ gives the Pt(IV) complexes *fac*-[Pt(CN$^{(1)}$)Me₃I] (*fac*-**5.24**) and *fac*-[Pt(PC$^{(2)}$)Me₃I] (*fac*-**5.23**). *Fac*-**5.24** decomposes *via* a route that produces imidazolium salts.

Interaction of [Rh(μ-OMe)₂(COD)] with two equivalents of the *in situ* generated free carbenes PC$^{(1)'}$ or PC$^{(2)'}$ gives complexes [Rh(PC$^{(1)'}$)₂]⁺Br⁻ (**6.10**) and [Rh(PC$^{(2)'}$)₂]⁺Br⁻ (**6.11**) respectively (COD = 1,5-cyclooctadiene; PC$^{(1)'}$ = 3-(2,4,6-trimethyl-phenyl)-1-(diphenylphosphanyl-methyl)-2,3 dihydro-1*H*-imidazol-2-ylidene). Reaction of the *in situ* generated carbene PC$^{(2)}$ with [Rh(COD)(py)₂]⁺BPh₄⁻ gives a 1:1 mixture of complexes [Rh{η⁶-Ph-BPh₃}(PC$^{(2)}$)] (**6.12**) and [Rh(COD)(PC$^{(2)}$)]⁺BPh₄⁻ (**6.13**). When the *in situ* generated carbene PC$^{(2)}$ was reacted with [Rh(COD)(PPh₃)₂]BF₄⁻ or [Rh(COE)₂acac] (COE = cyclooctene, acac = acetylacetonate anion) gave the dimmer [Rh(μ-Br)(PC$^{(2)}$)]₂ (**6.15**) and complex [Rh(PC$^{(2)}$)acac] (**6.14**). Complex **6.14** catalyses the insertion of aryl-boronic acids into aldehydes while it readily reacts at room temperature and atmospheric pressure with CO or syn-gas to give complexes *cis*-[Rh(PC$^{(2)}$)(acac)(CO)₂] (**6.18**) and *cis*-[Rh(PC$^{(2)}$)(acac)(H)₂] (**6.19**) respectively. Complex **6.19** cannot be prepared by reaction of **6.14** with H₂ under similar conditions. Interaction

of $PC^{(2)}$ with $[Ir(COD)(\mu\text{-}Cl)_2(\mu\text{-}H)]_2$ gives the five coordinate iridium complex $[Ir(COD)($ $PC^{(2)})Br]$ (**6.17**) where the carbene adopts an abnormal binding to the metal centre.

Finally, in an attempt to synthesise bulky-alkyl phosphine functionalised imidazolium salts we have managed to prepare the following synthones: 3-(2,6-diisopropyl-phenyl)-1-(2-X-ethyl)-3H-imidazol-1-ium (X = Br: **7.12**; X = OH: **7.13**), 1-Xmethyl-3--(2,6-diisopropyl-phenyl) -3H-imidazol-1-ium (X = chloro: **7.8**; X = iodo: **7.9**), 3-(2,6-Diisopropyl-phenyl)-1-vinyl-3H-imidazol-1-ium (**7.15**) and 2-(di-*tert*-butyl-phosphanyl)-ethanol (**7.20**). Microwave irradiation has been used to promote the synthesis of **7.12**, **7.13** and **7.8** quickly, cleanly and in very good yields.

List of Contents

Chapter 2: Synthesis of pyridine and phosphine functionalised NHC imidazolium salt precursors

Chapter 3: Functionalised *N*-heterocyclic carbene complexes of Palladium (II)

Chapter 5: Synthesis and reactivity of pyridine and phosphine functionalised NHC complexes of Pt(II).................................157-200

List of Tables

Chapter 2

Chapter 3

Chapter 4

Chapter 5

Chapter 6

List of Figures

Chapter 1

Chapter 2

Chapter 3

Chapter 4

Chapter 5

ORTEP representation of the structure of **5.22**

ORTEP representation of the structure of *fac*-**5.24**

Chapter 6

Functionalised NHC complexes of Rh(I) and Ir(I)
ORTEP representation of the cation in **6.10**
ORTEP representation of the zwitterion **6.12**
ORTEP representation of the crystal structure of **6.15**
ORTEP representation of **6.14**
ORTEP representation of **6.17**

Chapter 7

ORTEP representation of **7.1**

Chapter 8

Complex *fac*-**5.24**

List of Schemes

Chapter 1

Chapter 5

Chapter 8

List of abbreviations

acac	acetylacetonate anion
Ad	2-adamantyl
Ar	aryl group
Ar^F	$3,5\text{-}(CF_3)_2\text{-}C_6H_3$
Bu^t	*tert*-butyl
br.	broad
COD	1,5-cyclo-octadiene
COE	cyclooctene
Cy	cyclohexyl
d	doublet
DEPT	Decoupled Polarisation Transfer
DMAC	N,N-dimethyl-acetamide
DMF	dimethylformamide
DMS	dimethylsulphide
DMSO	dimethylsulphoxide
d_n	deuterated solvent with n deuteriums
dt	doublet-triplet
ES	Electrospray
Et	ethyl
ether	diethyl-ether
fac	facial
GC	Gas Chromatography
H.O.M.O.	Highest Occupied Molecular Orbital
HR	High resolution
hrs	hours
^iPr	*iso*-propyl
IR	infrared
J	coupling constant
Lt.	Litter
L.U.M.O.	Lowest Unoccupied Molecular Orbital
Me	methyl group
Mes	$2,4,6\text{-}(CH_3)_3\text{-}C_6H_2$

MS	Mass Spectrometry
mL	millilitre
nbd	Norbornadiene ([2.2.1]-biscyclo-1,4-heptadiene)
NHC	*N*-Heterocyclic Carbene
NMP	N-methyl-2-pyrrolidinone
NMR	Nuclear Magnetic Resonance
NOESY	Nuclear Overhauser Effect Spectroscopy
OTf⁻	triflate anion (trifluoro-sulphonic anion)
Ph	phenyl group
PE	Petroleum Ether
ppm	parts per million
py	pyridine
R	alkyl or hydrogen
s.	singlet
t.	triplet
*t*Bu	*tert*-butyl
TFA	trifluoroacetic acid
THF	Tetrahydrofuran
tmeda	N,N,N',N'-tetramethyl-1,2-diamino-ethane
TMS	Trimethyl-sylil group
Ts	tosyl
tt	triplet of triplets
ylid.	ylidene
µL	microlitre
η	hapto
μ	mijou

Acknowledgements

First and foremost I would like to thank my supervisor Dr. Andreas Danopoulos for giving me the opportunity to experience first hand the joys as well as the trials and tribulations of organometallic chemistry. His support and input throughout my project were more than valuable and without them I must admit I would be lost.

My deepest thanks are extended to Dr. Robin Porter for being a very good friend and lab mate, Dr. Joseph Wright for his efforts in teaching us to do Crystallography the right way, help with solving troublesome X-ray data sets and his patience into sharing his knowledge, Dr. Lisa Titcomb, Dr. Melissa Matthews, Neoklis Stylianides, Stephen Downing and everyone who has worked in Lab 30:2007 during my time there.

To my parents, sister and grandparents, I can find no words to express my dearest thanks for their support. My dearest thanks to all the friends I have met in Southampton (Simos, Leonidas, Lefteris, Jiakomo, Paolo, Clelia…) and especially my housemates Benedetta Guizzardi, Julien Michel and Daniela Demurtas and Sue Emmer for her support during the preparation of this manuscript.

I would especially like to thank Prof. Michael Hursthouse for the provision of X-ray facilities and everyone in the EPSRC X-ray Crystallography Service.

Finally I would like to thank my industrial supervisor Dr. Arran Tulloch for helpful discussions and help with VT-NMR experiments, Johnson-Matthey and the University of Southampton for financial support, my advisor Dr. Michael Paver for his input and his patience reading my reports, the NMR and MS service of the Chemistry Department in Southampton and Dr. Richard Brown for the provision of the GC.

To my nanny

Chapter 1: Introduction

Chapter 1:Introduction

The introduction of carbenes into inorganic and organometallic chemistry, by Fischer in 1964,[1] planted the seeds of what now has become a very active area of research within the scientific community and chemical industry. Since then, suffice it to say that the significance of metal carbenes in organic synthesis,[2] catalysis[3] and macromolecular chemistry[4] has increased enormously.

It was shortly after the isolation of the first well-defined metal carbene complex 1[1] (Figure 1.1), when independently, Öfele and Wanzlick reported the isolation of 2[5] and 3[6] (Figure 1.1), respectively, where N-heterocyclic carbenes made their debut as ligands. Although, these two reports received little attention, the foundations of a very interesting area of research in organometallic chemistry were laid.
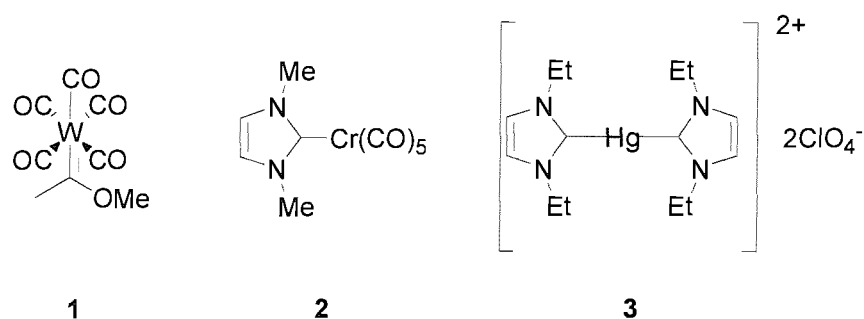
Figure 1.1: First metal carbene complex (1) and N-heterocyclic carbene complexes by Öfele (2) and Wanzlick (3).

The preparation of complexes 2 and 3 was achieved by the deprotonation of the corresponding imidazolium salts. In the case of 2 a carbonylmetallate was used, while the mercury complex 3 was obtained by deprotonating the imidazolium salt with Hg(OAc)$_2$ (Scheme 1.1).
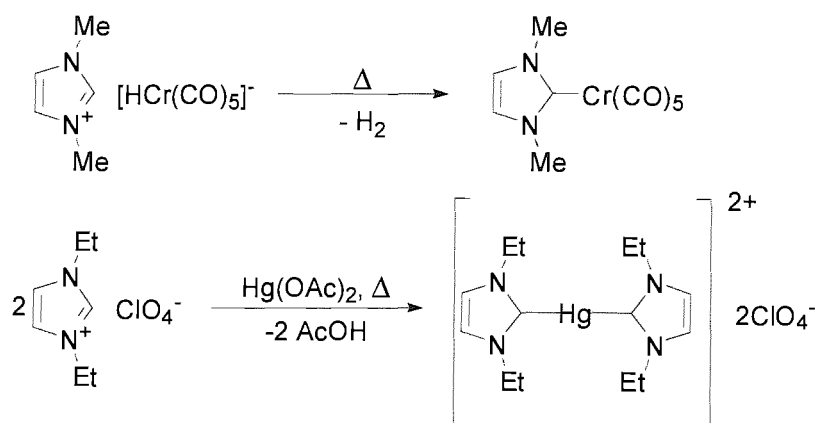
Scheme 1.1: Preparation of complexes **2** and **3**.

The major breakthrough occurred in 1991 when Arduengo isolated the first free *N*-heterocyclic carbene, by deprotonation of the imidazolium salt with NaH in the presence of catalytic amounts of KOBu^t or DMSO (Scheme 1.2).[7] Even though the methodology has limitations regarding the substituents on the nitrogen heteroatoms, it demonstrates that isolable and thermodynamically stable carbenes do exist, and rekindled the interest in the area. As a result, *N*-heterocyclic carbenes were transformed from lab curiosities to one of the most extensively studied and researched family of ligands.
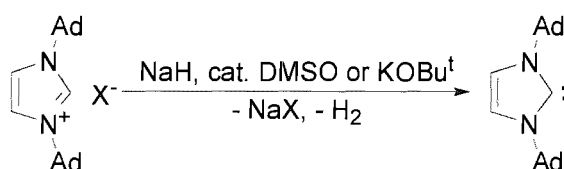
Scheme 1.2: Preparation of the first isolated free NHC from Arduengo.

1.1 Carbenes

Carbenes are uncharged species, of the type :CR$_1$R$_2$, with a divalent carbon and a pair of unshared electrons that can be assigned to two non-bonding orbitals in different ways. This in turn means that two types of carbenes exist: singlet state carbenes and triplet state ones. The spin multiplicity of the ground state (S =1 for singlet and S = 3 for triplet) is determined by the energy difference between the σ and π orbital of the sp^2- hybridized carbene carbon. The magnitude of this energy gap is dependant on the nature of the R$_1$, R$_2$ substituents of the carbene carbon.[8]

In triplet state carbenes, the R_1, R_2 substituents are not electron donors. These species are very unstable and their isolation is achieved by steric protection of the carbene carbon, in order to suppress its reactivity. Tomioka *et.al.* managed to stabilize diphenyl carbenes with methyl or chloro substituents in *ortho* positions.[9] In 1995 the same group reported the synthesis of carbene 4 (Figure 1.2) by photolysis of the corresponding diazo compound. The latter carbene is stable in the solid state at room temperature.[10]
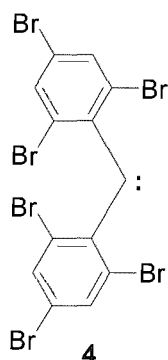
Figure 1.2: Triplet state carbene 4 isolated by Tomioka *et.al.*

On the other hand, the R_1, R_2 substituents in singlet state carbenes are heteroatom donor groups (R_1, R_2 = O, S, N, P, Si). Due to the low electronegativity of the carbene carbon, they are considered to be very strong nucleophiles. Their propensity to donate their electron pair exceeds that of amines. Some characteristic examples synthesised by Alder *et.al.*[11, 12] and Bertrand *et.al.*[13, 14] are shown in Figure 1.3.

5a: X = O, R = iPr, R' = tBu   5e: R = iPr
5b: X = O, R = Me, R' = tBu   5f: R = Me
5c: X = O, R = iPr, R' = Me
5d: X = S, R = iPr, R' = Me

5g

5h: R = iPr
5i: R = Cy
5j: R = Ph
5k: R = tBu
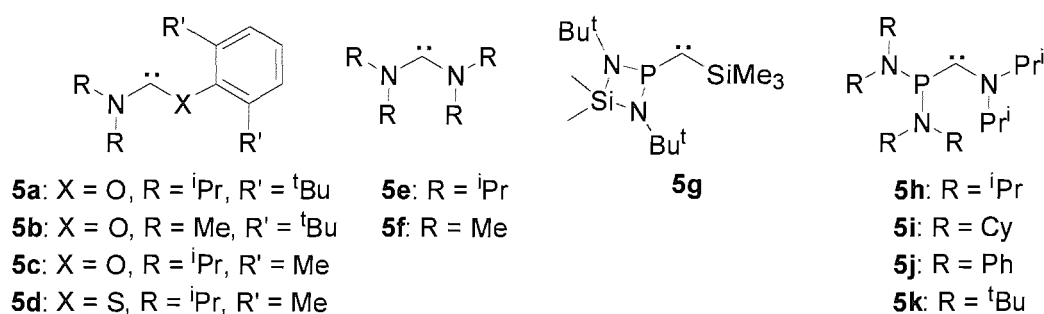
Figure 1.3: Singlet state acyclic carbenes 5a-k prepared by Alder (5a-f) and Bertrand (5g-k).

3

Finally the two different types of carbenes, described above, exhibit different reactivities. Triplet state carbenes show a radical-like reactivity, whereas singlet state carbenes are expected to participate in reactions as either nucleophiles or electrophiles, due to the σ-type lone pair and the empty p orbital.

1.2 *N*-Heterocyclic Carbenes (NHCs)

1.2.1 Nomenclature of NHCs

NHCs are singlet state carbenes of type (**I**) (Scheme 1.3). Their main characteristic is that the carbene carbon is flanked by two heteroatoms one of which is at least nitrogen. The whole system exists usually in a five-membered ring, although six-membered ring NHCs have been reported. [15]
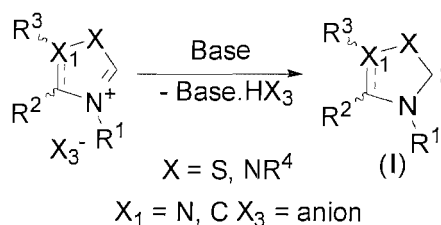
Scheme 1.3: *N*-heterocyclic carbenes and their synthesis. When X_1 is N there is no R^3.

Their preparation involves the deprotonation of the parent salt with a base, as illustrated above. Their name derives from the parent azolium salt using the suffix ylidene. The addendum –ylidene describes the substitution of two hydrogens with two electrons or a pair of electrons. So when X= NR^4, X_1 = C the name is 1-R^1-3-R^4-4-R^3-5-R^2-2,3-dihydro-1*H*-imidazole-2-ylidene. *N*-heterocyclic ylidenes where X = NR^4, and X_1 = C and the backbone of the five-membered ring is saturated are called 1-R^1-3-R^4-4-R^3-5-R^2-2,3-dihydro-1*H*-imidazolidine-2-ylidene. Finally ylidenes deriving from triazolium or thiazolium salts (X = NR^4, X_1 = N and X = S, X_1 = C respectively) are named as follows: 1-R^4-3-R^2-4-R^1-4,5-dihydro-1*H*-triazole-5-ylidene and 1-R^1-4-R^3-5-R^2-2,3-dihydro-thiazol-2-ylidenes. Even though the correct nomenclature demands the use of the 2,3-dihydro-1*H* addendum, the literature norm is to ignore it.[8]

1.2.2 Electronic properties of NHCs

Most of the attention has been centred on ylidenes deriving from imidazolium and imidazolinium salts. Their investigation begun in the early 1960's, when Wanzlick focused on imidazolinidines like **6** (Scheme 1.4). [16] Unfortunately instead of the desired compound **6**, only the electron rich olefin **7** was isolated. Furthermore, no equilibrium between the 'monomeric' carbene **6** and the dimer **7** was experimentally substantiated. Electron rich (Wanzlick) olefins like **7** were utilised by Lappert *et.al.* for the development of a general synthetic route for the isolation of metal-NHC complexes. [17]
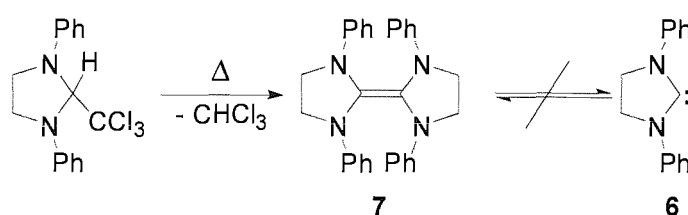
Scheme 1.4: Attempted isolation of free NHC from Wanzlick.

It was only after the groundbreaking work of Arduengo *et.al.* [7] that stable, crystalline ylidic carbenes were isolated (Scheme 1.2). The steric bulk around the carbene carbon was thought to be crucial for their isolation. Shortly after, this speculation was overthrown by the isolation of ylidenes without bulky substituents attached to the nitrogen heteroatoms. Many examples of free NHCs have emerged and some of them are depicted at Figure 1.4. [18]
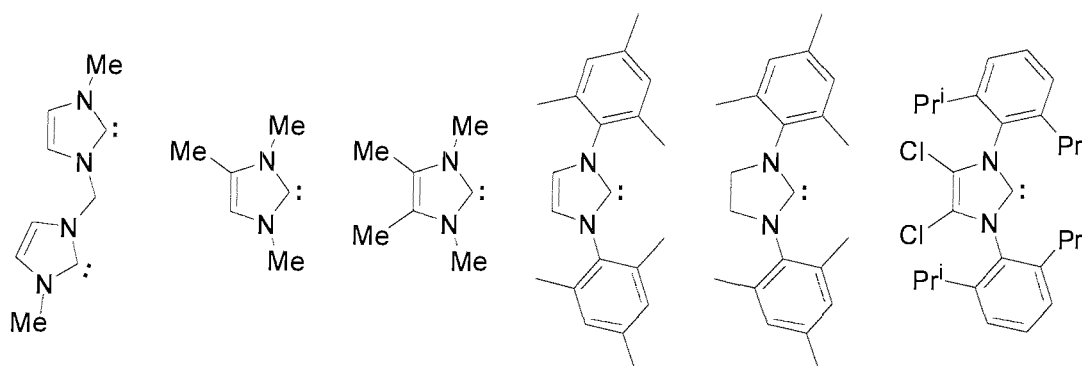
Figure 1.4: Examples of free NHCs.

The isolation of stable, sterically unencumbered NHC, made it clear that thermodynamic (electronic effects) rather than kinetic (steric hindrance) stabilisation, was responsible for their isolation. Two are the major electronic effects that should be taken into consideration. Firstly, the difference in electronegativity between the carbene carbon and the nitrogen substituents, induces a strong $-I$ σ effect which stabilises the lone pair in the in-plane carbene σ-orbital. Secondly, further stabilisation is achieved by donation of electron density, from the nitrogen heteroatoms, to the unoccupied p orbital of the carbene carbon lying perpendicular to the plane of the heterocycle (+M effect). The two phenomena are illustrated in Figure 1.5. Although the electronic situation in the N-C-N moiety is crucial, steric hindrance does account for stability, especially in the case of imidazolinidines.[8]
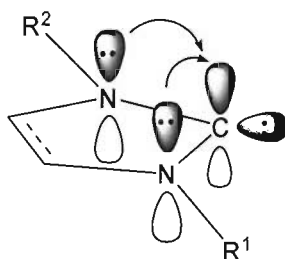
Figure 1.5: -I inductive effect along the N-C-N σ bonds and +M effect from p_N-p_C orbital interaction.

1.2.3 Reactivity of NHCs

NHCs, unlike triplet state carbenes or other transient singlet state carbenes, are reluctant towards reaction with unsaturated nucleophiles such as alkenes, allenes, acetylenes or arenes. Moreover, in contrast to other nucleophilic singlet state carbenes, stabilized by interaction of the empty p-orbital with a delocalized π system, they are indifferent to electrophiles like fumaric esters. NHCs can be easily handled in donor solvents like THF. The reason behind the reduced electrophilic character of the carbene carbon can be found in the fact that the $p\pi$ L.U.M.O. orbital lies low in energy due to the nitrogen pair conjuration. This also rationalises their susceptibility towards dimerisation,

which can be considered as a nucleophilic attack of one singlet carbene at the vacant-perpendicular to the plane-orbital of another singlet carbene.[8]

Due to their nucleophilic character, NHCs could be utilized as catalysts to promote many organic transformations. Indeed, imidazole and triazole ylidenes have found catalytic applications in organic synthesis. They are very active catalysts for the benzoin condensation of higher aldehydes to α-hydroxyketones, [19] the Michael-Stetter reaction,[20] the formoin reaction [21] and transesterifications.[22] Asymmetric variants of ylidene catalysed benzoin consenstaion and Michael-Stetter reaction were achieved using chiral triazolium salts as catalyst precursors. [23] Recently, NHCs made their premier as catalysts in macromolecular chemistry when, 1,3-bis(2,4,6-trimethyl-phenyl)-2,3-dihydro-1H-imidazol-2-ylidene was used to promote the living ring-opening polymerisation of cyclic esters. [24]

Finally, it is worth mentioning their potential role as catalytic species in biological systems. Breslow *et.al.* found evidence that the active catalyst for the decarboxylation of pyruvic acid to acetaldehyde is in fact a thiazole-ylidene deriving from the naturally occurring thiazolium salt vitamin B_1 enzyme cofactor. [25]
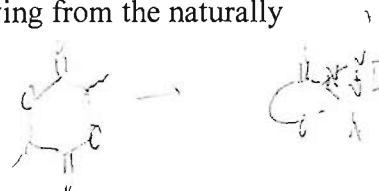
1.3 Metal carbene complexes

Organometallic compounds bearing fragments of the type $:CR_1R_2$ are known as carbene complexes and their main characteristic is that there is formally a double bond between the metal and the divalent carbon of the carbene moiety. This is indicated by the shorter carbon-metal distances, than those found in complexes with metal-carbon single bonds. As conventional carbenes are poor σ donors, π backdonation from the metal centre accounts for the shorter metal carbon bond distances observed in metal-carbene complexes, than those found in metal-alkyl complexes. [26]

Carbene complexes can be categorised in two general classes. Those where the metal centre is a late transition metal in a low oxidation state and one or both of the substituents R_1, R_2 are π donors, are known as Fischer carbenes. Carbene complexes containing an early transition metal in a high oxidation state and alkyl or hydrogen substituents on the carbene carbon are known as Schrock carbenes. [27]

These two classes are also representative of different types of chemical behaviour. In Fischer type carbenes the carbon is electrophilic while in Schrock type carbenes the carbon is nucleophilic. The last statement in molecular orbital terminology could be

7

rephrased as, that in Fischer carbenes the H.O.M.O. is of metal character, while in the case of Schrock carbenes the H.O.M.O. has carbon character. In either case common carbenes :CR$_1$R$_2$ (R$_1$, R$_2$ = H, alkyl, alkoxy, amino, aryl) are not considered as spectator ligands, as the reactions of metal-carbene complexes proceed either *via* metal-carbon bond cleavage or by transfer of the carbene moiety to one of the substrates. [2]

1.4 *N*-heterocyclic carbenes as ligands

1.4.1 Synthesis of NHCs

One of the reasons of the recent popularity of NHCs as ligands could be lying in the fact that the imidazolium (or imidazolnium) precursors can be made along various reliable routes. The one-pot synthesis starting from glyoxal, primary amine and formaldehyde allows the preparation of symmetrically substituted imidazolium salts (Scheme 1.5a). Variations of this method allow the formation of unsymmetrically substituted imidazolium salts (Scheme 1.5b). Finally the orthoformate route presents another way towards (un)symmetrically substituted imidazolinium salts (Schemes 1.5c and 1.5d). [28]

The next step *i.e.* the synthesis of the free carbene by deprotonation of the azolium salt can be achieved in many ways. The most common method follows the Arduengo protocol, using NaH or KH in the presence of catalytic amount of KOBu^t. Another successful way of deprotonation utilizes liquid ammonia. [29] The use of K[N(SiMe$_3$)$_2$] or Li(N^{i}Pr$_2$) is applicable to relative large scale synthesis of heterocyclic ylidenes as demonstrated by Danopoulos *et.al.*. [30] The advantage of this method is that in most cases it selectively generates the free carbene, leaving hydrocarbon bridges and other moieties intact. Finally, although harsh, the use of potassium in refluxing THF is another way to accessing free carbenes from their azolium salts. Nevertheless, care should be taken with the choise of the deprotonating agent, as certain side reactions leading to undesired products are known. [31, 32]

(a) $\text{(glyoxal)} + 2\ \text{R-NH}_2 + \text{(CH}_2\text{O)} \xrightarrow[-3\ \text{H}_2\text{O}]{+\ \text{HX}} \text{R-N}^+\text{=CH-N-R}\ \ \text{X}^-$

(b) $\text{(glyoxal)} + \text{R}^1\text{-NH}_2 + \text{NH}_4\text{Cl} + \text{(CH}_2\text{O)} \xrightarrow[-3\ \text{H}_2\text{O}]{\text{acid}} \text{N=CH-N-R}^1 \xrightarrow{+\ \text{R}^2\text{-X}} \text{R}^2\text{-N}^+\text{=CH-N-R}^1\ \ \text{X}^-$

$\uparrow\ \text{HNO}_3$

$\text{R}^1\text{-NH}_2 + \text{Cl}_2\text{CS} + \text{NH}_2\text{CH}_2\text{CH(OEt)}_2 \xrightarrow{\text{HCl}} \text{N=CH-N-R}^1 \quad (\text{SH})$

(c) $\text{(glyoxal)} + 2\ \text{R}^1\text{-NH}_2 \longrightarrow \text{R}^1\text{-N=CH-CH=N-R}^1 \xrightarrow[\text{HCl}]{\text{NaBH}_4} \text{R}^{1+}\text{NH}_2\ \ ^+\text{NH}_2\text{R}'\ \ 2\text{Cl}^- \xrightarrow{\text{HC(OEt)}_3} \text{R}^1\text{-N}^+\text{=CH-N-R}'\ \ \text{Cl}^-$

$\text{reduction} \nearrow\ \text{HCl}$

(d) $\text{(Cl-CO-CO-OEt)} \xrightarrow{+\ \text{R}^1\text{-NH}_2} \text{(R}^1\text{-NH-CO-CO-OEt)} \xrightarrow[\Delta]{+\ \text{R}^2\text{-NH}_2} \text{(R}^1\text{-NH-CO-CO-NH-R}^2)$
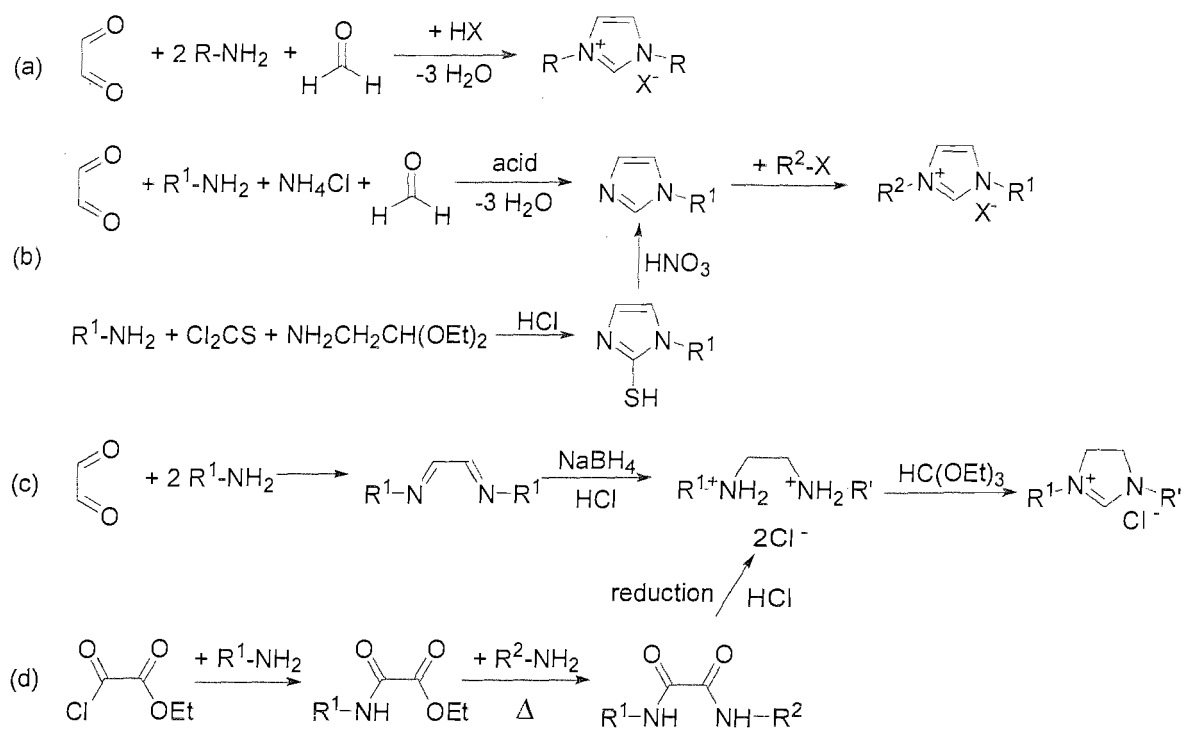
Scheme 1.5: Preparation of azolium precursors for the synthesis of NHCs (R' = R^1 for method (c) and R' = R^2 for method (d)).

1.4.2 Electronic properties of NHC complexes

The electronic properties of NHCs portrayed above exert a significant role on the nature of their bonding to metals. The textbook discrimination of Fischer and Schrock type carbenes does not hold for NHCs. Although at first glance they could be placed in the Fischer type class, NHCs exhibit some 'abnormalities' compared to the carbene moieties found in metal-carbene complexes conforming to either the Fischer or Schrock type.

First and foremost, due to the partial fulfilment of the vacant pπ orbital through π conjugation from the nitrogen heteroatoms, π-backdonation from the metal centre to the carbene carbon of a NHC is insignificant. Their π acceptor ability is very near to that of pyridine.

Secondly, unlike conventional carbene moieties, they are very strong σ donors. By comparing the v(CO) stretching frequencies of compounds of the type *trans*-[RhL₁L₂(CO)X] (X = Cl, Br, I, L₁, L₂ = phosphine or ylidene) it was deduced that their electronic characteristics resemble those of electron-rich alkyl phosphines and N donors as

9

nitriles and pyridine.[33, 34] Quoting the conclusions, of Nolan *et.al.* deriving from structural and thermodynamical studies: "in general these ligands behave as better donors than the best phosphine ligands with the exception of the sterically demanding (adamantyl) carbene".[35]

Furthermore the non-conformity of NHCs to either class of Fischer or Schrock carbenes is validated by X-ray single crystal diffraction studies of numerous of their complexes. The NHC-metal bond distances were found to be longer compared to the carbene-metal bond lengths found in Fischer and Schrock type complexes, due to the absence of backbonding.[36]

Finally it is noticeable to say that upon complexation of imidazole-2-ylidenes onto group 6 transition metal centres, as well as platinum group metals, there is little to no π-aromaticity. This was evidenced by the OsO_4-addition to the unsaturated backbone of a NHC complex (Scheme 1.6).[37] This experiment came in agreement with recent charge-density studies.[38]
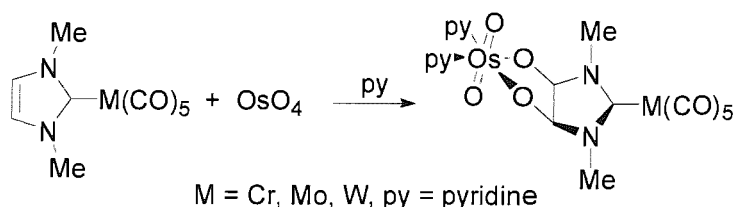
Scheme 1.6: Addition of OsO_4 to the unsaturated backbone of a NHC.

The electronic properties discussed above, sum up to the conclusion that NHCs upon complexation, do not exhibit the reactivity of Fischer or Schrock type carbene moieties. Because of this chemical behaviour they could be considered as spectator ligands in organometallic catalysis.

1.4.3 Tunability of NHCs

The spectator ligand properties of heterocyclic ylidenes, have shifted a considerable amount of attention towards them, as potentially successful alternatives to phosphines in homogeneous catalysis. None the less, NHCs have to possess some of the key characteristics that contributed to the popularity of phosphines in homogeneous

catalysis, *i.e.* steric and electronic tunability of the active metal centre. Chirality is of course another desired attribute that NHCs should have.

From Scheme 1.5 it is apparent that the ability to control the steric and electronic environment of the metal centre is great. Variation of the R^1, R^2 substituents on the nitrogen heteroatoms, can alter the steric and electronic characteristics around the metal centre. The electronic environment can also be manipulated through substitution of the backbone with electron donating or electron withdrawing groups. Moving from imidazole-2-ylidenes (unsaturated backbone) to imidazolidine-2-ylidenes (saturated backbone), affects the electronic environment of the metal centre as well.

Chirality can be introduced through the R^1, R^2 substituents. In the case of imizolidine-2-ylidenes, stereogenic centres can also be located at the saturated backbone. Examples of chiral NHCs or their azolium precursors are shown in Figure 1.6.
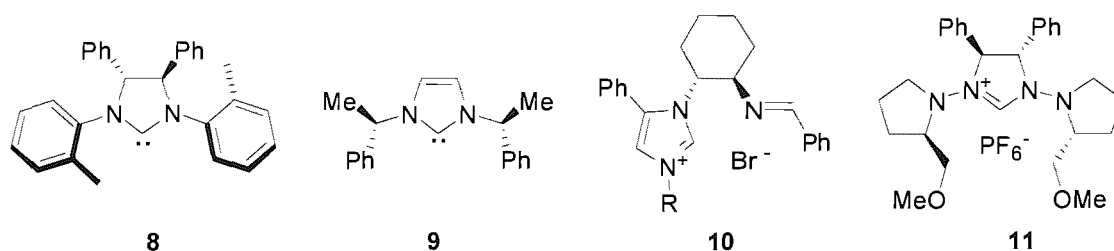
Figure 1.6: Two chiral ylidenes (**8** and **9** synthesised by Grubbs [39] and Herrmann [40] respectively) and two chiral imidazolium precursors (**10** and **11** synthesised by Douthwaite [41] and Alcarazo [32] respectively).

Immobilisation to achieve catalyst recycling and minimum leaching is also a possibility.

The scope of tunability is further extended by the isolation of bidenate, tridentate and pincer heterocyclic ylidenes. Crucial parameters in homogeneous catalysis like bite angle can be manipulated. Some examples are illustrated in Figure 1.7.[42-45]

R = Me, Bu^t, Ar = 2,6-(Pr^i)$_2$-Ph

12 **13** **14** **15**
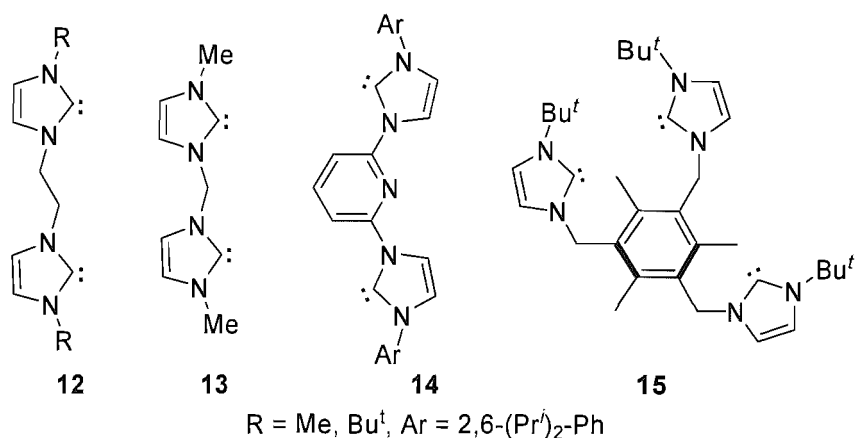
Figure 1.7: Bidentate NHCs with different bite angles (**12** [42] and **13** [43]), pincer tridentate NHCs [44] (**14**) and tridentate NHCs [45] (**15**).

The above discussion can be summarised schematically in Figure 1.8. It is quite clear that there are seemingly endless possibilities for novel ligand architectures.

chirality, immobilization, electonic and steric tuning

chirality, immobilization and electonic tuning
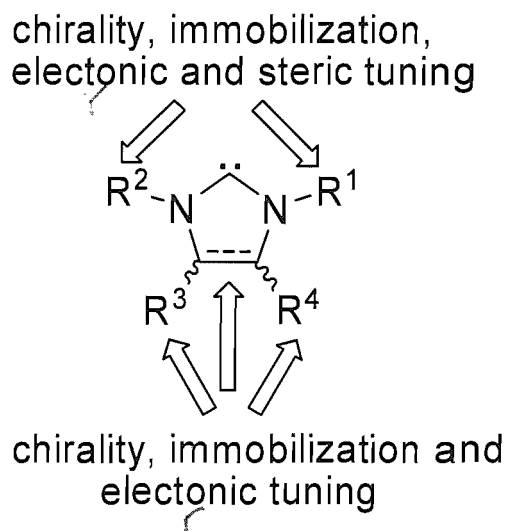
Figure 1.8: Summary of the "good ligand" characteristics of NHCs.

12

1.5 Metal Coordination Chemistry

1.5.1 Synthesis of NHC complexes

Keeping in mind the backround discussed above it is no surprise that metals incapable of π-backdonation coordinate NHCs as nucleophilic two electron donor ligands. The synthesis of a multitude of main group and rare earth metal complexes has been described by Schumann *et.al.*.[46] Although these complexes show interesting coordination chemistry, most of the up to date interest has been focused on transition metal complexes of NHCs, due to their potential applications in catalysis.

The introduction of a heterocyclic ylidene to a metal centre can be achieved with one of the following methods: a) Simple substitution reactions using the isolated free carbene and a suitable metal precursor. [47]A variation of this method involves the *in situ* generation of the free carbene, followed by complexation (usually through a substitution reaction) with a metal.[48] b) Metal vapour synthesis, applicable in the case of sublimable NHCs. [49] c) Reaction of the azolium salts with metal bases like metal amides, alkoxides, hydrides, alkyls and carboxylates. [50] d) Transmetallation reactions from silver NHC complexes to transition metals. This method has been utilized by many research groups and is one of the most popular ones in the literature. Its popularity is based on the relative easy synthesis of the silver complexes as well as on the mild conditions under which the transmetallation works. The reaction is driven by the precipitation of AgX (X = halide) that can easily be separated by filtration. It is important to say that this method is particularly effective in the case of functionalised NHCs with ''dangling'' substituents.[51, 52, 53] e) The Metalla-Ugi reaction. [54] This reaction can be characterised as a one-pot domino process involving the cycloaddition between an amine an isocyanide, an aldehyde and a CN⁻ ligand bound on a metal cente. The metal centre can be considered as the template. This is illustrated in Scheme 1.7.

$$NEt_4[Mn_2(CO)_2CN] + [PhNH_3]^+ Cl^- + Bu^tNC + PhCHO \xrightarrow{\text{MeOH}} (OC)_9Mn_2$$
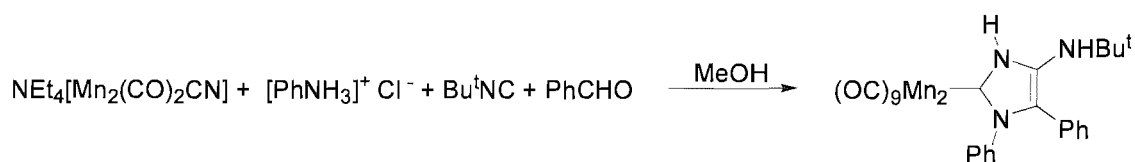
Scheme 1.7: A typical example of Metalla-Ugi reaction.

1.5.2 Transition Metal Complexes of NHCs

The plethora of transition metal complexes that have been accessed using the synthetic protocols described above is proof of the interest in the area. Some examples from each group are given below.

1.5.2.1 Group 3

Examples of group 3 NHC complexes are very rare. The only reported examples are an amido functionalised NHC complex of yttrium (**16**) [55] and the anionic scandium complex **17** [56] (Scheme 1.8).
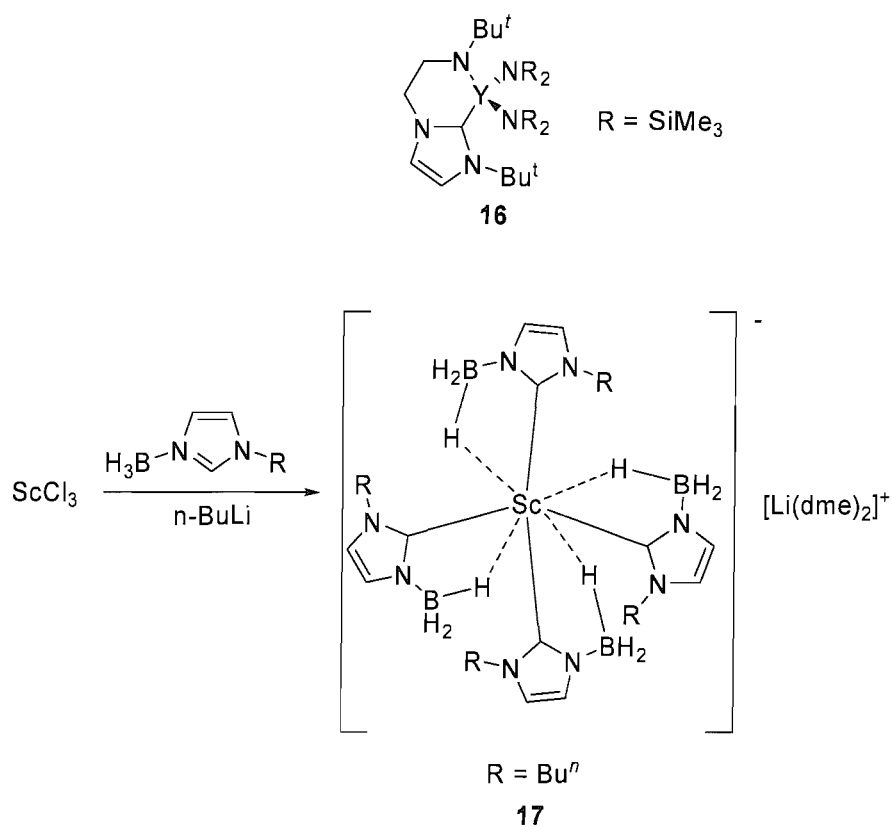
Scheme 1.8: Group 3 metal NHC complexes reported by Arnold *et.al.* [55] (**16**) and Wacker *et.al.* [56] (**17**).

1.5.2.2 Group 4

Group 4 ylidene metal complexes have been only recently isolated. They are prepared either by direct reaction of the metal amides or alkyls with the imidazolium salt or by the reaction of the free isolated carbenes with the appropriate metal precursor. Their catalytic activity has not been studied yet. Some examples are illustrated in Scheme 1.8. [57, 58]
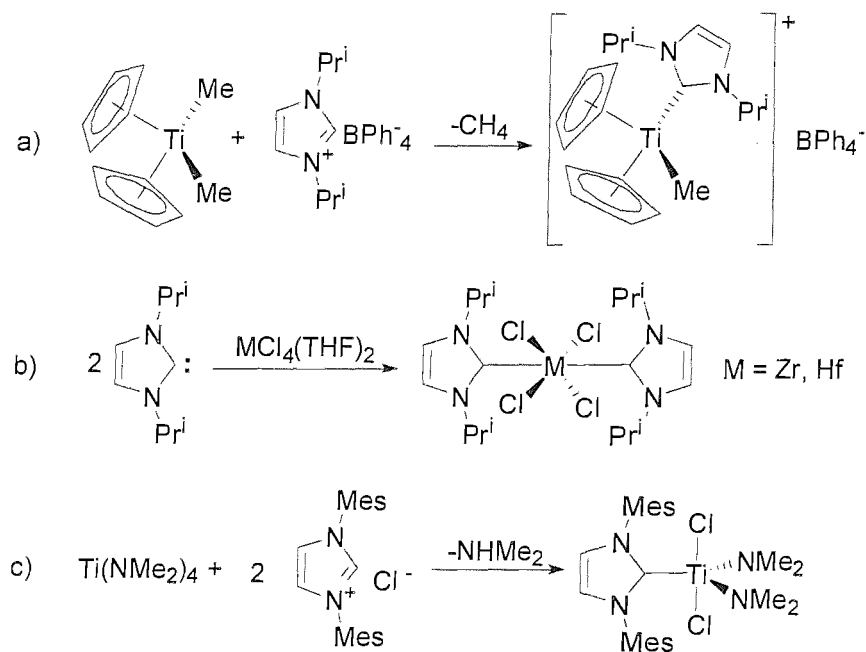
Scheme 1.9: Group 4 metal NHC complexes deriving from a) metal alkyls, [57] b) interaction of free carbene with metal precursor [57] and c) metal amides. [58]

1.5.2.3 Group 5

The first group 5 NHC complexes were reported by Herrmann and coworkers. [36] Their synthesis is outlined in Scheme 1.10.
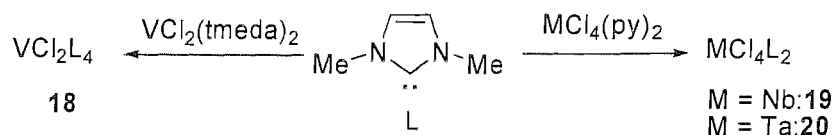
Scheme 1.10: Group 5 metal NHC complexes reported by Herrmann et.al. [36]

Recently the V(V) oxo NHC complex (**18**) was synthesised by interaction of V(O)Cl$_3$ with 1,3-bismesityl-imidazol-2-ylidene (Scheme 1.11). [59] It is interesting to note that complex **21** is resilient towards hydrolysis.
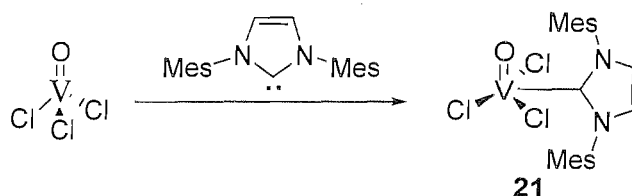
Scheme 1.11: Preparation of a V(V) NHC complex.

1.5.2.4 Group 6

Complexes of the type M(CO)$_{6-n}$L$_n$ (L = heterocycle ylidene, M = Cr, Mo, W, n = 1, 2, 3) were probably some of the first transition metal NHC complexes. Their synthesis played an important role into establishing the electronic properties of NHCs as ligands by probing their CO stretching frequencies. [8] Herrmann *et.al.* also described the preparation of Mo(VI) and W(VI) dioxo NHC complexes (Scheme 1.12). [60]

M = Mo: **22**
M = W: **23**
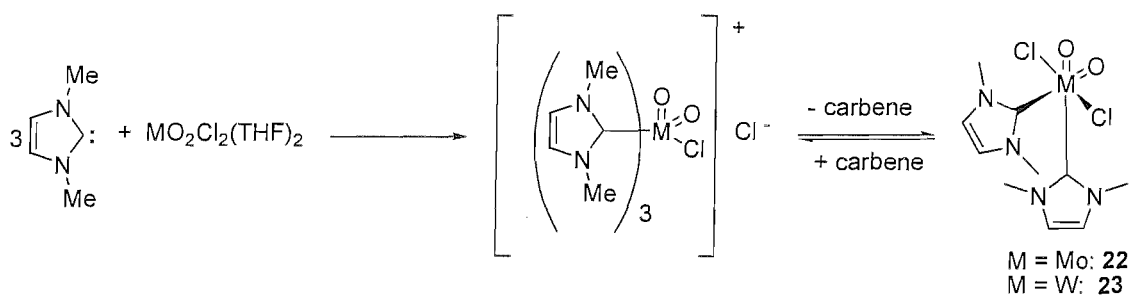
Scheme 1.12: Synthesis of Mo(VI) and W(VI) NHC complexes.

It is interesting that in this paper, the issue of the lability of NHCs as ligands is addressed. Moreover, complex **22** decomposes in acidic media in the presence of water to give molybdate (IV) and imidazolium salt. Danopoulos and coworkers have also reported the synthesis of Cr(II) NHC complexes by interaction of Cr(Mes)$_2$(THF)$_3$ with 1,3-diisopropyl-4,5-dimethyl-imidazole-2-ylidene (Scheme 1.13). [61]

the synthesis of Cr(II) NHC complexes by interaction of Cr(Mes)$_2$(THF)$_3$ with 1,3-diisopropyl-4,5-dimethyl-imidazole-2-ylidene (Scheme 1.13). [61]

Cr(Mes)$_2$(THF)$_3$
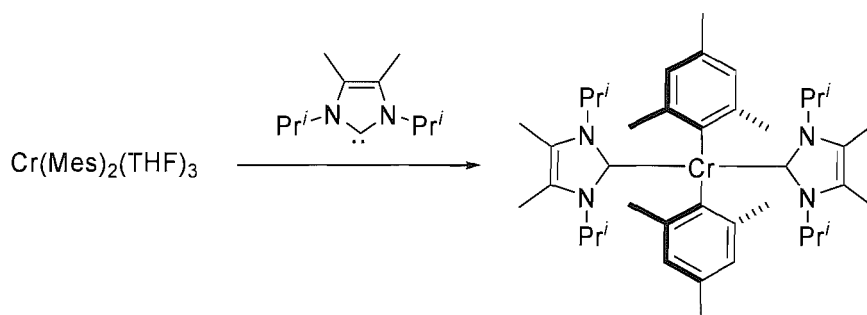
Scheme 1.13: Synthesis of aryl Cr(II) NHC complexes.

1.5.2.5 Group 7

Examples of group 7 NHC complexes are very few. *trans*-Re(O)$_3$MeL (L = 1,3-dimethylimidazole-2-ylidene) was reported by Hermann in 1994.[36] Braband *et.al.* have reported the synthesis of complexes of the type [MO$_2$L$_4$]$^+$ (M = Re, Tc; L = 1.3-diisopropyl-4,5-dimethyl-imidazol-2ylidene) (Scheme 1.14). [62]

[MOCl$_4$]$^-$ + excess

trace H$_2$O

M = Re, **24**
M = Tc, **25**
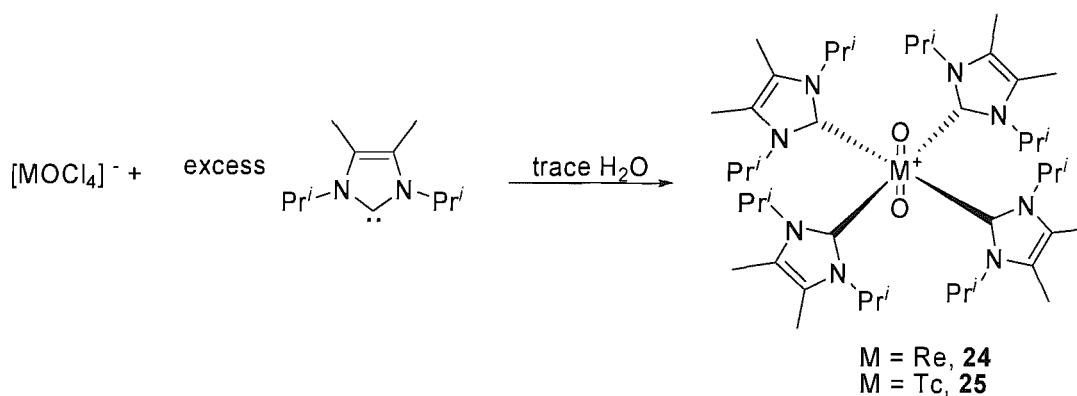
Scheme 1.14: Synthesis of Re(V) (**19**) and Tc(V) (**20**) dioxo NHC complexes.

The same group has also reported the synthesis technetium-nitrido NHC complexes by interaction of [TcNCl$_2$P(Me$_2$Ph)$_3$] with 1,3-diethyl-4,5-dimethylimidazol-2-ylidene (Scheme 1.15). [63] Complex **26** could not be isolated without concurrent contamination from complex **27**, when silicon grease was used as a sealant. When silicon-

free fittings were used, only complex **26** formed and upon addition of silicon grease to its THF solution it produced a reaction mixture consisting of **26** and **27**.

When [TcNCl₂P(Me₂Ph)₃] was reacted with 1,3-diethyl-4,5-dimethylimidazol-2-ylidene in CH₃CN instead of THF the formation of the ligand exchange intermediate complex **28** was isolated (Scheme 1.15). Complex **26** was also present in solution along with a number of side products.
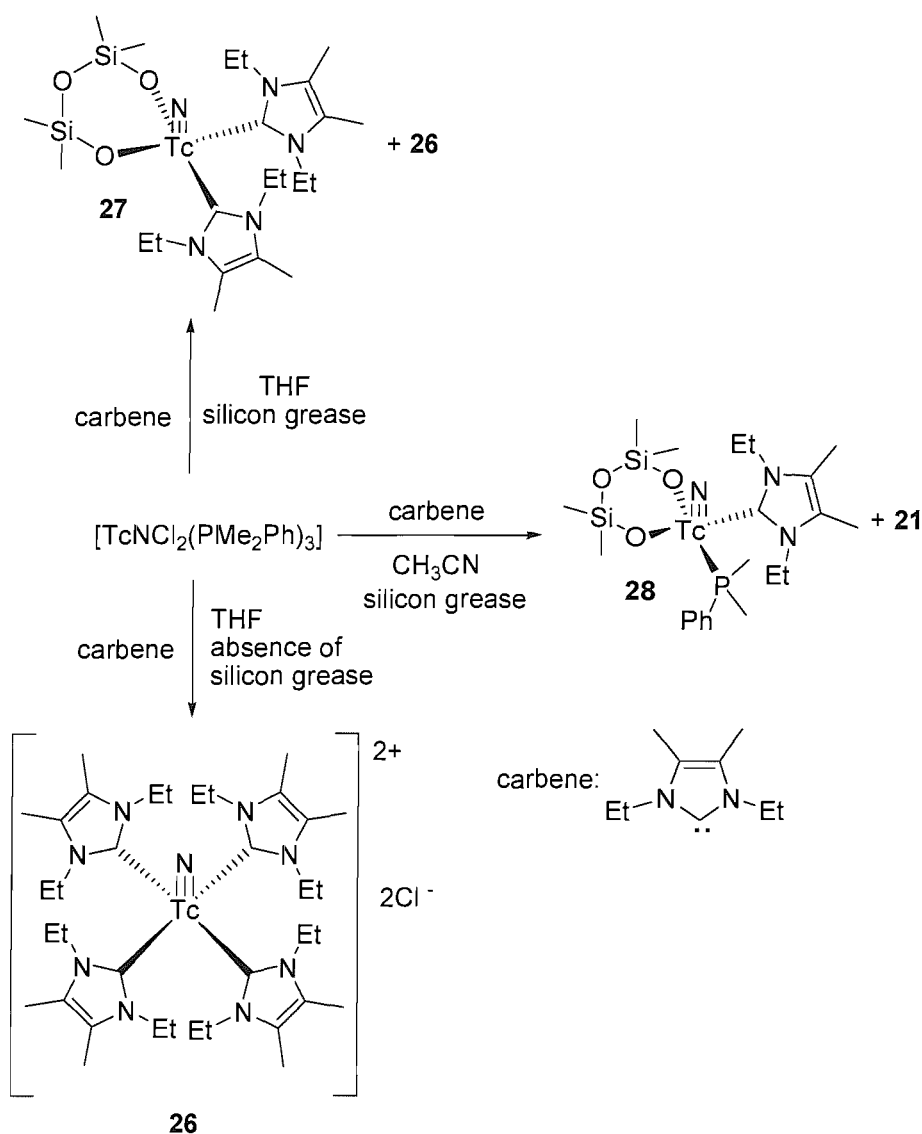
Scheme 1.15: Preparation of Tc-nitrido NHC complexes.

Roesky and coworkers have reported the isolation of Mn(II) complexes of the type [ML$_2$X$_2$] (L = 1.3-diisopropyl-4,5-dimethyl-imidazol-2ylidene; X = Cl (**29**); X = I (**30**); X = OAc (**31**)) (Scheme 1.16). [64]
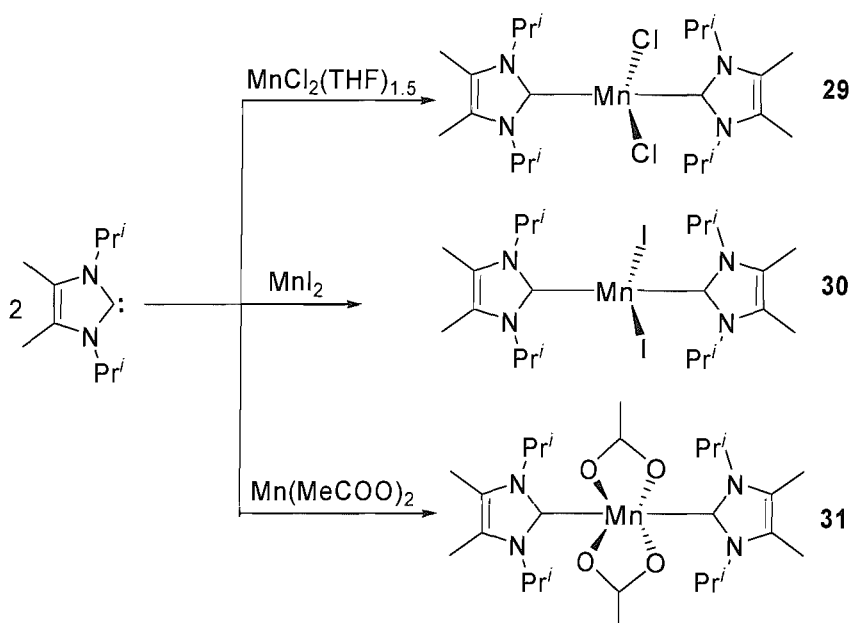
Scheme 1.16: Preparation of Mn(II) NHC complexes.

The same group has also reported the synthesis of Mn(II) NHC complexes bearing the β-diketiminate ligand. They have the formula [ML{CH(CMeNAr)$_2$}X}] (L = 1.3-diisopropyl-4,5-dimethyl-imidazol-2ylidene; X = I (**32**); X = NHAr (**33**)) and their synthesis is outlined in Scheme 1.17. [65]
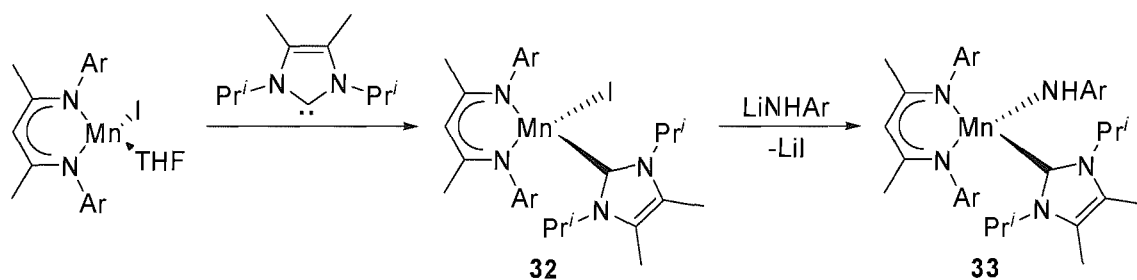
Scheme 1.17: Preparation of Mn(II) NHC complexes incorporating the β-diketiminate ligand (Ar = 2,6-diisopropyl-phenyl).

The effect of different substituents on the reactivity of NHCs was demonstrated by the reaction of 1,3-bis(aryl)-imidazol-2-ylidene (aryl = mesityl or 3-bromo-*m*-xylene) or

19

tetramethylimidazol-2-ylidene with manganocene (Scheme 1.18).[66] In the first case, X-ray diffraction studies showed that only one NHC is bound to the metal centre while the Cp rings are bound to manganese in an η^2 and η^4 mode (Complexes 34a-b). When tetramethylimidazol-2-ylidene was used the manganese coordination sphere comprised of two NHC ligands and two Cp ligands (Complex 35). X-ray diffraction studies on 35 showed that one of the Cp ligands bonds to the metal centre in an η^1 fashion, while the other adopts an orientation intermediate of an η^1 and η^2 bonding mode.[66]
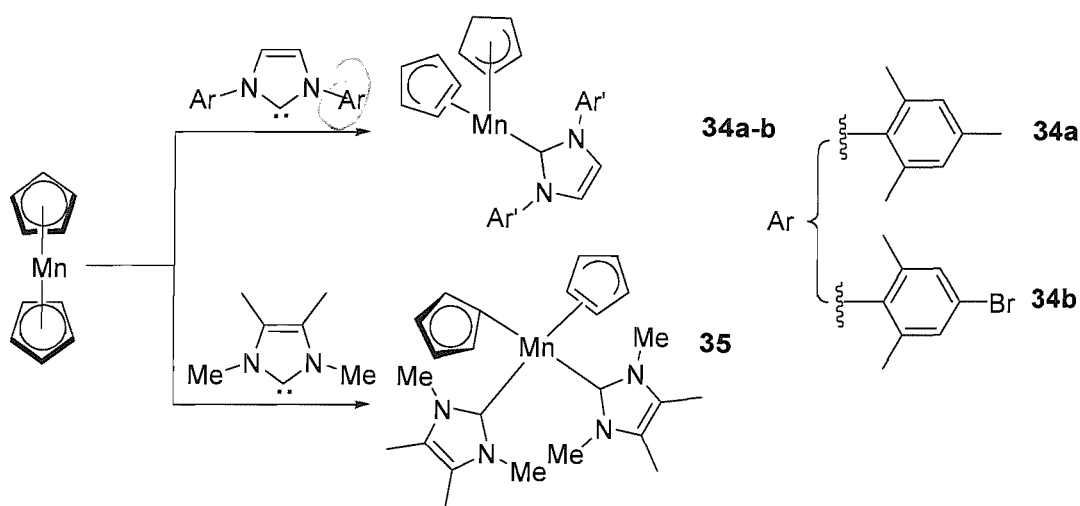
Scheme 1.18: Preparation of Cp Mn(II) NHC complexes.

1.5.2.6 Group 8

The incorporation of a heterocyclic ylidene moiety in the second-generation Grubbs catalyst (37), leading to superior reactivities (compared to the first generation catalyst 36), had a paramount contribution to the success story of NHCs as ligands. Since then the volume of papers dealing with different NHC ligand architectures and the reactivities of their ruthenium alkylidene complexes, resembles that of a tidal wave.[67] The synthesis of the chiral second-generation Grubbs catalyst (38),[36] showed the enormous potential of NHC metal carbene complexes as useful catalysts. The preparation of the complexes is shown in Scheme 1.19.
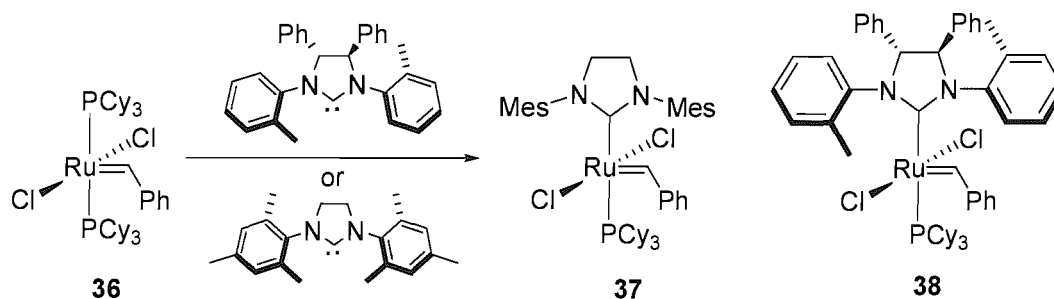
Scheme 1.19: Synthesis of Grubbs'second-generation (37) catalyst and its chiral analogue (38).

The catalytic properties of compounds **36-38** and their analogues, in many organic transformations are astonishing. They catalyse a range of reactions with applications in total organic synthesis (cross metathesis,[68] ring closing metathesis,[69] ene-yne metathesis[70] and self metathesis[71]) and in macromolecular chemistry (ring opening metathesis polymerisation[72] and acyclic diene metathesis polymerisation[67]). Finally, the immobilisation of second type generation Grubbs catalysts has been achieved, and preliminary results regarding their activity and recyclability are very encouraging.[67] Other ruthenium NHC complexes have been used in catalytic transformations like furan synthesis[73] (complexes **39** and **40**), hydrogenation and hydroformylation (complex **41**) [Scheme 1.14].[74]
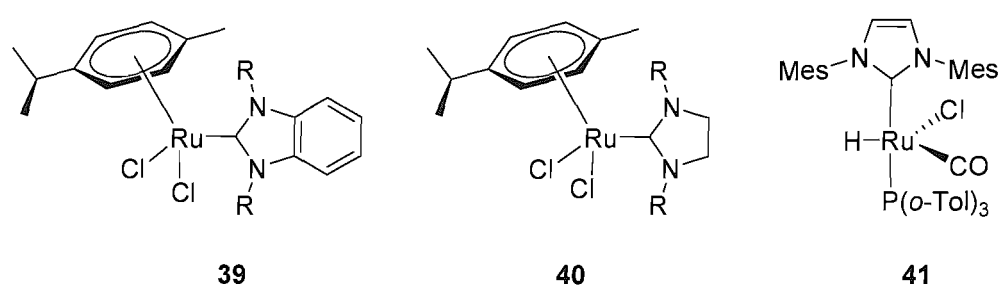
Figure 1.9: Ruthenium complexes **39**, **40** used as catalysts in furan synthesis (R = Cy, Mes). Complex **41** shows activity in hydrogenation and hydroformylations.

Iron NHC complexes are scarce. There are only two papers reporting the synthesis of heterocyclic ylidene complexes of iron from Danopoulos et.al.[75] and Grubbs et.al..[76]

The tetrahedral iron(II) complex **42** (Figure 1.9) reported by Grubbs works as an atom transfer radical polymerisation (A.T.R.P.) catalyst for styrene.[76]
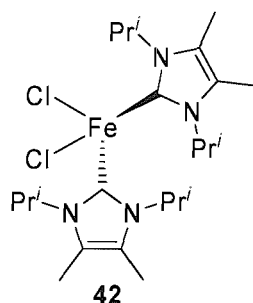
Figure 1.10: Complex **42** used as A.T.R.P. catalyst yielding poly-(styrene) with low polydispersities.

Recently the preparation of osmium-alkylidene NHC complexes has been reported (Scheme 1.20). These complexes have been found to be efficient catalysts for olefin metathesis reactions.[77]
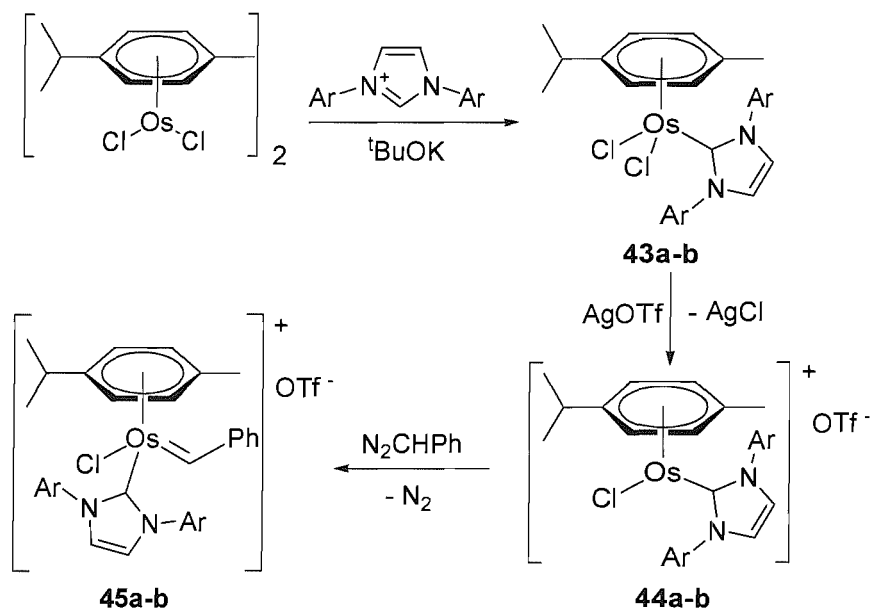
Scheme 1.20: Synthesis of osmium NHC complexes (Ar = Mes:**a**; Ar = 2,6-diisopropylphenyl:**b**)

Since phosphine based rhodium and iridium catalytic systems are very well established, it is hoped that NHCs can be used as alternative ligands in developing a new more active generation of catalysts. There are many examples of rhodium and iridium complexes incorporating NHCs as ligands. Some rhodium and iridium complexes are described in Figure 1.10. Complex 46 has been utilized as an effective chiral catalyst for the hydrosilylation of ketones.[78] Complexes 47a-b and 48 have displayed good to moderate activities as hydrogenation, [79] hydroformylation [79] and transfer hydrogenation catalysts.[80] Complex 51 catalyses the cyclopropanation of olefins with diazoalkanes.[81] The cationic complex 52, incorporating a chelating bis carbene ligand, is catalytically active towards the intramolecular hydroamination of alkynes.[82] Finally, immobilized on polymer supports, rhodium NHC catalysts have also been reported to be very active as hydroformylation catalysts.[83]
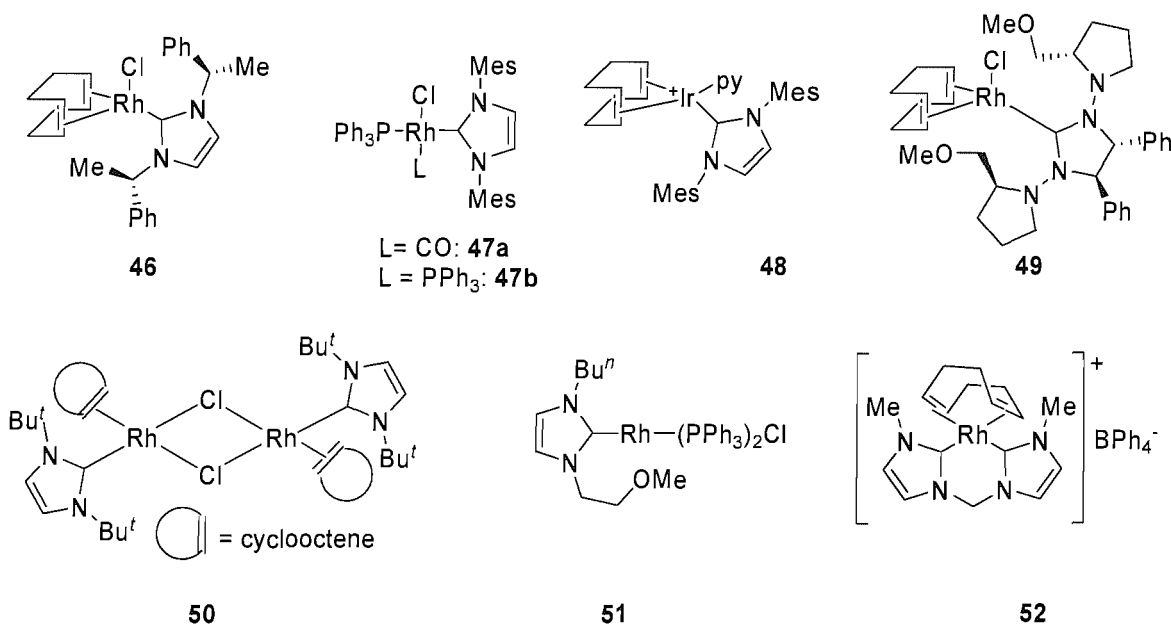
Figure 1.11: Some characteristic examples of Rh(I) and Ir(I) NHC complexes.

Cobalt complexes containing NHC ligands have been known for some time. Lappert reported the earliest examples. [84] Later examples include a number of cyclopentadienyl derivatives like complexes 53 [85] and 54. [86] Interestingly in complex 53 the NHC has unexpectedly displaced the tethered phosphine instead of the ethene ligand.

Other examples include hexacoordinate cationic Co(III) complexes containing a tripodal carbene ligand of the Trofimenko type,[87] dicobalt NHC complexes [88] (complex **55**) and cobalt complexes with a pincer carbene pyridine ligand (complex **56**). [89] The above examples are illustrated in Figure 1.11.
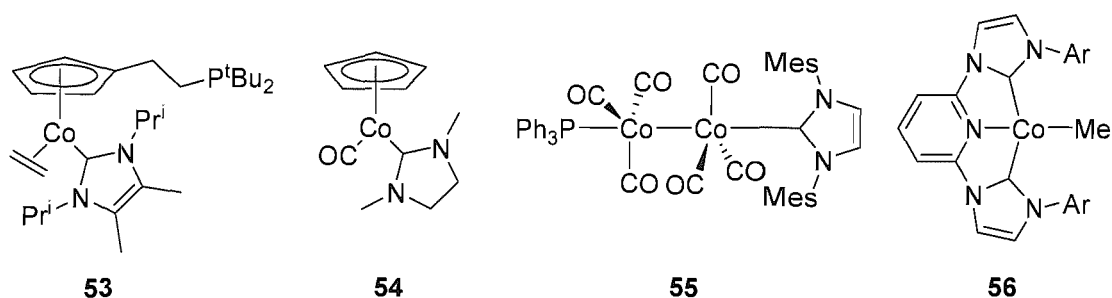
Figure 1.12: Cobalt NHC complexes. For **56**, Ar = 2,6-(Pr^i)$_2$-Ph.

1.5.2.8 Group 10

The use of NHCs as ligands with group 10 metals paved the way to systems revolutionising catalytic C-C bond formation reactions. This is evidenced by the always-increasing amount of group 10 NHC complexes surfacing in the literature. Some examples of monodentate palladium NHC complexes are given in Figure 1.12.

24

R₁ = R₂ = Me: **57a**
R₁ = R₂ = CF₃: **57b**
R₁ = Me, R₂ = CF₃: **57c**

58

59

60

61

62a-e

R₃ = Cy(**a**), Ad(**b**), Mes(**c**), Prⁱ(**d**),
2,6-(Prⁱ)-Ph (**e**)
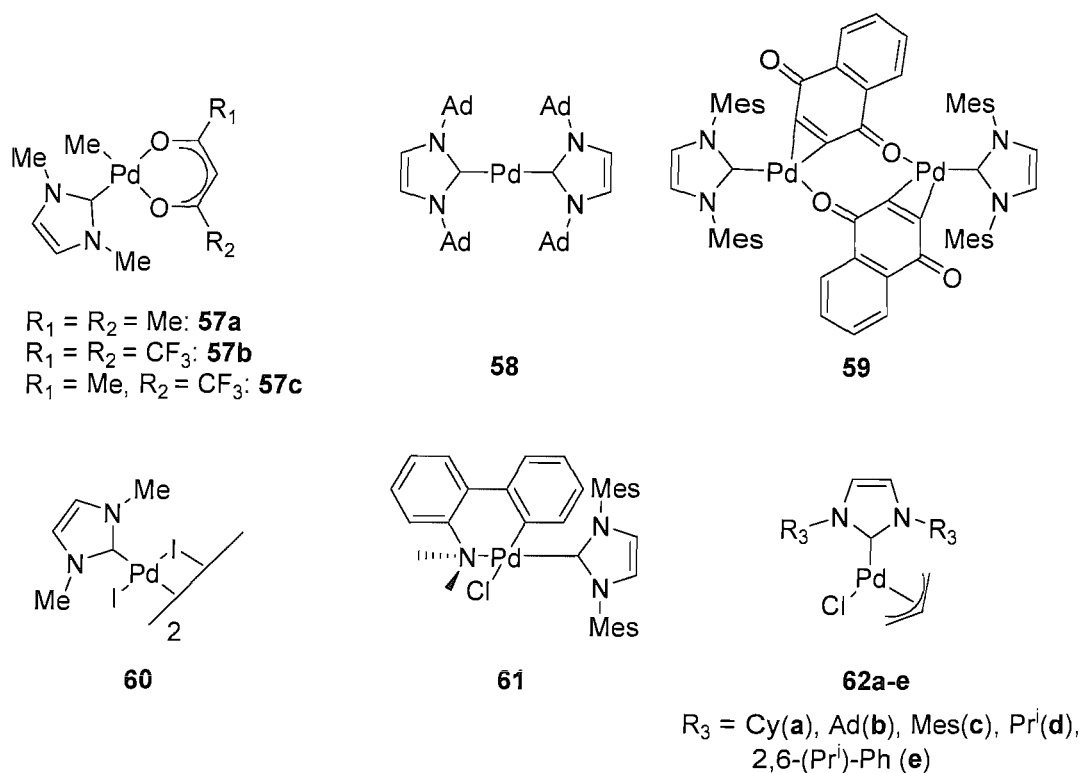
Figure 1.13: Monodentate palladium NHC complexes.

The Pd(0) complex **58** is a very effective catalyst for the Suzuki coupling at ambient temperatures of inactivated substrates, such as electron rich aryl chlorides. [90] Complexes **61** [91] and **62a-e**, [92] reported by Nolan *et.al.*, exhibit very good reactivities for the catalytic amination of aryl halides. In certain cases, even challenging substrates provided very good catalytic turnovers. The Heck olefination of aryl halides proceeds very well, when complexes **57a-c** are employed as catalysts. [93] Finally compound **59** reported, by Beller *et.al.*, was shown to be an effective catalyst for Heck couplings as well. [94]

Bidentate NHC complexes of palladium and nickel have also been synthesized. They show structural diversities depending on the size of the chelate ring (Figure 1.13). A characteristic example of this behaviour is found in complexes **67a-b**, **68** and **69**. It is interesting to notice that complexes **68** and **69** co-exist in solution and in the solid state as proved by NMR spectroscopy and X-ray single crystal diffraction studies. [52]

X = Cl, Br, I, R₁ = Me: **63a-c**
X = Br, R₁ = Buᵗ: **64**

65

66

67a-b
Ar = Mes (a), 2,6-(Prⁱ)-Ph (b)

68

69

X = BF₄⁻, R₁ = Me: **70a**
X = PF₆⁻, R₁ = Mes: **70b**
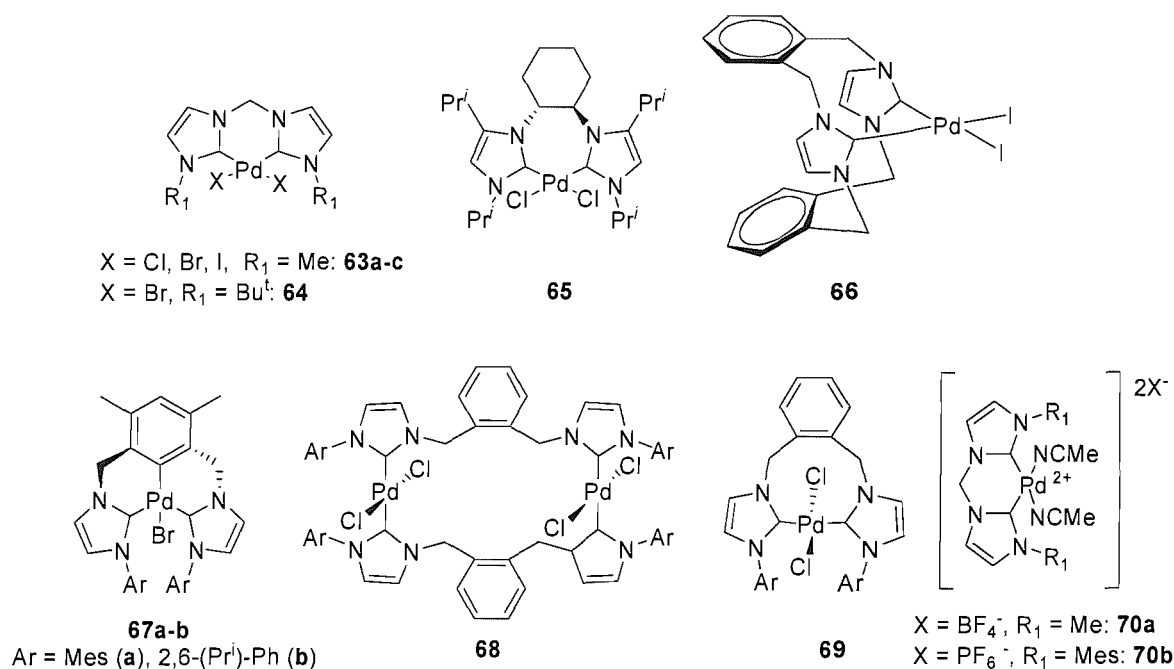
Figure 1.14: Bidentate NHC complexes of palladium (in the case of **68** and **69**, Ar = 2,6-(Prⁱ)₂-Ph).

Complexes **63a-c** are catalytically active towards Heck couplings in the presence of smooth reducing agents.[95] Catalyst loadings are exceptionally low for the case of aryl bromides. Heck olefinations are also promoted in good to excellent yields by complexes **66**[96] and **67a-b**.[52] Methane activation is achieved by complex **64**, in the presence of trifluoroacetic anhydride and potassium peroxodisulphate, under mild conditions (20-30 bar CH_4, 80-90°C), to yield the methyl ester of trifluoroacetic acid.[97] Finally, bidentate cationic complexes **70a-b** have found applications in the catalytic copolymerisation of ethylene-carbon monoxide, yielding high molecular weight, strictly alternating poly(C_2H_4-alt-CO).[98]

It is worth noticing the small number of well-defined nickel NHC complexes. These are very scarce and few examples are known (Figure 1.14). Complex **71** represents one example of bidentate nickel(II) NHC complex.[99] Compound **72** reacts with dioxygen to generate μ-hydroxo species with parallel loss of prop-2-ene-aldehyde through a radical mechanism.[100] Herrmann et.al. have reported that compound **73** has shown good activity in the Suzuki coupling of activated aryl chlorides.[101]

71   **72**   **73**
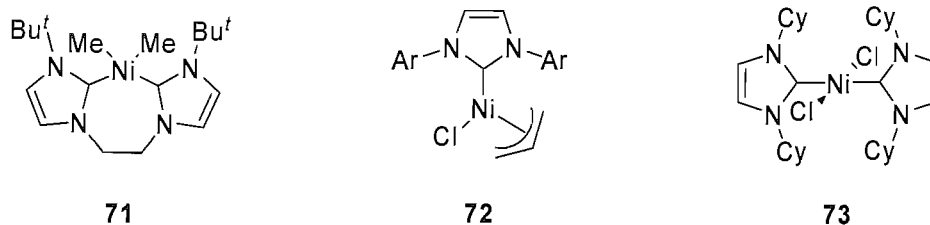
Figure 1.15: Examples of nickel NHC complexes.

The existence of homoleptic 14 and 16e⁻ Ni(0) NHC complexes has also been reported, and they have been found to readily undergo oxidative addition of aryl-halides (Scheme 1.15).[102]
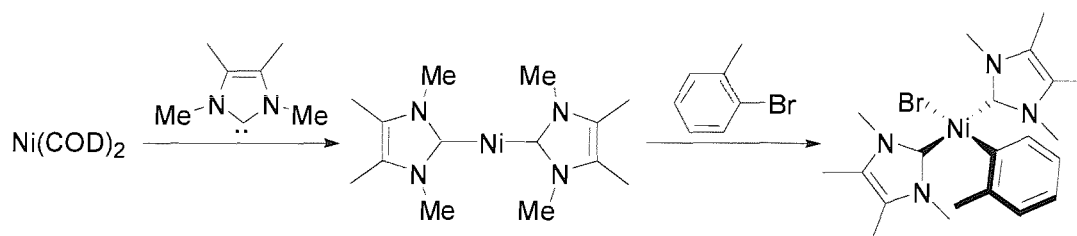
Scheme 1.21: Oxidative addition in Ni(0) 14e⁻ homoleptic NHC complex.

Platinum NHC complexes have also been characterised and their activity as moderate hydrosilylation catalysts has been demonstrated.[103] Very interesting reactivity between Pt(0) NHC complexes and imidazolium salts has been observed by Cavell *et.al..* Interaction of Pt(0) complexes of the type Pt(NHC)(alkene)₂ with imidazolium salts, leads to oxidative addition of the acidic C-H bond onto the metal centre, yielding *trans*-(carbene)₂PtHX (X = I). It is interesting to notice that the reaction proceeds at ambient temperature.[104]

The impact of NHCs in catalytic transformations promoted by group 10 metals, is also highlighted by the increased use of their azolium precursors in conjunction with simple commercially available metal precursors, to generate the catalytically active species *in situ*. This synthetic protocol, which avoids the use of well-defined catalysts, is very popular in organic labs. Employing such a methodology has certain advantages, like the availability of the air-stable, straightforward prepared-from cheap chemicals-imidazolium (or imidazolinium) salts in multi-gram quantities. This practice has been indeed applied and in many instances has yielded catalytic systems that rival similar

protocols utilising phosphines. Examples include the hydroamination [105, 106] and Heck olefination [106] of aryl halides, amide α-arylation, [107] hydrosylilation, [108] Suzuki, [109] Kumada, [110, 111] Sonagashira [112] and Stille [113] couplings.

1.5.2.9 Lanthanide and Actinide metals

Examples of f-block NHC complexes are very rare. Oldham *et.al.* has reported NHC complexes of uranyl dichloride (**74a-b**),[114] while Arnold *et.al.* has synthesised samarium [55] (**75**) and cerium [115] (**76**) mixed amido-NHC complexes (**56**) (Figure 1.15).

R = H, **74a**
R = Me, **75b**

M = Sm: **75**
M = Ce: **76**
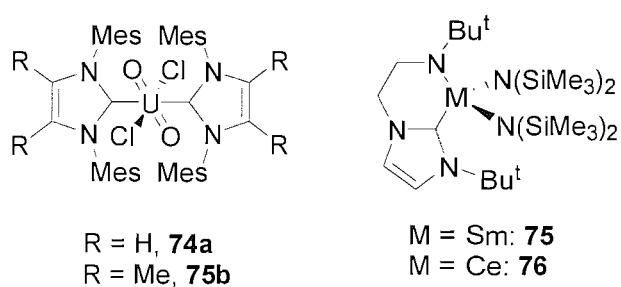
Figure 1.16: NHC complexes of samarium, cerium and uranium.

References:

1. Fischer, E. O.; Maasböl, A. *Angew. Chemie Int. Ed. Engl.* **1964**, *76*, 580.
2. Cornils, B.; Herrmann,W. A. *Applied Homogeneous Catalysis with Organometallic Compounds*; VCH: Weinheim, Germany, 1996; Vol. 1
3. Grubbs, R. H., *Complehensive Organometallic Chemistry*. Pergamon: Oxford, U.K. 1982; p. 499.
4. Brookhart, M.; Studabaker, W. B. *Chem. Rev.* **1987**, *87*, 411.
5. Öfele, K. *J. Organomet. Chem* **1968**, *12*, P42.
6. Wanzlick, H. -W.; Schonherr, H. -J. *Angew. Chemie Int. Ed.* **1968**, *7*, 141.
7. Arduengo III, A. J.; Harlow, R. L.; Kline, M. *J. Am. Chem. Soc* **1991**, *113*, 361.
8. Herrmann, W. A.; Köcher, C. *Angew. Chemie Int. Ed.* **1997**, *36*, 2162.
9. Hirai, K.; Komatsu, K.; Tomioka, H. *Chem. Lett.* **1994**, *33*, 148.
10. Tomioka, H.; Watanabe, T.; Hirai, K.; Furukawa, K.; Takui, T. *J. Am. Chem. Soc* **1995**, *117*, 6376.
11. Alder, R. W.; Allen, P. R.; Murray, M.; Orpen, A. G. *Angew. Chemie Int. Ed.* **1996**, *35*, 1121.
12. Alder, R. W.; Butts, C. P.; Orpen A. G. *J. Am. Chem. Soc.* **1998**, *120*, 11526.
13. Kato, T.; Gornitzka, H.; Baceiredo, A.; Bertrand, G. *J. Am. Chem. Soc.* **2000**, *122*, 998.
14. Merceron, N.; Miqueu, K.; Baceiredo, A.; Bertrand, G. *J. Am. Chem. Soc.* **2002**, *124*, 6806.
15. Yun, J.; Marinez, E. R.; Grubbs, R. H. *Organometallics* **2004**, *23*, 4173.
16. Wanzlick, H. W.; Schikora, E. *Angew. Chemie* **1960**, *72*, 494.
17. Lappert, M. F.; Pye, P. L. *J. Chem. Soc., Dalton Trans.* **1978**, 837.
18. Bourissou, D.; Guerret, O.; Gabai, F.; Bertrand, G. *Chem. Rev.* **2000**, *100*, 39.
19. Kreizer, W. *Nachr. Chem. Tech. Lab.* **1981**, *29*, 172.
20. Stetter, H., *Angew. Chem. Int. Ed. Engl.* **1976**, *15*, 639.
21. Stetter, H.; Kuhlmann, H. *Org. React.* **1991**, *40*, 407.
22. Grasa, G. A.; Kissling, R. M.; Nolan, S. P. *Org. Lett.* **2002**, *4*, 3583.
23. Enders, D.; Breuer, K.; Telles, J. H. *Helv. Chim. Acta* **1996**, *79*, 1217.
24. Nice, G. W.; Clauser, T.; Connor, E. F.; Mock, A.; Waymouth, R. M.; Hedrick, J. L. *J. Am. Chem. Soc* **2003**, *125*, 3046.
25. Breslow, R. *J. Am. Chem. Soc* **1958**, *80*, 3719.
26. Bochmann, M. *Organometallics 1*. Oxford University Press: Oxford, U.K., 1994.
27. Cotton, F. A.; Wilkinson, G. *Advanced Inorganic Chemistry*. Wiley Interscience: New York, U.S.A., 2001.
28. Waltman, A. W.; Grubbs, R. H. *Organometallics* **2004**, *23*, 3105.
29. Herrmann, W. A.; Köcher, C.; Artus, G. R. J. *Chem. Eur. J.* **1996**, *2*, 162.
30. Danopoulos, A. A.; Winston, S.; Gelbrich, T.; Hursthouse, M. B.; Tooze, R. P. *Chem. Commun.* **2002**, 482.
31. Craig, H. A.; Goerlich, J. R.; Marshall, W. J.; Unverjagt, M. *Tetrahedron* **1999**, *55*, 14523.
32. Alcarazo, M.; Roseblade, S. J.; Allonso, E.; Fernandez, R.; Alvarez, E.; Lahoz, F. J.; Lassaletta, J. M. *J. Am. Chem. Soc* **2004**, *126*, 13242.
33. Öfele, K.; Kreiter, C. G. *Chem. Ber.* **1972**, *105*, 529.
34. Öfele, K.; Herberhold, M. *Z. Naturforsch.* **1973**, *28b*, 306.
35. Huang, I.; Schanz, H. -J.; Stevens, E. D.; Nolan, S. P. *Organometallics* **1999**, *18*, 2370.
36. Herrmann, W. A. *Angew. Chem. Int. Ed.* **2002**, *41*, 1290.

37. Herrmann, W. A.; Roesky, P. W.; Elison, M.; Artus, G. R. J.; Öfele, K. *Organometallics* **1995**, *14*, 1085.

38. Tafipolsky, M.; Scherer, W.; Artus, G. R. J.; Herrmann, W. A. *J. Am. Chem. Soc* **2002**, *124*, 3766.

39. Seiders, T. J.; Ward, D. W.; Grubbs, R. H. *Org. Lett.* **2001**, *3*, 3225.

40. Herrmann, W. A.; Köcher, C.; Artus, G. R. J. *Angew. Chem. Int. Ed. Engl.* **1996**, *108*, 2980.

41. Bonnet, L.G.; Douthwaite, R. E. *Organometallics* **2003**, *22*, 4187.

42. Douthwaite, R.E.; Hausinger, D.; Green, M. L. H.; Silock, P.J.; Gomes, P.T.; Martius, A. M.; Danopoulos, A. A. *Organometallics* **1999**, *18*, 4584.

43. Herrmann, W. A.; Köcher, C.; Elison, M.; Fischer, J. *Chem. Eur. J.* **1996**, *2*, 772.

44. Danopoulos, A. A.; Winston, S.; Motherwell, W. B. *Chem. Commun.* **2002**, 1376.

45. Dias, H. V. R.; Jin, W. *Tetrahedron Lett.* **1994**, *35*, 1365.

46. Schumann, H.; Glanz, M.; Dechert, S.; Demtschuk, J. *J.Organomet. Chem.* **2001**, *617-618*, 588.

47. Herrmann, W.A.; Reisemberg, C. -P.; Spiegler, M. *J. Organomet. Chem* **1998**, *557*,

48. Baker, V. M.; Skelton, W. B.; White, H. A.; Williams, C. V. *J. Chem. Soc. Dalton Trans.* **2001**, 111.

49. Arnold, P. L.; Cloke, F. G. N.; Geldbach, T.; Hitchcock, P. B. *Organometallics* **1999**, *18*, 3228.

50. Tulloch, A. A. D.; Danopoulos A. A.; Winston, S.; Kleimenz, S.; Eastham, G. J. *J. Chem. Soc., Dalton Trans.* **2000**, 4499.

51. Arnold, P. L.; Scaribrick, A. C.; Blake A. J.; Wilson, C. *Chem. Commun.* **2001**, 2340.

52. Danopoulos, A. A.; Tulloch, A. A. D.; Winston, S.; Eastham, G. J.; Hursthouse, M. B. *J. Chem. Soc., Dalton Trans.* **2003**, 1009.

53. Rieger, D.; Lotz, S. D.; Kernbach, U.; Fellhammer, W. P. *J. Organomet. Chem.* **1995**, *491*, 135.

54. Niehues, M.; Erker, G.; Kehr, G.; Schwab, P.; Roesky, P. W.; Berke, H. *Organometallics* **2002**, *21*, 2905.

55. Arnold, P. L.; Blake, A. J.; Wilson, C. *Angew. Chem. Int. Ed. Engl.* **2003**, *42*, 5981.

56. Wacker, A.; Yan, C. G.; Kaltenpoth, G.; Ginsberg, A.; Arif, A. M.; Ernst, R. D.; Pritzkow, H.; Siebert, W. *J. Organomet. Chem.* **2002**, *641*, 195.

57. Niehues, M.; Erker, G.; Kehr, G.; Wibbeling, B.; Blacque, O.; Berke, H. *J. Organomet. Chem.* **2002**, *663*, 192.

58. Shukla, P.; Johnson, J. A.; Vidovic, D.; Cowley, A. H.; Abernethy, C. D. *Chem. Commun.* **2004**, 360.

59. Abernethy, C. D.; Spicer, M. D.; Taylor, M. K. *J. Am. Chem. Soc.* **2003**, *125*, 1129.

60. Herrmann, W. A.; Lobawaier, G. M.; Elison, M. *J. Organomet. Chem.* **1996**, *520*, 231.

61. Danopoulos, A. A.; Hankin, D. M.; Wilkinson, G.; Cafferkey, S. M.; Sweet, T. K. N.; Hursthouse, M. B. *Polyhedron* **1997**, *16*, 3879.

62. Braband, H.; Zahn, T. I.; Abram, U. *Inorg. Chem.* **2003**, *42*, 6160.

63. Braband, H.; Abram, U.; *Organometallics* **2005**, *24*, 3362.

64. Chai, J.; Zhu, H.; Peng, Y.; Roesky, H. W.; Singh, S.; Schmidt, H. -G.; Noltemeyer, M. *Eur. J. Inorg. Chem.* **2004**, 2673.

65. Chai, J.; Zhu, H.; Kerstin, M.; Roesky, H. W.; Vidovic, D.; Schmidt, H. -G.; Noltemeyer, M. *Eur. J. Inorg. Chem.* **2003**, 4332.

66. Abernethy, C. D.; Cowley, A. H.; Jones, R. A.; Mcdonald, C. L. B.; Shukla, P.; Thomson, L. K. *Organometallics* **2001**, *20*, 3629.

67. Connon, S. J.; Blechert, S. *Angew. Chem. Int. Ed. Engl.* **2003**, *42*, 1900.

68. Kitamura, T.; Suzuki, Y.; Moti, M. *Chem. Commun.* **2001**, 1258.

69. Stragies, R.; Voigtmann, U.; Blechet, S. *Tetrahedron Lett.* **2000**, *41*, 5465.

70. Forman, G. S.; McConnel, A. E.; Hanton, M. J.; Slawin, A. M. Z.; Tooze, R. P.; Meyer, W. H.; Kirk, M. M.; Dwyer, C.; Serfontein, D.W. *Organometallics* **2004**, *23*, 4824.

71. Hamilton, G. J.; Kohl, F. J.; Weskamp, T.; Rooney, J. J.; Herrmann, W. A. *J. Organomet. Chem.* **2000**, *606*, 8.

72. Craig, S. W.; Manzer, J. A.; Couglin, E. B. *Macromolecules* **2001**, *34*, 7929.

73. Kücükbay, H.; Cetinkaya, B.; Guesmi, S.; Difneux, P. H. *Organometallics* **1996**, *15*, 2434.

74. Cetinkaya, B.; Özdemir, I.; Difneux, P. H. *J. Mol. Cat. A* **1997**, *118*, L1.

75. Danopoulos, A. A.; Tsoureas, N.; Wright, J. A.; Light, M. E. *Organometallics* **2004**, *23*, 166.

76. Louise, J.; Grubbs, R. H. *Chem. Commun.* **2000**, 1479.

77. Castarlenas, R.; Esteruelas, M. A.; Oñate, E. *Organometallics* Published on the web 29/07/2005.

78. Koscher, C.; Herrmann, W. A. *J. Organomet. Chem.* **1997**, *532*, 231.

79. Lee, H. M.; Stevens, E. D.; Nolan, S. P. *Organometallics* **2001**, *20*, 1255.

80. Hillier, A. C.; Lee, H. M.; Stevens, E. D.; Nolan, S. P. *Organometallics* **2001**, *20*, 4246.

81. Cetinkaya, B.; Özdemir, I.; Difneux, P. H. *J. Organomet. Chem.* **1997**, *534*, 153.

82. Suzanne, B.; Turner, P.; Hsiu, L.; Li, D.; Messerle, B. *Eur. J. Inorg. Chem.* **2003**, 3179.

83. Procop, J.; Merica, R.; Glatz, F.; Verpek, S.; Klingan, F.-R.; Herrmann, W. A. *J. Non-Cryst. Solids* **1996**, 2638.

84. Lappert, M. F. *J. Chem. Soc., Dalton Trans.* **1977**, 2172.

85. Macomber, D. W.; Rogers, R. D. *Organometallics* **1985**, *4*, 1485.

86. Foerstener, J.; Kakoschke, A.; Gobbard, R.; Rust, J. *J. Organomet. Chem.* **2001**, *617-618*, 412.

87. Kernbach, U.; Bakola-Christianopoulou, M.; Plaia, U.; Ponikwar, W.; Fehlhammer, W. P. *J. Organomet. Chem.* **2001**, *617-618*, 530.

88. Gibson, S. E.; Johnstone, G.; Loch, J. A.; Steed, J. W.; Stevenazzi, A. *Organometallics* **2003**, *22*, 5375.

89. Danopoulos, A. A.; Wright, J. A.; Motherwell, M. B.; Ellwood, S. *Organometallics* **2004**, *23*, 4807.

90. Gstottmayr, C. W. K.; Bohm, V. P. W.; Herdtweck, E.; Grosche, M.; Herrmann, W. A. *Angew. Chem. Int. Ed. Engl.* **2002**, *41*, 1363.

91. Viciu, M. S.; Stevens, E. D.; Nolan, S. P. *Org. Lett.* **2003**, *5*, 1479.

92. Grasa, G. A.; Viciu, M. S.; Huang, J.; Zhang, C.; Trudel, M. L.; Nolan, S. P. *Organometallics* **2002**, *21*, 2866.

93. McGuiness, D. S.; Cavell, K. J.; Skelton, B. W.; White, A. H. *Organometallics* **1999**, *18*, 1596.

94. Selvakumar, K.; Zapf, A.; Beller, M. *Org. Lett.* **2002**, *4*, 3031.

95. Herrmann, W.A.; Elison, M.; Fischer, J.; Köcher, C.; Artus, G. R. J. *Angew. Chem. Int. Ed. Engl.* **1995**, *34*, 2371.

96. Baker, M. V.; Skelton, B. W.; White, A. H.; Williams, C. C. *J. Chem. Soc., Dalton Trans.* **2001**, 111

97. Muhlhofer, M.; Strassner, T.; Herrmann, W. A. *Angew. Chem. Int. Ed. Engl.* **2002**, *114*, 2359.

98. Gardiner, M. G.; Herrmann, W. A.; Reisinger, C.-P.; Spiegler, M. *J. Organomet. Chem.* **1999**, *572*, 239.

99. Douthwaite, R. E.; Green, M. L. H.; Silcock, P. J.; Gomes, P. T. *Organometallics* **2001**, *20*, 2611.

100. Dible, B. R.; Sigman, M. S. *J. Am. Chem. Soc.* **2003**, *125*, 872.

101. Herrmann, W. A.; Gerstberger, G.; Spiegler, M. *Organometallics* **1997**, *16*, 2209.

102.McCuiness, D. S.; Cavell, K. J.; Skelton, B. W.; White, A. H. *Organometallics* **1999**, *18*, 1596

103. Duin, M. A.; Clement, N. D.; Cavell, K. J.; Elsevier, C. J. *Chem. Commun.* **2003**, 400.

104. Stauffer, S. R.; Lee, S.; Stambuli, J. P.; Hauck, S. I.; Hartwig, J. F. *Org. Lett.* **2000**, *2*, 1423.

105. Lee, S.; Hartwig, J. F. *J. Org. Chem.* **2001**, *66*, 3402.

106. Zhang, C.; Huang, J.; Trudell, M. L.; Nolan, S. P. *J. Org. Chem.* **1999**, *64*, 3804.

107.Cetinkaya, E.; Hitchcock, P. B.; Kücükbay, H.; Lappert, M. F.; Al-Juaid, S. *J. Organomet. Chem.* **1994**, *481*, 89.

108. Sprengers, J. W.; Mars, M. J.; Duin, M. A.; Cavell, K. J.; Elsevier C. J. *J. Organomet. Chem.* **2003**, *679*, 149.

109. Yang, C.; Lee, H. M.; Nolan, S. P. *Org. Lett.* **2001**, *3*, 1511.

110. Bohm, V. P. W.; Weskamp, T.; Herrmann, W. A. *Angew. Chem. Int. Ed. Engl.* **2000**, *39*, 1602.

111. Huang, J.; Nolan, S. P. *J. Am. Chem. Soc.* **1999**, *121*, 9889.

112. Yang, C.; Nolan, S. P. *Synlett.* **2002**, *9*, 187.

113. Grasa, G. A.; Nolan, S. P. *Org. Lett.* **2000**, *3*, 119.

114. Oldham, W. J.; Oldham, S. M.; Scott, B. L.; Abney, K. D.; Smith, W. H.; Costa, D. A. *Chem. Commun.* **2001**, 1348.

115.Liddle, S. T.; Arnold, P. L. *Organometallics* **2005**, *24*, 2597.

Chapter 2: Synthesis of pyridine-and phosphine-functionalised NHC imidazolium salts

2.1 Introduction:

The use of functionalised nucleophilic heterocyclic cabenes ligands is a recent development in successful ligand designs incorporating NHCs.[1] Their synthesis allows us to tailor the metal coordination sphere by combining a strongly bound, robust functional group (NHC) with a "classical" donor able to further facilitate electronic and steric tuning. In addition to the manipulation of the steric and electronic environment around a metal centre, these hybrid ligand architectures can impose chirality and electronic differentiation of the *trans* coordination sites to the chelating ligand (Figure 2.1).
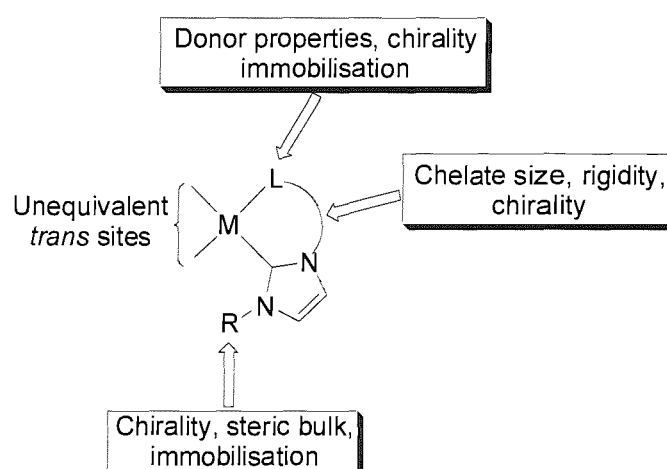
Figure 2.1: Features of mixed donor NHC ligands.

The integration of phosphine and pyridine functionalities into ligand architectures similar to the one shown in Figure 2.1, could prove advantageous for the following reasons: (i) the coordination chemistry of the donors is well documented allowing the easier manipulation of the steric and electronic environment of the centre; (ii) the adjustment of chelate size and rigidity is possible (*i.e.* by using variable length linkers), (iii) donor properties and steric bulk could lead to hemilability[2] with possible implications on the catalytic activity (Figure 2.2). The appropriate hemilabile L donor could trigger the formation of coordinatively unsaturated species, thus initiating a catalytic cycle.
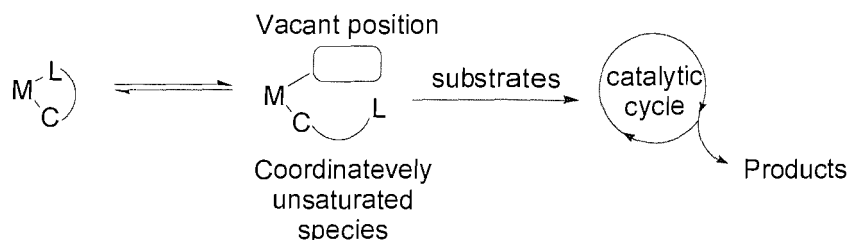
Figure 2.2: Hemilability initiating a catalytic cycle.

The use of pyridine functionalities in such ligand architectures has already been investigated and catalytic studies of systems involving those ligands are very encouraging.[3] On the other hand very few examples of phosphine functionalised NHC complexes are known[4] and theoretical studies suggest that such integration would give rise to a new class of efficient ligands for catalytic transformations such as C-C coupling reactions.[5] To further our insight into the reactivity and catalytic activity of systems incorporating these ligand architectures, we have decided to synthesise NHCs incorporating pyridine (A) and phosphine (B) functionalities (Figure 2.3).
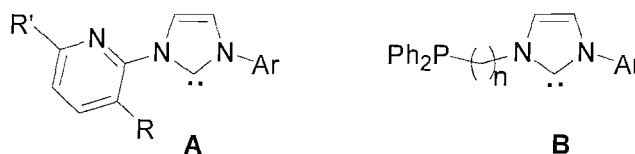
Figure 2.3: Pyridine (R = H, Me then R' = H; R' = SiMe$_3$ then R = H; Ar = bulky aryl) and phosphine functionalised NHCs target compounds.

The synthesis and crystal structures of phosphine (n = 2, Ar = 2,6-(^{i}Pr)$_2$-C$_6$H$_3$) and pyridine (R' = SiMe$_3$, Ar = 2,6-(^{i}Pr)$_2$-C$_6$H$_3$) functionalised NHCs has already been published by Danopoulos and co-workers.[6] Ligands such as (A) and (B) can adopt a monodentate, bridging or chelating mode (Figure 2.4).

Monodentate   Bridging   Chelating
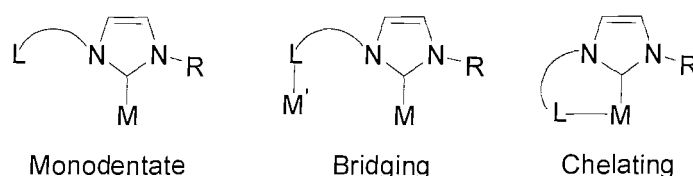
Figure 2.4: Binding modes of hybrid ligands.

34

The choice of donors can of course include chiral ligands, allowing the control of the stereochemistry of the product molecule. Chirality can also be introduced at the linker joining the NHC with the L donor ligand. Some examples of chiral functionalised imidazolium salt NHC precursors are illustrated in Figure 2.5.
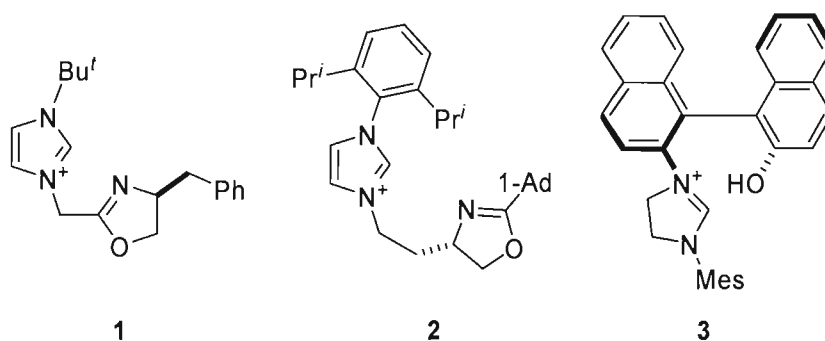
Figure 2.5: Chiral imidazolium salt NHC precursors [7, 8, 11].

The oxazoline functionalised NHC precursors 1 and 2 represent two examples of chiral imidazolium salts where the chirality can be introduced either on the donor ligand or the space linker.[7, 8] A cationic Ir(I) NHC complex derived from 2 has given > 90% enantiomeric excess in the hydrogenation of unfunctionalised alkenes.[7] High enantioselectivity can be obtained for several substrates under low H_2 pressures (up to 5 bar). The results obtained are comparable to the best phosphine or phosphite-oxazoline systems that require pressures of 50 bar H_2.[9, 10] Imidazolinium 3 introduces chirality due to axial chirality. When the carbene and the phenolic oxygen coordinate to the metal centre, the aromatic group is locked into a twisted, chiral conformation.[11]

The appropriate choice of functionality can also allow the immobilisation on polymer supports of imidazolium salt NHC precursors or their NHC metal complexes. For instance the functionalised alcohol NHC rhodium complex 4 was immobilised on a polymer support after its formation (Scheme 2.1).[12]
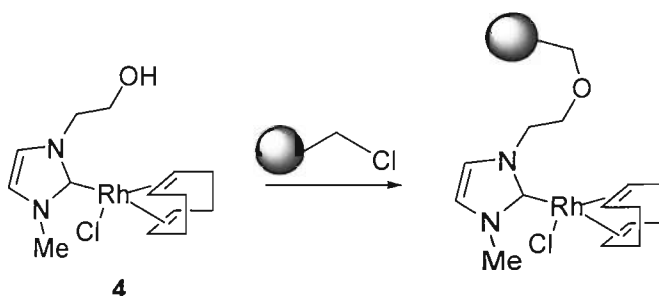
Scheme 2.1: Immobilisation of a functionalised NHC Rh complex.

The integration of NHCs with other donor ligands can give rise to a wide range of other ligand designs like pincer and tripodal architectures (Figure 2.6).

Ia, Ib

a: L = 'L, b: L ≠ 'L

II

III

Pincer

IV
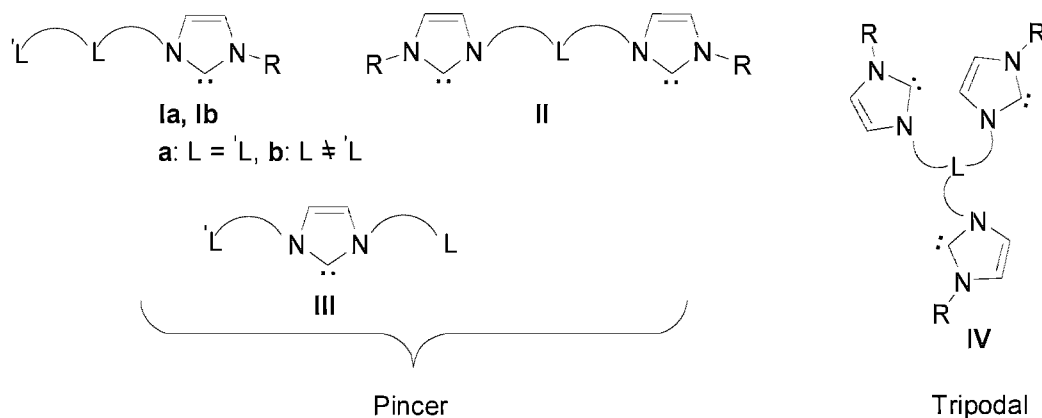
Tripodal

Figure 2.6: Pincer and tripodal architectures integrating NHCs with other donor ligands.

Some examples of each type of ligand are given in Figure 2.7. Danopoulos *et al.* have made pioneering steps towards the synthesis and coordination chemistry of carbenes of type **Ia-b** and **II**.[13, 14, 15] Recently pincer carbenes of type **III** have been prepared where the NHC is flanked by two phosphines.[4]
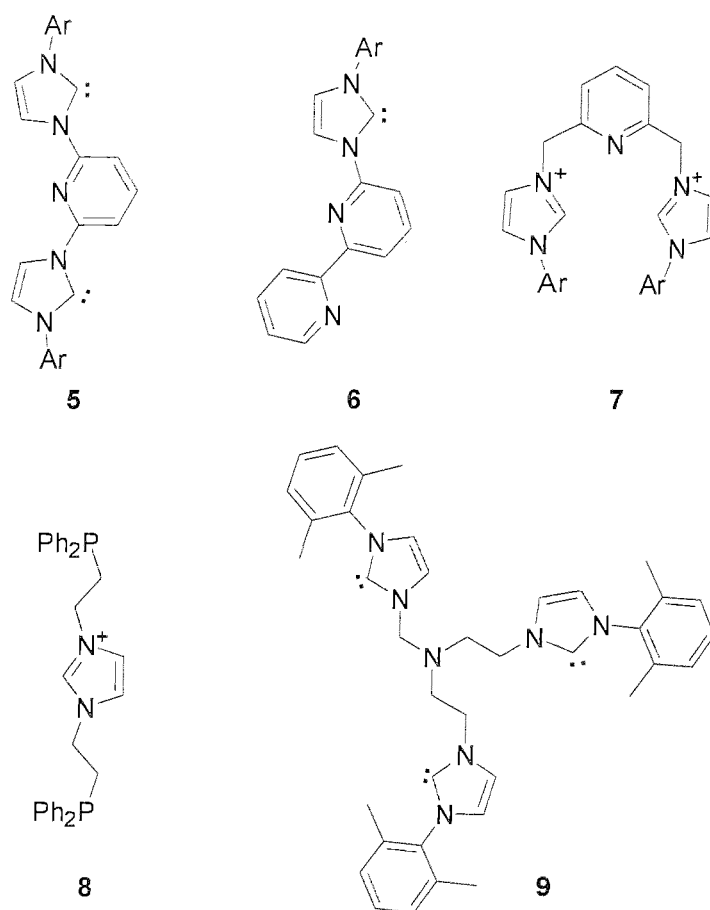
Figure 2.7: Examples of different functionalised NHC architectures (**5**, **6** and **9**) or functionalised NHC precursors (**7** and **8**). NHCs **5** and **6** as well those deriving from imidazolium salts **7** and **8** belong to the pincer type ligand family, while **9**[16] to the tripodal ligand families (Ar = 2,6-(^{i}Pr)$_2$ –C$_6$H$_3$)).

Interestingly, when **7** is used as a NHC precursor chirality is induced without any chiral information originating from asymmetric centres in the ligand architecture or from steric constrictions in the ligand design. Scheme 2.2 illustrates the situation. Complex **10** contains a C_2 stereogenic axis, giving rise to atropisomeric chirality without any backbone chirality. The two enantiomers were differentiated using a chiral shift reagent in a NMR experiment, but were otherwise unresolved.[17]
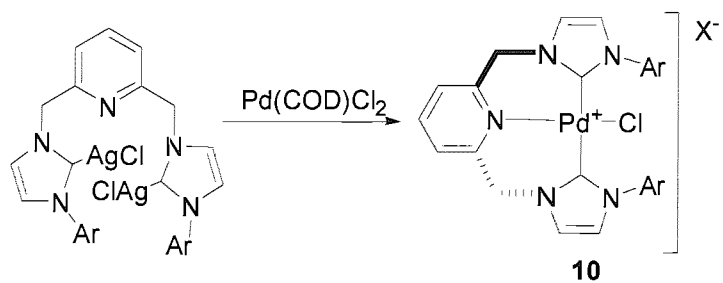
Scheme 2.2: Atropisomeric chirality induced by a non chiral functionalised NHC precursor (Ar = 2,4,6-Me$_3$C$_6$H$_2$, 2,6-Pr^i-C$_6$H$_3$; X$^-$ = Cl$^-$, AgCl$_2^-$).

Other functionalities that could be introduced include nitriles,[18] amines,[19] imines,[20] ethers,[21] thioethers, [22]carboxylates[21, 23] and alkenes.[24]

2.2 Results and discussion:

2.2.1 Synthesis of ligands and ligand precursors

The novel phosphine, phosphine oxide and pyridine functionalised imidazolium salt NHC precursors, as well the pyridine functionalised NHCs, that have been synthesized are illustrated in Figure 2.7.

2.1a, 2.1b **2.2a, 2.2b** **2.3a, 2.3b** **2.4a, 2.4b**

2.5 **2.6**

2.7 **2.8c, 2.8d** **2.9c, 2.9d**
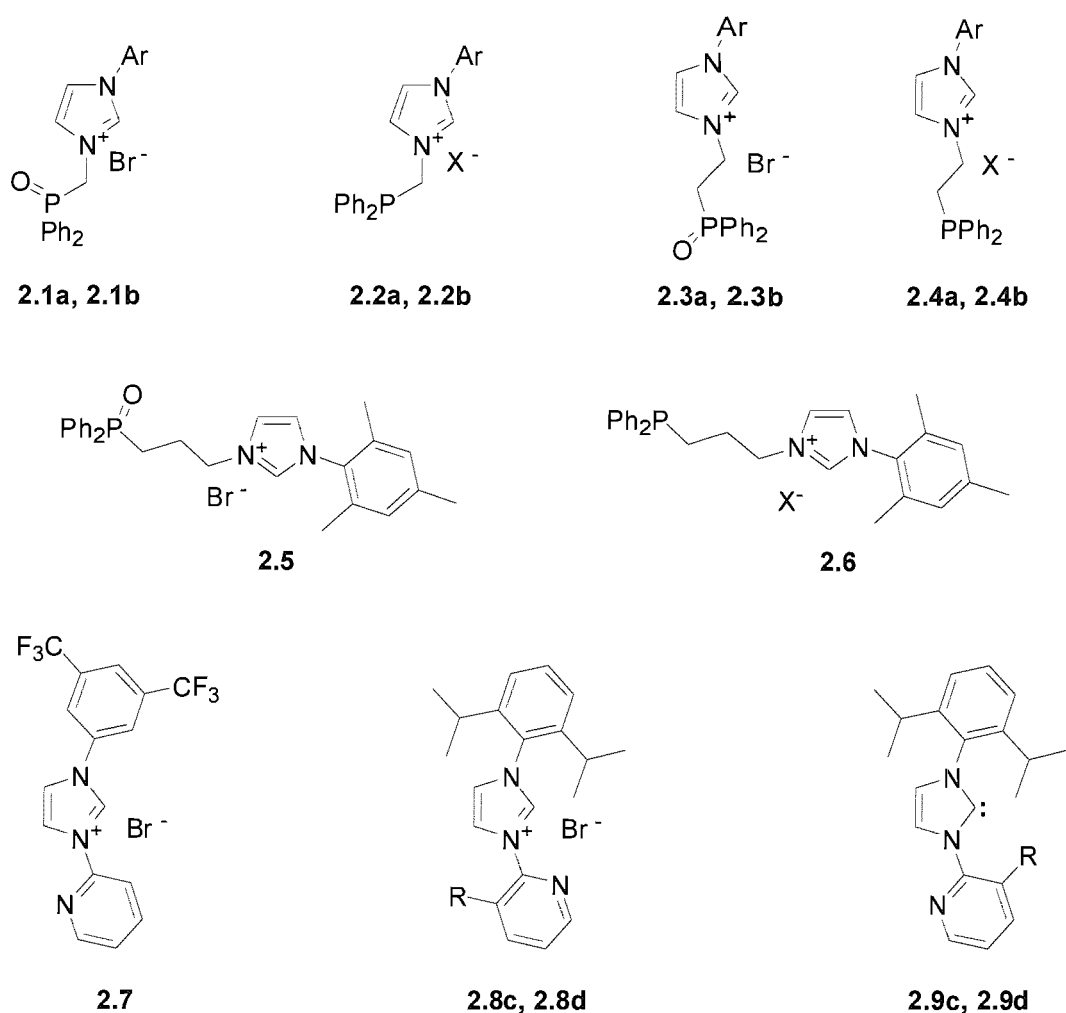
Figure 2.8: Functionalised imidazolium salts and NHCs that have been synthesised (Ar = 2,6-Pr^i-C$_6$H$_3$: **a**; Ar = 2,4,6-Me$_3$-C$_6$H$_3$: **b**; R = H: **c**; R = Me: **d**. X⁻ = Cl⁻, Br⁻).

In the case of the phosphine functionalized imidazolium salts the synthetic strategy is outlined in Scheme 2.3. It is based in the quaternization of 3-arylimidazoles with (ω-bromoalkyl)diphenylphosphinoxide followed by reduction with SiHCl$_3$. A similar

procedure was used for the synthesis of 1-(β-(diphenylphosphino)ethyl)-3-methyl imidazolium salt.[25] However, under the previously reported conditions, both reaction steps failed with the bulky, less nucleophilic 3-arylimidazoles. When the quaternization reactions were carried out at 150-160 °C (most conveniently in the melt, in the absence of solvent), they gave good yields. Furthermore, the yield of the subsequent reduction was also dramatically improved when using SiHCl$_3$ in refluxing chlorobenzene as a reducing agent. All imidazolium phosphine salts were isolated as white, air-sensitive powders and were characterised by spectroscopic and analytical methods. The microanalysis data support the presence of mixed chloride/bromide salts. The chloride anion originates from the hydrolytic workup of the excess SiHCl$_3$ during the reduction step. Mixed halide imidazolium salts and palladium NHC complexes have been observed before.[21]
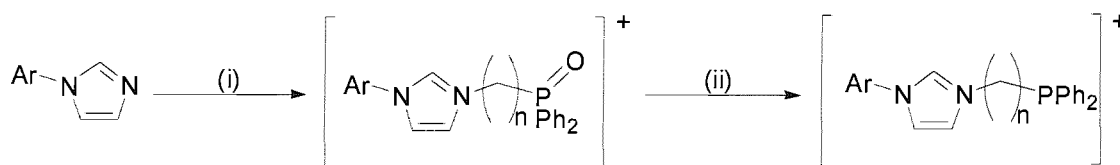
Scheme 2.3: Synthesis of phosphine functionalized imidazolium salts. Reagents and conditions: (i) Ph$_2$P(O)(CH$_2$)$_n$Br, 150-160 °C, 7 days. (ii) SiHCl$_3$ in chlorobenzene 120 °C (n = 1, 2, 3).

Nolan *et al.* have described the synthesis of 1-(β-(diphenylphosphino)ethyl)-3-mesitylimidazolium bromide (**2.4b**) from 1-(β-bromoethyl)-3-mesitylimidazolium and Ph$_2$PH in DMSO in the presence of KOBu^t,[26] but the reported overall yield was very poor. The synthetic protocol shown in Scheme 2.3 allows the access of a range of ligand architectures, enabling the manipulation of parameters, *e.g.* the bite angle or the electronic and steric environment around a metal centre once the NHC ligand has coordinated. Moreover the imidazolium salt NHC precursors can be prepared in large scale, pure and in good overall yields.

When n = 2 or 3 the (ω-bromoalkyl)phosphine oxides were prepared by a simple Arbusov reaction between Ph$_2$POEt and an excess of 1,2-dibromoethane (n = 2) or 1,3-dibromopropane (n = 3). The reaction takes place in refluxing α,ω-dibromide. This is illustrated in Scheme 2.4 along with the mechanism of the Arbusov reaction.[27]

Ph$_2$P–OEt + Br$\frown$Br$_m$ $\longrightarrow$ Ph–P$^+$(Et, O:)–Br$_m$ Br$^-$ $\longleftrightarrow$ Ph–P(=O, Et O$^+$)–Br$_m$ Br$^-$ $\longrightarrow$ Ph$_2$P(=O)–Br$_m$ + EtBr
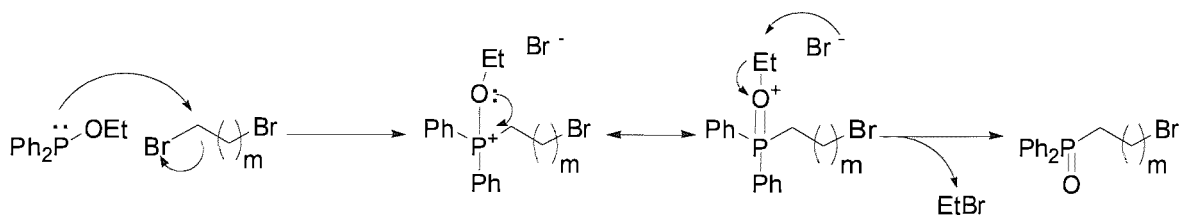
Scheme 2.4: Synthesis of (ω-bromoalkyl)-phosphine oxides (m = n-1) and mechanism of Arbusov reaction.

The use of an excess of the α,ω-dibromide, inhibits the formation of α,ω-bis-(diphenylphosphine oxide)-alkyls. It is also very important to remove the EtBr that is produced, firstly because it can undergo an Arbusov reaction and secondly in order to drive the reaction to completion. This is achieved by equipping the reaction apparatus with a Dean-Stark trap to distil the low-boiling EtBr out of the reaction mixture.

Ph$_2$PCl $\xrightarrow[\text{80-90 °C, air}]{\text{HCHO, HCl}}$ Ph$_2$P(O)CH$_2$OH $\xrightarrow[\text{THF, RT}]{\text{TsCl}}$ Ph$_2$P(O)CH$_2$OTs $\xrightarrow[\text{reflux. DMF}]{\text{KBr}}$ Ph$_2$P(O)CH$_2$Br

Scheme 2.5: Preparation of (diphenylphosphine-oxide)bromomethane.

In the case of n =1, the synthesis of the phosphine oxide is achieved *via* the different route illustrated at Scheme 2.5. The rational behind using (ω-bromoalkyl)phoshine oxides instead of (ω-bromoalkyl)phoshines in the quaternization with arylimidazoles is to avoid any side reactions. Under the forcing conditions the quaternization takes place, two competing reactions could occur if phosphines were used: nucleophilic attack of the arylimidazole to the (ω-bromoalkyl)phosphine to yield the desired product, and intermolecular quaternization between two (or more) phosphine molecules to give phosphonium salts (Scheme 2.6). In the case of the phosphine oxides the lone electron pair of the phosphorus atom is unavailable, and the side reaction described above cannot take place. Furthermore the ease of preparation and handling of the phosphine oxides makes this synthetic route very attractive.
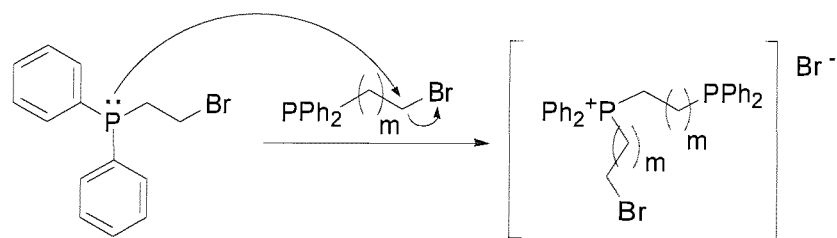
Scheme 2.6: Formation of phosphonium salts (m = n-1).

The use of microwave irradiation, to reduce the above quaternization reaction times, was also considered. Unfortunately they did not proceed to completion, neither when using a solvent or by heating the two reactants neat. ^{1}H-NMR spectroscopy revealed in all cases the presence of unreacted phosphine oxide, even when longer reaction times (*i.e.* overnight), or elevated temperatures were employed.

The pyridine functionalised imidazolium salts **2.7**, **2.8c-d**, were prepared by employing the quaternization strategy between the appropriate 3-arylimidazole and 2-bromopyridine (**2.7**, **2.8c**) or 3-methyl-2-bromopyridine (**2.8d**). The reaction was carried out in the melt in the absence of solvent. In the case of **2.7** the reaction took place under more forcing conditions, by heating at 160 °C, due to the reduced nucleophilicity of 3-[3,5-bis(trifluoromethyl)phenyl]imidazole. In most cases the reaction proceeded cleanly, producing the imidazolium salts in very good yields.

The imidazolium salts discussed so far, except **2.7**, are readily soluble in dichloromethane chloroform and water, while the phosphine and phosphine oxide functionalised imidazolium salts exhibit some solubility in THF as well. Imidazolium salt **2.7** is soluble only in acetonitrile and dimethylsulfoxide and unlike the pyridine functionalised imidazolium salts **2.8c-d**, is insoluble in acetone. The lipophilic nature of the trifluoromethyl groups explains the insolubility of **2.7** in water, but does not account for its insolubility in the polar organic solvents described above.

Danopoulos *et al.* have described the preparation of phosphine and pyridine functionalised NHCs.[5] Following the method described in the literature the pure NHCs **2.9c-d** were isolated. The deprotonation occurs smoothly, even at -78 °C and is completed at -30 °C overnight, when K[N(SiMe$_3$)$_2$] is used as a base.

2.2.2 NMR spectroscopy

The formation of the imidazolium salt ligand precursors was evidenced by the existence in the ^{1}H-NMR spectrum of the acidic imidazolium proton. This characteristic peak appears in the region between 10-11 ppm. The ^{13}C$\{^1$H$\}$-NMR spectra of the compounds also back up the formation of the imidazolium salts, from the existence of the imidazolium carbon in the region of 140 ppm. Table 2.1 summarises the ^{1}H-NMR and ^{13}C$\{^1$H$\}$-NMR shifts of the imidazolium protons and carbons respectively of the ligand precursors that were synthesised. This is in agreement with reported values for other functionalised imidazolium salts.[28] In all cases the spectra were recorded in CDCl$_3$, except **2.7** which was recorded in (CD$_3$)$_2$SO.

Imidazolium salt	^{1}H-NMR shift (ppm), [multiplicity, J (Hz)]	^{13}C$\{^1$H$\}$-NMR shift (ppm)
2.1a	10.2 [broad doublet, 1.1]	145.5
2.1b	9.95 [broad singlet]	142.1
2.2a	10.5 [triplet, 1.5]	144.3
2.2b	10.4 [singlet]	139.5
2.3a	10.3 [singlet]	145.4
2.3b	10.1 [singlet]	141.3
2.4a	10.4 [broad singlet]	145.5
2.4b	10.6 [broad singlet]	141.3
2.5	10.4 [singlet]	142.3
2.6	10.9 [singlet]	141.5
2.7	10.9 [triplet, 1.5]	136.1
2.8c	11.0 [singlet]	148.7
2.8d	11.0 [singlet]	148.8

Table 2.1: ^{1}H-NMR and ^{13}C$\{^1$H$\}$-NMR chemical shifts of imidazolium protons and carbons.

As seen in the above table, in most cases the imidazolium proton appears as a singlet. Compounds **2.1a**, **2.2a** and **2.7** are the exception. The H-H correlation experiment

for compound **2.7**, revealed coupling between the acidic imidazolium proton and a broad doublet integrating for two protons, centred at 8.8 ppm. This doublet was assigned to the imidazolium backbone protons, based on the C-H correlation. In the case of imidazolium salts **2.1a**, **2.2a**, the observed splitting is not fully understood.

The imidazolium carbon appears in most cases between 140 and 150 ppm. This trend is not observed in the case of **2.7**. Although in the $^{13}C\{^1H\}$-NMR spectrum a peak at 149.4 ppm does exist, this cannot be assigned to the imidazolium carbon. The DEPT-135 proves that it is not quaternary, but it does not correlate with the imidazolium proton as proved from the C-H correlation. The peak that does show correlation with the imidazolium proton is the one at 136.1 ppm. The nature of this upfield shift is not understood.

The ^1H-NMR and $^{13}C\{^1H\}$-NMR spectra of the phosphine functionalised imidazolium salts, as well as their phosphine oxide precursors, exhibit some other characteristic peaks. These are assigned to the protons and the carbons of the different methylenic space linkers. In the ^1H-NMR spectra of the two and three carbon bridged imidazolium salts, these appear as multiplets due to P-H and H-H coupling. In the case of compounds **2.1a,b** and **2.2a,b** these appear as doublets. A summary of these shifts, multiplicities and coupling constants is given in table 2.2.

Imidazolium salt	^{1}H-NMR shift (ppm), [multiplicity, J_{PH} (Hz)]	^{13}C-$\{^1$H$\}$-NMR shift (ppm), [multiplicity, $^nJ_{PC}$ (Hz)]
2.1a	6.25 [doublet, 6.5]	49.5 [doublet, 24.5]
2.1b	6.11 [doublet, 6.6]	49.6 [doublet, 25.3]
2.2a	5.77 [doublet, 6.4]	47.7 [doublet, 19.5]
2.2b	5.71 [doublet, 6.4]	49.4 [doublet, 19.4]
2.3a	3.42, 5.14 [multiplets]	28.7, 44.6 [singlets]
2.3b	3.38, 4.82 [multiplets]	49.5 [singlet]
2.4a	2.87, 4.87 [multiplets]	30.0 [doublet, 13.0], 48.2 [doublet, 18.1]
2.4b	2.88, 4.91 [multiplets]	29.8 [doublet, 16.0], 48.9 [doublet, 21.9]
2.5	2.41, 2.72, 5.00 [multiplets]	24.6 [doublet, 11.6], 27 [singlet], 50.8 [singlet]
2.6	2.23 [multiplet], 5 [broad triplet]	24.4 [doublet, 10.6], 27.1 [doublet, 18.1], 50.6 [doublet, 19.1]

Table 2.2: ^{1}H-NMR and ^{13}C$\{^1$H$\}$-NMR shifts and multiplicities of methylenic bridges (n = 1-3; for **2.5** each multiplet integrates for 2H; for **2.6** the upfield multiplet integrates for 4H).

It is worth noticing that in the case of the phosphine oxides **2.3a,b** no splitting of the methylenic bridges due to P-C coupling is observed in their ^{13}C-$\{^1$H$\}$-NMR spectra. Moreover in the case of **2.3b** the methylene carbon in the α position to the phosphorus does not appear in the spectrum. This trend is also present in the case of the imidazolium salt **2.5**, where only one methylene carbon appears as a doublet. On the other hand, the methylene carbon in phosphine oxides **2.1a,b** appears as a doublet. The assignment of these methylenic bridges is based on the grounds of their chemical shifts. The carbon shifted more downfield is assigned to the one attached to the quaternary imidazolium nitrogen. The assignment of the methylenic protons is also based on the same principle.

On the other hand, the expected splitting of the methylenic carbons, is indeed observed in the case of the phosphine-imidazolium salts. Two additional interesting

observations can also be made. Firstly, the J_{PC} coupling constant increases in the order $^3J_{PC} > {}^2J_{PC} > {}^1J_{PC}$. Secondly, upon reduction of the phosphine oxide functionalised imidazolium salts (**2.1a-b**, **2.3a-b** and **2.5**) to the corresponding phosphines (**2.2a-b**, **2.4a-b** and **2.6**), a decrease in the J_{PC} coupling constants for these methylenic space linkers, is observed.

The protons of the methylenic bridges in compounds **2.3a-b**, **2.4a-b**, **2.5** and **2.6** appear as multiplets in the ^{1}H-NMR spectra. The peaks assigned to the protons of the methylenic bridges α and β to the phosphorus in compound **2.6**, coincide giving rise to a multiplet integrating for 4 protons. In compounds **2.1a-b**, **2.2a-b**, these protons are split into doublets due to phosphorus coupling. It is worth noticing that after the reduction of **2.1a-b** to the corresponding phosphines **2.2a-b**, these doublets are shifted upfield. This is because of the removal of the electronegative oxygen atom.

When the aryl is 2,6-diisopropylphenyl, the ^{1}H-NMR spectrum has two doublets centred in the region between 1.0 and 1.3 ppm and a septet centred at 2.4 ppm. These are assigned to the methyl and methine protons of the isopropyl groups, respectively. The appearance of the methyl protons as two doublets means that they are diastereotopic.

The characterisation of NHCs **2.9c-d**, was achieved by spectroscopic methods. The absence of the imidazolium protons in their ^{1}H-NMR spectra, as well as the appearance of the electron deficient carbene carbon in their ^{13}C-$\{^1$H$\}$-NMR spectra, at 214.5 for **2.9c** and 215 for **2.9d**, was of important diagnostic value.

2.2.3 X-ray Crystallography

2.2.3.1 X-ray Crystallographic study of 2.7

Although compound **2.7** was characterised by NMR spectroscopy and mass spectrometry, its unusual spectral characteristics led us to use X-ray single crystal diffraction as another characterisation method. Crystals of imidazolium salt **2.7** were grown by slow evaporation of an acetonitrile solution in air. An ORTEP diagram of **2.7** is shown in Figure 2.9.
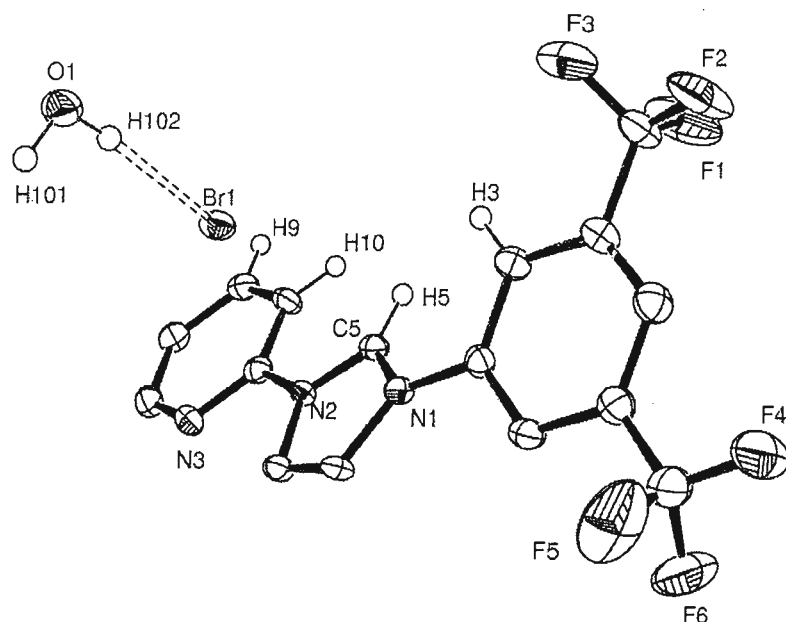
Figure 2.9: ORTEP representation of the crystal structure of **2.7** showing 50% probability ellipsoids. Bond lengths and angles are in agreement with previous reported structures of pyridine functionalised imidazolium salts.[29]

The water molecule originates from the solvents used and the crystallisation procedure. This water molecule interacts with a pair of symmetry equivalent bromide anions *via* hydrogen bonding. The hydrogen bond distance [d(H102...Br)] is 2.48(7) Å. The crystal structure of a similar imidazolium salt, synthesised by quaternization of 3-*tert*-butyl-imidazole and picolyl bromide, shows such an interaction.[29] The d(H102...Br) bond distance, in this occasion is slightly shorter. It is also interesting that the pyridine nitrogen atom is oriented towards the opposite direction of the imidazolium proton. The packing in the lattice also shows some other intermolecular interactions. Firstly, there is an interaction between the fluorines of the CF_3 groups belonging to different molecules. Secondly, a bromide counter anion interacts with the imidazolium proton (H5), and protons H10, H3. Finally, the nitrogen atom of the pyridine interacts intermoleculary with the H9 hydrogen of another pyridine molecule. The last two interactions could be the reason why the nitrogen atom of the pyridine is directed away from the imidazolium proton. These two interactions are illustrated in Figure 2.10.
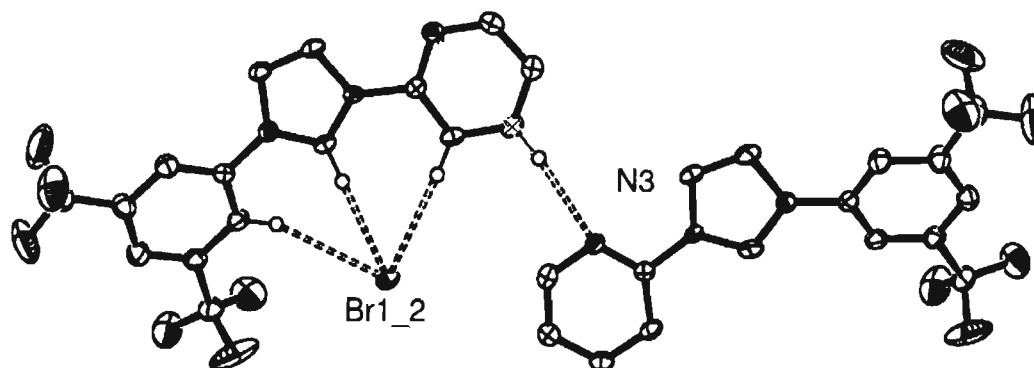
Figure 2.10: ORTEP diagram showing 50% probability ellipsoids, of the intermolecular interactions observed in the crystal lattice of **2.7**. Bond distances: d(H3...Br1_2) 2.92(2) Å, d(H5...Br1_2) 2.64(5) Å, d(H10...Br1_2) 2.91(1) Å, d(H9...N3) 2.54(3) Å.

2.2.3.2 X-ray Crystallographic study on free carbene 2.9c

The isolation of crystalline pyridine functionalised NHCs as bottle-able reagents stable at room temperature[6] has been a major contribution to the study of the transition metal chemistry of these asymmetric ligands.[30, 37] Their existence has been verified by spectroscopic methods, but few examples of crystallographically characterised NHCs of this type are known.[6, 37]

The isolation of NHC **2.9c** was confirmed by NMR spectroscopy as mentioned above. Its identity was further verified by a single crystal X-ray diffraction study. An ORTEP diagram of the crystal structure of **2.9c** is given in Figure 2.11.
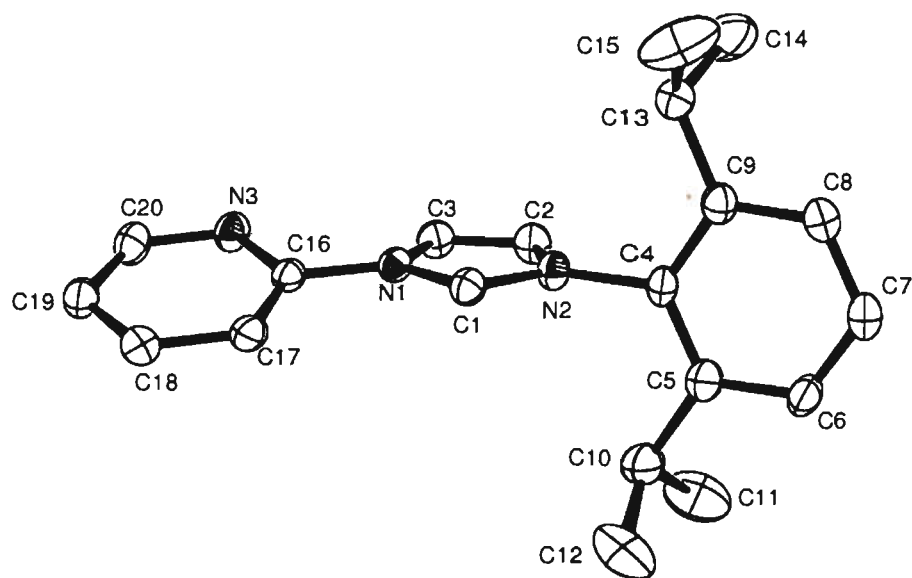
Figure 2.11: ORTEP representation of the crystal structure of **2.9c** showing 50% probability ellipsoids. Hydrogens have been omitted for clarity. Selected bond lengths (Å) and angles (°): C(1)-N(2) 1.357(2), C(1)-N(1) 1.371(2), N(2)-C(1)-N(1) 101.32(15).

The pyridine nitrogen is again pointing to the opposite direction of the carbene carbon. This characteristic has been observed in other functionalized NHCs.[6] The rational behind this trend is to minimize the repulsion of the two lone electron pairs the in molecule. Finally, bond lengths and angles are in agreement with previously reported pyridine functionalized NHCs.[37]

2.3 Conclusions

The synthesis of novel pyridine and phosphine functionalized imidazolium salt precursors has been achieved. The synthetic methodology utilized in the case of phosphine functionalized imidazolium salts, allows the access to a wide range of ligand architectures. This new family of ligands, upon coordination, could provide us with the opportunity to manipulate the metal coordination sphere. Steric and electronic control of the metal environment could also be imposed. By varying the size of the chelate, hemilability issues could also be addressed. Differences in reactivities could also been explained based on the differences of the ligands characteristics.

Pyridine functionalized imidazolium salts and the corresponding free NHCs have also been isolated. Compound **2.7** exhibits some interesting features in its NMR spectra, while a single crystal X-ray analysis of it showed the existence of some unusual interaction within its lattice.

Finally free functionalized NHCs were prepared following well-established procedures. They were isolated as pure crystalline materials in reasonably good yields and were characterised by spectroscopic methods including X-ray single crystal diffraction (for **2.9c**).

The coordination chemistry of these new ligands will be the subject of the following chapters. Aspects of the reactivity of their complexes will also be addressed.

2.4 Experimental

General materials: Ph_2POEt,[31] $Ph_2P(O)(CH_2)_2Br$,[31] $Ph_2P(O)CH_2X$ (X = OH,[32] OTs,[33] Br[34]), 1-(2,4,6-trimethyl-phenyl)-imidazole[35] and 1-(2,6-diisopropyl-phenyl)-imidazole[36] were prepared according to literature procedures. 1-(3,5-bis(trifluoromethyl)-phenyl)-imidazole was prepared in a way analogous to 1-(2,6-diisopropyl-phenyl)-imidazole and was isolated pure *via* recrystallisation from light petroleum ether. $Ph_2P(O)(CH_2)_3Br$ was prepared by a method analogous to $Ph_2P(O)(CH_2)_2Br$ from Ph_2POEt and 1,3-dibromopropane. 1,2-Dibromoethane, 1,3-dibromo-propane, TsCl, 2-bromopyridine 2-bromo-3-methylpyridine, thiophosgene and 3,5-bis(trifluoromethyl)aniline were purchased from Aldrich and were used with no further purification. Ph_2PCl and 2,3-diethoxy-propylamine were purchased from Lancaster and were used as received.

2.1a: 3.0 g (10 mmol) of $Ph_2P(O)CH_2Br$ and 3.5 g (15 mmol) of 1-(2,6-diisopropyl-phenyl)-imidazole were charged in an ampoule which was sealed under vacuum. The ampoule and its contents were heated at 140 °C for a week in a thermostated oil bath. After the completion of the reaction, the contents of the ampoule were dissolved in dichloromethane. Removal of volatiles produced a brown sticky solid. This was re-dissolved in the minimum amount of dichloromethane and was precipitated by addition of a 4:1 (v/v) mixture of Et_2O/PE. The solid was immediately filtered and washed with diethylether (3 × 60 mL). Due to its hydroscopic nature, the compound adopted a glue-like form during the filtration. It was therefore dissolved in the minimum amount of THF and was precipitated with Et_2O. The white solid thus isolated was used without further purification in the next step. Analytically pure compound was isolated by cooling the filtrate of the last precipitation at 5 °C. ^{1}H-NMR $\delta(CDCl_3)$: 1.01 (6H, d, $^3J_{HH}$ = 6.8 Hz, CH(CH_3)$_2$), 1.12 (6H, d, $^3J_{HH}$ = 6.8 Hz, CH(CH_3)$_2$), 1.94 (2H, sept., $^3J_{HH}$ = 6.8 Hz, CH(CH$_3$)$_2$), 6.25 (2H, d, $^2J_{PH}$ = 6.6 Hz, $Ph_2P(O)CH_2$- imidazolium), 6.99 (1H, dd, J_{HH} = 1.7 Hz, J_{HH} = 1.9 Hz, imidazole backbone), 7.21 (2H, d, $^3J_{HH}$ = 7.7 Hz, aromatic), 7.32 (1H, broad s., imidazole backbone), 7.50 (1H, t, $^3J_{HH}$ = 7.7 Hz, aromatic), 7.55-7.63 (6H, m, aromatic), 8.22-8.31 (5H, m, aromatic), 10.19 (1H, broad d, J_{HH} = 1.13 Hz, NCHN); ^{13}C{^{1}H}-NMR $\delta(CDCl_3)$: 24.5 (s, CH(CH$_3$)$_2$), 24.6 (s, CH(CH$_3$)$_2$), 28.9 (s, CH(CH$_3$)$_2$), 49.5 (d, $^1J_{PC}$ = 64.5 Hz), 124.0 (s, imidazolium backbone), 124.6 (s, imidazolium backbone), 125.1 (s, aromatic), 128.3 (d, $^1J_{PC}$ = 19.0 Hz, aromatic), 129.6 (d, J_{PC} = 12.6 Hz, aromatic), 130.1 (s, aromatic), 131.9 (d, J_{PC} = 10.3 Hz, aromatic), 132.4 (s, aromatic), 133.5 (d, J_{PC} = 2.3 Hz, aromatic), 138.3 (s, *ipso* to the imidazole moiety), 145.5 (s, (s,

NC(H)N); ^{31}P$\{^1$H$\}$-NMR δ(CDCl$_3$): 36.6 (s, Ph$_2$$P$(O)CH$_2$-imidazolium) HRES$^+$: Found: 443.2242. Calcd for [C$_{28}$H$_{32}$N$_2$PO]$^+$: 443.2247.

2.1b: 2.0 g (5 mmol) Ph$_2$P(O)CH$_2$Br and 1.1 g (6 mmol) of mesitylimidazole were placed in a glass ampoule, which was sealed under vacuum. The ampoule was submerged in an oil bath heated at 160 °C for ten days. The brown-black solid was dissolved in dichloromethane and activated charcoal was added. It was then filtered through a Celite plug and the volume of the solution was reduced to half. Et$_2$O was then added to facilitate the precipitation of the imidazolium salt as a white solid. This was isolated from the mother-liquor by filtration and was washed with Et$_2$O (3 × 50 mL). Yield: 1.2 g (65 %). ^{1}H-NMR δ(CDCl$_3$): 1.68 (6H, s, o-methyls of mesityl), 2.31 (3H, s, p-methyl of mesityl), 6.11 (2H, d, $^2J_{PH}$ = 6.5 Hz, Ph$_2$P(O)CH_2- imidazolium), 6.88 (2H, s, aromatic), 7.10 (1H, s, imidazole backbone), 7.49 (4H, br. s, aromatics), 8.30 (7H, m, aromatics), 9.95 (1H, s, NCHN); ^{13}C$\{^1$H$\}$-NMR δ(CDCl$_3$): 18.2 (s, o-methyls of mesityl), 22.1 (s, p-methyl of mesityl), 49.6 (d, $^1J_{PC}$ = 65.3 Hz Ph$_2$P(O)CH$_2$-imidazolium), 122.5 (s, imidazolium backbone), 123.2 (imidazolium backbone), 127.0 (d, J_{PC} = 7.2 Hz), 128.1 (s, aromatic), 129.4 (s, aromatic), 131.7 (d, J_{PC} = 16.6 Hz), 132.9 (s, aromatic), 134.1 (s, aromatic), 139.8 (s, *ipso* to the imidazolium moiety), 142.1 (s, NC(H)N); ^{31}P$\{^1$H$\}$-NMR δ(CDCl$_3$): 35 (s, Ph$_2$$P$(O)CH$_2$-imidazolium). Anal. Found: C, 59.42; H, 5.48; N, 5.70 %. Calcd for C$_{25}$H$_{26}$N$_2$BrPO.H$_2$O: C, 60.13; H, 5.65; N, 5.61 %.

2.2a: The phosphine oxide **2.1a** (2 g, 3.8 mmol) was placed in a three-neck 1 L flask fitted with a nitrogen inlet, double jacket condenser, and a pressure-equalizing funnel, and freshly dried-degassed chlorobenzene was added (110 mL). **2.1a** was dissolved by heating to the reflux temperature under a nitrogen atmosphere. The temperature was then maintained at 120 °C, and excess trichlorosilane was added in small portions (10 mL, 72 mmol, 19-fold excess). After completion of the addition the reaction mixture was heated at 130 °C for 3 hrs and then cooled at room temperature. After addition of 100 mL of dichloromethane, the excess SiHCl$_3$ was quenched by careful dropwise addition of degassed 10% (w/v) NaOH$_{(aq.)}$ at 0 °C. The organic phase was separated and the aqueous phase was washed with dichloromethane (3 × 50 mL). The combined organic extracts were dried over MgSO$_4$, filtered and volatiles were removed under reduced pressure. The resulting white solid was washed with diethyl ether (2 × 150 mL) and dried under vacuum overnight. The imidazolium salt was further dried azeotropically with toluene and was stored in the glovebox. Yield 1.0 g (52 %). ^{1}H-NMR δ(CDCl$_3$): 1.03 (6H, d, $^3J_{HH}$ = 6.8 Hz, CH(CH_3)$_2$), 1.15 (6H, d, $^3J_{HH}$ = 6.8 Hz, CH(CH_3)$_2$), 2.01 (2H, sept., $^3J_{HH}$ = 6.8 Hz,

CH(CH$_3$)$_2$), 5.77 (2H, d, $^2J_{PH}$ = 6.4 Hz, Ph$_2$PCH_2- imidazole), 6.91 (1H, t, $^3J_{HH}$ = 1.7 Hz,

aromatic), 7.08 (2H, d $^3J_{HH}$ = 7.7 Hz, aromatic), 7.31-7.38 (6H, m, aromatic), 7.41 (1H, t,

$^3J_{HH}$ = 7.7 Hz, aromatic), 7.51 (1H, t, $^3J_{HH}$ = 1.7 Hz, aromatic), 7.58-7.77 (4H, m,

aromatic), 10.51 (1H, t, $^3J_{HH}$ = 1.5 Hz, NCHN); ^{13}C{^{1}H}-NMR δ(CDCl$_3$): 23.1 (s,

CH(CH_3)$_2$), 23.3 (s, CH(CH_3)$_2$), 27.6 (s, CH(CH$_3$)$_2$), 47.7 (d, $^1J_{PC}$ = 19.52 Hz, Ph$_2$PCH_2-

imidazolium), 121.4 (d, J_{PC} = 5.1 Hz, aromatic), 122.6 (s, imidazolium, backbone) 123.6

(s, imidazolium backbone), 128.2 (d, J_{PC} = 7.6 Hz, aromatic), 129.1 (s, aromatic), 129.3 (s,

aromatic), 130.8 (s, aromatic), 131.6 (d, J_{PC} = 11.5 Hz, aromatic), 132.6 (d, J_{PC} = 20.3 Hz,

aromatic), 138.2 (s, *ipso* to the imidazolium moiety), 144.3 (s, NC(H)N); ^{31}P{^{1}H}-NMR:

δ(CDCl$_3$): -10 (s, Ph$_2$$PCH_2$- imidazolium). Anal. Found: C, 69.31; H, 6.77; N, 5.70 %.

Calcd for C$_{56}$H$_{64}$BrClN$_4$P$_2$ (1:1 bromide/chloride salt): C, 69.31; H, 6.65; N, 5.77 %.

2.2b: This compound was prepared as **2.2a** starting from 1.1 g (2.3 mmol) of **2.1b**. Yield:

900 mg (85 %). ^{1}H-NMR δ(CDCl$_3$): 1.66 (6H, s, *o*-methyls of mesityl), 2.28 (3H, s, *p*-

methyl of mesityl), 5.71 (2H, d, $^2J_{PH}$ = 6.37 Hz, Ph$_2$PCH_2- imidazolium), 6.93 (2H, broad

s., aromatic), 7.01 (1H, s, imidazole backbone), 7.48 (5H, broad s, aromatic), 7.83 (1H, s,

imidazole backbone), 7.91 (4H, m, aromatic), 10.38 (1H, s, NCHN); ^{13}C{^{1}H}-NMR

δ(CDCl$_3$): 17.9 (s, *o*- methyls of mesityl), 21.6 (s, *p*-methyl of mesityl), 49.4 (d, $^1J_{PC}$ =

19.4 Hz, Ph$_2$PCH$_2$-imidazolium), 123.3 (s, imidazolium backbone), 127.7 (s, imidazolium

backbone), 129.2 (s, aromatic), 129.8 (s, aromatic), 130.4 (d, J_{PC} = 2.8 Hz, aromatic),

130.9 (s, aromatic), 133.3 (d, J_{PC} = 11.80 Hz, aromatic), 134.2 (s, aromatic), 134.4 (s,

aromatic), 134.8 (s, *ipso* to the imidazolium moiety), 139.5 (s, NC(H)N); ^{31}P{^{1}H}-NMR:

δ(CDCl$_3$): -10.0 (s, Ph$_2$$PCH_2$- imidazolium). Anal. Found: C, 68.01; H, 6.06; N, 6.33 %.

Calcd for C$_{50}$H$_{52}$BrClN$_4$P$_2$ (1:1 bromide/chloride salt): C, 67.76; H, 5.91; N, 6.32 %.

2.3a: 9.7 g (31 mmol) of Ph$_2$P(O)(CH$_2$)$_2$Br and 7.2 g (32 mmol) of 1-(2,6-diisopropyl-

phenyl)-imidazole were placed in a glass ampoule which was sealed under vacuum and

immersed in an oil bath heated at 150-160 °C for 1 week. After the ampoule was opened,

the brown solid was dissolved in dichloromethane and the volatiles were removed under

reduced pressure to give a beige solid, which was washed with ether (2 × 50 mL). It was

then redissolved in the minimum amount of dichloromethane and re-precipitated by

addition of ether giving the product as a white powder. Yield: 15.2 g (90 %). ^{1}H-NMR

δ(CDCl$_3$): 0.92 (6H, d, $^3J_{HH}$ = 6.9 Hz, CH(CH_3)$_2$), 1.10 (6H, d, $^3J_{HH}$ = 6.9 Hz CH(CH_3)$_2$),

2.10 (2H, sept., $^3J_{HH}$ = 6.9 Hz, CH(CH$_3$)$_2$), 3.42 (2H, m, Ph$_2$P(O)CH_2CH$_2$-imidazolium),

5.14 (2H, m, Ph$_2$P(O)CH$_2$CH_2-imidazolium), 6.93 (1H, s, imidazolium backbone), 7.12-

7.19 (3H, m, aromatics and imidazolium backbone proton) 7.40-7.70 (8.5H, m,

aromatics), 7.81-8.03 (4.5H, m, aromatics), 8.72 (1H, s, aromatic), 10.33 (1H, s, NCHN);

^{13}C{^{1}H}-NMR δ(CDCl$_3$): 24.4 (s, CH(CH_3)$_2$), 24.5 (s, CH(CH$_3$)$_2$), 28.7 (s,

Ph$_2$P(O)CH$_2$CH$_2$-imidazolium), 44.6 (s, Ph$_2$P(O)CH$_2$$CH_2$-imidazolium), 123.9 (s,

imidazolium backbone), 124.8 (s, aromatic), 125.2 (s, imdazolium backbone), 129.2 (d,

J_{PC} = 12.1 Hz, aromatic), 130.2 (s, aromatic), 130.9 (d, J_{PC} = 9.8 Hz, aromatic), 132.1 (s,

aromatic), 132.5 (s, aromatic), 138.4 (s, ipso at imidazolium moiety), 145.4 (s, NC(H)N);

^{31}P{^{1}H}-NMR δ(CDCl$_3$): 33.4 (s, Ph$_2$$P$(O)CH$_2CH_2$-imidazolium). Anal. Found: C, 61.93;

H, 6.14; N, 5.12 %. Calcd for C$_{29}$H$_{34}$N$_2$BrOP.H$_2$O: C, 62.70; H, 6.63; N, 5.04 %.

2.3b: This was prepared by a method analogous to **2.3a** from 10 g (32.5 mmol) of

Ph$_2$P(O)(CH$_2$)$_2$Br and 6.1 g (32.6 mmol) of 1-(2,4,6-trimethyl-phenyl)-imidazole. Yield:

13.4 g (83 %). ^{1}H-NMR δ(CDCl$_3$): 1.79 (6H, s, o-methyls of mesityl), 2.66 (3H, s, p-

methyl of mesityl), 3.38 (2H, m, Ph$_2$P(O)CH_2CH$_2$-imidazolium), 4.82 (2H, m,

Ph$_2$P(O)CH$_2$CH_2-imidazolium), 6.59 (1H, s, imidazolium backbone), 6.88 (1H, s,

imidazolium backbone), 7.21-7.50 (5H, m, aromatics), 7.71-7.87 (4H, m, aromatics), 8.41

(1H, s, aromatic), 10.1? (1H, s, NCHN); ^{13}C{^{1}H}-NMR δ(CDCl$_3$): 17.8 (s, o-methyls of

mesityl), 21.2 (s, p-methyl of mesityl), 44.5 (s, Ph$_2$P(O)CH$_2$$CH_2$-imidazolium), 122.8 (s,

imidazolium backbone), 124.8 (s, imidazolium backbone), 129.1 (d, J_{PC} = 12.8 Hz,

aromatic), 129.8 (s, aromatic), 131.? (d, J_{PC} = 18.1 Hz, aromatic), 131.4 (aromatic), 132.2

(s, aromatic), 134.7 (s, aromatic), 138.3 (s, ipso to the imidazolium moiety) 141.3 (s,

NC(H)N); ^{31}P{^{1}H}-NMR δ(CDCl$_3$): 31.0 (s, Ph$_2$$P$(O)CH$_2CH_2$-imidazolium). Anal. Found:

C, 62.90; H, 5.70; N, 5.64 %. Calcd for C$_{26}$H$_{28}$N$_2$BrOP: C, 63.04; H, 5.70; N, 5.64 %.

2.4a: The phosphine oxide **2.3a** (4.5 g, 8.4 mmol) was placed in a three-neck 1 L flask

(Schlenk adapter, double jacket condenser, and a pressure-equalizing funnel) and freshly

dried-degassed chlorobenzene (110 mL) was added. The phosphine oxide **2.3a** was

dissolved by heating to the reflux temperature under a nitrogen atmosphere. The

temperature was then maintained at 120 °C, and excess trichlorosilane was added in small

portions (14 mL, 100 mmol, 12-fold excess). After completion of the addition the reaction

mixture was heated at 130 °C for 3 hrs and then cooled at room temperature. After

addition of 100 mL of dichloromethane, the excess trichlorosilane was quenched by

careful dropwise addition of degassed 10% (w/v) NaOH$_{(aq.)}$ at 0 °C. The organic phase was

separated and the aqueous phase was washed with dichloromethane (3×50 mL). The

combined organic extracts were dried over MgSO$_4$, filtered and volatiles were removed

under reduced pressure. The resulting white solid was washed with ether (2 × 150 mL)

and dried under vacuum overnight. The imidazolium salt was further dried azeotropically

with toluene and was stored in the glovebox. Yield: 3.3 g (75 %). ^{1}H-NMR δ(CDCl$_3$):

1.09 (6H, d, $^3J_{HH}$ = 6.8 Hz, CH(CH_3)$_2$), 1.17 (6H, d, $^3J_{HH}$ = 6.8 Hz CH(CH_3)$_2$), 2.41 (2H,

septet, $^3J_{HH}$ = 6.8 Hz CH(CH$_3$)$_2$), 2.87 (2H, m, Ph$_2$PCH_2CH$_2$-imidazolium), 4.87 (2H, m,

Ph$_2$PCH$_2$CH_2-imidazolium), 6.88 (1H, s, imidazolium backbone), 7.07-7.77 (13H, m,

aromatics), 8.01 (1H, s, aromatic), 10.40 (1H, s, NCHN); ^{13}C{^{1}H}-NMR δ(CDCl$_3$): 24.5

(s, CH(CH_3)$_2$), 28.8 (s, CH(CH$_3$)$_2$), 30.0 (d, $^1J_{PC}$ = 13.0 Hz, Ph$_2$PCH$_2$CH$_2$-imidazolium),

48.2 (d, $^2J_{PC}$ = 18.1 Hz, Ph$_2$PCH$_2$$CH_2$-imidazolium), 123.8 (s, imidazolium backbone),

124.0 (s, imidazolium backbone), 124.8 (s, aromatic), 129.1 (d, J_{PC} = 6.8 Hz, aromatic),

130.3 (s, aromatic), 130.8 (s, aromatic), 132 (s, aromatic), 132.9 (d, J_{PC} = 19.7 Hz,

aromatic), 136.2 (d, J_{PC} = 11.3 Hz, aromatic), 138.6 (s, *ipso* to imidazolium moiety,

aromatic) 145.5 (s, NC(H)N); ^{31}P{^{1}H}-NMR δ(CDCl$_3$): -22.4 (s, Ph$_2$$PCH_2CH_2$-

imidazolium). Anal. Found: C, 69.07; H, 6.63; N, 5.08 %. Calcd for C$_{58}$H$_{68}$BrClN$_4$P$_2$ (1:1

bromide/chloride salt): C, 69.77; H, 6.86; N, 5.61 %.

2.4b: This was prepared by a method analogous to **2.4a** starting from 5.0 g (10.1 mmol) of

phosphine oxide **2.3b**. Yield: 3.6 g (75 %). ^{1}H-NMR δ(CDCl$_3$): 2.07 ppm (6H, s, *o*-

methyls of mesityl), 2.41 ppm (3H, s, *p*-methyl of mesityl), 2.88 (2H, m,

Ph$_2$P(O)CH_2CH$_2$-imidazolium) 4.91 (2H, m, Ph$_2$P(O)CH$_2$CH_2-imidazolium), 6.73 (1H, s,

imidazolium backbone), 6.92 (1H, s, imidazolium backbone), 7.04 (aromatics of mesityl)

7.5 (5H, br, aromatics), 7.65 (4H, br s., aromatic), 7.89 (1H, s aromatic) 10.61 (1H, s,

NCHN); ^{13}C{^{1}H}-NMR δ(CDCl$_3$): 17.8 (s, *o*-methyls of mesityl), 21.2 (s, *p*-methyl of

mesityl), 29.8 (d,$^1J_{PC}$ = 16.0 Hz, Ph$_2$PCH$_2$CH$_2$-imidazolium), 48.1 (d, $^1J_{PC}$ = 21.9 Hz,

Ph$_2$PCH$_2$$CH_2$-imidazolium), 123.0 (s, imidazolium backbone),123.5 (s, imidazolium

backbone), 129.0 (d, J_{PC} = 6.8 Hz, aromatic), 129.1 (d, J_{PC} = 8.3 Hz, aromatic), 129.9 (s,

aromatic), 130.8 (s, aromatic), 132.9 (d, J_{PC} = 18.9 Hz, aromatic), 134.4 (s, aromatic),

136.3 (d, J_{PC} = 11.3 Hz, aromatic), 138.5 (s, *ipso* to imidazolium moiety), 141.3 (s,

NC(H)N); ^{31}P{^{1}H}-NMR δ(CDCl$_3$): -22.4 (s, Ph$_2$$PCH_2CH_2$-imidazolium). Anal. Found:

C, 63.57; H, 5.69; N, 5.31 %. Calcd for C$_{52}$H$_{56}$BrClN$_4$P$_2$ (1:1 bromide chloride salt): C,

63.70; H, 5.85; N, 5.61 %.

2.5: This was prepared by following a method analogous to **2.3a** from 4.34 g (13.5 mmol)

of Ph$_2$P(O)(CH$_2$)$_3$Br and 2.8 g (15 mmol) of mesitylimidazolium. ^{1}H-NMR δ(CDCl$_3$):

1.88 (6H, s, *o*-methyls of mesityl), 2.41 (3H, s, *p*-methyl of mesityl), 2.31-2.51 (2H, m, ,

Ph$_2$P(O)CH_2(CH$_2$)$_2$-imidazolium), 2.72 (2H, m, Ph$_2$P(O)CH$_2$CH_2CH$_2$-imidazolium), 5.00

(2H, m, Ph$_2$P(O)(CH$_2$)$_2$CH_2- imidazolium), 6.92 (2H, s, aromatics of mesityl), 7.11 (1H, s,

imidazolium backbone), 7.31 (1H, s, imidazolium backbone), 7.52 (5H, br. s, aromatics of

phosphinoxide), 7.69-7.86 (4H, m, aromatic), 8.21 (1H, s, aromatic), 10.4? (1H, s, NCHN); ^{13}C{^{1}H}-NMR δ(CDCl$_3$): 17.9 (s, o-methyls of mesityl), 21 (s, p-methyl of mesityl), 24.6 (d, $^1J_{PC}$ = 11.6 Hz, Ph$_2$P(O)CH$_2$(CH$_2$)$_2$-imidazolium), 27.4 (s, Ph$_2$P(O)CH$_2$$CH_2CH_2$-imidazolium), 50.8 (s, Ph$_2$P(O)(CH$_2$)$_2$$CH_2$-imidazolium), 122.5 (s, imidazolium backbone), 123.9 (imidazolium backbone), 127.5 (d, J_{PC} = 6.6 Hz), 128.3 (s, aromatic), 129.1 (s, aromatic), 131.3 (d, J_{PC} = 17.3 Hz), 131.6 (s, aromatic), 132.9 (s, aromatic), 133.6 (s, aromatic), 138.8 (s, $ipso$ to the imidazolium moiety), 142.3 (s, NC(H)N); ^{31}P{^{1}H}-NMR δ(CDCl$_3$): 33.8 (s, Ph$_2$$P$(O)(CH$_2$)$_3$-imidazolium). Anal. Found: C, 65.83; H, 6.17; N, 5.69 %. Calcd for C$_{27}$H$_{30}$N$_2$BrPO: C, 65.72; H, 6.13; N, 5.68 %.

2.6: This compound was prepared by following a method analogous to **2.4a**, starting from 4.5 g (8.8 mmol) of oxide **2.5**. Yield: 3.3 g (75 %). ^{1}H-NMR δ(CDCl$_3$): 2.00 (6H, s, o-methyls of mesityl), 2.23 (4H, m, Ph$_2$PCH_2(CH$_2$)$_2$-imidazolium and Ph$_2$PCH$_2$CH_2CH$_2$-imidazolium), 2.41 (3H, s, p-methyl of mesityl), 5.00 (2H, t, Ph$_2$P(O)(CH$_2$)$_2$CH_2-imidazolium), 6.91 (2H, br. s, aromatics), 7.13 (2H, br. s., imidazolium backbone), 7.41-7.68 (10H, m, aromatics of phosphine), 10.88 (1H, s, NCHN); ^{13}C{^{1}H}-NMR δ(CDCl$_3$): 17.8 (s, o- methyls of mesityl), 21.2 (s, p-methyl of mesityl), 24.4 (d, $^1J_{PC}$ = 10.6 Hz, Ph$_2$PCH$_2$CH$_2$CH$_2$-imidazolium), 27.1 (d, $^2J_{PC}$ = 18.1 Hz, Ph$_2$PCH$_2$$CH_2CH_2$-imidazolium), 50.6 (d, $^3J_{PC}$ = 19.1 Hz, Ph$_2$PCH$_2$CH$_2$$CH_2$-imidazolium), 122.3 (s, imidazolium backbone), 123.3 (s, imidazolium backbone), 128.8 (d, J_{PC} = 6.8 Hz, aromatic), 129.1 (s, aromatic), 130.0 (s, aromatic), 130.8 (s, aromatic), 132.9 (d, J_{PC} = 19.2 Hz, aromatic), 134.3 (s, aromatic), 137.6 (d, J_{PC} = 12.4 Hz, aromatic), 139.1 (s, ipso to the imidazolium moiety), 141.5 (s, NC(H)N); ^{31}P{^{1}H}-NMR: δ(CDCl$_3$): -16.6 (s, Ph$_2$$PCH_2CH_2CH_2$-imidazolium). Anal. Found: C, 68.66; H, 6.28; N, 6.39 %. Calcd for C$_{54}$H$_{60}$BrClN$_4$P$_2$ (1:1 bromide/chloride salt): C, 68.82; H, 6.42; N, 5.95 %.

1-(3,5-bis(trifluoromethyl)phenyl)-imidazole: 2.6 g (22 mmol) of thiophosgene was added at 30 mL of distilled water. To this 5.0 g (22 mmol) of 3,5-bis(trifluoromethyl)-aniline was added over a period of 10 minutes under vigorous stirring. After the addition was complete the reaction mixture was left to stir vigorously at room temperature for 2 hours. The reaction mixture was extracted with chloroform (3 × 50 mL) and volatiles were removed under reduced pressure using an external liquid nitrogen trap, to yield a yellow-green viscous oil. This was added to a solution of 5.9 g (22 mmol) of 2,3-diethoxy-propylamine in 40 mL of ethanol. After the addition was complete the mixture was heated under reflux for 30 minutes and was stripped of ethanol. The arylacetalylthiourea was then heated at reflux for 60 minutes with 50 mL of 10% aqueous hydrochloric acid. The acid

solution was cooled to 0 °C and the mercaptane was isolated by filtration. This was further purified by recrystalisation from a 1:1 (v/v) ethanol/water mixture. 2.5 g (8.1 mmol) (36.8 % crystalline yield) of the recrystalised mercaptane was placed in a 100 mL Erlenmeyer flask, suspended in 10 mL of distilled water and cooled down to 0 °C. This suspention was treated with four times the weight of the mercaptane of 20% aqueous nitric acid. After stirring for 30 minutes at 0 °C, 1-2 drops of concentrated nitric acid were added and the ice bath was removed. The oxidation started shortly after the removal of the ice bath as evidenced by the appearance of brown fumes. The suspention changed colour from pale yellow to green and when the oxidation had finished to bright yellow. The reaction mixture was then cooled down to 0 °C and was made basic with 15 % aqueous ammonia. It was then extracted with chloroform (3 × 30 mL). The organic phase was dried over $MgSO_4$ and volatiles were removed by means of a rotary evaporator, yielding a yellow-brown oil. This was dissolved in PE and was placed in the freezer (- 30 °C) overnight, to give the title compound as pale yellow crystals that were isolated by filtration and dried under vacuum. Yield: 1.0 g (45 %). ^{1}H-NMR δ($CDCl_3$): 7.21 (1H, broad s, aromatic), 7.31 (1H, br. s., aromatic), 7.77 (3H, br. s., aromatic), 7.91 (1H, br. t, aromatic); ^{13}C$\{^1$H$\}$-NMR δ($CDCl_3$): 118.0 (br. s, aromatic), 120.9 (s, aromatic), 121.2 (quintet, J_{FC} = 8.8 Hz aromatic), 121.5 (br. d, J_{FC} = 3.7 Hz), 124.5 (s, aromatic), 131.7 (s, aromatic), 134.1 (quartet J_{FC} = 32.9 Hz), 138.7 (s, aromatic); ^{19}F$\{^1$H$\}$-NMR δ($CDCl_3$): -63.4 (CF_3); ES$^+$: 281[M+H]$^+$, 322 [M+H+CH$_3$CN]$^+$.

2.7: 900 mg (3.24 mmol) of 1-(3,5-bis(trifluoromethyl)-phenyl)-imidazole and 658 mg (4.16 mmole) of 2-bromo-pyridine were charged in an ampoule which was sealed under vacuum. The ampoule and its contents were submerged in an oil bath thermostated at 160 °C for one week. The ampoule was then opened and to the black solid, dichloromethane was added up to ¾ of the ampoule volume. The whole was left stirring at room temperature overnight. During this time a colourless crystalline solid formed. This was isolated by filtration, washed with Et$_2$O and PE and dried under vacuum. This solid was soluble in acetonitrile and dimethylsulfoxide and insoluble in chloroform, acetone, water and toluene. Mass spectrometry as well as NMR spectroscopy proved that it is the title compound. The dichloromethane filtrate was reduced to half volume and was cooled at − 30 °C to give a second crop of the compound, which was not as pure. Yield: 650 mg (46 %). ^{1}H-NMR δ((CD_3)$_2$SO): 7.71 (1H, ddd, J_{HH} = 1.0 Hz, 4.8 Hz, 8.2 Hz, aromatic pyridine), 8.25 (1H, t, J_{HH} =8.2 Hz, aromatic pyridine), 8.29 (1H, dt, J_{HH} = 1.7 Hz, 8.2 Hz, aromatic pyridine), 8.44 (1H, br. s, aromatic), 8.75 (1H, ddd, J_{HH} = 0.8 Hz, 1.7 Hz, 4.8

Hz, aromatic pyridine), 8.81 (2H, br. d, J_{HH} = 1.5 Hz, imidazolium backbone), 8.85 (2H, br. t., aromatic), 10.93 (1H, t, J_{HH} = 1.5 Hz, NCHN); ^{13}C$\{^{1}$H$\}$-NMR δ(CD$_3$)$_2$SO): 114.8 (s, imidazolium backbone), 119.8 (s, imidazolium backbone), 120.8 (s, aromatic), 122.6 (s, aromatic), 124.1 (broad t, J_{FC} = 27.6 Hz, aromatic), 125.7 (s, aromatic), 132.8 (quartet, $^{1}J_{FC}$ = 33.9 Hz, CF$_3$), 132.9 (s, aromatic), 135.6 (s, aromatic), 136.1 (s, NC(H)N), 140.7 (s, aromatic), 146.1 (s, *ipso* to the imidazolium), 149.4 (s, aromatic); ^{19}F$\{^{1}$H$\}$-NMR δ(CD$_3$)$_2$SO): - 61.1 (s, CF_3); ES$^+$: 358.1 [M]$^+$; HRES$^+$: Found: 358.0769. Calcd for: [C$_{16}$H$_{10}$F$_6$N$_3$]$^+$: 358.0773

2.8c: 10 g (44 mmol) of 1-(2,6-diisopropylphenyl)imidazole and 5.8 g (37 mmol) of 2-bromopyridine were placed in an ampoule, which was sealed under vacuum. The two solids were heated at 140 °C for one week by means of a thermostated oil bath. The brown-beige solid was dissolved in dichloromethane and volatiles were removed by means of a rotary evaporator. The fluffy brown solid was then stirred with diethyl ether for 2 hours to remove the excess of imidazole. The ether was decanted off and the solid was dissolved in the minimum amount of dichloromethane and precipitated with ether. The solid was immediately filtered, washed with more ether (2 × 100 mL) and PE (50 mL) and dried under vacuum. Water was removed by azeotropic distillation with toluene and the solid was kept in the glove box. Yield: 12 g (85.1%). Spectroscopic data agree with ones reported in literature.[37]

2.8d: This was prepared as above from 10 g (44 mmol) of 3-(2,6-diisoproylphenyl)-imidazole and 6.3 g (37 mmol) 2-bromo-3-methyl-pyridine. Yield: 10 g (68 %). Spectroscopic data agree with those reported in literature.[37]

2.9c: In the glove box 3.0 g (7.8 mmol) of dry **2.8c** were placed in a 250 mL Schlenk tube that had been left in a 120 °C oven overnight. A second Schlenk tube was charged with 1.7 g (8.5 mmol) of KN(SiMe$_3$)$_2$. The imidazolium salt was suspended in approximately 50 mL of THF and was cooled down to -78 °C using a dry-ice-acetone slush bath. To this suspention a cooled at -78 °C solution of KN(SiMe$_3$)$_2$ in THF (approx. 30 mL) was added slowly by means of cannula. The reaction mixture was placed in the freezer (-30 °C) overnight. Volatiles were removed under reduced pressure and the beige solid was extracted thrice (3 × 40 mL) with toluene and filtered through a Celite plug. The volume of the solution was reduced to *ca.* 25 mL and 60 mL of PE were added with vigorous stirring. The mixture was then cooled at - 30 °C to afford the title compound as beige crystals, which were separated by filtration by means of a filter cannula and dried under vacuum. As second crop was collected by removing the solvent from the filtrate,

dissolving in the minimum amount of Et_2O, adding more PE and re-cooling at - 30 °C. Yield: 1.3 g (55 %). Spectroscopic data agree with ones reported before within the group.[38]

2.9d: This was prepared as above from 3 g (7.5 mmol) of **2.8d** and 1.65 g (8.3 mmol) of $KN(SiMe_3)_2$ to yield 1.0 g (42 %) of the title compound as pale yellow crystals. Spectroscopic data agree with ones reported in literature.[37]

Crystallographic data for 2.7 and 2.9c:

	2.9c	2.7
Chemical Formula	$C_{20}H_{23}N_3$	$C_{16}H_{12}BrF_6N_3O$
Formula weight	305.41	456.20
Crystal system	Monoclinic	Monoclinic
Space group	$P\ 2_1/c$	Pc
a / $\mathring{A}$	5.8255(14)	5.0631(4)
b / $\mathring{A}$	18.479(7)	22.659(3)
c / $\mathring{A}$	15.878(8)	7.5481(3)
α / $^\circ$	90	90
β / $^\circ$	98.54(3)	95.561(6)
γ / $^\circ$	90	90
Z	4	2
T/K	120(2)	120(2)
μ / mm^{-1}	0.072	2.458
No. of data collected	21831	15925
No. of unique data	3899	3860
Goodness of fit on F^2	0.974	1.065
$R_{int.}$	0.1050	0.0449
Final $R(|F|)$ for $F_o > 2\sigma(Fo)$	0.0574	0.0330
Final $R(F^2)$ for all data	0.1321	0.0428

References:

1. Herrmann, W. A., *Angew. Chem. Int. Ed.* **2002**, *41*, 1290.

2. Naud, F.; Braunstein, P. *Angew. Chem. Int. Ed.* **2001**, *40*, 680.

3. McGuiness, D. S.; Cavell, K. J. *Organometallics* **2000**, *19*, 741.

4. a) Lee, H. M.; Zeng, J. Y.; Hu, C.-H.; Lee, M.-T. *Inorg. Chem.* **2004**, *43*, 6822. b) Lang, H.; Vittal, J. J.; Leung, P. -H. *J. Chem. Soc., Dalton Trans.*, **1998**, 2109. c) Seo, H.; Park H.; Kim, B. Y.; Lee, J. H.; Son, S. U.; Chung, Y. K. *Organometallics*, **2003**, *22*, 618.

5. a) Lee, M.-T.; Hu, C.-H. *Organometallics* **2004**, *23*, 976. b) Herrmann, W. A.; Kocher, C.; Artus, G. R. J. *Chem. Eur. J.*, **1996**, *2*, 1627 c) Yang, C.; Lee, H. M.; Nolan S. P. *Org. Lett.*, **2001**, *3*, 1511; d)Wang, A.-E.; Zhong, J.; Xie, J.-H.; Li, K.; Zhou, Q.-L. *Adv. Synth. Cat.*, **2004**, *6*, 595.

6. Danopoulos, A. A.; Gelbrich, T.; Hursthouse, M. B.; Winston, S. *Chem. Commun.* **2002**, 482.

7. Enders, D.; Breuer, K.; Raabe, G.; Runsink, J.; Telles, J. H.; Melder, J. P.; Ebel, K.; Brode, S. *Angew. Chem. Int. Ed.* **1995**, *34*, 1021.

8. Perry, M. C.; Cui, X.; Powell, M. T.; Hou, D.-R.; Reibenspies, J. H. *J. Am. Chem. Soc.* **2003**, *125*, 114.

9. Broene, R. D.; Buchwald, S. L. *J. Am. Chem. Soc.* **1993**, *115*, 12569.

10. Blankenstein, J.; Pfaltz, A. *Angew. Chem. Int. Ed.* **2001**, *40*, 4445.

11. Van Velhuisen, J. J.; Garber, S. B.; Kingsbury, J. S.; Hoveyda, A. H. *J. Am. Chem. Soc.* **2002**, *124*, 4954.

12. Weberskirch, R.; Kotre, T.; Tobias, Z. M. *Polymer Preprints* **2004**, *45*, 393.

13. Danopoulos, A. A.; Winston, S.; Motherwell, W. B. *Chem. Commun.* **2002**, 1376.

14. Danopoulos, A. A.; Tsoureas, N.; Wright, J. A.; Light, M.E. *Organometallics* **2004**, *23*, 166.

15. Danopoulos, A. A.; Wright, J. A.; Motherwell, M. B.; Elwood, S. *Organometallics* **2004**, *23*, 4807.

16. Hu, X.; C.-Rodriguez, I.; Meyer, K. *J. Am. Chem. Soc.* **2004**, *126*, 6997.

17. Tulloch, A. A. D.; Danopoulos, A. A.; Tizzard, G. J.; Coles, S. J.; Hursthouse, M. B.; Motherwell, R. H.; Motherwell, W. B. *Chem. Commun.* **2001**, 1270.

18. Horrath, A., *Synthesis* **1994**, 102.

19. Arnold, P. L.; Blake, A. J.; Wilson, C. *Angew. Chem. Int. Ed.* **2003**, *42*, 5981.

20. Bonnet, C.; Douthwaite, R. E.; Hodgson, R.; Houghton, J.; Kariuki, B. M.; Simonovic, S. *J. Chem. Soc. Dalton Trans.* **2004**, 3528.

21. Tulloch A. A. D.; Winston, S.; Danopoulos, A. A.; Eastham, G.; Hursthouse, M. B. *J. Chem. Soc. Dalton Trans.* **2003**, 699.

22. 13. Seo, H.; Park, H.-J.; Kim, B.Y.; Lee, J. H.; Son, S. U.; Chung, Y. K. *Organometallics* **2003**, *22*, 618.

23. Batey, R. A.; Shen, M.; Lough, A. J. *Org. Lett.* **2002**, *4*, 1411.

24. Furstner, A.; Ackermann, L.; Gabor, B.; Coddard, R.; Lehmann, C. W.; Mynott, R.; Stelzer, F.; Thiel, O. R. *Chem. Eur. J.* **2001**, *7*, 3236.

25. Herrmann, W. A.; Goosen, L. J.; Artus, G. R. J. *Chem. Eur. J.* **1996**, *2*, 1627.

26. Yang, C.; Lee, H. M.; Nolan, S. P. *Org.Lett.* **2001**, *3*, 1511.

27. Toke, L.; Petnehazy, I.; Stacal, C. *J. Chem. Soc. Res. Synop.* **1978**, *5*, 155.

28. Tulloch, A. A. D.; Danopoulos, A. A.; Winston, S.; Kleinhenz, S.; Eastham, G. *J. Chem. Soc. Dalton Trans.* **2000**, 4499.

29. Kleinhenz, S.; Tulloch, A. A. D.; Danopoulos, A. A. *Acta Cryst.* **2000**, *C56*, e476.

35. Arduengo, A. G., III. U.S. Patent 6,177,575, 2001.
36. Johnson, A. L.; Del, W. U.S. Patent 3,637,731, 1972.
37. Winston, S.; Stylianides, N.; Tulloch, A. A. D.; Wright, J. A.; Danopoulos, A. A. *Polyhedron*, **2004**, *23*, 2813
38. Personal communication with Dr. A. A. Danopoulos and Neoklis Stylianides.

Chapter 3: Functionalised *N*-heterocyclic carbene complexes of Palladium (II)

3.1 Introduction

The use of Pd-NHC complexes in important catalytic transformations, such as C-C[1,2] and C-N[3] bond formation reactions, has been a milestone. There is therefore a continuing effort to improve our understanding of the organometallic transformations and catalytic reactions involving Pd-NHC complexes. The reductive elimination of methylimidazolium salts from $[Pd(tmim)CH_3(L)_2]^+$ [(tmim) = tetramethylmethylimidazol-2-ylidene, L = phosphine, phosphite)][4] and the microscopic reverse, oxidative addition,[5] have been observed in simple systems and studied by theoretical methods;[4,5] methyl migration to the NHC carbon has also been observed in a Pd complex with a preorganized "pincer" NHC ligand and studied theoretically.[6] The extent of these reactions is critically dependent on the nature of the coligating functionalities, the presence and size of chelating rings, and other structural variables. Consequently, the design of successful carbene catalysts should be based on ligands promoting productive catalytic steps while inhibiting decomposition or deactivation. Incorporation of the carbene functionality into ligand systems containing other "classical" donor groups could achieve this, while in the same time facilitate electronic tuning of the metal coordination sphere.[7] A number of functionalised NHC complexes have been reported by others [8,9] and us.[10,11] Complexes containing multi-dentate carbenes,[12] as well as polymer- supported systems [13] have also been reported.

In this chapter the syntheses of a number of phosphine and pyridine *N*-heterocyclic palladium(II) complexes are described (Figure 3.1). These have been characterised by spectroscopic and analytical methods. X-ray diffraction studies have been undertaken, where possible, and they have revealed some interesting structural characteristics.

Ar = 2,6-diisopropylphenyl : **3.1a**
Ar = 2,4,6trimethylphenyl: **3.1b**

Ar = 2,6diisopropylphenyl : **3.2a**
Ar = 2,4,6trimethylphenyl: **3.2b**

3.3

3.4

R = H : **3.5a**
R = Me : **3.5b**

3.6

3.7
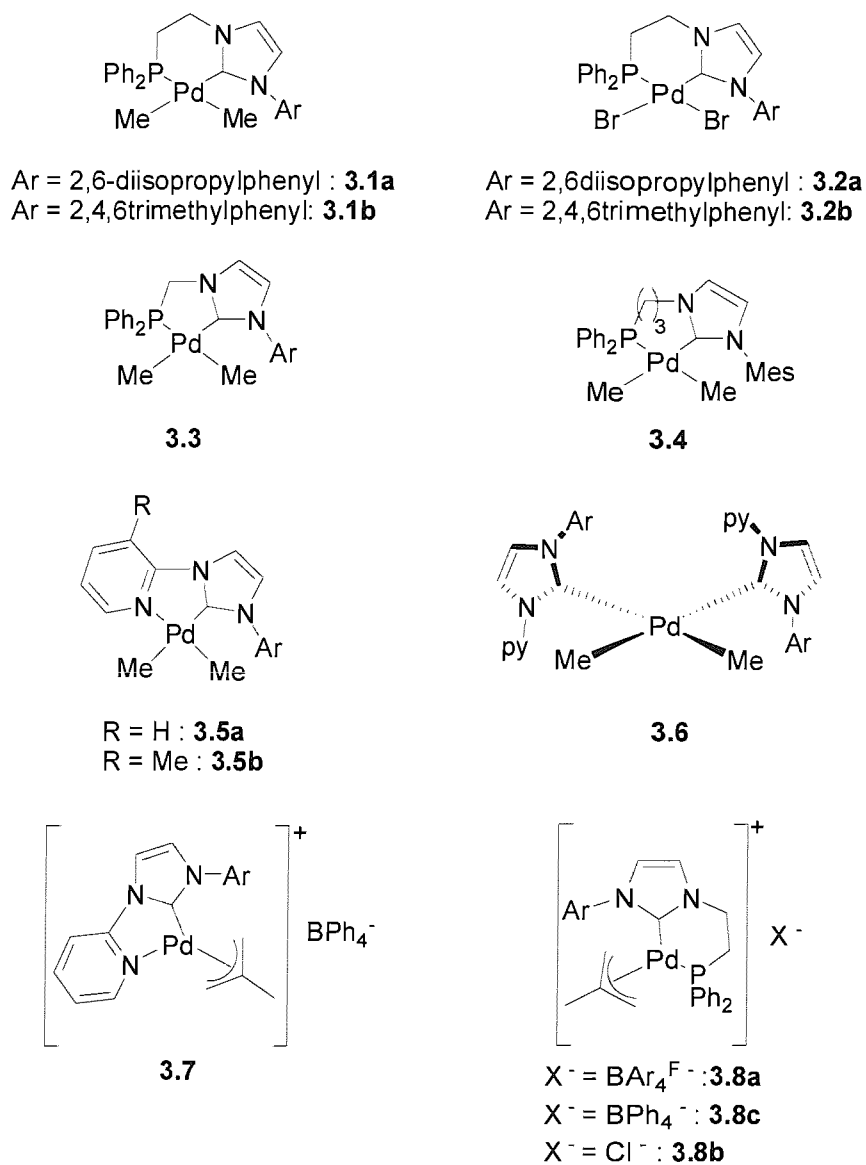
X $^-$ = BAr$_4$$^{F-}$:**3.8a**
X $^-$ = BPh$_4$ $^-$: **3.8c**
X $^-$ = Cl $^-$: **3.8b**

Figure 3.1: Synthesised Pd(II) complexes (Unless otherwise stated, Ar = 2,6-diisopropyl-phenyl. py = pyridine. BAr$_4$$^{F-}$ = tetrakis[3,5-bis(trifluoromethyl)phenyl]borate).

64

3.2 Results and discussion

3.2.1 Synthesis of phosphine functionalised NHC neutral Pd(II) complexes

The best method for the introduction of the new phosphine-functionalised NHC ligands onto a palladium centre is by trapping the *in situ* generated free carbene with a suitable metal precursor (Scheme 3.1). The generation of these carbenes by deprotonation of the appropriate imidazolium precursors with $KN(SiMe_3)_2$ in THF is complete within a few minutes at -78 °C. Reaction of the carbenes with $Pd(tmeda)Me_2$ or $Pd(1,5\text{-}COD)Br_2$ gave good yields of complexes **3.1-3.4**. Although the isolation and characterisation of the free phosphine-functionalised NHC has been communicated,[14] the synthetic methodology described above was employed due to the thermal instability of this free carbene.

m = 0, Ar = 2,6-Pr^i-C$_6$H$_3$: **3.3**
m = 1, Ar = 2,6-Pr^i-C$_6$H$_3$: **3.1a**
m =1, Ar = Mes : **3.1b**
m = 2, Ar = Mes : **3.4**

Ar = 2,6diisopropylphenyl : **3.2a**
Ar = 2,4,6trimethylphenyl: **3.2b**
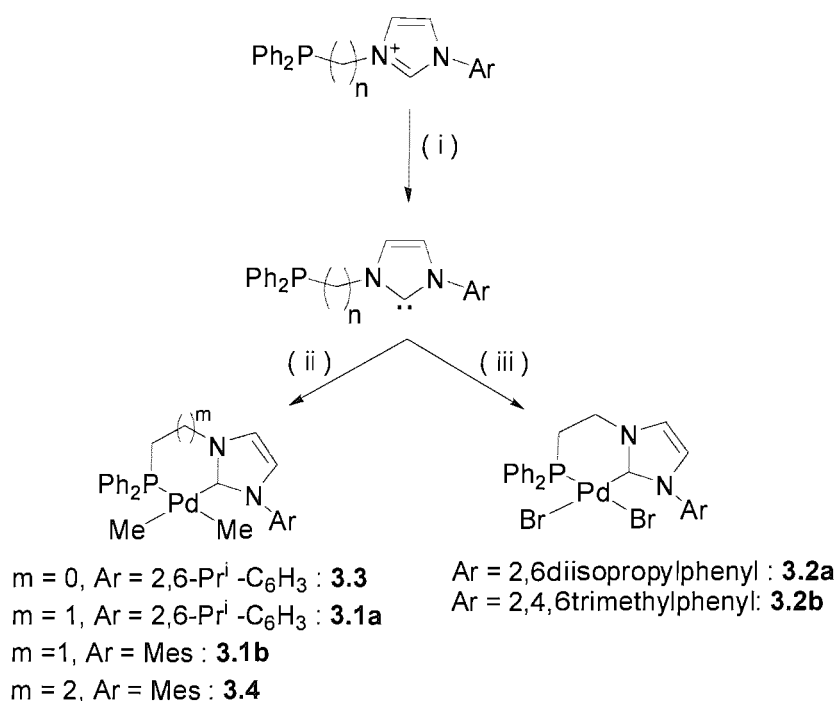
Scheme 3.1: Synthetic protocol for the preparation of phosphine functionalised NHC complexes (n = 1, 2, 3; m = n-1). Reagents and conditions: (i): 1.1 equiv. $KN(SiMe_3)_2$, THF -78 °C. (ii): 1 equiv. $Pd(tmeda)Me_2$. (iii): 1 equiv. $Pd(1,5\text{-}COD)Br_2$.

The reasons for choosing this methodology are: 1) the mild conditions of the reaction; 2) The clean deprotonation achieved using $KN(SiMe_3)_2$ as a base and the nature of the side products (KX (X = Br$^-$, Cl$^-$) and the volatile $NH(SiMe_3)_2$) and finally 3)

simplicity provided by substituting a ligand with a carbene. This of course minimises the formation of side-products.

The colourless, air-stable complexes **3.1**, **3.3** and **3.4** are soluble in THF, pyridine, chlorobenzene and CH_2Cl_2, although their solutions in the latter develop a dark colouration upon standing at room temperature for 2-3 hours. Rapid decomposition occurs when they are dissolved in $CHCl_3$. Complexes **3.2a** and **3.2b** are soluble in THF and CH_2Cl_2 but insoluble in $CHCl_3$.

3.2.2 Synthesis of pyridine functionalised NHC neutral Pd(II) complexes
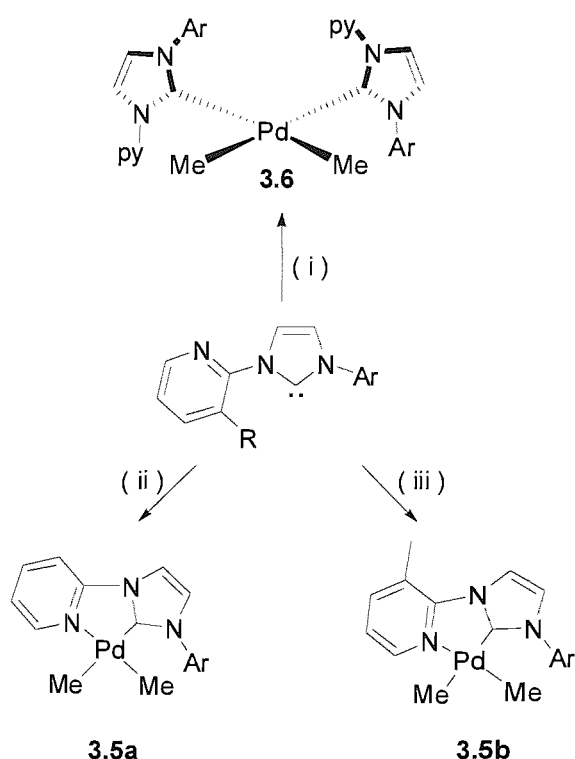
Scheme 3.2: Synthesis of complexes **3.5a**, **3.5b** and **3.6** (R = H, Me; Ar = 2,6-diisopropylphenyl). Reagents and conditions: (i): 0.5 equiv. Pd(tmeda)Me$_2$, THF, RT. (ii): 0.6 equiv. Pd(tmeda)Me$_2$, THF, -78 °C to RT. (iii): 1 equiv. Pd(tmeda)Me$_2$, THF, -78 °C to RT.

The synthesis of the pyridine functionalised NHC neutral Pd(II) complexes **3.5a**, **3.5b** and **3.6** was achieved by reacting the isolated free pyridine functionalised carbene with Pd(tmeda)Me$_2$ in the appropriate stoichiometry (Scheme 3.2).

In the case of **3.6**, the reaction was carried out at room temperature, and the metal precursor was added to the solution of the free carbene. This method of addition ensures an excess of the free carbene, in solution to avoid the formation of species **3.5a**. Complexes **3.5a** and **3.5b** are yellow air-stable compounds, soluble in CH_2Cl_2, toluene, THF and acetone, while they exhibit some solubility in Et_2O. Compound **3.6** is a pale yellow, air-stable solid, soluble in toluene, CH_2Cl_2, THF and acetone, whilst it is sparingly soluble in Et_2O.

Although complex **3.5b** was isolated by trapping the functionalised NHC with one equivalent of Pd(tmeda)Me_2, complex **3.5a** was not obtained in a pure form when a similar stoichiometry was used. The ^{1}H-NMR spectrum of an aliquot of the reaction mixture showed that the reaction had not proceeded to completion after stirring at room temperature overnight. Increasing the reaction time did not improve the situation, as unreacted Pd(tmeda)Me_2 remained in the solution, as demonstrated by ^{1}H-NMR spectroscopy. Using a 40 % excess of the free carbene circumvented the problem. The excess free carbene was removed by washing the product with cold (0 °C) Et_2O. Although this led to the isolation of the title compound pure by ^{1}H and ^{13}C\{^{1}H\}-NMR spectroscopy, the yield was substantially lower than that of the analogous compound **3.5b**. This is possibly due to the partial solubility of the compound in Et_2O.

3.2.3 Synthesis of cationic η^3-allyl NHC Pd(II) complexes

The synthesis of complexes **3.7** and **3.8a-c** is outlined in Scheme 3.3. Their isolation was achieved by following the synthetic protocols for either the phosphine or the pyridine functionalised NHC neutral palladium (II) complexes. The cationic complex **3.8b** was prepared by interaction of the *in situ* generated free NHC with [Pd(η^3-methallyl)(μ-Cl)]$_2$, in the absence of NaX (X$^-$ = BPh$_4$$^-$ or BAr$_4$^{F} $^-$). Complex **3.7** was isolated as the product of the reaction between the isolated free pyridine functionalised NHC with [Pd(η^3-methallyl)(μ-Cl)]$_2$ in the presence of NaBPh$_4$, but the intermediate chloride complex was not isolated. This intermediate may adopt two distinct molecular structures (Scheme 3.3). In the first case, the pyridine-NHC acts as a bidentate ligand, giving rise to a salt with the chloride being the counter anion (intermediate A). On the other case, the pyridine is not coordinating, and the NHC ligand is monodentate giving rise to a neutral complex (intermediate B). Such behaviour has been observed .[15]
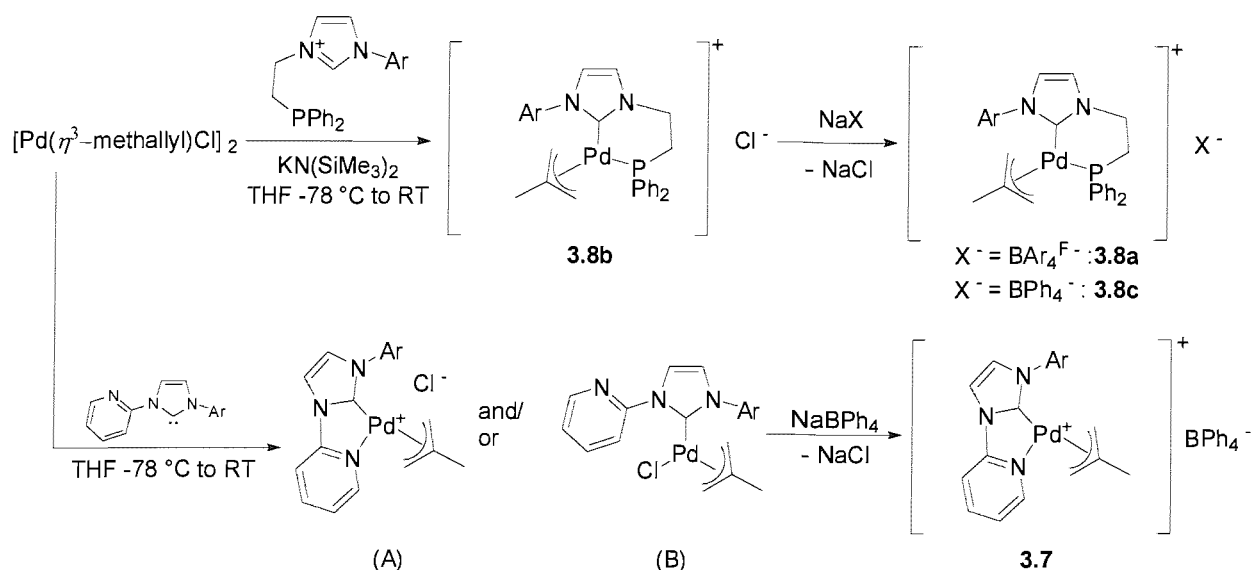
Scheme 3.3: Synthesis of cationic Pd(II) complexes (Ar = 2,6-diisopropylphenyl).

3.2.4 Characterisation of complexes 3.1a-b, 3.3 and 3.4

3.2.4.1 NMR spectroscopy

The most useful spectroscopic technique for verifying the formation of the phosphine functionalised NHC complexes **3.1a-b**, **3.3** and **3.4**, has proved to be $^{31}P\{^1H\}$-NMR spectroscopy. It serves as a sensitive probe, since upon complexation the chemical shift of the phosphine part of the ligand was significantly shifted downfield. This, in combination with the absence of the imidazolium proton in their ^1H-NMR spectra and the appearance of the carbene carbon at their $^{13}C\{^1H\}$-NMR spectra, supports the presence of chelating ligand. These characteristic shifts are outlined in Table 3.1.
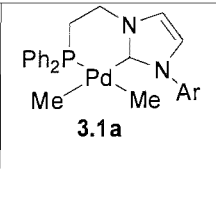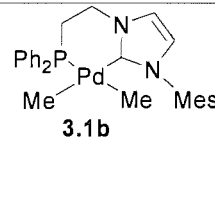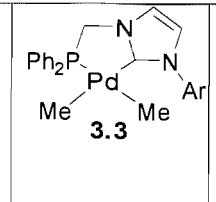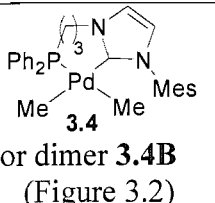
Complex	3.1a	3.1b	3.3	3.4 or dimer 3.4B (Figure 3.2)
$^{31}P\{^1H\}$-NMR δ(ppm)	12.4 (-22.4)	12.2 (-22.4)	32.7 (-10)	1.8 (-16.6)
$\delta(^{13}C\{^1H\})$-NCN	187.8	185.8	190.4	179.8

Table 3.1: ^{31}P-$\{^1H\}$-NMR chemical shifts of complexes **3.1a-b**, **3.3** and **3.4**. The values in parenthesis are the ^{31}P-$\{^1H\}$-NMR shifts of the imidazolium NHC precursors.

It is worth that noticing the $^{31}P\{^1H\}$ upfield shift of compounds **3.1a**, **3.1b** (12.4 and 12.2 ppm, respectively) compared to complex **3.3** (32.7 ppm), demonstrating the dependence of ^{31}P-NMR shifts on the size of the chelate ring. The proximity of the electronegative nitrogen atom could also account for this observed downfield shift.

Although compound **3.4** was not structurally characterised, a plausible structure is given in Figure 3.2. Alternative geometries with the ligand acting as bridging rather than chelating cannot be excluded (*i.e.* **3.4B**), especially bearing in mind the formation of a seven membered chelate ring (Figure 3.2). The dimeric structure **3.4A** (Figure 2) is not adopted as in such a conformation where the carbene-carbon and the phosphine are arranged *trans* to each other would result in the splitting of this carbon into a doublet. This is not observed in the $^{13}C\{^1H\}$-NMR spectrum of the compound (one singlet centred at 179.8 ppm). Mass spectrometry was unfortunately not informative.
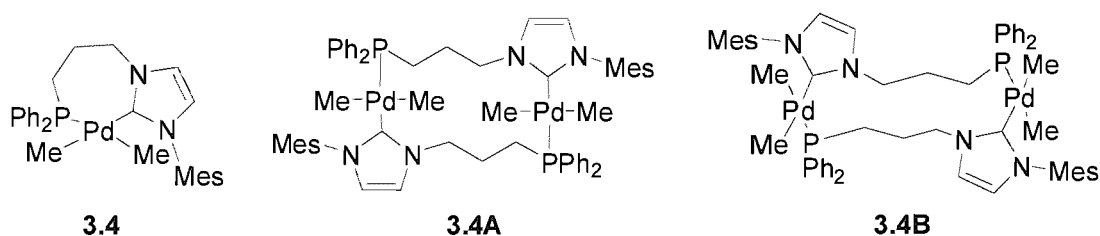
Figure 3.2: Possible structures for **3.4**.

The observed ^1H-NMR spectra of the new dimethyl complexes are consistent with nonsymmetric structures. They contain high field peaks assignable to inequivalent Pd-CH$_3$ groups (Table 3.2). These methyl peaks appear as a set of doublets, due to P-H coupling,

in the range of δ –0.6 to –0.1. They are almost isochronous to the methyls of Pd(tmeda)Me₂,[16] but more shielded relative to the methyls of cis-Pd(P₂)Me₂ (P = tertiary phosphine) [17] and the reported PdMe₂[(NHC-CH₂)₂].[18]

Complex	δ(^{1}H)-PdCH_3 (multiplicity, $^3J_{PH}$)
3.1a	-0.62 (d, 7.2 Hz), -0.41 (d, 8.2 Hz)
3.1b	-0.63 (d, 7.7 Hz), -0.48 (d, 6.5 Hz)
3.3	-0.53 (d, 8.1 Hz), -0.32 (d, 8.2 Hz)
3.4	-0.33 (d, 7.3 Hz), -0.19 (8.2 Hz)

Table 3.2: Pd-CH_3 NMR shifts (ppm) and their splittings.

The o-isopropyl methyls are diastereotopic and appear as a set of doublets. The nonsymmetric structure of complex **3.4** is further proved by the appearance of the mesityl methyl groups as three different singlets. This means that the plane of the mesityl group is not perpendicular to the plane of the ylidene moiety and the adaptation of an asymmetric conformation is the most plausible explanation.

The ethylene bridge protons appear as multiplets. In complex **3.3**, the methylenic bridge appears as a distinct doublet with a $^2J_{PH}$ of 3.30 Hz. The assignment of these protons was achieved on the basis of their shifts. The protons in the proximity of the ylidene moiety of the ligand are shifted downfield compared to the ones closer the phosphine moiety. The carbons of these methylenic space linkers appear as doublets. Their assignment is again based on the grounds of their relative NMR shifts. These shifts are provided in Table 3.3 along with the multiplicities due to ^{31}P splitting.
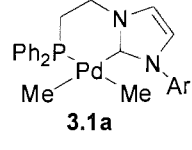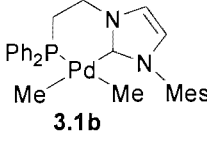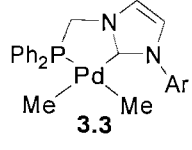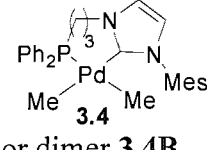
Complex	Ph₂P–Pd(Me)(Me)–N...N–Ar **3.1a**	Ph₂P–Pd(Me)(Me)–N...N–Mes **3.1b**	Ph₂P–Pd(Me)(Me)–N...N–Ar **3.3**	Ph₂P–Pd(Me)(Me)–N...N–Mes **3.4** or dimer **3.4B**
$\delta(^{13}C\{^1H\})$-CH₂ (multiplicity, $^nJ_{PC}$ [Hz])	30.3 (d, $^1J_{PC}$ = 14.6), 49.3 (d, $^2J_{PC}$ = 10.6)	31.1 (d, $^1J_{PC}$ = 14.2), 49.2 (d, $^2J_{PC}$ = 10.3)	51.9 (d, $^1J_{PC}$ = 24.5)	31.8 (d, $^1J_{PC}$ = 14.2), 35.6 (d, $^2J_{PC}$ = 11.1), 41.8 (d, $^3J_{PC}$ = 9.0)

Table 3.3: Chemical shifts (ppm) and multiplicities of methylenic bridge carbons

From the table above we can observe that the $^nJ_{PC}$ coupling constant increases in the order $^1J_{PC} > {}^2J_{PC} > {}^3J_{PC}$, as expected. It is also worth noticing that the magnitude of the $^1J_{PC}$ in the dimethyl complex **3.3** is significantly larger than the corresponding ones observed for the other dimethyl complexes. This methylenic carbon is also more de-shielded and it is shifted further downfield in comparison with the other carbon methylenic spacers α to the ylidene moiety of the phosphine-NHC hybrid ligand.

3.2.4.2 X-ray diffraction studies on complexes 3.1a and 3.3

Complexes **3.1a** and **3.3** were also characterised by single crystal X-ray diffraction. X-ray quality crystals of **3.1a** were obtained by layering a THF solution of the complex with ether. The structure of **3.1a** as determined by single crystal X-ray diffraction studies is shown in Figure 3.3. The geometry around the palladium centre is square planar and the ligand acts as a chelate occupying two *cis* positions. The two Pd-CH₃ bond lengths, 2.098(5) and 2.111(5) Å, are equal within the esds. The Pd-C(carbene) bond length at 2.088(5) Å is comparable to that recently reported,[16] where the NHC is *trans* to an alkyl group. The six-membered chelate ring is puckered, and the ligand bite angle is 91.06(14)°.

It is interesting to note that due to the fact that NHC ligands are better σ-donors than trialkylphosphines, they should be exerting a higher *trans* influence, which is not evidenced by the structural data of **3.1a**. The plane of the ylidene moiety of the ligand is also tilted relative to the plane defined by Pd(1), C(30) and C(31) by approximately 43.05°. This conformation is another proof of the low π-acidity of the NHC ligands.

Figure 3.3: ORTEP representation of the structure of **3.1a**, showing 50 % probability ellipsoids. H atoms have been omitted for clarity. Selected bond lengths (Å) and angles (°): C(1)-Pd(1) = 2.088(5), P(1)-Pd(1) = 2.2994(13), C(30)-Pd(1) = 2.098(5), C(31)-Pd(1) = 2.111(5); N(1)-C(1)-Pd(1) = 124(4), N(2)-C(1)-Pd(1) = 131.6(4), C(1)-Pd(1)-P(1) = 91.06(14), C(30)-Pd(1)-P(1) = 89.23(15), C(31)-Pd(1)-P(1) = 172.31(14), C(1)-Pd(1)-C(31) = 95.84(18), C(1)-Pd(1)-C(30) = 177.0(2), C(30)-Pd(1)-C(31) = 84.05(19).

Crystals of the homologous compound **3.3** were grown by slow diffusion of petroleum ether to a THF solution of the complex. An ORTEP diagram of **3.3** is shown in Figure 3.4. Again the complex adopts a square planar geometry with the ligand occupying two *cis* positions. The ylidene plane forms a dihedral angle of approximately 20.83° with the plane defined by the Pd-alkyl bonds. This dihedral angle is significantly smaller than the one observed for complex **3.1a**. This is probably due to the formation of a more rigid five-membered ring. This X-ray diffraction study again shows a trend of suppressed *trans* influence, as the two inequivalent Pd-Me group bond lengths are the same within esds. The bite angle of the ligand is 80.39(14)° and is smaller compared to that of **3.1a** (91.06(14)°). This decrease is expected due to the formation of a five-membered chelate.
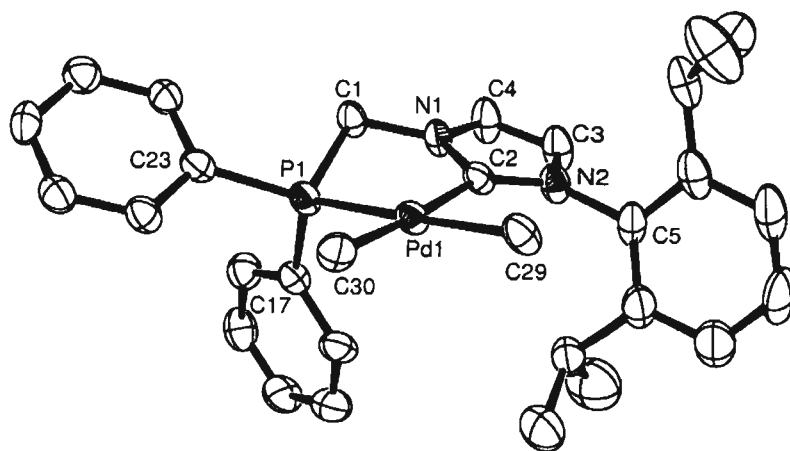
Figure 3.4: ORTEP representation of the structure of **3.3**, showing 50 % probability ellipsoids. H atoms have been omitted for clarity. Selected bond lengths (Å) and angles (°): C(2)-Pd(1) = 2.068(5), P(1)-Pd(1) = 2.293(3), C(30)-Pd(1) = 2.067(5), C(29)-Pd(1) = 2.090(5); C(2)-Pd(1)-P(1) = 80.39(14), C(30)-Pd(1)-P(1) = 98.61(14), C(29)-Pd(1)-P(1) = 176.56(14), C(2)-Pd(1)-C(29) = 96.17(19), C(30)-Pd(1)-C(2) = 176.0(2), C(30)-Pd(1)-C(29) = 84.82(19).

Table 3.4 contains a list of selected bond lengths of the complexes **3.1a** and **3.3**. A comparison of this bond lengths reveals that they are in the same range within esds.

Bond	Bond lengths for **3.1a** (Å)	Bond lengths for **3.3** (Å)
Pd-C(carbene)	2.088(5)	2.068(5)
Pd-P	2.2994(13)	2.293(3)
Pd-CH$_3$ *trans* to carbene	2.098(5)	2.067(5)
Pd-CH$_3$ *trans* to phosphorous	2.111(5)	2.090(5)

Table 3.4: Comparison of bond lengths between complexes **3.1a** and **3.3**.

73

3.2.5 Characterisation of complexes 3.5a, 3.5b and 3.6

3.2.5.1 NMR spectroscopy

The ^{1}H-NMR spectra of complexes **3.5a** and **3.5b** (Figure 3.5) account for non-symmetric structures. This lack of symmetry is evidenced by the existence of a pair of singlets in the metal-alkyl region of their spectra. ThePd-CH_3 are shifted further downfield (0.01 and 0.12 ppm for **3.5a**, and 0.12 and 0.22 for **3.5b**) compared to the dimethyl complexes incorporating the phosphine-NHC hybrid ligand, which is probably due to the less electron-donating character of the pyridine-NHC, compared to the mixed phosphine-NHC ligand.

3.5a   **3.5b**   **3.6**
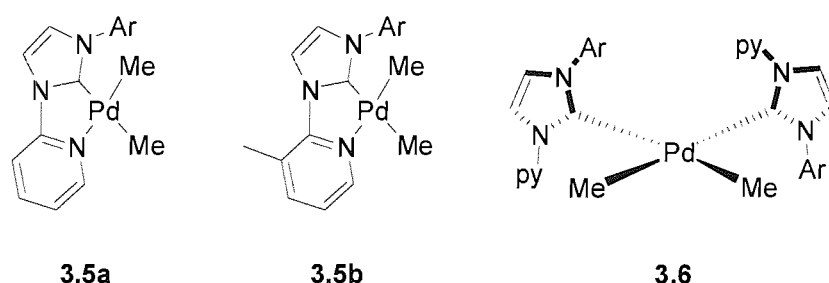
Figure 3.5: Pyridine functionalised NHC Pd(II) neutral complexes (Ar = 2,6-diisopropylphenyl).

The relative location of the inequivalent Pd-CH$_3$ groups in complexes **3.5a** and **3.5b** was determined by NOESY experiments. In both cases, they revealed a cross-peak between the metal alkyl group shifted further downfield and the α-CH hydrogen of the pyridine heterocycle. This means that this CH$_3$ group is *trans* to the NHC moiety of the ligand (Figure 3.6).
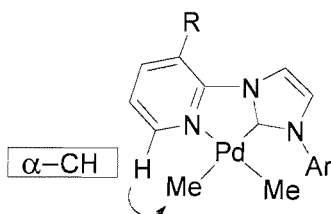
Figure 3.6: Topology of Pd-CH$_3$ groups as determined by NOESY.

The $^{13}C\{^1H\}$-NMR spectra of **3.5a** and **3.5b** contained peaks assignable to the Pd-CH3 methyls (-0.1 and 0.0 ppm for **3.5a**/0.12 and 0.22 ppm, for **3.5b**). Unfortunately, in both cases, the carbene carbons could not be located.

In contrast to the unsymmetrical compounds discussed above, the ^1H-NMR spectrum of complex **3.6**, suggests the existence of a C_2 symmetry rotation axis. The alkyl region of the spectrum contains two pairs of doublets and one pair of septets. This means that there are four different isopropyl methyl environments and two inequivalent methinic protons. Furthermore the spectrum has only one singlet at the metal alkyl region (- 0.11 ppm) integrating for six protons. The latter signal correlates with a singlet at –0.4 ppm found in the $^{13}C\{^1H\}$-NMR spectrum of the complex. Finally, unlike 3.5a and 3.5b only one carbene carbon was located at 200.1 ppm in the $^{13}C\{^1H\}$-NMR spectrum. The structure proposed in Figure 3.5 complies with these observations.

3.2.5.2 X-ray diffraction studies on complexes 3.5b and 3.6

The dimethyl complex **3.5b** was crystallised by slow diffusion of petroleum ether in a toluene solution of the complex. The yellow crystals were analysed by X-ray diffraction. Although the R factor of the model is just above 10%, connectivity can be addressed and comparisons with molecules **3.1a**, **3.3** can be made. The ORTEP representation of this crystal structure is given in Figure 3.7.
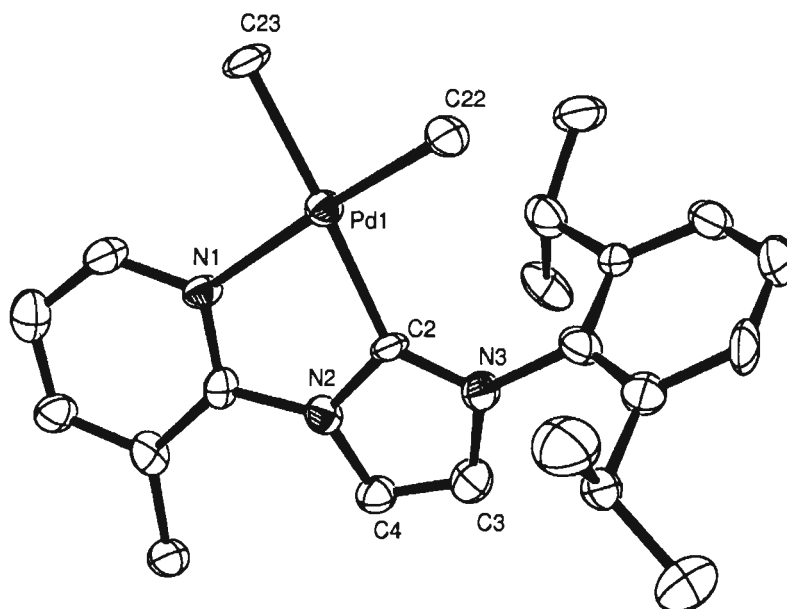
Figure 3.7: ORTEP representation of the structure of **3.5b**, showing 50% probability ellipsoids. H atoms have been omitted for clarity. Selected bond lengths (Å) and angles (°): C(2)-Pd(1) = 2.038(10), N(1)-Pd(1) = 2.130(9), C(22)-Pd(1) = 2.017(11), C(23)-Pd(1) = 2.082(11); C(22)-Pd(1)-C(2) = 100.7(5), C(22)-Pd(1)-C(23) = 85.1(5), C(2)-Pd(1)-C(23) = 172.2(5), C(22)-Pd(1)-N(1) = 174.5(5), C(2)-Pd(1)-N(1) = 76.8(4), C(23)-Pd(1)-N(1) = 97.8(4)

The geometry around the metal centre is square planar with the ligand occupying two *cis* positions. The trend of suppressed *trans* influence from the NHC moiety of the ligand is again apparent, as evidenced by the Pd-CH$_3$ bond lengths that are as previously seen, equal within esds. The ligand adopts an almost coplanar conformation with the pyridine plane tilted, in order to accommodate the steric requirements of the methyl in the three position of the pyridine heterocycle. The ligand bite angle of 76.8(4)° is smaller than the ones observed for complexes **3.1a** (91.06(14)°) and **3.3** (80.39(14)°) due to the extra rigidity of the ligand architecture.

The bond lengths of the two different types of Pd-C bonds (Pd-NHC and Pd-CH$_3$) in compounds **3.1a**, **3.3** and **3.5b** are similar within esds. This indicates that any π-backbonding in **3.5b** is negligible.

The C_2 symmetrical conformation of complex **3.6** was confirmed by an X-ray diffraction study performed on crystals grown from slow cooling of a toluene solution of

the complex. It revealed that the compound adopts the expected symmetry in the solid state as well. An ORTEP diagram of this crystal structure is shown in Figure 3.8.
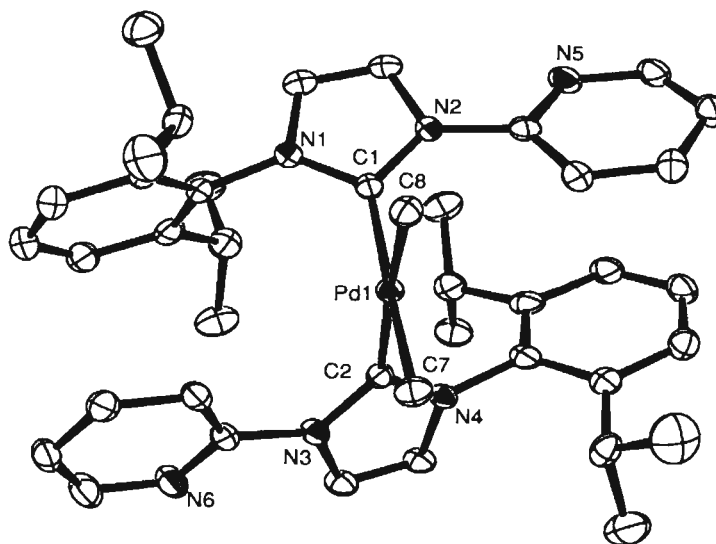
Figure 3.8: ORTEP representation of the structure of **3.6**, showing 50% probability ellipsoids. H atoms have been omitted for clarity. Selected bond lengths (Å) and angles (°): C(1)-Pd(1) = 2.058(3), C(2)-Pd(1) = 2.064(5), Pd(1)-C(7) = 2.101(1), Pd(1)-C(8) = 2.103(5); C(8)-Pd(1)-C(2) = 170.87(11), C(7)-Pd(1)-C(1) = 171.08, C(1)-Pd(1)-C(8) = 87.96(15), C(2)-Pd(1)-C(7) = 87.73(17), C(1)-Pd(1)-C(2) = 101.16(16).

The two ligand molecules are monodentate occupying two *cis* positions, with the geometry around the metal centre being square planar. The C_2 rotation axis passes through the plane defined by the palladium carbon bonds. The Pd-C(carbene) bond distances are identical and are in the same range (within esds) with the ones observed for the bidenate complexes described above. The same applies for the Pd-CH$_3$ bond lengths. The planes of the ylidene moieties form a dihedral angle of approximately 75.5° with the plane of the metal centre. The molecule adopts this C_2 symmetric conformation in order to accommodate the steric requirements of the bulky aryl groups, which are probably responsible for the C(1)-Pd(1)-C(2) angle of 101.16(16)°.

The nitrogen donor atom of the pyridine heterocycle is pointing at the opposite direction of the carbene palladium bond. This was observed in the crystal structure of the free carbene and was attributed to the minimisation of electrostatic repulsion between the two lone electron pairs. The pyridine heterocycle is not coplanar with the ylidene moiety

77

but is tilted in respect with the carbene plane by approximately 19.25°. This dihedral angle is very close to the value of found for the free carbene **2.9c** (18.85°) (Figure 3.9). This also suggests that there is no π-conjugation between the pyridine and the ylidene moieties of the ligand.

The above observations suggest that there is an energy rotation barrier for the pyridine group. This in turn means that when the ligand is forced to act as bidentate, through adjustment of the reaction stoichiometry, the substitution of the labile ligand (in this case tmeda) happens in two steps: coordination of the carbene carbon, followed by rotation of the pyridine heterocycle to donate its lone pair, thus forming a five-membered ring. The rotation of the pyridine moiety is possible as electrostatic destabilisation seizes to be an important factor due to the coordination of the carbene carbon lone pair. Of course in the case of **3.6**, this rotation is not achieved due to the saturation of the available coordination sites by two carbene ligands.
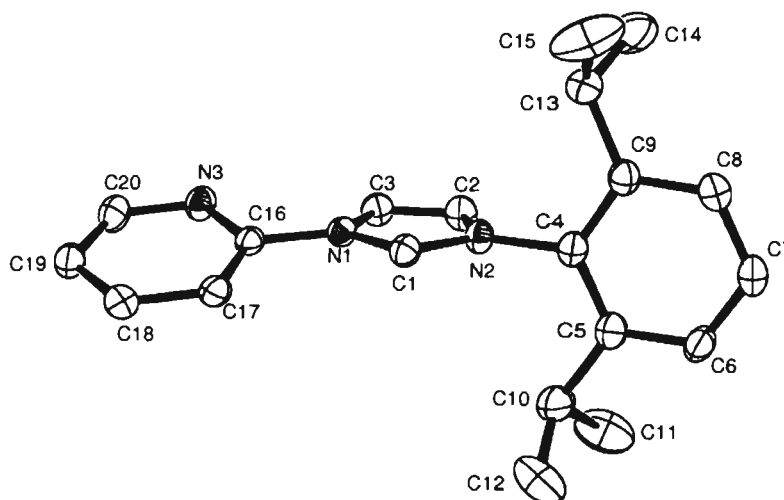
Figure 3.9: ORTEP representation of structure of **2.9c**. Hydrogens have been omitted for clarity.

3.2.6 Characterisation of complexes 3.2a and 3.2b

3.2.6.1 NMR spectroscopy

The existence of complexes **3.2a** and **3.2b** (Figure 3.10) in solution was confirmed by NMR spectroscopy. Their $^{31}P\{^{1}H\}$-NMR spectra consisted of one peak at 21 ppm for

3.2a and 19 ppm for **3.2b**. These peaks are significantly shifted downfield compared to the $^{31}P\{^1H\}$ shifts (-22.4 ppm) of the imidazolium NHC precursors signifying that the phosphine part of the ligand has coordinated. Further proof of their formation was the absence of the 2 position imidazolium proton in their ^1H-NMR spectra, and the appearance in their $^{13}C\{^1H\}$-NMR spectra of the carbene carbon (160.8 ppm for **3.2a** and 162.4 for **3.2b**).
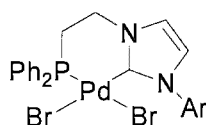
Figure 3.10: Complexes **3.2a-b** (Ar = 2,6-Pr^i-C$_6$H$_3$:**3.2a**; Ar = Mes:**3.2b**).

Unlike the dimethyl complexes **3.1a** and **3.1b**, no splitting, due to P-C coupling, is observed for the methylenic space linkers and they appear as two singlets in their $^{13}C\{^1H\}$-NMR spectra (29.8 and 48.0 ppm for **3.2a** and 30.1 and 48.0 ppm for **3.2b**). The ^1H-NMR resonances for these methylenic protons exhibit the same characteristics discussed for the dimethyl complexes **3.1a** and **3.1b**.

The o-isopropyl methyls of the aryl group in **3.2a** are diastereotopic and appear as a set of doublets in its ^1H-NMR spectrum. The alkyl region in the ^1H-NMR spectrum of **3.2b** consists of two singlets in a 2:1 ratio, assignable to the methyls of the mesityl group.

3.2.6.2 X-ray diffraction study of complex 3.2b

X-ray quality crystals of **3.2b** were obtained by slow diffusion of ether in a CH$_2$Cl$_2$ solution of the complex. The structure of the molecule as determined by single crystal X-ray diffraction, is shown in Figure 3.11. The geometry around the metal is square planar, with the ligand occupying two cis sites. The Pd-Br bond distance $trans$ to the phosphorus is longer than that $trans$ to the NHC by $ca.$ 0.03 Å. This observation is in contrast to that expected on the basis of the relative $trans$ influence of the phosphine and the NHC ligands. The Pd-C(carbene) is, within error, the same as that observed for the complexes discussed above. The Pd-P bond length in **3.2b** (2.2461(7) Å) is shorter than those observed for **3.1a** (2.2994(13) Å), **3.3** (2.090(5) Å) as expected. The dihedral angle of the ylidene and metal centre planes, is approximately 59.2° and is significantly larger than the

one observed for **3.1a** (43.05°). This is probably because of the less bulky mesityl group allowing the ligand architecture to be more flexible.
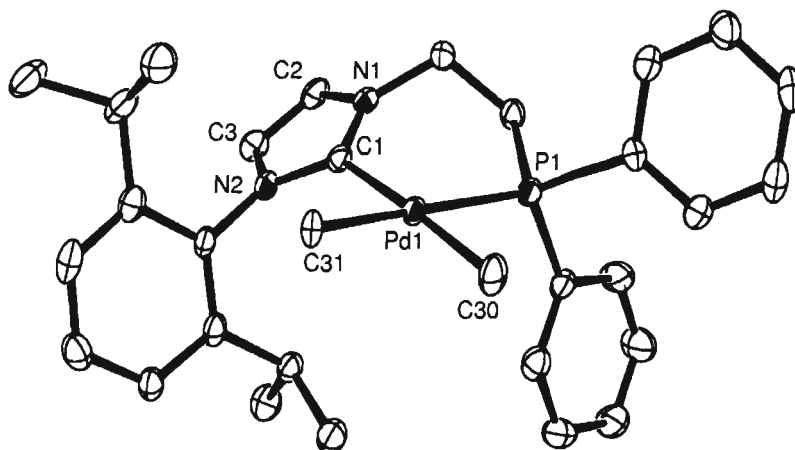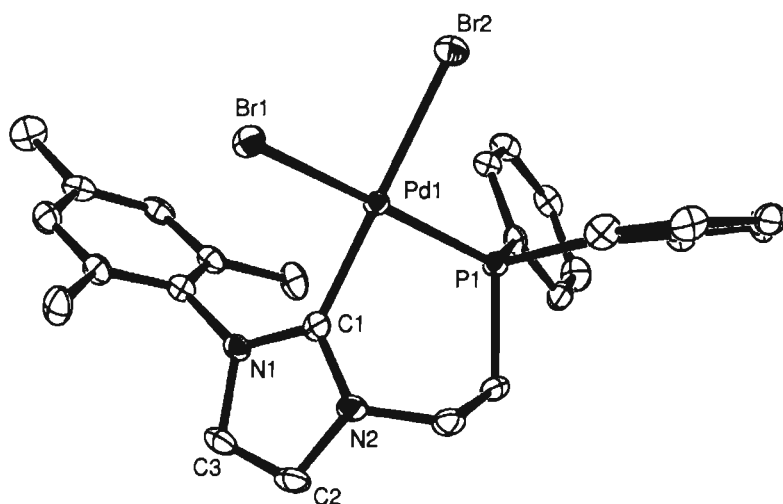

Figure 3.11: ORTEP representation of the structure of **3.2b**, showing 50 % probability ellipsoids. H atoms have been omitted for clarity. Selected bond lengths (Å) and angles (°): C(1)-Pd(1) = 1.996(3), P(1)-Pd(1) = 2.2461(7), Pd(1)-Br(1) = 2.4989(3), Pd(1)-Br(2) = 2.4708(3); C(1)-Pd(1)-Br(2) = 176.63(7), C(1)-Pd(1)-P(1) = 89.24(8), C(1)-Pd(1)-Br(1) = 90.37(7), P(1)-Pd(1)-Br(1) = 168.96(2), P(1)-Pd(1)-Br(2) = 89.32(2), Br(2)-Pd(1)-Br(1) = 91.622(11).

3.2.7 Characterisation of complexes 3.8a-c and 3.7

3.2.7.1 NMR spectroscopy

The formation of **3.8a-c** and **3.7** (Figure 3.12) was verified by ^{1}H, ^{13}C$\{^1$H$\}$ and ^{31}P$\{^1$H$\}$- NMR spectroscopy. The ^{1}H, ^{13}C$\{^1$H$\}$ and DEPT-135 spectra showed a lack of symmetry in the molecule. The ^{1}H-NMR showed a multiplet corresponding to the isopropyl methyls as opposed to the two doublets characteristically seen for these groups. The methylenic protons of the η^3-methallyl are diasteretopic and appear as unresolved multiplets due to geminal and phosphorus coupling in complexes of series **3.8**. In complex **3.7** these protons appear as a set of broad singlets centred at 3.2 and 4.1 ppm and as a broad multiplet coinciding with the methinic septet.

X⁻ = BAr₄ᶠ⁻ :**3.8a**
X⁻ = Cl⁻ :**3.8b**
X⁻ = BPh₄⁻ : **3.8c**

3.7
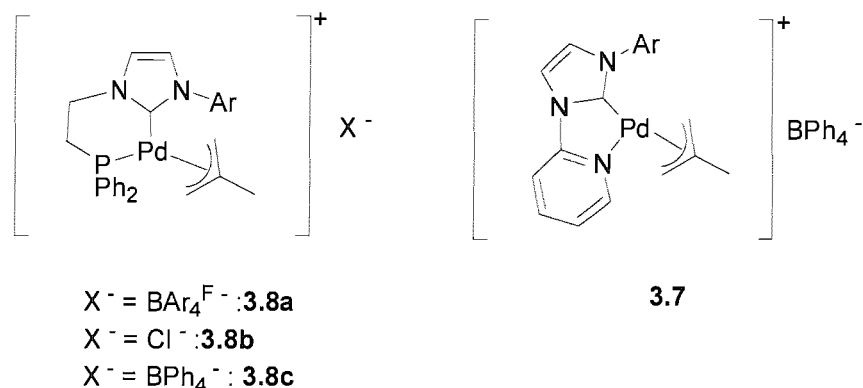
Figure 3.12: Cationic Pd(II) complexes **3.8a-c** and **3.7**.

The DEPT-135 spectrum consisted of seven peaks in the methyl region (six for the methyls and methines of the two *o*-isopropyl groups, and one for the methyl of the η^3-allyl moiety). Four different methylenic carbons were also observed (two for the bridge and two for the methylene carbons of the η^3-methallyl). The nonsymmetric structure of these compounds was also evidenced by the appearance of extra peaks at the aromatic region of their $^{13}C\{^1H\}$ spectra. These peaks are assigned to the quaternary aromatic carbons *ipso* to the inequivalent isopropyl groups. This lack of symmetry is further induced to all carbons of the aryl group adjusted to the ylidene part of the ligand. Unfortunately in none of these complexes was the carbene carbon observed.

The formation of complex **3.8b** is based on its spectroscopic characterisation. Its ^1H-NMR spectrum exhibits the same features as for its other cationic analogues **3.8a** and **3.8c**. Further proof that the ligand acts as a bidentate is provided by the $^{31}P\{^1H\}$-NMR shift of the compound (21.0 ppm), which is isochronous with its well defined cationic analogues **3.8a** and **3.8c** (22.0 and 22.3 ppm respectively).

The existence of one isomer in solution was confirmed by $^{31}P\{^1H\}$, $^{13}C\{^1H\}$ and ^1H-NMR spectroscopy. The $^{31}P\{^1H\}$ spectrum of any compound of series **3.8** consisted of one singlet in the region of 21-22 ppm. Moreover the ^1H spectra of these complexes had only one characteristic singlet for the methyl of the allylic moiety. Finally, there was only one characteristic peak for the allylic quaternary carbon in the area of 127-128 ppm.

Layering a CH_2Cl_2 solution of the complex with ether afforded X-ray-quality crystals of **3.8c**. An ORTEP diagram of the cationic species is shown in Figure 3.15. The complex adopts a square planar geometry, with the ligand occupying two *cis* positions. The Pd-C(carbene) and Pd-P bond distances are within experimental errors the same as the ones observed for complex **3.1a**.
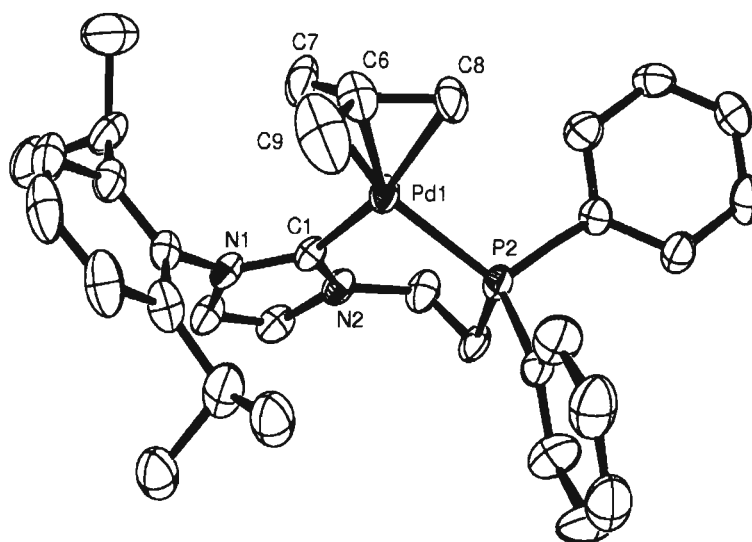
Figure 3.13: ORTEP representation of the structure of the cation in **3.8c**, showing 50 % probability ellipsoids. The BPh_4^- counter anion and H atoms have been omitted for clarity. Selected bond lengths (Å) and angles (°): C(1)-Pd(1) = 2.046(4), P(2)-Pd(1) = 2.2815(12), C(8)-Pd(1) = 2.154(4), C(6)-Pd(1) = 2.202(5), C(7)-Pd(1) = 2.168(5), C(8)-C(6) = 1.429(7), C(9)-C(6) = 1.504(9), C(6)-C(7) = 1.375(8); C(1)-Pd(1)-P(2) = 92.51(13), C(1)-Pd(1)-C(8) = 167.74(19), C(1)-Pd(1)-C(7) = 101.87(19), C(8)-Pd(1)-C(7) = 66.98(19), C(1)-Pd(1)-C(6) = 133.84(18), C(8)-Pd(1)-C(6) = 38.27(18), C(7)-Pd(1)-C(6) = 36.8(2), C(8)-Pd(1)-P(2) = 97.99(13), C(7)-Pd(1)-P(2) = 163.89(16), C(6)-Pd(1)-P(2) = 132.08(15), C(7)-C(6)-C(8) = 116.5(5), C(8)-C(6)-C(9) = 118.2(6), C(7)-C(6)-C(9) = 123.8(6).

The Pd-C(carbene) and Pd-P bond distances are in agreement with reported NHC [19] or phosphine [20] η^3-allyl palladium (II) complexes. The Pd-C(methylenic allyl) bond

lengths are virtually the same, while the Pd-C(quaternary allyl) bond distance is lengthened by *ca.* 0.05 Å. The allylic unit adopts a conformation where its methylenic carbons (C(7) and C(8)) are coplanar with the metal centre, while the quaternary (C(6)) and methyl carbons (C(9)) are pointing outwards. The two planes form a dihedral angle of approximately 87.7°. This conformation accounts for the asymmetry observed in the isopropyl region of the complex's ^{1}H and ^{13}C{^{1}H} spectra (four different methyls: up and down, right and left).

The analogous complex **3.7** was crystallized by slow diffusion of ether into a CH_2Cl_2 solution of the complex. Figure 3.14 shows the ORTEP diagram of the complex. The geometry around the metal centre is square planar with the allylic unit adopting a conformation with almost similar metric data (dihedral angle of 89.56°) to that observed for **3.8c**. The ligand occupies two *cis* positions with the ligand being almost planar.
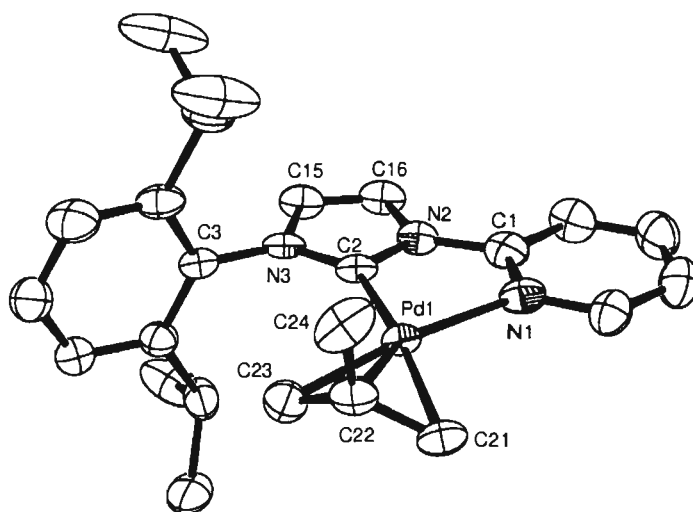
Figure 3.14: ORTEP representation of the cation in **3.7**, showing 50 % probability ellipsoids. The BPh_4^- counter anion and H atoms have been omitted for clarity. Selected bond lengths (Å) and angles (°):C(2)-Pd(1) = 2.014(3), C(21)-Pd(1) = 2.165(4), C(22)-Pd(1) = 2.160(4), C(23)-Pd(1) = 2.096(5), N(1)-Pd(1) = 2.113(4); C(2)-Pd(1)-C(23) = 106.53(18), C(2)-Pd(1)-N(1) = 78.44(16), C(23)-Pd(1)-N(1) = 173.28(15), C(2)-Pd(1)-C(22) = 139.74(18) C(23)-Pd(1)-C(22) = 38.73(17), N(1)-Pd(1)-C(22) = 138.40(15), C(2)-Pd(1)-C(21) = 172.87(18), C(23)-Pd(1)-C(21) = 68.06(18), N(1)-Pd(1)-C(21) = 106.59(16), C(22)-Pd(1)-C(21) = 37.66(17), C(21)-C(22)-C(23) = 116.3(4), C(21)-C(22)-C(24) = 120.2(4), C(23)-C(22)-C(24) = 121.8(4).

The Pd-C(carbene) bond is similar to the one described above within esds. A comparison of selected bond distances is given in Table 3.5.

Bond	Bond lengths for **3.8c** (L = phosphine) (Å)	Bond lengths for **3.7** (L = pyridine) (Å)
Pd-C(carbene)	2.046(4)	2.014(3)
Pd-L (L = pyridine, phosphine)	2.2815(12)	2.113(4)
Pd-CH$_2$ *trans* to carbene	2.154(4)	2.165(4)
Pd-CH$_2$ *trans* to L	2.168(5)	2.096(5)
Pd-C (quaternary)	2.202(5)	2.160(4)

Table 3.5: Comparison of selected bond distances of complexes **3.8c, 3.7**.

Firstly, the Pd-C(23) bond distance (allylic methylene *trans* to the pyridine) is significantly shorter than the Pd-C(21) bond distance (allylic methylene *trans* to the carbene). This is consistent with the stronger *trans* influence exerted by the NHC. On the other hand we can see that the analogous distances in **3.8c** are similar within experimental errors. Secondly, the Pd-(η^3-allyl) bond distances in **3.8c** are significantly elongated in comparison to **3.7**. This is probably due to the overall stronger *trans* influence of the phosphine functionalised carbene, compared to the pyridine-NHC hybrid architecture.

3.3 Conclusions

In this chapter the synthesis of novel chelate phosphine and pyridine functionalised NHC complexes of palladium(II) has been described. This new family of square-planar complexes exhibits some interesting characteristics such as electronic asymmetry imposed by the combination of a "classical" donor ligand and a NHC within the ligand architecture. X-ray diffraction studies on some of these complexes have revealed interesting structural motifs like the suppression of *trans* influence of the NHC part of the ligand *versus* that of the "classical" donor ligand.

3.4 Experimental:

General materials: Pd(tmeda)Me$_2$,[14] Pd(1,5-COD)Br$_2$[21] and [Pd(η^3-methallyl)Cl]$_2$[22] were prepared according to literature procedures.

Preparation of palladium complexes 3.1a,b, 3.2a,b, 3.3 and 3.4. General Method: To a mixture of the appropriate imidazolium salt (1 equiv.) and KN(SiMe$_3$)$_2$ cooled to -78 °C was added precooled THF (-78 °C) with vigorous stirring. The solution of the free carbene generated in this way was added after 10 min *via* cannula to a solution of the palladium precursor in THF at -78 °C. After the mixture was stirred for 10 min at –78 °C it was allowed to reach room temperature and stirred for 2 hours. Evaporation of the volatiles under reduced pressure, extraction of the residue into cold (0 °C) dichloromethane, filtration of the cold solution through Celite, concentration of the filtrates to 1-3 mL, and addition of ether precipitated the product as a white to beige solid, which was collected by filtration and dried under vacuum.

3.1a: This was prepared using 110 mg (0.397 mmol) of Pd(tmeda)Me$_2$, 232 mg **2.4a** (1 equiv.) and 95 mg (1.1 equiv.) of KN(SiMe$_3$)$_2$. ^{1}H-NMR δ(CD$_2$Cl$_2$) : -0.62 (3H, d, $^3J_{PH}$ = 7.2 Hz, PdCH_3), -0.41 (3H, d, $^3J_{PH}$ = 8.2 Hz, PdCH_3), 1.05 (6H, d, $^3J_{HH}$ = 6.7 Hz, CH(CH_3)$_2$), 1.12 (6H, d, $^3J_{HH}$ = 6.7 Hz, CH(CH_3)$_2$), 2.32 (2H, m, (PPh$_2$CH_2CH$_2$-ylid)PdMe$_2$), 2.74 (2H, sept., $^3J_{HH}$ = 6.7 Hz, CH(CH$_3$)$_2$), 4.35 and 4.42 (1H each, dt, (PPh$_2$CH$_2$CH_2-ylid)PdMe$_2$), 6.81 (1H, d, $^3J_{HH}$ = 1.5 Hz ylidene backbone), 7.05 (1H, d, $^3J_{HH}$ = 1.49 Hz, ylidene backbone),7.12 (1H, s, aromatic), 7.23 (1H, s, aromatic), 7.30-7.44 (m, 7H, aromatics), 7.61-7.78 (m, 4H, aromatics); ^{13}C{^{1}H}-NMR δ(d_5-py): 0.1 (d, $^2J_{PC}$ = 10 Hz, PdCH_3), 2.4 (d, $^2J_{PC}$ = 9.3 Hz, PdCH$_3$), 24.4 (s, CH(CH_3)$_2$), 26.0 (s, CH(CH_3)$_2$), 29.7 (s, CH(CH$_3$)$_2$), 30.3 (d, $^1J_{PC}$ =14.6 Hz, (PPh$_2$CH$_2$CH$_2$-ylid)PdMe$_2$), 49.4 (d, $^2J_{PC}$ =10.6 Hz, (PPh$_2$CH$_2$CH$_2$-ylid)PdMe$_2$), 121.0 (s, ylidene backbone), 125.2 (s, aromatic), 125.4 (s, aromatic), 129.7 (d, J_{PC} = 9.0 Hz, aromatic), 130.3 (d, J_{PC} = 7.0 Hz, aromatic), 130.8 (s, aromatic), 134.7 (s, aromatic), 134.8 (d, J_{PC} = 5.0 Hz, aromatic), 147.1 (s, *ipso* carbon of the aryl group), 187.8 (s, NC N); ^{31}P{^{1}H}-NMR: δ(CD$_2$Cl$_2$): 12.4 (s, (*P*Ph$_2$CH$_2$CH$_2$-ylid)PdMe$_2$). ES$^+$: 561 [(PPh$_2$CH$_2$CH$_2$-ylid)PdMe]$^+$, 602 [M+CH$_3$CN]$^+$. Anal. Found: C, 64.50; H, 6.77; N, 4.81 %. Calcd for C$_{31}$H$_{39}$N$_2$PPd: C, 64.52; H, 6.81; N, 4.85 %. X-ray quality crystals were grown by layering a THF solution of **3.1a** with Et$_2$O.

3.1b: This was prepared using 100 mg (0.397 mmol) of Pd(tmeda)Me$_2$, 194 mg(1 equiv.) of **2.4b** and 87mg of KN(SiMe$_3$)$_2$ (1.1 equiv.). Yield: 162 mg (75 %). ^{1}H-NMR δ(CD$_2$Cl$_2$): -0.63 (3H, d, $^3J_{PH}$ = 7.7 Hz, PdCH_3), -0.48 (3H, d, $^3J_{PH}$= 6.5 Hz PdCH_3), 2.01

(6H, s, *o*-methyls), 2.18 (2H, br. s, (PPh$_2$C*H$_2$*CH$_2$-ylid)PdMe$_2$), 2.34 (3H, s, *p*-methyl), 4.41 and 4.53 (1H each, dt (PPh$_2$CH$_2$C*H$_2$*-ylid)PdMe$_2$), 6.71 (1H, d, $^3J_{HH}$ = 1.5 Hz, ylidene backbone), 6.93 (2H, br. s, aromatics), 7.02 (1H, d, $^3J_{HH}$= 1.5 Hz ylidene backbone), 7.44 (5H, m, aromatics), 7.52-7.77 (5H, m, aromatics); ^{13}C{^{1}H}-NMR δ(*d$_5$*-py): 0.04 (d, $^2J_{PC}$ = 9.9 Hz, PdC*H$_3$*), 1.9 (d, $^2J_{PC}$ = 9.3 Hz, PdC*H$_3$*), 18.1 (s, *o*-methyls), 22.2 (s, *p*-methyls), 31.1 (d, $^1J_{PC}$ = 14.2 Hz, (PPh$_2$C*H$_2$*CH$_2$-ylid)PdMe$_2$), 49.2 (d, $^2J_{PC}$ = 10.3 Hz, (PPh$_2$CH$_2$C*H$_2$*-ylid)PdMe$_2$), 120 (s, ylidene backbone), 120.5 (s, ylidene backbone), 122.5 (s, aromatic), 123.8 (d, J_{PC} = 8.1 Hz, aromatic), 124.2 (s, aromatic), 124.7 (s, aromatic), 126.2 (d, J_{PC} = 9.1 Hz, aromatic), 126.4 (d, J_{PC} = 5.0 Hz), 128.6 (s, aromatic), 148.5 (s, *ipso* carbon of the aryl group), 185.8 (s, NC*N*); ^{31}P{^{1}H}-NMR δ(CD$_2$Cl$_2$) 12.2 (s, (*P*Ph$_2$CH$_2$CH$_2$-ylid)PdMe$_2$); ES$^+$: 519 [(PPh$_2$CH$_2$CH$_2$-ylid)PdMe]$^+$, 560 [M+CH$_3$CN]$^+$. Anal. Found: C, 57.33; H, 5.73; N, 4.49 %. Calcd for C$_{28}$H$_{33}$N$_2$PPd.CH$_2$Cl$_2$: C, 56.19; H, 5.69; N, 4.52 %.

3.2a: This was prepared using 100 mg (0.267 mmol) Pd(COD)Br$_2$, 143 mg of **2.4a** (1 equiv.) and 59 mg of KN(SiMe$_3$)$_2$ (1.1 equiv.). Yield: 134 mg (70 %).

^{1}H-NMR δ(CD$_2$Cl$_2$) : 0.92 (6H, d, $^3J_{HH}$ = 6.8 Hz, CH(C*H$_3$*)$_2$), 1.33 (6H d, $^3J_{HH}$ = 6.8 Hz, CH(C*H$_3$*)$_2$), 1.91 (2H, m, (PPh$_2$C*H$_2$*CH$_2$-ylid)PdBr$_2$), 2.12 (2H, sept., $^3J_{HH}$ = 6.8 Hz, C*H*(CH$_3$)), 4.32 and 4.41 (1H each, dt, (PPh$_2$CH$_2$C*H$_2$*-ylid)PdBr$_2$), 6.93 (1H, s, (PPh$_2$C*H$_2$*CH$_2$-ylid)PdBr$_2$), 7.40-7.72 (11H m, aromatics), 7.73-7.82 (3H, m, aromatics); ^{13}C{^{1}H}-NMR δ(CD$_2$Cl$_2$): 20.0 (s, CH(C*H$_3$*)$_2$), 23.5 (s, CH(C*H$_3$*)$_2$), 26.2 (s, C*H*(CH$_3$)$_2$), 29.8 (s, (PPh$_2$C*H$_2$*CH$_2$-ylidene)PdBr$_2$), 48.0 (s, (PPh$_2$CH$_2$C*H$_2$*-ylidene)PdBr$_2$), 122.2 (s, ylidene backbone), 124.6 (s, ylidene backbone), 127.1 (s, aromatic), 129.4 (d, J_{PC} = 10.7 Hz, aromatic), 130.3 (s, aromatic), 131.5 (s, aromatic), 132.1 (d, J_{PC} = 2.9 Hz, aromatic), 134.4 (d, J_{PC} = 9.7 Hz, aromatic), 136.8 (s, aromatic), 146.1 (s, ipso carbon of the aryl group), 160.8 (s, NC*N*); ^{31}P{^{1}H}-NMR δ(CD$_2$Cl$_2$): 21 (s, (*P*Ph$_2$CH$_2$CH$_2$-ylidene)PdBr$_2$). Anal. Found: C, 50.88; H, 4.94; N, 3.55 %. Calcd for C$_{29}$H$_{33}$Br$_2$N$_2$PPd.Et$_2$O: C, 50.76; H, 5.55; N, 3.59 %.

3.2b: This was prepared using 100 mg (0.267 mmol) Pd(1,5-COD)Br$_2$, 130 mg **2.4b** (1 equiv.) and 60 mg KN(SiMe$_3$)$_2$ (1.1 eq). Yield: 120 mg (70 %). ^{1}H-NMR δ(CD$_2$Cl$_2$) : 0.91 (6H, s, *o*-methyls), 1.33 (3H, s, *p*-methyl), 1.82 (2H, m, (PPh$_2$C*H$_2$*CH$_2$-ylid)PdBr$_2$), 4.34 and 4.47 (1H each, dt, (PPh$_2$CH$_2$C*H$_2$*-ylid)PdBr$_2$), 6.88 (1H, d, $^3J_{HH}$ = 1.5 Hz, ylidene backbone), 7.11 (1H, s br., ylidene backbone), 7.22 (2H, s, mesityl aromatic protons), 7.23-7.76 (10H, m, aromatics); ^{13}C{^{1}H}-NMR δ(CD$_2$Cl$_2$): 17.9 (s, *o*-methyls), 21.8 (s, *p*-methyl), 30.1 (s, (PPh$_2$C*H$_2$*CH$_2$-ylidene)PdBr$_2$), 48.0 (s, (PPh$_2$CH$_2$C*H$_2$*-ylidene)PdBr$_2$),

121.1 (s, ylidene backbone), 124.4 (s, ylidiene backbone), 127.9 (s, aromatic), 128.9 (d, J_{PC} = 9.1 Hz, aromatic), 130.3 (s, aromatic), 132.3 (s, aromatic), 133.5 (s, aromatic), 134.2 (d, J_{PC} = 3.0 Hz, aromatic), 135.0 (d, J_{PC} = 12.1 Hz, aromatic), 138.2 (s, aromatic), 147.1 (s, *ipso* carbon of the aryl group), 162.4 (s, NCN); ^{31}P{^{1}H}-NMR: δ(CD$_2$Cl$_2$): 19.0 (s, (*P*Ph$_2$CH$_2$CH$_2$-ylid)PdMe$_2$). Anal. Found: C, 44.24; H, 3.93; N, 3.85 %. Calcd for C$_{26}$H$_{27}$Br$_2$N$_2$PPd.CH$_2$Cl$_2$: C, 43.26; H, 3.90; N, 3.74 %. Yellow crystals appropriate for single X-ray diffraction were grown by layering a CH$_2$Cl$_2$ solution of **3.2b** with Et$_2$O.

3.3: This was prepared from 80 mg (0.317 mmol) of Pd(tmeda)Me$_2$, 161 mg of **2.2a** (1 equiv.) and 70 mg of KN(SiMe$_3$)$_2$ (1.1 equiv.). Yield: 130 mg (73 %). ^{1}H-NMR δ(CD$_2$Cl$_2$): -0.53 (3H, d, $^3J_{PH}$ = 8.1 Hz, PdCH_3), -0.32 (3H, d, $^3J_{PH}$ = 8.2 Hz, PdCH_3), 1.06 (6H, d, $^3J_{HH}$ = 6.9 Hz, CH(CH_3)$_2$), 1.23 (6H, d, $^3J_{HH}$ = 6.9 Hz, CH(CH_3)$_2$), 2.55 (2H, sept. $^3J_{HH}$ = 6.9 Hz, CH(CH$_3$)$_2$), 4.21 (2H, d, $^2J_{PH}$ = 3.3 Hz, (PPh$_2$CH_2-ylid)PdMe$_2$), 6.84 (1H, s, ylidene backbone), 7.32 (4H, br. d, aromatic), 7.44 (6H, br. s, aromatic), 7.62 (4H, m, aromatic); ^{13}C{^{1}H}-NMR δ(CD$_2$Cl$_2$): -0.4 (d, $^2J_{PC}$ = 18.2 Hz, PdC H$_3$), 0.2 (d, $^2J_{PC}$ = 19.2 Hz, PdC H$_3$), 22.4 (s, CH(C H$_3$)$_2$), 23.7 (s, CH(C H$_3$)$_2$), 27.5 (s, C H(CH$_3$)$_2$), 51.9 (d, $^1J_{PC}$ = 24.5 Hz, (PPh$_2$C H$_2$-ylid)PdMe$_2$), 117.9 (s, ylidene backbone), 122.6 (s, ylidene backbone), 123.8 (s, aromatic), 127.8 (d, J_{PC} = 8.85 Hz, aromatic), 128.1 (s, aromatic), 128.3 (s, aromatic), 129.4 (s, aromatic), 131.7 (d, J_{PC} = 26.1 Hz, aromatic), 132.3 (d, J_{PC} = 13.5 Hz, aromatic), 144.9 (s, *ipso* carbon of the aryl group), 190.4 (s, NCN); ^{31}P{^{1}H}-NMR δ(CD$_2$Cl$_2$): 32.7 (s, (*P*Ph$_2$CH$_2$-ylid)PdMe$_2$). X-ray quality crystals were grown by slow diffusion of PE to a THF solution of the complex.

3.4: This was prepared as **3.2a** using 100 mg (0.397 mmol) of Pd(tmeda)Me$_2$, 196 mg of **2.6** (1 equiv.) and 119 mg of KN(SiMe$_3$)$_2$ (1.1 equiv.). Yield: 171 mg (77 %). ^{1}H-NMR δ(CD$_2$Cl$_2$): -0.33 (3H, d, $^3J_{PH}$ = 7.3 Hz, PdCH_3), -0.19 (3H, d, $^3J_{PH}$ = 8.2 Hz, PdCH_3), 0.33 (2H, m, (PPh$_2$CH_2CH$_2$CH$_2$-ylid)PdMe$_2$), 2.03 (3H, s, CH_3 of mesityl), 2.42 (3H, s, CH_3 of mesityl), 2.64 (3H, s, CH_3 of mesityl), 4.15 and 4.24 (1H each, (PPh$_2$CH$_2$CH_2CH$_2$-ylid)PdMe$_2$), 5.62 (2H, m, (PPh$_2$CH$_2$CH$_2$CH_2-ylid)PdMe$_2$), 6.84, 6.91, 7.14 and 7.23 (1H each, 4 br. s, aromatics of mesityl and ylidene backbone), 7.45-7.63 (7H, m, aromatics), 7.92-8.13 (3H, aromatics); ^{13}C{^{1}H}-NMR δ(d_5-py): 0.03 (d, $^2J_{PC}$ = 9 Hz, PdC H$_3$), 0.9 (d, $^2J_{PC}$ = 8.1 Hz, PdC H$_3$), 17.8 (s, CH$_3$ of mesityl), 17.9 (s, C H$_3$ of mesityl), 22.4 (s, C H$_3$ of mesityl), 31.8 (d, $^1J_{PC}$ = 14.2 Hz, (PPh$_2$C H$_2$CH$_2$CH$_2$-ylid)PdMe$_2$), 35.6 (d, $^2J_{PC}$ = 11.1 Hz, (PPh$_2$CH$_2$C H$_2$CH$_2$-ylid)PdMe$_2$), 41.8 (d, $^3J_{PC}$ = 9.0 Hz, (PPh$_2$CH$_2$CH$_2$C H$_2$-ylid)PdMe$_2$), 120.2 (s, ylidene backbone), 120.9 (s, ylidene backbone), 121.5 (s, aromatic), 121.8 (s, aromatic), 121.9 (s, aromatic), 122.5 (d, J_{PC} = 8.0 Hz, aromatic), 123.1 (s, aromatic), 124.2

87

(d, J_{PC} = 3.0 Hz, aromatic), 126.2 (d, J_{PC} = 9.1 Hz, aromatic), 128.2 (s, aromatic), 145.8 (s, *ipso* carbon of the aryl group), 179.8 (s, NCN); ^{31}P{^{1}H}-NMR δ(d_5-py): 1.8 (s, (PPh$_2$CH$_2$CH$_2$CH$_2$-ylid)PdMe$_2$).

3.5b: In the glove-box 80 mg (0.317 mmol) of Pd(tmeda)Me$_2$ were placed in a Schlenk. A second Schlenk was charged with 101 mg (0.317 mmol) of free carbene **2.9d**. The contents of the two Schlenks were cooled at -78 °C using an acetone-dry ice bath and were dissolved in dry-degassed THF (approx 15 mL). The solutions were allowed to cool down to the temperature of the slush baths, and the solution of the free carbene was transferred by means of cannula to the solution of the Pd(tmeda)Me$_2$. The slush-baths were removed and the reaction mixture was allowed to warm to RT and stir overnight. The volatiles were removed under reduced pressure and the pale yellow solid was washed with PE (3 × 10 mL) and cold Et$_2$O (-30 °C, 5 mL). The compound is readily soluble in acetone, dichloromethane and toluene, while it has some solubility in ether. Prolonged exposure in toluene or dichloromethane leads in the formation of palladium black. Yield: 100 mg (81 %). ^{1}H-NMR δ(CD$_2$Cl$_2$): 0.12 (3H, s, PdCH_3), 0.22 (3H, s, PdCH_3), 1.12 (6H, d, $^3J_{HH}$ = 6.9 Hz, CH(CH_3)$_2$), 1.31 (6H, d, $^3J_{HH}$ = 6.9 Hz, CH(CH_3)$_2$), 2.71 (2H, sept., $^3J_{HH}$ = 6.9 Hz, CH(CH$_3$)$_2$), 2.91 (3H, s, 3-CH_3-pyridine), 6.92 (1H, s, ylidene backbone), 7.31 (3H, m, aromatic), 7.41 (1H, br. t, aromatic), 7.72 (1H, br dd, aromatic), 8.07 (1H, d, $^3J_{HH}$ = 2.5 Hz, aromatic), 8.61 (1H, d, $^3J_{HH}$ = 5 Hz, aromatic); ^{13}C{^{1}H}-NMR δ(CD$_2$Cl$_2$): -0.2 (s, PdCH_3), 0.0 (s, PdCH_3), 19.8 (s, 3-CH$_3$-pyridine), 21.7 (s, CH(CH$_3$)$_2$), 22.8 (s, CH(CH$_3$)$_2$), 26.9 (s, CH(CH$_3$)$_2$), 115.9 (s, ylidene backbone), 120.4 (s, ylidene backbone), 120.8 (s, aromatic), 122.1 (s, aromatic), 122.5 (s, aromatic), 128.3 (s, aromatic), 141.5 (s, aromatic), 143.8 (s, aromatic), 144.1 (s, aromatic), 144.5 (s, aromatic), 147.2 (s, *ipso* carbon of the aryl group). Yellow crystals were grown by layering a toluene solution of the complex with PE.

3.5a: This was prepared as above starting from 80 mg (0.317 mmol) of Pd(tmeda)Me$_2$ and 135 mg (0.443 mmol, 1.4 equiv.) of free carbene **2.9c**. Yield: 50 mg (42 %). ^{1}H-NMR δ(CD$_2$Cl$_2$): 0.01 (3H, s, PdCH_3), 0.12 (3H, s, PdCH_3), 1.09 (6H, d, $^3J_{HH}$ = 6.9 Hz, CH(CH_3)$_2$), 1.21 (6H, d, $^3J_{HH}$ = 6.9 Hz, CH(CH_3)$_2$), 2.73 (2H, sept., $^3J_{HH}$ = 6.9 Hz, CH(CH$_3$)$_2$), 6.91 (1H, d, $^3J_{HH}$ = 1.5 Hz, ylidene backbone), 7.22 (2H, distorted ddd, J_{HH} = 5.7 Hz, 5.4 Hz and 7.6 Hz, pyridine), 7.31 (2H, d, $^3J_{HH}$ = 7.9 Hz, aromatic), 7.52 (1H, t, $^3J_{HH}$ = 7.9 Hz, aromatic), 7.92 (1H, distorted ddd, J_{HH} = 1 Hz, 0.7 Hz and 8.2 Hz, pyridine), 8.06 (1H, d, $^3J_{HH}$ = 1.5 Hz, ylidene backbone), 9.18 (broad dt, 1H, pyridine);

^{13}C{^{1}H}-NMR δ(CD$_2$Cl$_2$): -0.1 (s, PdCH$_3$), 0.0 (s, PdCH$_3$), 21.7 (s, CH(CH$_3$)$_2$), 22.2 (s, CH(CH$_3$)$_2$), 26.9 (s, CH(CH$_3$)$_2$), 118.9 (s, ylidene backbone), 120.4 (s, ylidene backbone), 121.4 (s, aromatic), 122.1 (s, aromatic), 123.7 (s, aromatic), 128.3 (s, aromatic), 141.5 (s, aromatic), 143.8 (s, aromatic), 144.1 (s, aromatic), 145.5 (s, aromatic), 147.2 (s, *ipso* carbon of the aryl group).

3.6: In the glove-box 80 mg (0.317 mmol) of Pd(tmeda)Me$_2$ were placed in a Schlenk. A second Schlenk was charged with 194 mg (0.636 mmol) of free carbene **2.9c**. The contents of the two Schlenks were dissolved in dry-degassed THF and the solution of Pd(tmeda)Me$_2$ was transferred at RT *via* cannula to the solution of the free carbene. The reaction mixture was stirred overnight, volatiles were removed and the pale yellow solid was washed with PE 40-60. The compound is air stable, soluble in dichloromethane, toluene and ether. Yield: 201 mg (85 %). ^{1}H-NMR δ(d$_8$-tol.): -0.11 (6H, s, PdCH$_3$), 0.82 (6H, d, $^3J_{HH}$ = 6.9 Hz, CH(CH$_3$)$_2$), 0.98 (6H, d, $^3J_{HH}$ = 6.7 Hz, CH(CH$_3$)$_2$), 1.09 (6H, d, $^3J_{HH}$ = 6.7 Hz, CH(CH$_3$)$_2$), 1.42 (6H, d, $^3J_{HH}$ = 6.7 Hz, CH(CH$_3$)$_2$) 2.62 (2H, sept., $^3J_{HH}$ = 6.7 Hz, CH(CH$_3$)$_2$), 3.12 (2H, sept., $^3J_{HH}$ = 6.7 Hz, CH(CH$_3$)$_2$), 6.45 (1H, d, $^3J_{HH}$ = 1.9 Hz, ylidene backbone), 6.51 (1H, d, J_{HH} = 1.6 Hz, aromatic), 6.55 (1H, d, J_{HH} = 1.4 Hz), 6.63 (1H, ddd, J_{HH} = 1.1 Hz, 4.9 Hz and 7.1 Hz), 6.83 (2H, t, $^3J_{HH}$ = 7.8 Hz, aromatic) 6.85 (1H, d, $^3J_{HH}$ = 1.9 Hz, ylidene backbone), 6.92 (3H, m, aromatic), 7.03 (1H, br.s, aromatic), 7.09 (1H, d, J_{HH} = 1.6 Hz, aromatic), 7.11 (1H, m, aromatic), 8.14 (2H, dd, J_{HH} = 1.1 Hz, 3.8 Hz, aromatic), 8.42 (2H, d, J_{HH} = 2.2 Hz, aromatic), 9.33 (2H, d, J_{HH} = 8.2 Hz, aromatic); ^{13}C{^{1}H}-NMR δ(d$_8$-tol.): -0.4 (s, PdCH$_3$), 22.1 (s, CH(CH$_3$)$_2$), 24.1 (s, CH(CH$_3$)$_2$), 26.5 (s, CH(CH$_3$)$_2$), 27.3 (s, CH(CH$_3$)$_2$), 28.6 (s, CH(CH$_3$)$_2$), 28.8 (s, CH(CH$_3$)$_2$), 117.1 (s, ylidene backbone), 119.1 (ylidene backbone), 121.3 (s aromatic), 123.8 (s, aromatic), 124.7 (s, aromatic), 125.2 (s, aromatic), 130.7 (s, aromatic), 138 (s, aromatic), 138.9 (s, aromatic), 145.7 (s, aromatic), 147 (s, aromatic), 148.6 (s, aromatic), 152.2 (s, aromatic), 200.1 (s, NCN). Anal. Found: C, 67.61; H, 7.16; N, 11.01 %. Calcd for C$_{42}$H$_{52}$N$_6$Pd: C, 67.50; H, 7.01; N, 11.25 %. Colourless crystals were grown, by cooling a saturated solution of the compound in toluene to 5 °C.

3.7: In the glove-box, one Schlenk was charged with 40 mg (0.10 mmol) of [Pd(η^3-methallyl)Cl]$_2$. A second Schlenk was charged with 61 mg (0.20 mmol) of free carbene **2.9c**. The contents of the two Schlenks were dissolved in THF and the corresponding solutions were cooled to -78 °C using a dry ice-acetone slush bath. The solution of the free carbene was transferred by cannula to the solution of [Pd(η^3-methallyl)Cl]$_2$ and the

reaction mixture was allowed to warm to RT. After it reached RT, the reaction mixture was allowed to stir for a further twenty minutes, upon which time 68 mg (0.20 mmol) of NaBPh$_4$ were added in one go. After the addition, the reaction mixture was allowed to stir for another 15 minutes. Volatiles were removed *in vacuo* and the remaining solid was dissolved in CH$_2$Cl$_2$. It was then filtered through Celite and the solvent was removed under reduced pressure. The solid was washed with petroleum ether and dried under vacuum. Yield: 110 mg (69 %). ^{1}H-NMR δ(CD$_2$Cl$_2$): 1.11-1.23 (12H, m, CH(C*H$_3$*)$_2$), 1.82 (3H, s, CH$_2$CC*H$_3$*CH$_2$), 2.01-2.41 (4H, broad m, C*H*(CH$_3$)$_2$ and C*H$_2$*CCH$_3$CH$_2$), 3.25 (1H, s, CH$_2$CCH$_3$CH*H*), 4.12 (1H, s, CH$_2$CCH$_3$C*H*H), 6.84 (2H, tt, J_{HH} = 1.3 Hz, 8.5 Hz, aromatic), 7.09 (4H, two coinciding d, J_{HH} = 7.4 Hz, 7.5 Hz, aromatic), 7.12 (1H, d, $^3J_{HH}$ = 2.1 Hz, ylidene backbone), 7.35 (12H, broad m, aromatic), 7.55 (1H, broad t, aromatic), 8.17 (4H, m, aromatic), 8.45 (1H, d, $^3J_{HH}$ = 2.1 Hz, ylidene backbone), 8.51 (1H, ddd, J_{HH} = 0.8 Hz, 1.7 Hz, 5.4 Hz, aromatic); ^{13}C{^{1}H}-NMR δ(CD$_2$Cl$_2$): 22.? (s, CH(C*H$_3$*)$_2$), 22.1 (s, CH(C*H$_3$*)$_2$), 22.4 (s, CH$_2$CC*H$_3$*CH$_2$), 23.8 (s, CH(C*H$_3$*)$_2$), 24.1 (s, CH(C*H$_3$*)$_2$), 27.2 (s, C*H*(CH$_3$)$_2$), 27.3 (s, C*H*(CH$_3$)$_2$), 48.1 (s, C*H$_2$*CCH$_3$CH$_2$), 52.5 (s, CH$_2$CCH$_3$C*H$_2$*), 118.1 (s, ylidene backbone), 119 (ylidene backbone), 121.3 (s aromatic), 123.7 (s, aromatic), 124.8 (s, aromatic), 125.3 (s, aromatic), 125.7 (s, aromatic), 126.3 (broad s, aromatic), 127.2 (s, aromatic), 127.9 (s, CH$_2$*C*CH$_3$CH$_2$), 128.8 (s, aromatic), 132.5 (s, aromatic) 138.1 (s, aromatic), 139.2 (s, aromatic), 145.7 (s, aromatic), 146.6 (s, aromatic), 149.4 (s, *ipso* aromatic to aryl group). Colourless crystals were obtained by layering a CH$_2$Cl$_2$ solution of **3.7** with petroleum ether.

3.8a: In the glove-box a Schlenk tube was charged with 212 mg (0.41 mmol) of imidazolium salt **2.4a** and 89 mg (0.45 mmol) of KN(SiMe$_3$)$_2$. A third Schlenk was charged with 80 mg (0.20 mmol) of [Pd(η^3-methallyl)Cl]$_2$, while a fourth Schlenk was charged with 361 mg (0.41 mmol) of NaBAr$_4$^{F}. [Pd(η^3-methallyl)Cl]$_2$ and NaBAr$_4$^{F} were dissolved in approximately 15 mL THF, while the Schlenk containing the imidazolium salt and the base was cooled to -78 ° C and cooled THF was added to this solid mixture under vigorous stirring. The free carbene generated this way was transferred *via* cannula to the THF [Pd(η^3-methallyl)Cl]$_2$ solution and was left to warm to RT. To this pale yellow solution, NaBAr$_4$^{F} was added *via* cannula and the mixture was allowed to stir at RT for one hour. Volatiles were removed and the remaining solid was dissolved in CH$_2$Cl$_2$ and filtered through Celite to give a pale yellow solution. Solvent was removed in vacuum and the solid was washed with petroleum ether and dried in vacuum to give an orange-yellow product. Yield: 490 mg (75 %) ^{1}H-NMR δ(CD$_2$Cl$_2$): 0.31-0.40 (12H, m, CH(C*H$_3$*)$_2$), 1.12

(3H, s, CH$_2$CCH_3CH$_2$), 1.63-1.71 (3H, m, CHHCCH$_3$CH$_2$ and [(PPh$_2$CH_2CH$_2$-ylid)Pd(η^3-methallyl)]$^+$), 1.92 (1H, sept., $^3J_{HH}$ = 6.8 Hz, CH(CH$_3$)$_2$), 2.20-2.31 (2H, m, CHHCCH$_3$CH$_2$ and CH(CH$_3$)$_2$), 3.01 and 3.32 (each 1H, br.s, CH$_2$CCH$_3$CH_2), 3.91-4.13 (2H, m, [(PPh$_2$CH$_2$CH_2-ylid)Pd(η^3-methallyl)]$^+$), 6.77 (1H, s, ylidene backbone), 6.81-6.92 (4H, m, aromatic), 7.07-7.22 (10H, m, aromatic), 7.55 (8H, br.s, aromatics); ^{13}C{^{1}H}-NMR δ(CD$_2$Cl$_2$): 21.9 (s, CH(CH$_3$)$_2$), 22.1 (s, CH(CH$_3$)$_2$), 22.7 (s, CH$_2$CCH$_3$CH$_2$), 24.1 (s, CH(CH$_3$)$_2$), 24.2 (s, CH(CH$_3$)$_2$), 26.7 (d, $^1J_{PC}$ = 29.2 Hz, [(PPh$_2$$CH_2CH_2$-ylid)Pd($\eta^3$-methallyl)]$^+$), 27.6 (s, CH(CH$_3$)$_2$), 27.8 (s, CH(CH$_3$)$_2$), 47.2 (s, CH$_2CCH_3CH_2$), 62.5 (s, [(PPh$_2CH_2$$CH_2$-ylid)Pd($\eta^3$-methallyl)]$^+$), 68.4 (d, J_{PC} = 32.3 Hz, CH$_2$CCH$_3$$CH_2$), 116.6 (s, ylidene backbone), 122.1 (s, ylidene backbone), 122.4 (s, aromatic), 123.5 (d, J_{PC} = 5.1 Hz, aromatic), 125.1 (s, aromatic), 127.7 (s, CH$_2$$CCH_3CH_2$), 127.9 (s, aromatic), 128.2 (d, J_{PC} = 12.3 Hz, aromatic), 128.6 (br. s, aromatic), 129.9 (s, aromatic), 130.3 (d, J_{PC} = 9.0 Hz), 131.2 (br. s., aromatic), 132.2 (s, aromatic), 134 (br. s., aromatic), 134.9 (s, aromatic), 135.? (s, aromatic), 144.6 (s, *ipso* aromatic to aryl group), 160.9 (q, $^1J_{CF}$ = 49.9 Hz, CF$_3$); ^{31}P{^{1}H}-NMR δ(CD$_2$Cl$_2$): 22.0 (s, [(PPh$_2$CH$_2$CH$_2$-ylid)Pd(η^3-methallyl)]$^+$); ^{19}F{^{1}H}-NMR δ(CD$_2$Cl$_2$): 100.2.

3.8b: This was prepared as above, using the same amount of starting materials, but with the exclusion of NaBAr$_4$^{F}. Yield: 160 mg (65 %). ^{1}H-NMR δ(CD$_2$Cl$_2$): 0.88-1.03 (12H, m, CH(CH_3)$_2$), 1.51 (3H, s, CH$_2$CCH_3CH$_2$), 2.21-2.31 (1H, m, CHHCCH$_3$CH$_2$), 2.33 (1H, sept., $^3J_{HH}$ = 6.7 Hz, CH(CH$_3$)$_2$), 2.44 (1H, sept., $^3J_{HH}$ = 6.7 Hz, CH(CH$_3$)$_2$), 2.92 (3H, m, CHHCCH$_3$CH$_2$ and [(PPh$_2$CH_2CH$_2$ylid)Pd(η^3-methallyl)]Cl), 3.12 and 3.74 (each 1H, broad s, CH$_2$CCH$_3$CH_2), 5.04 (2H, m, [(PPh$_2$CH$_2$CH_2ylid)Pd(η^3-methallyl)]Cl), 6.91 (1H, s, ylidene backbone), 7.22 (3H, br.d, aromatic), 7.53 (10H, br. s, aromatic), 8.47 (1H, s, aromatic); ^{13}C{^{1}H}-NMR δ(CD$_2$Cl$_2$): 21.8 (s, CH(CH$_3$)$_2$), 22.1 (s, CH(CH$_3$)$_2$), 22.4 (s, CH$_2$CCH$_3$CH$_2$), 24.1 (s, CH(CH$_3$)$_2$), 24.3 (s, CH(CH$_3$)$_2$), 26.3 (d, $^1J_{PC}$ = 28.81 Hz, [(PPh$_2$$CH_2CH_2$-ylid)Pd($\eta^3$-methallyl)]Cl), 27.5 (s, CH(CH$_3$)$_2$), 27.8 (s, CH(CH$_3$)$_2$), 47.1 (s, CH$_2$CCH$_3$CH$_2$), 61.5 (d, $^2J_{PC}$ = 10.08 Hz [(PPh$_2$CH$_2$$CH_2$-ylid)Pd($\eta^3$-methallyl)]Cl), 66.4 (d, J_{PC} = 30.47 Hz, CH$_2$CCH$_3$$CH_2$), 117.1 (s, ylidene backbone), 122.? (s, ylidene backbone), 122.4 (s, aromatic), 123.3 (d, J_{PC} = 4.0 Hz, aromatic), 125.1 (s, aromatic), 127.8 (s, CH$_2$$CCH_3CH_2$), 128.5 (s, aromatic), 129.1 (d, J_{PC} = 10.6 Hz, aromatic), 129.9 (s, aromatic), 130.3 (d, J_{PC} = 6.0 Hz), 139.2 (s., aromatic), 143.2 (s, *ipso* aromatic to aryl group); ^{31}P{^{1}H}-NMR δ(CD$_2$Cl$_2$): 21.0 (s, [(PPh$_2$CH$_2$CH$_2$-ylid)Pd(η^3-methallyl)]Cl).

3.8c: Complex **3.8b** (40 mg, 0.066 mmol) was dissolved in CH$_2$Cl$_2$ (10 mL). To this solution, 23 mg (0.066 mmol) of NaBPh$_4$ dissolved in approximately 10 mL of a 1:1 (v/v)

mixture of CH_2Cl_2/CH_3CN, were added at RT. The solution became immediately dusky, and was left stirring for one hour at RT. The solution was filtered though Celite and volatiles were removed under reduced pressure. The solid was washed with petroleum ether and ether and dried under vacuum. Yield: 55 mg (90 %). ^{1}H-NMR δ(CD_2Cl_2): 0.71-0.89 (12H, m, $CH(CH_3)_2$), 1.35 (3H, s, $CH_2CCH_3CH_2$), 2.28-2.37 (2H, m, CHHCCH$_3$CH$_2$ and $CH(CH_3)_2$), 2.43 (1H, sept., $^3J_{HH}$ = 6.8 Hz, $CH(CH_3)_2$), 2.91-3.09 (3H, m, CHHCCH$_3$CH$_2$ and [(PPh$_2$CH_2CH$_2$ylid)Pd(η^3-methallyl)]$^+$), 3.12 and 3.73 (each 1H, br.s, $CH_2CCH_3CH_2$), 4.82 (2H, m, [(PPh$_2$CH$_2$CH_2ylid)Pd(η^3-methallyl)]$^+$), 6.91 (1H, s, ylidene backbone), 7.11-7.33 (6H, m, aromatic), 7.35 (5H, broad d., aromatic), 7.52 (12H, broad s., aromatic), 7.61-7.72 (10H, m, aromatic), 8.17 (1H, s, ylidene backbone); ^{13}C{^{1}H}-NMR δ(CD_2Cl_2): 21.9 (s, $CH(CH_3)_2$), 22.? (s, $CH(CH_3)_2$), 22.3 (s, $CH_2CCH_3CH_2$), 23.9 (s, $CH(CH_3)_2$), 24.2 (s, $CH(CH_3)_2$), 26.5 (d, $^1J_{PC}$ = 27.9 Hz, [(PPh$_2$CH$_2$CH$_2$-ylid)Pd(η^3-methallyl)]Cl), 27.4 (s, $CH(CH_3)_2$), 27.6 (s, $CH(CH_3)_2$), 47.? (s, $CH_2CCH_3CH_2$), 62.5 (d, $^2J_{PC}$ = 9.1 Hz, [(PPh$_2$CH$_2$CH$_2$-ylid)Pd(η^3-methallyl)]$^+$), 68.4 (d, J_{PC} = 30.3 Hz, $CH_2CCH_3CH_2$), 117.6 (s, ylidene backbone), 122.8 (s, ylidene backbone), 123.1 (s, aromatic), 124.2 (d, J_{PC} = 3.6 Hz, aromatic), 125.8 (s, aromatic), 127.7 (s, $CH_2CCH_3CH_2$), 127.9 (s, aromatic), 128.2 (d, J_{PC} = 11.7 Hz, aromatic), 128.6 (br. s., aromatic), 129.9 (s, aromatic), 130.3 (d, J_{PC} = 8.6 Hz), 131.2 (br. s., aromatic), 133.2 (s, aromatic), 134.4 (br. s., aromatic), 134.9 (s, aromatic), 135.2 (s, aromatic), 149.6 (s, *ipso* aromatic to aryl group); ^{31}P{^{1}H}-NMR δ(CD_2Cl_2): 22.3 (s, [(*P*Ph$_2$CH$_2$CH$_2$-ylid)Pd(η^3-methallyl)]$^+$). Colourless crystals were grown by layering a CH_2Cl_2 solution of **3.8c** with Et_2O.

Crystalographic data for 3.1a, 3.2b, 3.3 and 3.8c:

	3.1a	3.3	3.2b	3.8c
Chemical Formula	$C_{31}H_{39}N_2PPd$	$C_{30}H_{37}N_2PPd$	$C_{26}H_{27}Br_2N_2PPd$	$C_{57}H_{60}BN_2PPd$
Formula weight	577.01	562.99	664.69	921.25
Crystal system	Monoclinic	Orthorhombic	Triclinic	Monoclinic
Space group	$P2_1/n$	$P\,2_1\,2_1\,2_1$	$P\text{-}1$	Cc
a / $\mathring{A}$	12.7219(5)	10.031(13)	9.3880(2)	16.0703(8)
b / $\mathring{A}$	15.2549(8)	11.34(2)	10.4022(2)	16.4224(9)
c / $\mathring{A}$	15.3658(6)	24.499(8)	13.8831(3)	19.7579(11)
α / °	90	90	69.2150(10)	90
β / °	110.421(3)	90	88.9380(10)	112.768(2)
γ / °	90	90	77.9220(10)	90
Z	4	4	2	4
T/K	150(2)	120(2)	150(2)	120(2)
μ / mm^{-1}	0.743	0.743	4.062	0.458
No. of data collected	28963	24799	10490	13505
No. of unique data	6290	6316	5607	8588
Goodness of fit on F^2	1.012	1.028	1.079	1.000
$R_{int.}$	0.1825	0.1060	0.0188	0.0532
Final $R(|F|)$ for $F_0 > 2\sigma(F_0)$	0.0676	0.0483	0.0283	0.0457
Final $R(F^2)$ for all data	0.1053	0.0785	0.0347	0.0684

93

Crystallographic data for 3.5d, 3.6 and 3.7:

	3.5b	3.6	3.7
Chemical Formula	$C_{22}H_{29}N_3Pd$	$C_{42}H_{52}N_6Pd$	$C_{48}H_{50}BN_3Pd$
Formula weight	455.9	747.30	786.12
Crystal system	Monoclinic	Monoclinic	Triclinic
Space group	$P\,2_1/c$	$P\,2_1/n$	$P\text{-}1$
a / $\mathring{A}$	10.408(6)	10.936(14)	13.1744(3)
b / $\mathring{A}$	12.139(7)	27.06(3)	14.1774(6)
c / $\mathring{A}$	17.357(11)	13.47(4)	15.6806(7)
α / °	90	90	114.991(2)
β / °	105.97(4)	107.64(19)	90.710(2)
γ / °	90	90	114.308(2)
Z	4	4	2
T/K	120(2)	120(2)	120(2)
μ / mm^{-1}	0.892	0.526	0.425
No. of data collected	22013	33787	40259
No. of unique data	3714	6436	10835
Goodness of fit on F^2	1.188	1.047	1.043
$R_{int.}$	0.1620	0.0674	0.0936
Final $R(|F|)$ for $F_0 > 2\sigma(F_0)$	0.1037	0.0363	0.0683
Final $R(F^2)$ for all data	0.1204	0.0507	0.0991

References:

1. Zhang, C.; Huang,, J.; Trudell, M. L.; Nolan, S. P. *J. Org. Chem.* **1999**, *64*, 3804.

2. Cornils, B.; Herrmann, W. A. *Applied Homogeneous Catalysis with Organometallic compounds.* Willey-VCH: Weinheim, 2000.

3. Caddick, S.; Cloke, F. G. N.; Clentsmith, G. K. B.; Hitchcock, P. B.; McKerrecher, D.; Titcomb, L. R.; Williams, M. R. V. *J. Organomet. Chem.* **2001**, *617-618*, 635.

4. McGuiness, S.; Saendig, N.; Yates, B. F.; Cavell, K. J., *J. Am. Chem. Soc.* **2001**, *123*, 4029.

5. McGuiness, S.; Cavell, K. J.; Yates, B. F.; Skelton, B. W.; White, A. H., *J. Am. Chem. Soc.* **2001**, *123*, 8317.

6. Danopoulos, A. A.; Tsoureas, N.; Green, J. C.; Hursthouse, M. B., *Chem. Commun.* **2003**, 2163.

7. Herrmann, W. A.; Köcher, C.; Goosen, L. J.; Artus, G. R. J., *Chem. Eur. J.* **1996**, *2*, 1627.

8. Herrmann, W. A.; Spiegler, L. G., M. *Organometallics* **1998**, *17*, 2162.

9. McGuiness, S.; Cavell, K. J. *Organometallics* **2000**, *19*, 741.

10. Tulloch, A. A. D.; Danopoulos, A. A.; Tooze, R. P.; Cafferkey, S. M.; Kleinhenz, S.; Hursthouse, M. B. *Chem. Commun.* **2000**, 1247.

11. Tsoureas, N.; Danopoulos, A. A.; Tulloch, A. A. D.; Light, M. E. *Organometallics* **2003**, *22*, 4750.

12. Hahn, F. E.; Foth, M. *J. Organomet. Chem.* **1999**, *585*, 241.

13. Schwarz , J.; Gardiner, M. G.; Grosche, M.; Herrmann, W. A.; Hieringer, W.; Raudaschl-Sieber, G. *Chem. Eur. J.* **2000**, *6*, 1773.

14. Danopoulos, A. A.; Gelbrich, T.; Hursthouse, M. B.; Winston, S. *Chem. Commun.* **2002**, 482.

15. Danopoulos, A. A.; Winston, S.; Hursthouse, M. B. *J. Chem. Soc. Dalton Trans.* **2002**, 3090.

16. de Graaf, W.; Boersma, J.; Smeets, W. J. J.; Spek, A. L.; van Koten, G. *Organometallics* **1989**, *8*, 2907.

17. Tooze, R. P.; Chiu, K. W.; Wilkinson, G. *Polyhedron* **1984**, *3*, 1025.

18. Douthwaite, R. E.; Green, M. L. H.; Silcock, P. J.; Gomes, P.T. *J. Chem. Soc. Dalton Trans.* **2002**, 1386.

19. Viciu, M. S.; Navarro, O.; Germaneau, R. F.; Kelly III, R. A.; Sommer, W.; Marion, N.; Stevens, E. D.; Cavallo, L.; Nolan, S. P. *Organometallics* **2004**, *23*, 1629.

20. Gomez, M.; Jancat, S.; Muller, G.; Panyella, D.; van Leeuwen, P. W. N. M.; Kamer, P. J.; Goubitz, K.; Fraanje, J. *Organometallics* **1999**, *18*, 4970.

21. Drew, D.; Doyle, J. R. *Inorg. Synth.* **1972**, *13*, 53.

22. Tatasuno, Y.; Yoshida, T.; Otsuka, S. *Inorg. Synth.* **1990**, *28*, 342.

Chapter 4: Reactivity of phosphine- and pyridine-functionalised NHC complexes of Pd(II)

Chapter 4: Reactivity of phosphine- and pyridine-functionalised NHC complexes of Pd(II)

4.1 Introduction

In this chapter, studies of the reactivity and catalytic properties of the Pd(II) neutral and cationic complexes described in Chapter 3 are undertaken. The incorporation of a NHC moiety with classical donor functionalities into one ligand architecture, imposes electronic asymmetry on the metal centre, which could account for distinct reactivities. For this reason the reactivity of the neutral dimethyl Pd(II) complexes towards heating, electrofiles and the oxidative addition of MeI was investigated. Finally, the catalytic activity of the Pd(II) complexes described in Chapter 3 and this chapter, towards C-C coupling reactions (mainly Heck olefination) was investigated.

4.2 Thermal stability of 3.1a and 3.3

The types of Pd-C bonds (*i.e.* Pd-Me and Pd-carbene) in **3.1a** and **3.3** (Scheme 4.1) are arranged in a way that one Pd-CH_3 bond is flanked by one Pd-CH_3 bond and one Pd-carbene bond. This provides the opportunity to test the preferred decomposition pathway by reductive elimination of either ethane or methylimidazolium salts (Scheme 4.1).
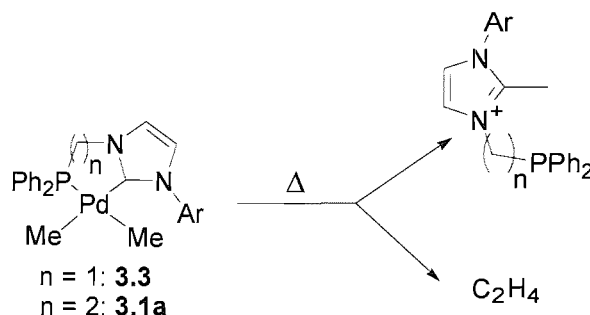
Scheme 4.1: Possible decomposition pathways of complexes **3.1a** and **3.3** (Ar = 2,6-diisopropylphenyl).

Complexes **3.1a** and **3.3** (Scheme 4.1) are stable at room temperature in the solid state or in solution. The thermal decomposition of **3.1a** in solution (d_8-THF) was studied by means of VT-NMR and showed that up to 60 °C no other species could be detected in

solution except **3.1a**, while formation of ethane or methane was not observed. The formation of palladium colloids and of a colourless solid was observed upon removal of the NMR tube from the NMR probe. Removal of the volatiles followed by extraction in dichloromethane and filtration through Celite resulted in a beige-yellow solution. The ES^+ mass spectrum of this solution contained a peak (in 100% abundance), at 471 Da with an isotopic pattern agreeing with the formula for 2-methyl-[3-(2,6-diisopropylphenyl)-1-(β-((diphenylphosphino)oxy)ethyl)]imidazolium. This mass spectrum also showed the existence of complex **3.1a** in solution, by the appearance in it of the cationic species [**3.1a**-Me]$^+$(= M) and $[M+CH_3CN]^+$ in a 1:1 ratio.

In a similar experiment, complex **3.3** was dissolved in d_5-PhCl in a Young's tap NMR tube and was heated to 50 °C. The spectrum of the compound remained unchanged for 20 minutes in this temperature. After an additional 20 minutes at this temperature the only change in the ^{1}H-NMR spectrum was observed in the $Pd-CH_3$ region where an extra peak (0.27 ppm) appeared almost coincident with the most upfield doublet (centred at 0.28 ppm) assignable to one of the Pd-Me protons. Upon the appearance of this singlet the total integration of the two peaks increased from 3H to 4H. Heating was continued for another 20 minutes, upon which time decomposition had occurred as seen from the formation of black aggregates. The ^{1}H-NMR spectrum showed no significant change, with the only difference that the integral in question had increased to 4.5H. A closer inspection of this region of the spectrum revealed that the relative height of the doublet attributed to the Pd-Me proton had decreased in comparison to the new peak (in a ratio 2.7:1 from 3:1 before, as judged by the integration of peaks of Cp_2Fe (ferrocene) which was added as an internal standard). This sharp singlet is attributed to methane (singlet at 0.23 ppm in $CDCl_3$) produced during the thermolysis. The formation can be explained through a mechanism, which involves α-hydrogen elimination followed by reductive elimination of methane. No 2-methylimidazolium or imidazolium proton peaks were observed. Furthermore, ^{1}H and $^{31}P\{^1H\}$-NMR spectroscopy revealed that only complex **3.3** was present in solution.

4.3 Synthesis and characterisation of cationic species

4.3.1 Synthesis and characterisation through NMR spectroscopy

Square planar cationic complexes of palladium and nickel stabilised by bidentate chelating ligands have received much attention due to their involvement in catalytic C-C bond-forming reactions.[1,2] The most studied ligands include diphosphines and diiminies,[2] although cationic complexes with chelating dicarbenes[1] have been observed spectroscopically and in some case structurally characterised.[3] The mixed donor chelates synthesised in Chapter 2 were potential sources of cationic complexes containing chelates with nonsymmetric NHC and classical donors that could provide useful insight into the mechanism of their formation and possible catalytic activity.

The asymmetry imposed by the ligand architectures in the neutral palladium(II) dimethyl complexes, described in Chapter 3 (Figure 4.1), prompted us to investigate their reactivity towards electrophilic reagents. The reactivity described below shows that the ligand environment imposes a kinetic differentiation of the two Pd-CH$_3$ bonds.

3.1a   **3.3**   **3.5b**
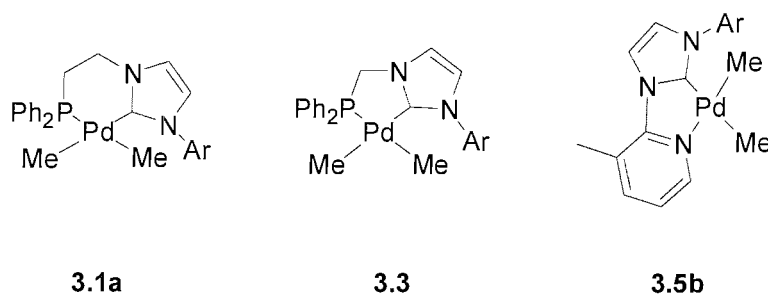
Figure 4.1: Neutral palladium(II) dimethyl complexes whose reactivity towards electrophiles has been studied (Ar = 2,6-diisopropyl-phenyl).

The use of alkyl abstracting agents such as Ph$_3$C$^+$OTf$^-$, Ph$_3$C$^+$BAr$_4$$^{F-}$ (BAr$_4$$^{F-}$ = tetrakis-[3,5-(bistrifluoromethyl)phenyl]borate) and B(C$_6$F$_5$)$_3$ was initially considered, in order to test the reactivity of complex **3.1a** towards electrophiles. Interaction of one of the above reagents with complex **3.1a** in CH$_2$Cl$_2$ resulted in the abstraction of one Pd-CH$_3$ bond as evidenced by ^{1}H-NMR spectroscopy. Unfortunately in most cases the reactions did not yield clean products. Nevertheless the ^{31}P{^{1}H} NMR spectra did contain a major peak in the region of 30 ppm, suggesting the formation of a cationic species.[4] To further

our insight into these reactions, variable temperature NMR studies were employed. In all cases the spectra obtained were broad and the formation of complex reaction mixtures from low temperatures hindered our understanding of the reaction.

Interaction of **3.1a** with one equivalent of the acidic alcohol[5] $(CF_3)_2CHOH$ in CH_2Cl_2 or CH_2Cl_2/ether at -78 °C and warming to -20 °C resulted in the formation of Pd black and unidentified decomposition products. The reaction was repeated on a NMR scale using d_5-pyridine as the solvent. Upon warming to room temperature the formation of cationic species **4.1** (Figure 4.2) was postulated due to the loss of the two doublets

$$n = 1: \textbf{4.1}$$
$$n = 2: \textbf{4.2}$$
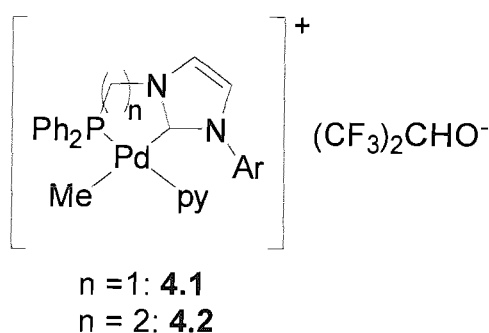
Figure 4.2: Cationic species formed by reaction of the neutral complexes **3.1a** or **3.3** with $(CF_3)_2CHOH$ in d_5-pyridine (n = 1, 2, Ar = 2,6-diisopropyl-phenyl and py = d_5-pyridine).

assigned to the Pd-CH_3 ($^3J_{PH}$ = 7.2 Hz and $^3J_{PH}$ = 8.2 Hz) protons and appearance of one doublet ($^3J_{PC}$ = 2.7 Hz), shifted downfield, integrating for three protons. The ^{1}H-NMR spectrum of this reaction also contained peaks for the $(CF_3)_2CHO^-$ counter-anion and the ligand. The ^{31}P{^{1}H}-NMR spectrum contained only one peak shifted downfield (35.2 ppm) in comparison with the neutral complex (12.4 ppm). Finally one carbene carbon and one Pd-CH_3 were located at 180.3 and 8.0 ppm (the latter appearing as a doublet with a $^2J_{PC}$ coupling constant of 4.6 Hz) respectively in the ^{13}C{^{1}H}-NMR spectrum. These observations imply the presence of one isomer in solution. The electrophilic attack, by the acidic alcohol, on one of the metal-alkyl bonds is further evidenced by the presence of methane (0.20 ppm) in the ^{1}H-NMR spectrum. The vacant coordination site is occupied by a pyridine molecule, thus providing a stable cationic species. The above spectroscopic evidence suggests that the complex is arranged such that pyridine occupies the site *trans* to the phosphorus. The downfield shift observed in the ^{31}P{^{1}H}-NMR spectrum is expected due to the formation of a cationic Pd(II) centre. Furthermore a geometry where

the coordinated pyridine is *trans* to the phosphorus atom accounts for such a downfield shift in the $^{31}P\{^1H\}$-NMR spectrum.

The same reaction was carried out in the case of complex **3.3**. This time the collapse of the two upfield Pd-CH$_3$ doublets ($^3J_{PH}$ = 8.1 Hz and $^3J_{PH}$ = 8.2 Hz) into one broad singlet was observed. Again, the metal-alkyl proton (0.04 ppm from –0.53 and – 0.32 ppm for **3.3**) was shifted downfield, suggesting the formation of a cationic species. The formation of the cationic species was further proved by the significant downfield shift in the $^{31}P\{^1H\}$-NMR (55.3 ppm) spectrum of the reaction mixture in comparison with the neutral complex **3.3** (32.7 ppm). The existence of one isomer in solution was evidenced firstly by the appearance of one singlet in the $^{31}P\{^1H\}$-NMR spectrum and secondly by the location of one signal for the carbene carbon and one signal for the Pd-CH$_3$ carbon in the $^{13}C\{^1H\}$-NMR spectrum at 194.1 and 2.1 ppm respectively. From the above observations it can be assumed that the vacant position occupied by the pyridine molecule is *trans* to the phosphorus. The above spectroscopic observations are summarised in Table 4.1.

Complex	δ-Pd-C*H$_3$*	δ-Pd-*C*H$_3$	δ-N*C*N	δ-^{31}P$\{^1$H$\}$
3.1a	-0.62 (d, $^3J_{PH}$ = 7.2 Hz) -0.41 (d, $^3J_{PH}$ = 8.2 Hz)	0.1 (d, $^2J_{PC}$ = 10 Hz) 2.4 (d, $^2J_{PC}$ = 9.3 Hz)	187.8	12.4
4.2	0.01 (d, $^3J_{PH}$ = 2.7 Hz)	8.0 (d, $^2J_{PC}$ = 4.6 Hz)	180.3	35.2
3.3	-0.53 (d, $^3J_{PH}$ = 8.1 Hz) -0.32 (d, $^3J_{PH}$ = 8.2 Hz)	-0.4 (d, $^2J_{PC}$ = 18.2 Hz) 0.2 (d, $^2J_{PC}$ = 19.2 Hz)	190.4	32.7
4.1	0.04 (broad singlet)	2.1 (singlet)	194.1	55.3

Table 4.1: Comparison of ^1H, $^{13}C\{^1H\}$ and $^{31}P\{^1H\}$-NMR chemical shifts (ppm) and multiplicities (Hz) (where observed) between the neutral and cationic species.

The susceptibility of the Pd-CH$_3$ bonds to electrophilic attack in complex **3.1a** was further tested by replacing (CF$_3$)$_2$CHOH with [H(OEt$_2$)]$^+$\{B[(3,5-CF$_3$)$_2$C$_6$H$_3$)]$_4$\}$^-$ ("Brookhart's acid"[40]). In this case the neutral complex and the electrophile were reacted at -78 °C, and the resulting reaction mixture was left to warm up to around -45 °C, upon which time a donor ligand was added to trap the electron deficient, coordinatively unsaturated cation (Scheme 4.2). This reaction was followed in order to ensure the

formation of a vacant position after the electrophilic attack by Brookhart's acid at the palladium-alkyl bond.
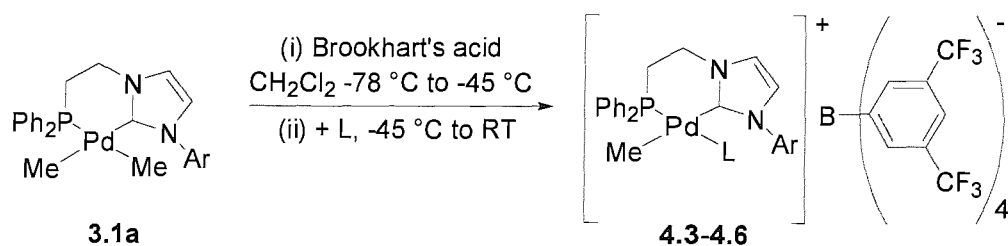
Scheme 4.2: Synthesis of cationic species (L = pyridine **4.3**, L = acetonitrile **4.4**, L = benzonitrile **4.5**, L = PMe$_3$ **4.6**; Ar = 2,6-diisopropyl-phenyl).

Complex	$\delta\text{-}^{31}P\{^1H\}$(multiplicity, J (Hz))
3.1a	12.4 (singlet)
4.3	34.8 (singlet)
4.4	36.5 (singlet)
4.5	35.3 (singlet)
4.6	-15.8 and 4.6 (d, $^2J_{PP}$ = 32.8 Hz)

Table 4.2: $^{31}P\{^1H\}$-NMR chemical shifts (ppm) of cationic species.

The observed $^{31}P\{^1H\}$ shifts for the cationic species **4.3-4.5**, are in the same region with the ones obtained from the reaction of **3.1a** with $(CF_3)_2CHOH$ in d_5-pyridine. Once again the existence of one isomer in solution was evidenced by the location of only one peak in their $^{31}P\{^1H\}$-NMR spectra, which were shifted downfield compared to the neutral complex **3.1a** (Table 4.2). This downfield shift can be accounted for by the occupation of the site *trans* to the phosphorus by an electronegative atom. In the case of **4.6**, two peaks appear in the $^{31}P\{^1H\}$-NMR spectrum of the compound. These are split into doublets due to phosphorus coupling. The range of this coupling constant ($^2J_{PP}$ = 32.8 Hz) suggests that the two phosphorus atoms are arranged *trans* to each other, and is in agreement with previously observed values.[6] From this spectrum we can clearly see that the trimethylphosphine is coordinated, while the upfield shift assigned to the phosphorus atom of the phosphine part of the ligand clearly suggests the existence of a strong σ-donor within the molecule.

Comparison of the metal-alkyl region of the ^{1}H-NMR spectra obtained from complexes **4.3-4.5** and the reaction of **3.1a** with $(CF_3)_2CHOH$ indicates the formation of similar cationic species. In all these cases, the region under discussion consists of one doublet due to P-H coupling. The coupling constants $^3J_{PH}$ (Table 4.3) are significantly smaller than the ones observed for the neutral complex **3.1a**. When the electrophilic attack of the Pd-CH$_3$ bond was followed by the addition of PMe$_3$ (complex **4.6**), the metal-alkyl bond protons appear as a broad triplet with a $^3J_{PH}$ of 7.3 Hz.

Complex	δ-^{1}H (multiplicity, J (Hz))
3.1a	-0.62 (d, $^3J_{PH}$ = 7.2 Hz), -0.41 (d, $^3J_{PH}$ = 8.2 Hz)
4.3	-0.33 (d, $^3J_{PH}$ = 2.7 Hz)
4.4	-0.10 (d, $^3J_{PH}$ = 1.8 Hz)
4.5	0.01 (d, $^3J_{PH}$ = 2.7 Hz)
4.6	0.01 (t, $^3J_{PH}$ = 7.3 Hz)

Table 4.3: ^{1}H-NMR chemical shifts (ppm) and multiplicities of Pd-CH_3 protons.

The o-isopropyl methyls are diastereotopic and appear as a set of doublets. The ethylene bridge protons appear as multiplets and their assignment was achieved on the basis of their relative shifts, with the ones shifted further downfield being attached on the ylidene moiety. These methylenic protons appear as a set of broad doublet triplets. Interestingly after the formation of the cationic species **4.3-4.5**, the methylenic protons at the α position to the phosphorus, are shifted downfield coinciding with the septet assigned to the methinic C-Hs of the o-ispropyl groups. This shift is another indication of the existence of an electronegative atom *trans* to the phosphine moiety of the hybrid ligand architecture. On the other hand, when L = PMe$_3$, the multiplet arising from the collapse of the methylenic CH$_2$s into the C-H septet is not observed. These CH$_2$s appear as a distinct multiplet in the same region as with the neutral complex **3.1a** (2.40 ppm for **4.6** *versus* 2.32 ppm for **3.1a**). The carbons of these methylenic space linkers appear in the same region as with the ones for the neutral complex **3.1a**. Interestingly the splitting due to ^{31}P coupling is not always observed. The above observations are summarised in table 4.4.

Complex	$\delta(^{13}C\{^1H\})$-CH_2 (multiplicity, $^nJ_{PC}$ [Hz])	δ-^{1}H-CH_2, $CH(CH_3)_2$
3.1a	30.3 (d, $^1J_{PC}$ = 14.6), 49.3 (d, $^2J_{PC}$ = 10.6)	2.32 (m, (PPh$_2$CH_2CH$_2$-ylid)PdMe$_2$), 2.74 (sept., CH(CH$_3$)$_2$)
4.3	32.0 (singlet) 47.9 (singlet)	2.49 (m, CH(CH$_3$)$_2$ and [PPh$_2$CH_2CH$_2$-ylidene]PdMe(py)$^+$)
4.5	31.6 (d, $^1J_{PC}$ = 34.2 Hz) 47.3 (singlet)	2.71 (m, CH(CH$_3$)$_2$ and [PPh$_2$CH_2CH$_2$-ylidene]PdMe(PhCN)$^+$)

Table 4.4: Comparison of $^{13}C\{^1H\}$ and ^{1}H-NMR chemical shifts (ppm), and multiplicities of methylenic protons and carbons between the neutral complex **3.1a** and cationic species in **4.3** and **4.5**.

Due to the thermal instability of complex **4.4** and **4.6** in CD$_2$Cl$_2$ during the acquisition of the ^{13}C(^{1}H)-NMR spectra, no data regarding the shifts and multiplicities of the corresponding methylenic carbons are available. Nevertheless the ^{1}H-NMR spectrum of **4.4** follows the trend of the α to the phosphorus methylenic protons coinciding with the methinic septet of the o-isoprpyl group, thus giving rise to a multiplet centred at 2.61 ppm. Finally the observed values for the methylenic carbon space linkers (singlets at 32.0 and 47.9 ppm) of the isolated complex **4.3**, are in close proximity with the ones obtained for the $in\ situ$ generated cationic complex from the reaction of **3.1a** with (CF$_3$)$_2$CHOH in d_5-pyridine (doublet ($^1J_{PC}$ = 34.2 Hz) at 31.0 ppm and singlet at 47.7 ppm). The overlap of the α to the phosphorus methylenic proton multiplet with the methinic septet is not observed in the case of the generated $in\ situ$ cation. Nevertheless there is a downfield shift of this multiplet from 2.32 ppm in **3.1a** to 2.80 ppm in the cationic species **4.1**.

The metal-alkyl region of the $^{13}C\{^1H\}$-NMR spectra of compounds **4.5** and **4.3** consists of a singlet located at 4.9 and 7.6 ppm respectively, assignable to the Pd-CH$_3$ carbon. A doublet appears in the case of the generated $in\ situ$ cation **4.2** with a $^2J_{PC}$

coupling constant of 4.6 Hz. The carbene carbon is located in the case of complex **4.3** at 180.3 ppm, while it is not observed in the case of complex **4.5**.

Neutral complex **3.3** was reacted with Brookhart's acid in the presence of pyridine or 4-tertbutylpyridine, following the synthetic protocol described above (Scheme 4.3).
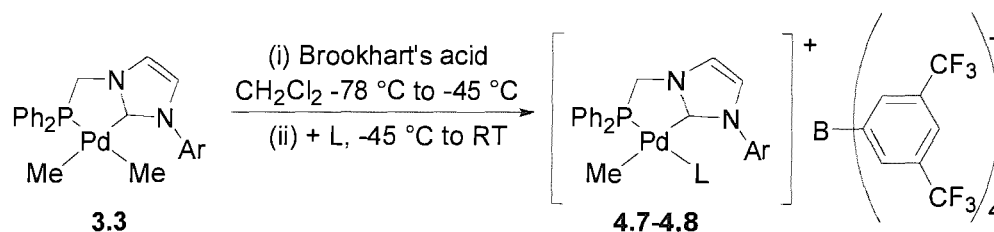
Scheme 4.3: Synthesis of cationic species **4.7** (L = pyridine) and **4.8** (L = 4-tertbutylpyridine) (Ar = 2,6-diisopropylphenyl).

When pyridine was used to trap the intermediate coordinatively unsaturated species, the reaction did not proceed cleanly. This was evidenced from the $^{31}P\{^1H\}$-NMR spectrum which consisted of two major peaks. The predominant peak at 54.0 ppm possibly represents the title compound **4.7**. Unreacted neutral complex **3.3** was recognised by the peak at 32.7 ppm in the $^{31}P\{^1H\}$-NMR spectrum of the reaction mixture. Attempts to purify the compound *via* crystallisation were unsuccessful.

On the other hand the reaction with 4-*tert*-butylpyridine afforded the cationic species **4.8** cleanly. The $^{31}P\{^1H\}$-NMR spectrum of the reaction mixture consisted of one peak at 53.8 ppm. As in the case of the cationic species discussed above, this peak is significantly shifted downfield in comparison to the $^{31}P\{^1H\}$ shift of compound **3.3** (32.7 ppm).

The proposed geometry in Scheme 4.3 is based on the same arguments as in the case of cationic species **4.3-4.6**. The formation of one isomer is verified firstly by the appearance of one Pd-CH$_3$ resonance in their ^1H and $^{13}C\{^1H\}$-NMR spectra and secondly by the existence of only one signal in their $^{31}P\{^1H\}$-NMR spectra (Table 4.5). From this table we can easily see that the $^{31}P\{^1H\}$ chemical shifts of the isolated complexes **4.7** and **4.8** almost coincide with the observed $^{31}P\{^1H\}$ chemical shift for the *in situ* generated cation **4.1**. The downfield shift of the Pd-CH$_3$ protons and carbon is probably due to the formation of the cation. Furthermore, an increase in the $^1J_{PC}$ and $^2J_{PH}$ coupling constants of the methylenic carbon and protons bridge is observed after the formation of the cationic

species. Unfortunately, the carbene carbon could not be observed in the $^{13}C\{^1H\}$-NMR spectra of **4.7** and **4.8**.

Complex	δ-Pd-CH_3 (ppm)	δ-Pd-CH$_3$ (ppm)	δ-{^{1}H}-CH_2 (ppm)	δ(^{13}C{^{1}H})-CH$_2$ (ppm)	δ-^{31}P{^{1}H} (ppm)
3.3	-0.53 (d, 8.1 Hz), -0.32 (d, 8.2 Hz)	-0.4 (d,$^2J_{PC}$ = 18.2 Hz), 0.2 (d, $^2J_{PC}$ = 19.2 Hz)	4.21 (d, $^2J_{PH}$ = 3.3 Hz)	51.9 (d, $^1J_{PC}$ = 24.5 Hz)	32.7
4.7 (L = py)	-0.09 (d, $^3J_{PH}$ = 2.5 Hz)	1.8 (singlet)	4.92 (d, $^2J_{PH}$ = 6.6 Hz)	53.7 (d, $^1J_{PC}$ = 48.4 Hz)	54
4.8 (L = 4-^{t}Bu-py)	-0.09 (d, $^3J_{PH}$ = 2.6 Hz)	1.9 (singlet)	4.93 (d, $^2J_{PH}$ = 6.6 Hz)	53.6 (d, $^1J_{PC}$ = 48.9 Hz)	53.8
4.1	0.04 (broad singlet)	2.1 (singlet)	5.54 (broad doublet)	52.5 (d, $^1J_{PC}$ = 53.6 Hz	55.3

Table 4.5: Comparison of characteristic peaks between **3.3**, **4.7**, **4.8** and **4.1**.

The selective electrophilic attack on one of the Pd-CH$_3$ was also observed upon the interaction of complex **3.5b** with one equivalent Brookhart's acid in the presence of pyridine (Scheme 4.4). Again the formation of one isomer in solution was evident, by the existence of one methyl peak at metal-alkyl region of the spectrum. This appears as a singlet at −0.09 ppm, while the two inequivalent Pd-CH$_3$ resonances for the neutral complex **3.5b** are located at 0.12 and 0.22 ppm. The reason for the upfield shift of the Pd-CH_3 resonance observed in the cationic species is not clear. The metal alkyl region of the $^{13}C\{^1H\}$-NMR spectrum consists of one peak at 7.7 ppm, assignable to the Pd-CH$_3$ carbon. This resonance is shifted downfield compared to the signals (-0.2 and 0.0 ppm) observed for the neutral complex **3.5b**.
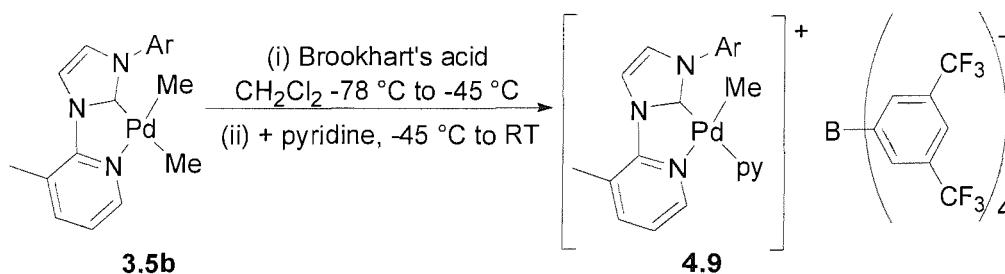
Scheme 4.4: Formation of cationic species **4.9**, from the reaction of **3.5b** with Brookhart's acid.

The geometry proposed in Scheme 4.4 was backed up by a long range ^{1}H-^{1}H NMR correlation experiment (NOESY). This revealed a cross peak between the Pd-CH_3 signal and one of the diastereotopic methyls of the isopropyl substituents of the aryl group. The observed correlation suggests that the metal-alkyl bond left intact is situated *cis* to the carbene moiety of the ligand. The selectivity with which the methyl abstraction occurs, is expected since the carbene moiety of the asymmetric bidenate ligand exerts a stronger *trans* effect than the pyridine.

4.3.2 Monitoring the formation of cationic species with VT ^{1}H-NMR spectroscopy

From the above spectroscopic data it can be deduced that the electrophilic attack takes place selectively at the site *trans* to the phosphorus in the case of complexes **3.1a** and **3.3**. This reactivity trend was not expected, as the metal-alkyl bond *trans* to the NHC moiety of the ligand should be attacked first due to the stronger *trans* influence imposed by the NHC on this site. The reaction of **3.1a** with (CF$_3$)$_2$CHOH in CD$_2$Cl$_2$ in the presence of pyridine was monitored by variable temperature ^{1}H-NMR. This experiment provides evidence that the only isomer is formed under kinetic control. The formation of the cationic species takes place selectively at −35 °C, at the site *trans* to the phosphorus as evidenced by the $^3J_{PH}$ coupling constant of 2.5 Hz (Figure 4.3).
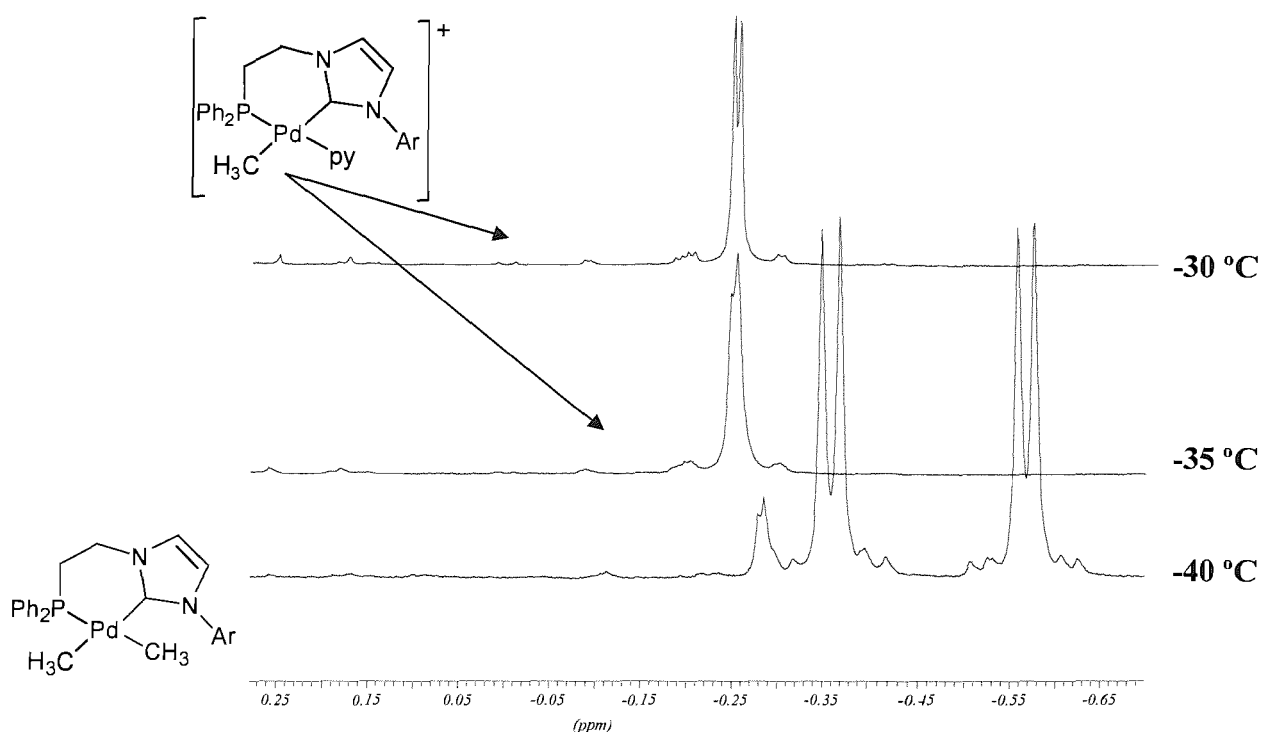
Figure 4.3: VT ^{1}H-NMR of the reaction of **3.1a** with $(CF_3)_2CHOH$ in CD_2Cl_2 in the presence of pyridine, showing the selective electrophilic attack at the Pd-CH$_3$ bond *trans* to the phosphorus atom.

4.3.3 Thermal stability of cationic species 4.3 and 4.4

Recent reports provide theoretical and experimental evidence that cationic complexes of the type *cis*-$[L_2Pd(NHC)(CH_3)]^+$ undergo facile concerted reductive elimination, resulting in the formation of alkylimidazolium salts.[7] However chelating ligands (*i.e.* L_2 = dppp) suppress this transformation.[8] The thermal stability of the cationic species reported above was investigated.

Complex **4.3** is stable in solid state and in solution. On prolonged standing at room temperature, it develops a yellow colouration, even though the compound is unchanged spectroscopically. Its stability could possibly arise from the *trans* arrangement of the Pd-Me bond and the NHC group, rendering methyl migration to the NHC carbon or reductive elimination of methylimidazolium salts unfavourable. Thermal decomposition of **4.3** occurs at 90 °C to colloidal Pd and intractable mixtures of organic products. On the other

hand complex **4.4** shows remarkable stability in d_3-MeCN up to 65 °C; the only process that can be detected involves exchange of coordinated and free acetonitrile.

4.3.4 X-ray diffraction studies of complexes 4.3, 4.4 and 4.9

The topology of the electrophilic attack at the Pd-CH$_3$ site *trans* to the phosphorus was further proved by single crystal X-ray studies carried out on complexes **4.3** (Figure 4.4) and **4.4** (Figure 4.5). Both complexes crystallise by slow diffusion of petroleum ether into ether solutions of the complexes.
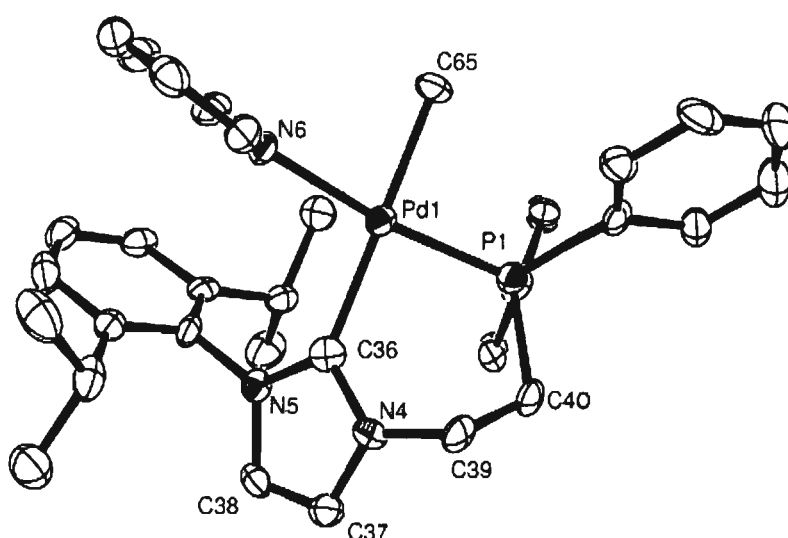
Figure 4.4: ORTEP representation of the cation in **4.3** showing 50% probability ellipsoids. The asymmetric unit consists of two cations and two anions. The BAr$_4$$^{F-}$ anion and H atoms are omitted for clarity. Selected bond lengths (Å) and angles (°): C(36)-Pd(1) = 2.092(6), C(65)-Pd(1) = 2.080(6), N(6)-Pd(1) = 2.126(4), P(1)-Pd(1) = 2.2219(17); C(36)-Pd(1)-C(65) = 173.7(2), C(36)-Pd(1)-N(6) = 97.38(16), C(65)-Pd(1)-N(6) = 84.10(17), C(36)-Pd(1)-P(1) = 89.81(16), C(65)-Pd(1)-P(1) = 89.18(17), N(6)-Pd(1)-P(1) = 171.77(13).

The geometry around the Pd centre in **4.3** is square planar; its coordination sphere comprises the ligand, one methyl group and one pyridine ligand that forms an angle of approximately 77.9° with the coordination plane. The methyl group is *trans* to the NHC functionality as proposed by spectroscopic data. The Pd-carbene and Pd-CH$_3$ bond lengths

and ligand bite angle (89.81(16)° for **4.3** and 91.06(14)° for **3.1a**) compare with the corresponding values observed in **3.1a** (Table 4.6).

Bond	**3.1a**	**4.3**
Pd-carbene	2.088(5) Å	2.092(6) Å
Pd-P	2.2994(13) Å	2.2221(18) Å
Pd-CH$_3$ *trans* to carbene	2.111(5) Å	2.099(6) Å

Table 4.6: Comparison of the bond lengths between complex **3.1a** and the cation in **4.3**.

Figure 4.5: ORTEP representation of the cation in **4.4** showing 50% probability ellipsoids. The BAr$_4^{F-}$ anion and H atoms are omitted for clarity. Selected bond lengths (Å) and angles (°):C(1)-Pd(01) = 2.090(4), C(6)-Pd(01) = 2.070(4), N(3)-Pd(01) = 2.091(3), P(1)-Pd(01) = 2.2043(9), C(7)-N(3) = 1.139(5); C(1)-Pd(01)-P(1) = 93.56(9), N(3)-Pd(01)-P(1) = 169.48(9), C(1)-Pd(01)-N(3) = 96.75(12), C(6)-Pd(01)-P(1) = 84.32(11), C(1)-Pd(01)-P(1) = 93.56(9), C(7)-N(3)-Pd(01) = 174.3(3), N(3)-C(7)-C(8) = 179.4(4).

Here too, the Pd centre in the cation is square planar with chelating ligand, one methyl group *trans* to the NHC end, and one acetonitrile ligand *trans* to the phosphine. The Pd-carbene and Pd-CH$_3$ bond distances compare with those observed in **4.4** (Table 4.7). The acetonitrile donor ligand is practically linear while the CN bond length suggests little to no π-backdonation from d$_\pi$ orbitals of the metal to the π* of the triple bond. [9] Finally the Pd-L (L = pyridine, acetonitrile) bond distances are equal within esds. The

ligand bite angle in **4.4** (93.56(9)°) is bigger than in **4.3** (89.81(16)°), accounting for a more flexible six member chelate. The reason for this is unclear but it could be due to the less steric restrictions imposed by the acetonitrile ligand.

Bond	**4.3**	**4.4**
Pd-carbene	2.092(6) Å	2.090(4) Å
Pd-P	2.2221(18) Å	2.2043(9) Å
Pd-CH$_3$ *trans* to carbene	2.099(6) Å	2.070(4) Å

Table 4.7: Comparison of selected bond distances of cations in complexes **4.3** and **4.4**.

From the above table it is observed that in the case of **4.4** the Pd-P distance is shorter than that in **4.3**. This could be attributed to the weaker *trans* influence the acetonitrile donor ligand has on this Pd-P bond compared to pyridine.

The geometry of the cation in complex **4.9** was unambiguously established by single crystal X-ray diffraction studies (Figure 4.6). Colourless crystals were grown by layering an ethereal solution of **4.9** with petroleum ether. The geometry around the Pd centre is square planar: its coordination sphere comprises the bidentate ligand, one pyridine and one methyl group. The ligand bite angle in the cationic species **4.9** has increased from 76.8(4)° at the neutral complex **3.5b** to 78.16(18)°. The Pd-carbene and Pd-CH$_3$ bond lengths compare with the corresponding values observed in the neutral complex **3.5b** (Table 4.8). The ligand adopts an almost isoplanar conformation with the pyridine plane tilted, in order to accommodate the steric requirements of the methyl in the three position of the pyridine heterocycle. The pyridine donor plane forms an angle of approximately 74.9° with the plane of the metal centre.

Figure 4.6: ORTEP representation of the cation in **4.9** showing 50% probability ellipsoids. The asymmetric unit consists of two cations and two anions. The BAr_4^{F-} anion and H atoms are omitted for clarity. Selected bond lengths (Å) and angles (°): C(2)-Pd(1) = 1.964(5) , N(4)-Pd(1) = 2.084(4), N(1)-Pd(1) = 2.154(4), C(27)-Pd(1) = 2.021(5), C(2)-Pd(1)-C(27) = 96.9(2), C(2)-Pd(1)-N(4) = 172.2(2), C(27)-Pd(1)-N(4) = 87.96(19), C(2)-Pd(1)-N(1) = 78.16(18), C(27)-Pd(1)-N(1) = 172.1(2), N(4)-Pd(1)-N(1) = 97.65(16).

Bond	**4.9**	**3.5b**
Pd-carbene	1.964(5) Å	2.038(10) Å
Pd-N(1)	2.154(4) Å	2.130(9) Å
Pd-CH$_3$ *trans* to N(1)	2.021(5) Å	2.017(11) Å

Table 4.8: Comparison of selected bond lengths in **3.5b** and **4.9**.

Table 4.9 compares some bond lengths between the cationic species in complexes **4.3** and **4.9**.

Bond	4.3	4.9
Pd-carbene	2.092(6) Å	1.964(5) Å
Pd-L'	2.2221(18) Å	2.154(4) Å
Pd-pyridine donor	2.126(4) Å	2.084(4) Å
Pd-CH$_3$	2.099(6) Å	2.021(5) Å

Table 4.9: Comparison of selected bond lengths between cations in **4.3** and **4.9** (L' = pyridine (**4.9**) or phosphine (**4.3**) moiety of the ligand).

The Pd-carbene bond in **4.9** is shorter than in the corresponding cation in **4.3**. This is probably due to the formation of a more rigid five member chelate than a six member one. The Pd-pyridine(donor) bond distances in both cases are the same within esds, while the Pd-CH$_3$ bond distance in **4.3** is elongated compared to **4.9** as a result of the stronger *trans* influence of the NHC functionality in **4.3** compared to the pyridine moiety of the ligand in **4.9**.

4.4 Reactivity of neutral Pd(II) complexes with MeI

4.4.1 Reaction of 3.1a with MeI

It is established that Pd(L-L)(CH$_3$)$_2$ complexes (L-L = tmeda, bipy, phen) react with CH$_3$I to form Pd(IV) complexes, [10] some of which have been structurally characterised. These Pd(IV) methyls can reductively eliminate ethane and form new Pd(II) complexes.[10,11] Reaction of **3.1a** with excess MeI in CH$_2$Cl$_2$ at room temperature gave rise to a complex reaction mixture. The ^{1}H-NMR spectrum of the reaction mixture showed the complete consumption of the starting material as evidenced by the absence of the two characteristic signals for the two Pd-CH$_3$ protons. Furthermore the two doublets assignable to the diastereotopic *o*-isopropyl methyls had been displaced by a broad multiplet, while the characteristic septet of the methinic C-Hs was replaced by two broad multiplets centred at 2.03 and 2.50 ppm. Finally two sharp singlets at 2.28 and 2.41 ppm appeared. The appearance of the last two resonances is indicative of the formation of 2-methylimidazolium salts.[7] The ^{31}P{^{1}H}-NMR spectrum showed the existence of two

phosphorus containing species in solution, with a predominant species being represented by a peak at 26.4 ppm and the second one giving rise to a signal at 20.9 ppm. Repeated recrystallisations of this complex reaction mixture from CH_2Cl_2/Et_2O at –30 °C gave a small crop of orange crystals of complex **4.10**. Its identity was unequivocally established by single-crystal X-ray diffraction and is shown in Figure 4.7.

Figure 4.7: ORTEP representation of the structure of **4.10** showing 50% probability ellipsoids. H atoms and a molecule of dicholoromethane have been omitted for clarity. Selected bond lengths (Å) and angles (°): P(4)-Pd(1) = 2.2481(18), Pd(1)-Cl(3) = 2.358(5), Pd(1)-I(1) = 2.6613(7), Pd(1)-I(2) = 2.6675(7); P(4)-Pd(1)-Cl(3)= 90.06(12), P(4)-Pd(1)-I(1)= 90.99(5), Cl(3)-Pd(1)-I(1) = 168.21(14), P(4)-Pd(1)-I(2) = 176.22(5), Cl(3)-Pd(1)-I(2) = 86.38(11), I(1)-Pd(1)-I(2) = 92.25(2).

The molecule comprises a square-planar Pd centre coordinated by one imidazolium functionalised phosphine, two iodides and one chloride. The chloride originates possibly from the use of dichloromethane as the reaction solvent. The two Pd-I bond distances are the same within esds.

113

A plausible mechanism for the formation of **4.10** is given in Scheme 4.5. This mechanism, although speculative of the exact stereochemistry of the intermediates, involves successive Pd(II)-Pd(IV) oxidative additions of MeI and reductive eliminations of ethane leading to the bis-iodo species **4.11**. The last oxidative addition is followed by reductive elimination of the methylimidazolium cation, leading to the observed species. Reductive elimination of methylimidazolium after the first oxidative addition step is also plausible, leading to iodo dimethyl species, which can undergo further oxidative addition steps to the observed product. An alternative pathway involving Pd(II)-Pd(0) cycles is less likely, on the basis of the high thermal stability of **3.1a** at room temperature.

Scheme 4.5: Proposed mechanism for the formation of **4.10**.

The above mechanism does not include a step that explains the chloride bound to the metal centre in **4.10**. It probably originates from oxidative addition of dichloromethane at the palladium centre, followed by reductive elimination of chloroethane to produce a

114

Pd(II) species that further undergo oxidative addition of MeI to give the observed product **4.10**.

The reaction was monitored by VT NMR spectroscopy (^{1}H and ^{31}P{^{1}H}). It showed that the reaction occurs at room temperature and that the formation of methylimidazolium (singlet at 2.40 ppm in the ^{1}H-NMR spectrum) happens overnight. This is accompanied by the disappearance of the two Pd-Me doublets and the formation of ethane. However, a complex reaction mixture prevented the full identification of all reaction products. The ^{31}P{^{1}H}-VT NMR experiment showed the complete consumption of the neutral complex **3.1a** (singlet at 12.4 ppm) at room temperature overnight, with the concurrent appearance of a predominant signal centred at 26.3 ppm. The latter spectrum also contained a multitude of other peaks.

4.4.2 Reaction of 3.3 with MeI

The reaction of **3.3** with MeI was also investigated. Upon addition of MeI the pale yellow dichloromethane solution of **3.3** changed to a bright orange. NMR spectroscopy revealed a complex reaction mixture. Nevertheless the absence of the upfield Pd-Me doublets in the ^{1}H-NMR spectrum was apparent, as well as one singlet at 2.1 ppm assignable to the methyl in the 2 position of a methylimidazolium salt. Two major species in a 1:1 ratio were also detected in the ^{1}H-NMR spectrum of the reaction, as evidenced by the existence of a pair of doublets centered at 4.52 ppm ($^2J_{PH}$ = 6.1 Hz) and 4.88 ppm ($^2J_{PH}$ = 6.8 Hz). Signals for the methyls of o-isopropyl groups appeared as two pairs of overlapping doublets, while two methinic CH septets centered at 2.52 and 2.56 ppm were also observed. The existence of two species in solution was further evidenced by the appearance in the ^{31}P{^{1}H}-NMR spectrum of two major peaks at 49.4 and 26.9 ppm. The latter spectrum also contained no resonance at 32.7 ppm corresponding to the neutral complex **3.3**, thus verifying its complete consumption. Upon standing at room temperature degradation occurred in the form of black aggregates. These were removed by filtration through Celite and the resulting orange solution was evaporated to dryness. Redissolving in CD_2Cl_2 and acquiring the spectra showed no significant improvement. Various methods of analysis (NMR, MS and X-ray diffraction) gave inconclusive results regarding the exact nature of these two species. Never the less, mass spectrometry (ES$^+$) consisted of peaks agreeing with the mass and isotopic patterns for species [**4.12**-I+CH$_3$CN]$^+$ (Scheme 4.6) and 3-(2,6-diisopropyl-phenyl)-1,2-dimethyl-imidazolium phosphinoxide (cation

generated from the breaking down of the methylimidazolium functionalized phosphine). Other palladium containing species, which could not be identified, were also present in solution.

Scheme 4.6: Reaction of **3.3** with MeI (X = I, Cl, two are iodides).

Based on the example of the reaction of **3.1a** with MeI it can be concluded that the species with the $^{31}P\{^{1}H\}$-NMR chemical shift at 49.4 ppm is **4.12**. The other species resonating at 26.9 ppm in the $^{31}P\{^{1}H\}$-NMR spectrum could not be identified. Nonetheless its relative upfield shift compared to the neutral complex **3.3** (32.7 ppm), means that it is the product of a chemical transformation shielding the phosphorus atom.

4.4.3 Reaction of 3.5b with MeI

The reactivity of the neutral complex **3.5b** towards oxidative addition with MeI was also tested. Unlike **3.1a** the reaction proceeded cleanly in an NMR scale, allowing the identification of the mixed complex **4.13** (Scheme 4.7).

The product of the oxidative addition of MeI was identified by its ^{1}H-NMR spectrum. The two singlets, assigned to the Pd-Me protons in **3.5b** (0.12 and 0.22 ppm), were replaced by a singlet, integrating for three protons, centred at 0.29 ppm. The other characteristic peaks of the molecule have the same appearance as in the precursor **3.5b**, showing that the molecule adopts a C_s symmetry. Finally the carbene carbon was located at 188.9 ppm in the $^{13}C\{^{1}H\}$-NMR spectrum. This spectroscopic evidence suggests the formation of one isomer. The exact stereochemistry of the molecule could not be determined by NMR correlation experiments.

Scheme 4.7: Oxidative addition reaction of MeI in **3.5b**.

When the sample was left overnight at room temperature in CD_2Cl_2, minor, but not negligible, peaks appeared in the ^1H-NMR spectrum (namely a second pair of doublets at 1.33 and 1.38 ppm, one septet at 2.65 ppm and a singlet between 2.91 and 2.92 ppm almost overlapping with the 3-CH_3-pyridyl signal at 2.91 ppm) . This suggests the formation of another product, which does not involve any oxidative addition of MeI excess (which was removed after the reaction was complete). Layering this CD_2Cl_2 solution with ether produced scarlet crystals, which were subjected to an X-ray diffraction study (Figures 4.8, 4.9). The geometry around the metal centre is practically square planar, with coordination sphere being comprised by the ligand, one iodide *trans* to the carbene, while the position *trans* to the pyridine functionality has a 50:50 mixed occupancy of carbon and chlorine. Thus complex **4.13** undergoes a second oxidative addition with dichloromethane, followed by reductive elimination of chloroethane to give complex **4.14**. The pyridine plane forms an angle of 14.36(1)° with the NHC plane, indicating no π-conjuration between the two functionalities. The Pd-X (X = Cl, I) compare with the ones observed in complex **4.10**. Finally the Pd-NHC and Pd-pyridine bond lengths are the same within esds with the ones observed in complex **3.5b**.

It is unclear why the formation of only one isomer is preferred. As a speculative reason it could be proposed that the methyl *trans* to the NHC functionality in the intermediate of the oxidative addition is more readily available for reductive elimination due to the stronger *trans* effect of the carbene moiety.
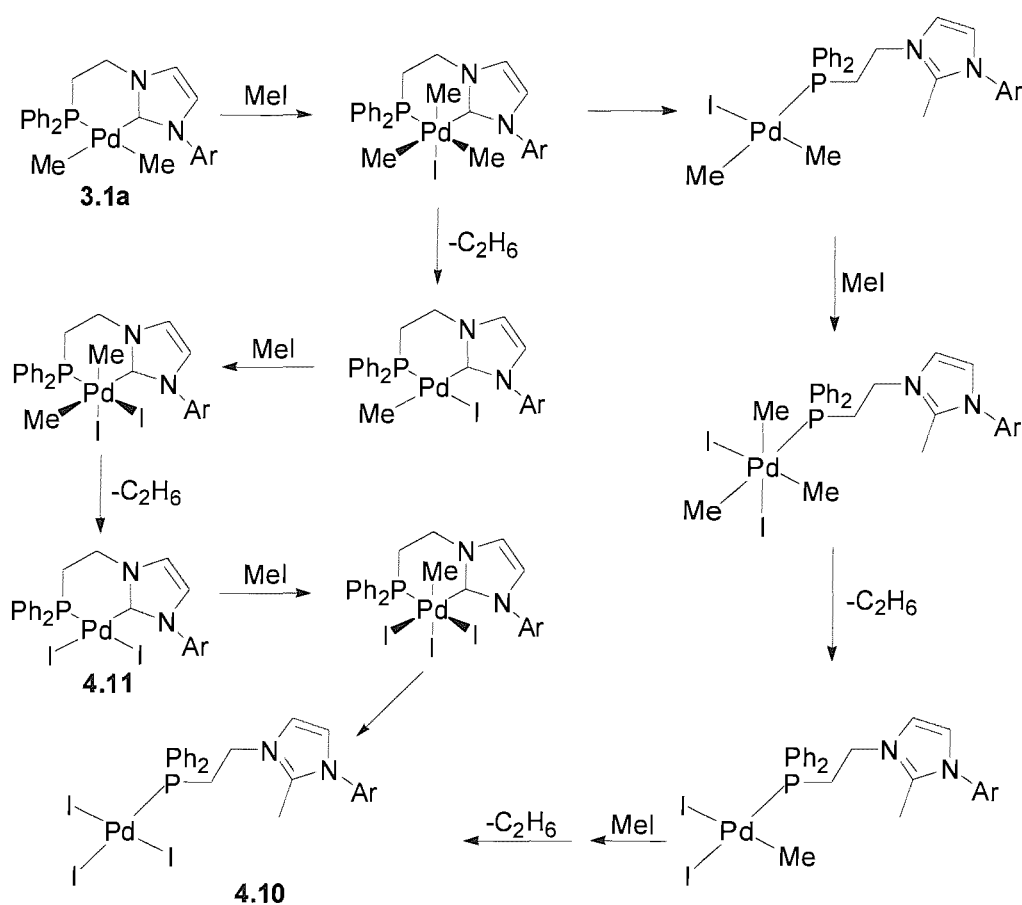
Figure 4.8: ORTEP representation of the structure of **4.13** showing 50% probability ellipsoids. H atoms have been omitted for clarity. Selected bond lengths (Å) and angles (°):C(2)-Pd(1) = 1.976(4), C(22)-Pd(1) = 2.228(2), I(1)-Pd(1) = 2.6441(6), N(1)-Pd(1) = 2.153(4); C(2)-Pd(1)-N(1) = 78.20(15), C(2)-Pd(1)-C(22) = 99.48(13), N(1)-Pd(1)-C(22) = 173.19(12), C(2)-Pd(1)-I(1) = 168.04(11), N(1)-Pd(1)-I(1) = 97.60(10), C(22)-Pd(1)-I(1) = 85.91(6).

Figure 4.9: ORTEP representation of the structure of **4.14** showing 50% probability ellipsoids. H atoms have been omitted for clarity. Metric data are the same as in Figure 4.8.

118

4.5 Synthesis and characterisation of dicationic species

Dicationic Pd(II) complexes incorporating bidentate bis-NHC ligands have been found to act as catalysts for the co-polymerisation of CO/C_2H_4.[12] In an attempt to access similar complexes incorporating phosphine functionalised NHC ligands, complex **3.2a** was reacted with $AgBF_4$ or AgOTf in CH_3CN to give complexes **4.15** and **4.16** respectively.

Scheme 4.8: Preparation of dicationic species (Ar = 2,6-diisopropylphenyl, $X^- = BF_4^-$ (**4.15**), OTf^- (**4.16**)).

Their formation was established by spectroscopic methods. The ^{1}H-NMR spectrum contained the characteristic peaks of the diastereotopic methyls as well as the methinic septet of the isopropyl groups. The signals attributed to the space linker methylenic protons are shifted downfield compared to the starting neutral complex **3.2a** (2.8 and 4.3/4.6 ppm for **4.15/4.16** respectively *versus* 1.9 and 4.3/4.4 ppm for **3.2a**). This downfield shift is probably due to the formation of the cationic species. Their formation was further confirmed by the downfield shift in the ^{31}P{^{1}H}-NMR spectrum of the reaction mixture from 21.0 ppm for **3.2a** to 29.9 ppm for both **4.15** and **4.16**. Unfortunately these species proved to be very unstable: after a twenty minutes period at room temperature, formation of black aggregates was observed. The contents of the solution were completely altered and further characterisation was inhibited. The reaction was also repeated with the use of MeOH instead of MeCN with no success. Finally use of $AgPF_6$ instead of $AgBF_4$ or AgOTf yielded far more unstable solutions, whose characterisation completely failed due to their rapid decomposition.

4.6 Catalytic activity of neutral and cationic Pd(II) complexes towards Heck olefinations

4.6.1 Introduction

Palladium catalysts have provided many catalytic transformations for synthetic organic chemistry. [13] Palladium-catalysed cross coupling of aryl-halides (or halide analogues) with nucleophiles is firmly established as one of the most important methods for C-C and C-N bond formation. [14] These cross-coupling reactions employ a range of transmetallating agents. A general catalytic cycle for palladium complex-mediated cross-coupling reactions is shown in Figure 4.10. While Heck and amination reactions do not strictly speaking involve a transmetallation step, they are generally included in discussions of cross-coupling chemistry since their catalytic cycles possess essentially the same features.

Figure 4.10: Catalytic cycle for palladium complex-mediated cross-coupling reactions;where Ar-M' is organoboronic acid, organomagnesium, organostannane, organosilicon, *etc.*

Palladium complexes containing phosphine ligands have been widely used as successful catalysts for the coupling of sp^2 carbons. The use of bulky electron-rich tertiary alkyl phoshines has been particularly effective. [15, 16, 17] Their success can be explained by

reference to the catalytic cycle depicted in Figure 4.10. The electron-richness imparted to the metal centre by the electron donating phosphine assists the oxidative addition of the Ar-X bond. On the other end of the cycle the steric bulk of the ligand promotes the reductive elimination of the Ar-Ar' coupling product.

Recently alternatives to phosphines have been sought after, due to their "user-unfriendly" properties, mainly air and moisture sensitivity. Highly promising and versatile alternatives to phosphines have been found in the NHC class of ligands. These neutral two electron σ-donors, exhibit greater thermal stability than phosphines and can bind to the metal centre very strongly. [18] In this way they eliminate the need for excess ligand during catalytic processes. Because of these properties they have proven to be extremely efficient ancillary ligands in many catalytic reactions [19] with activity surpassing those of phosphines

4.6.2 Heck olefination

The palladium catalysed arylation of an alkene with an organic halide was first reported by Mizoroki and Heck in the early 70's. [20] The reaction involves bond formation between two sp^2 carbon centres by an overall substitution of a C-H bond of an alkene by R_1 from the R_1X substrate (R_1 = vinyl or aryl; X = I or Br; R_2 = electron-withdrawing or releasing group) under basic conditions as depicted in Scheme 4.9.

$$R_1\text{-X} \quad + \quad \overset{R_2}{=\!\!/} \quad + \quad \text{Base} \quad \xrightarrow{\text{[Pd]}} \quad \overset{R_2}{\underset{R_1}{/\!\!=\!\!/}} \quad + \quad \text{Base.HX}$$

Scheme 4.9: Heck olefination.

The currently accepted mechanism for the Heck reaction is illustrated in Figure 4.11. The catalytically active species are believed to be 14 electron coordinatively unsaturated PdL_2 species which undergo oxidative addition of the aryl (or vinyl) halide, followed by cis-trans isomerization to give the more thermodynamically stable trans-PdL_2R_1X. The next step involves dissociation of an L ligand and complexation of the olefin, which is then followed by migratory insertion of the R_1 alkyl. The two final steps are the β-hydride elimination to produce a trans hydride species, which in the presence of base regenerates the catalytically active species.

Base.HX

Base   PdL$_2$ R$_1$-X

H
L–Pd–L
X

R$_1$
L–Pd–L
X

R$_2$

R$_2$
R$_1$

R$_2$
L–Pd–L
X
R$_1$

R$_1$
L–Pd
X
R$_2$

- L

+L

Figure 4.11: Postulated mechanism of Heck olefinations.

Variations of the mechanism illustrated in Figure 4.11 have been proposed for complexes with chelating ligands and weakly coordinating anions.[21] This generally accepted mechanism has been the subject of much debate, and there is much complexity in addition to the steps outlined above. One of the most debated issues is if the catalytic cycle follows a Pd(0)/Pd(II) or a Pd(II)/Pd(IV) step. Most of the Pd(II) catalytic systems show an induction period, implying that the cycle begins after the reduction of the Pd(II) metal centre to Pd(0). It is interesting to note that in these systems the use of reducing agents often results in the lowering of the observed induction periods. However this induction period is not observed with all complexes that are active pre-catalysts. This phenomenon has been observed in systems employing phosphine palladacycles and PCP pincer palladacycles.[22] To explain this, two mechanisms involving Pd(II)/Pd(IV) steps have been proposed by Jensen [23] and Shaw [24] (Figure 4.12 and 4.13 respectively).

Figure 4.12: Jensen's [23] Pd(II)/Pd(IV) mechanism (Q = CH_2, O; X = halide; R_1 = Ar).

The catalytic cycle illustrated above begins with the oxidative addition of a vinyl C-H of the alkene substrate to the Pd(II) pincer complex. This is followed by reductive elimination of HX to regenerate a Pd(II) species, which in turn undergoes a second oxidative addition of the R_1-X (R_1 = Ar) bond to give a Pd(IV) species. Reductive elimination of the desired product from this Pd(IV) species regenerates the catalyst.

o-Tol o-Tol

$$\left(\begin{array}{c}P\\ \\ C\end{array}\begin{array}{c}X\\Pd \quad Pd\\X\end{array}\begin{array}{c}C\\ \\ P\end{array}\right) = \left[\begin{array}{c}o\text{-Tol} \quad o\text{-Tol}\\P\\Pd \quad X\end{array}\right]_2$$
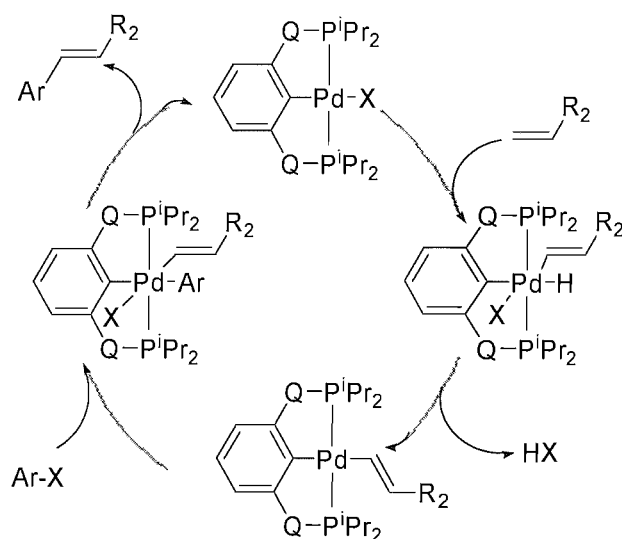
regeneration

Base.HX

Base

alkene coordination

R_2

attack by nucleophile

Nu

Nu

β-hydride elimination

R_2
R_1

oxidative addition

Nu

R_1-X

loss of nucleophile

Nu
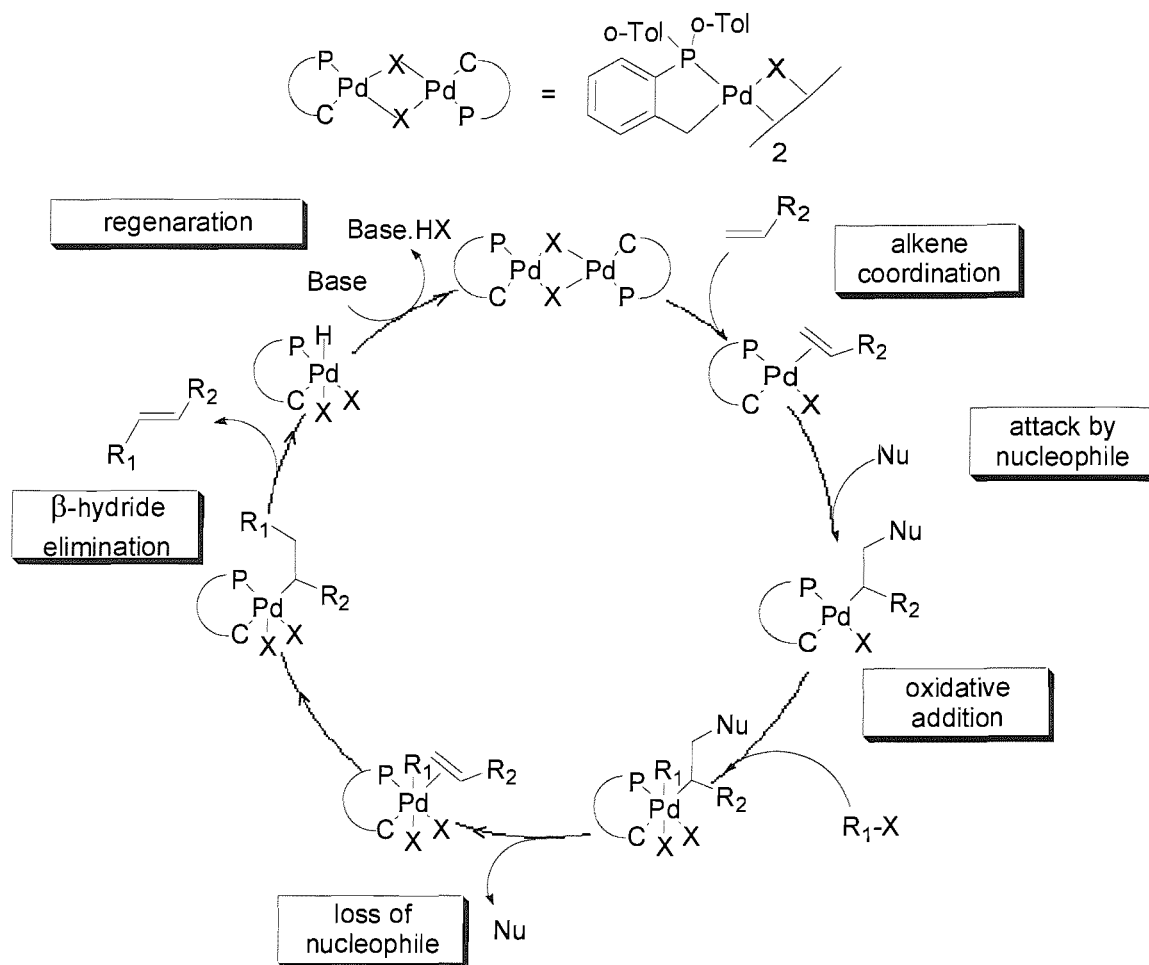
Figure 4.13: Shaw's [24] Pd(II)/Pd(IV) mechanism (R_1 = Ar; X = Cl, Br, I, OAc; Nu = OAc⁻, OH⁻, Br⁻, I⁻, amines).

The proposed catalytic cycle by Shaw, begins with the coordination of the alkene. This η^2-alkene complex undergoes attack by a nucleophile (e.g. the base) to give the σ-alkyl complex. This complex, which can have an overall negative charge if the nucleophile is not neutral, is sufficiently electron rich to oxidatively a R_1-X to form a Pd(IV) species. Loss of the nucleophile generates an η^2-alkene Pd(IV) species. Migration of the R_1 followed by β-hydride elimination creates the Pd-H complex. Regeneration of the catalyst is effected through the base promoted removal of HX.

Although there is proof that both mechanisms involve a Pd(II)/Pd(IV) step, it has been proposed that the success of these pincer palladacycles is due to the formation of colloidal palladium aggregates. This has huge repercussions as it means that the reaction is essentially heterogeneous.[25]

While monodentate phosphines have provided efficient catalysts, the use of bulky electron donating phosphines such as P^tBu_3 is needed when less reactive aryl halides are to be coupled.[26] At the elevated temperatures required for Heck chemistry, both phosphines and their Pd complexes are prone to decomposition, so higher catalyst loadings are needed. Increased stability can be imparted by using chelating phosphines but only limited success has been achieved in catalysis.

However a degree of efficiency has been observed in Heck reactions mediated by Pd-NHC complexes. The palladium complexes shown in Figure 4.14 reported by Herrmann [27, 28, 29] and Cavell [30, 31] have been demonstrated to be active catalysts for C-C bond formation in the Heck reaction.

4.17   **4.18**   **4.19**

4.20a: n = 2, X = I
4.20b: n = 3, X = Br

4.21

4.22a: R_1 = R_2 = Me
4.22b: R_1 = Me, R_2 = CF_3
4.22c: R_1 = R_2 = CF_3
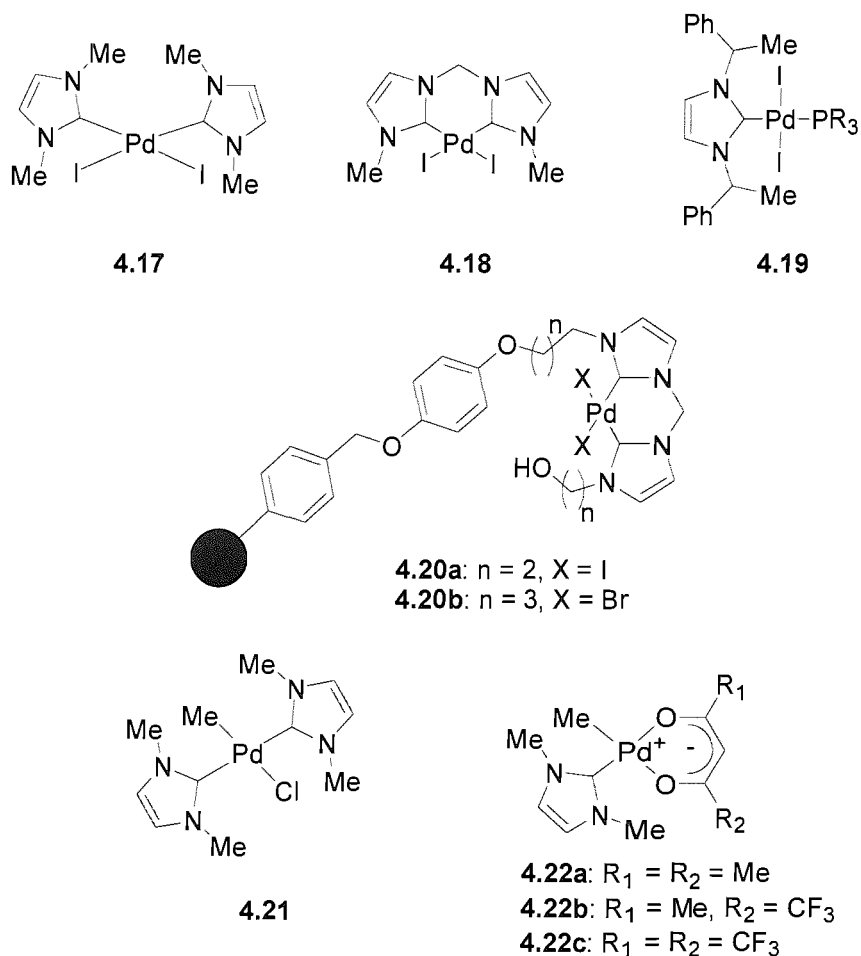
Figure 4.14: Complexes active in Heck couplings reported by Herrmann (**4.17-4.20a,b**) and Cavell (**4.21** and **4.22a-c**).

In the case of the complexes **4.17-4.19** shown above (Figure 4.14), the catalytic cycle is probably initiated by the formation of a biscarbene Pd(0) species. Oxidative addition of the aryl (vinyl) halide gives *trans*-Pd(bis-carbene)(aryl)X. Dissociation of X⁻ and coordination of the alkene to afford a monocationic complex is suggested to be the successive step of the catalytic cycle. *Cis-trans* isomerism is the necessary next step for the migratory intertion of the alkyl to the olefin. The last two steps of the cycle are the same as those described in Figure 4.11. Interestingly complexes **4.17-4.19** exhibit an induction period since the generation of the catalytic active species described above is achieved with the presence of reducing agents. In contrast, complexes **4.20-4.22** do not exhibit such a trend.

Other successful catalytic systems include Pd(II) NHC complexes with dangling *N*-substituents [32] (**4.23**), pyridine functionalised NHC Pd(II) complexes [33](**4.24a-b**) and C-N-C pincer Pd(II) [34] (**4.25**) complexes. The latter exhibit high thermal robustness in the Heck coupling of aryl bromides at 180 °C in air (Figure 4.15).

4.23

4.24a: n = 0
4.24b: n = 1

4.25
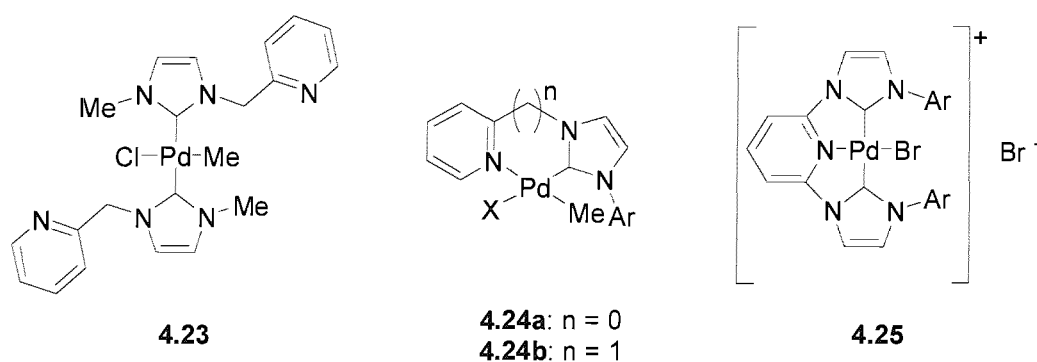
Figure 4.15: Pyridine functionalised NHC Pd(II) complexes employed in Heck couplings (Ar = 2,6-diisopropylphenyl, 2,4,6-trimethylphenyl; X = Cl, Br).

Following theoretical studies, [35] which suggested that mixed NHC-phosphine chelates were suitable for the Pd-catalysed Heck reaction, Nolan *et al.* prepared the imidazolium salt shown in Figure 4.16 and investigated its efficiency in the cross-coupling of aryl bromides with n-butyl acrylate.[36] No complexes were isolated though and the imidazolium salt was used as the precursor for the *in situ* generation of the NHC-phosphine chelate. To the best of our knowledge the only other system employing phosphine functionalized NHC Pd(II) complexes was recently reported by Hon Man Lee *et al.* (Figure 4.16).[37]

126

Ph2P

N+ N

Br-

2.4b

N N

P-Pd-P
Ph2 Ph2
X

X1-

4.26a: X = X1 = Cl
4.26b: X = MeCN, X1 = BF4
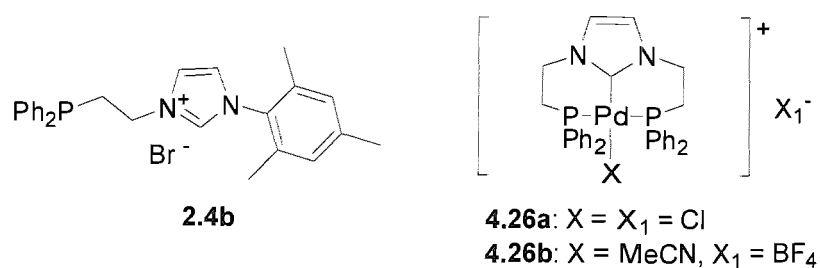
Figure 4.16: Phosphine functionalised imidazolium salts and NHC complexes used in Heck couplings.

4.6.3 Heck catalysis with complexes reported in Chapter 3 and Chapter 4

The catalytic activity of the neutral Pd(II) complexes, synthesised in Chapter 3 (Figure 4.17), was screened as Heck olefination catalysts.

Ph2P
Pd
Me Me

N
N Ar

Ar = 2,6-diiso -propylphenyl : **3.1a**
Ar = 2,4,6 -trimethylphenyl: **3.1b**

Ph2P
Pd
Br Br

N
N Ar

Ar = 2,6-diiso -propylphenyl : **3.2a**
Ar = 2,4,6-trimethylphenyl: **3.2b**

Ph2P
Pd
Me Me

N
N Ar

3.3

N
N
Pd
Me Me Ar

3.5b

Ar N
N
py Me Pd Me Ar N
N py

3.6
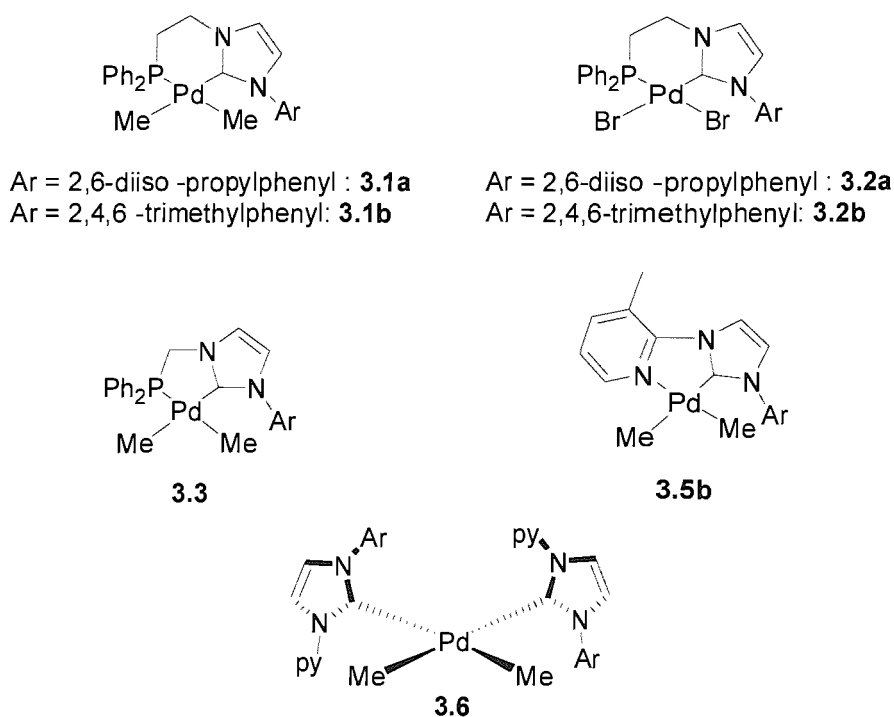
Figure 4.17: Neutral Pd(II) complexes used as catalysts for the Heck olefination of aryl halides.

The use of these complexes as catalysts for the Heck coupling of *p*-bromoacetophenone with methyl acrylate was initially studied. Using *N*-methyl-2-

pyrolidinone (NMP) as a solvent and NEt$_3$ as a base resulted in most cases in the complete conversion of the aryl halide to the desired product as determined by GC. The results are outlined in Table 4.10 and Figure 4.18. In the cases where complexes **3.5b** and **3.3** were used as catalysts, the product was isolated (almost quantitatively) and NMR spectroscopy showed that the substituents of the double bond are arranged *trans* to each other.
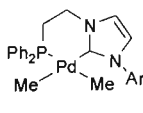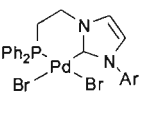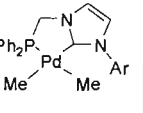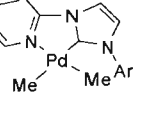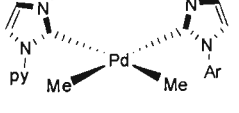
Complex	3.1a/b	3.2a/b	3.3	3.5b	3.6
Yield (%)	92/66.8	31/12	100	100	100
T.O.N.	184/134	62/24	200	200	200

Table 4.10: Heck olefination of *p*-bromoacetophenone with methyl-acrylate. Conditions: NMP, 1mmol of aryl bromide, 1.4 eq. of alkene, 2 eq of NEt$_3$ at 120 °C for 6hrs, with 0.5% mole catalyst loading. In the case of **3.2a/b** 1.1 eq. of N$_2$H$_4$.H$_2$O was added. (Ar = 2,6-diisopropyl-phenyl (**a**), 2,4,6-trimethyl-phenyl (**b**). For **3.3**, **3.5b** and **3.6** Ar = 2,6-diisopropyl-phenyl throughout).

Figure 4.18: Graphic representation of the catalytic results given in the above table 4.10.

From the above results it can be deduced that the dimethyl neutral Pd(II) complexes are better catalysts than the dibromide complexes. It is also apparent that the five member ring chelates are better catalysts than the six member ones. Finally, bidentate

128

complexes **3.3** and **3.5b** show the same activity with the monodentate complex **3.6**. It is also interesting to note the decrease in reactivity of complex **3.1b** compared to its analogue **3.1a**. This could be due to the fact that the bulkier aryl group in **3.1a** is facilitating the reductive elimination of the products. Black aggregates were observed where the phosphine functionalised NHC complexes were used, whereas such decomposition was not apparent with pyridine functionalised NHC complexes **3.5b** and **3.6**.

The use of other bases was also considered. Nolan *et al.* have reported the effective use of Cs_2CO_3 as a base for Heck coupling reactions.[36] The Heck olefination of *p*-bromoacetophenone with methyl acrylate was again the trial reaction. Table 4.11 and Figure 4.19 summarise the results.

Complex	3.1a/b	3.2a/b	3.3	3.5b	3.6
Yield (%)	4.3/54.3	0/0	32	100	100
T.O.N.	9/110	0/0	64	200	200

Table 4.11: Heck olefination of *p*-bromoacetophenone with methyl acrylate. Conditions: NMP, 1mmol of aryl bromide, 1.4 eq. of alkene, 2 eq of Cs_2CO_3 at 120 °C for 6hrs, with 0.5% mole catalyst loading. In the case of **3.2a/b** 1.1 eq. of $N_2H_4.H_2O$ was added. (Ar = 2,6-diisopropyl-phenyl (**a**), 2,4,6-trimethyl-phenyl (**b**). For **3.3**, **3.5b** and **3.6** Ar = 2,6-diisopropyl-phenyl throughout).
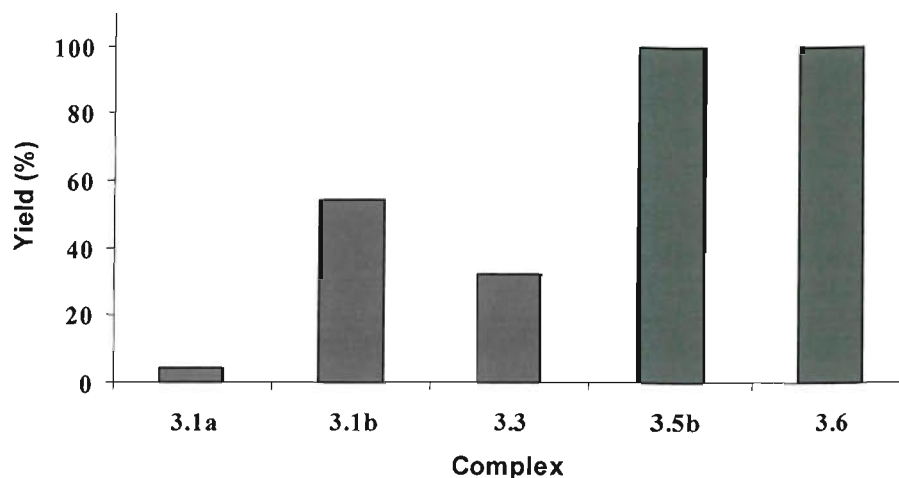
Figure 4.19: Graphic representation of the catalytic results given in the above table 4.11.

From these results it is easily seen that upon changing the base, there is a dramatic decrease in the observed yields where the phosphine functionalised NHC complexes were used. An exception is found in the case where complex **3.1b** was catalysing the reaction (54.3%). Still the product yield of this catalytic run is lower than the one observed when NEt$_3$ was the base (66.8%). It is worth noticing that the pyridine functionalised NHC catalysts **3.5b** and **3.6** were completely indifferent in the change of the base from NEt$_3$ to Cs$_2$CO$_3$.

The use of a different solvent was also considered. Using N,N'-dimethylacetamide (DMAC) as a solvent and Cs$_2$CO$_3$ as a base, under same conditions as above, the catalytic activity of complexes **3.1a/b** and **3.2a/b** towards the Heck olefination of p-bromoacetophenone with methyl acrylate, was tested. Complex **3.1a** performed almost the same (5.7%) as in the case of NMP/Cs$_2$CO$_3$ (4.3%) solvent-base system. Its mesityl analogue **3.1b** also underperformed (27% for the DMAC/Cs$_2$CO$_3$ *versus* 54.3% for NMP/Cs$_2$CO$_3$) while the dibromide complexes **3.2a** and **3.2b** showed very little activity (4.2% and 7.1% respectively).

The results of the catalytic runs displayed above are compared in Figure 4.20. From this figure we can see that for the Heck olefination of p-bromocetophenone with methyl acrylate the best solvent/base system is the NMP/NEt$_3$ one while the best catalysts are complexes **3.1a, 3.3, 3.5b** and **3.6**.

130
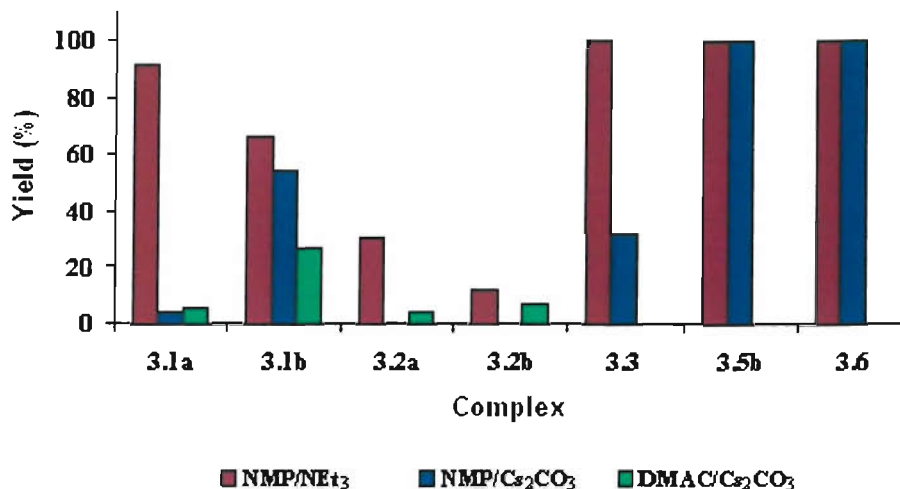
Figure 4.20: Graphic representation of the comparative study of Heck olefination of *p*-bromoacetophenone with methyl acrylate using neutral Pd(II) complexes as catalysts.

The Heck olefination, catalyzed by the neutral Pd(II) complexes of Figure 4.17, of un-activated aryl bromides was also tested. The results of the Heck coupling of bromobenzene with methyl acrylate are summarized in Table 4.12 and are represented graphically in Figure 4.21.
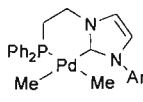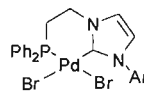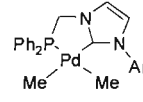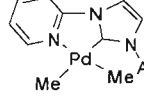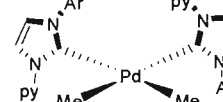
Complex	3.1a/b	3.2a/b	3.3	3.5b	3.6
Yield (%)	9.4/22	14/22	17	35	52
T.O.N.	19/44	28/44	34	70	104

Table 4.12: Heck olefination of bromobenzene with methyl-acrylate. Conditions: NMP, 1mmol of aryl bromide, 1.4 eq. of alkene, 2 eq. of NEt$_3$ at 120 °C for 6hrs, with 0.5% mole catalyst loading. In the case of **3.2a/b** 1.1 eq. of N$_2$H$_4$.H$_2$O was added. (Ar = 2,6-diisopropyl-phenyl (**a**), 2,4,6-trimethyl-phenyl (**b**). For **3.3**, **3.5b** and **3.6** Ar = 2,6-diisopropyl-phenyl throughout).

131
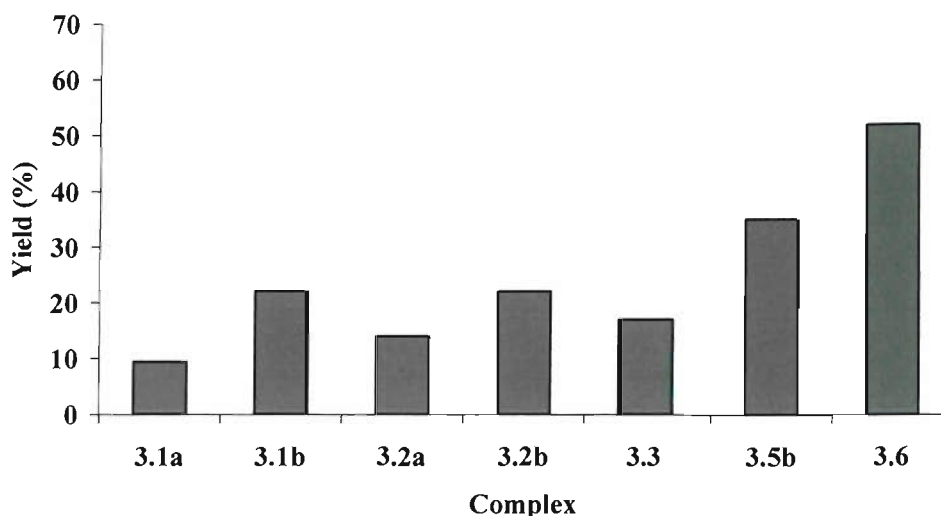
Figure 4.21: Graphic representation of the catalytic results given in the above table 4.12.

From the above table and figure, a decrease in reactivity is easily observed when bromobenzene is used as a substrate. The bidenate pyridine complex **3.5b** has superior catalytic activity compared to the phosphine functionalised NHC complexes. Its reactivity is surpassed by the neutral bis(monodentate) complex **3.6**. It is also worth noticing the higher activity of complex **3.1b** compared to **3.1a**. This result can explained on the grounds that in the case of the mesityl analogue **3.1b**, there is not as much steric crowding around the metal centre, facilitating the oxidative addition of bromobenzene. Once again complex **3.3** shows superior activity than complex **3.1a**.

The use of Cs_2CO_3 as a base in NMP or DMAC was also explored and the results of the catalytic runs are given in Tables 4.13 and 4.14, while they are graphically represented in Figures 4.22 and 4.23 respectively.
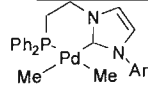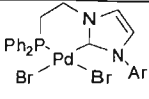
Complex	3.1a/b	3.2a/b
Yield (%)	15.3/17.4	14.4/25.3
T.O.N.	31/35	28/51

Table 4.13: Heck olefination of bromobenzene with methyl-acrylate. Conditions: NMP, 1mmol of aryl bromide, 1.4 eq. of alkene, 2 eq of Cs_2CO_3 at 120 °C for 6hrs, with 0.5% mole catalyst loading. In the case of **3.2a/b** 1.1 eq. of $N_2H_4.H_2O$ was added. (Ar = 2,6-diisopropyl-phenyl (**a**), 2,4,6-trimethyl-phenyl (**b**)).
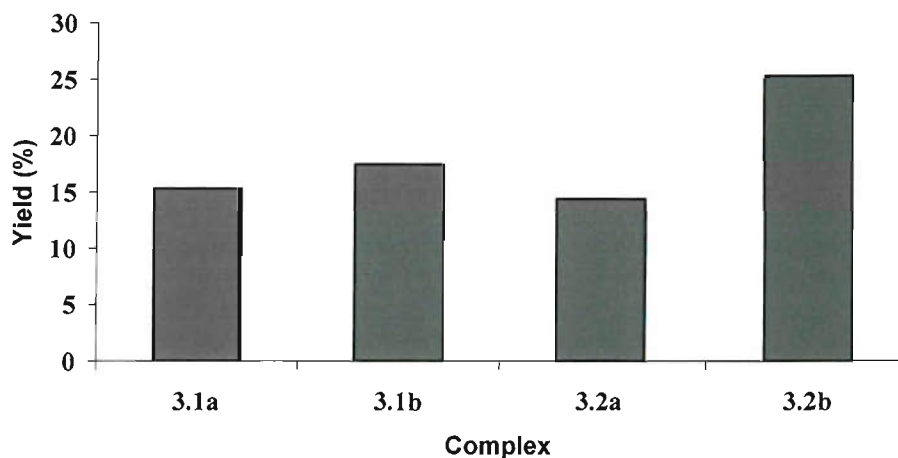
Figure 4.22: Graphic representation of the catalytic results given in the above table 4.13.
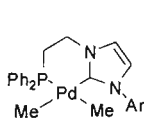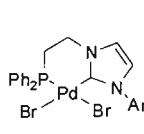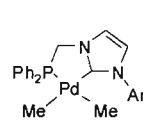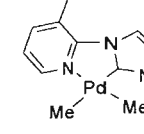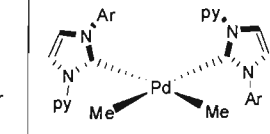
Complex	**3.1a/b**	**3.2a/b**	**3.3**	**3.5b**	**3.6**
Yield (%)	60.9/28	12/17	90	45	95
T.O.N.	122/56	24/34	180	90	190

Table 4.14: Heck olefination of bromobenzene with methyl-acrylate. Conditions: DMAC, 1mmol of aryl bromide, 1.4 eq. of alkene, 2 eq of Cs_2CO_3 at 120 °C for 6hrs, with 0.5% mole catalyst loading. In the case of **3.2a/b** 1.1 eq. of $N_2H_4.H_2O$ was added. (Ar = 2,6-diisopropyl-phenyl (**a**), 2,4,6-trimethyl-phenyl (**b**). For **3.3**, **3.5b** and **3.6** Ar = 2,6-diisopropyl-phenyl throughout).
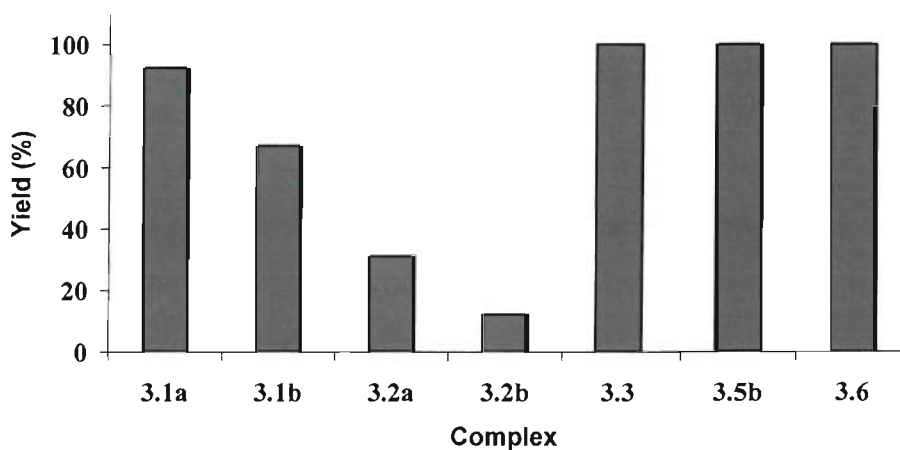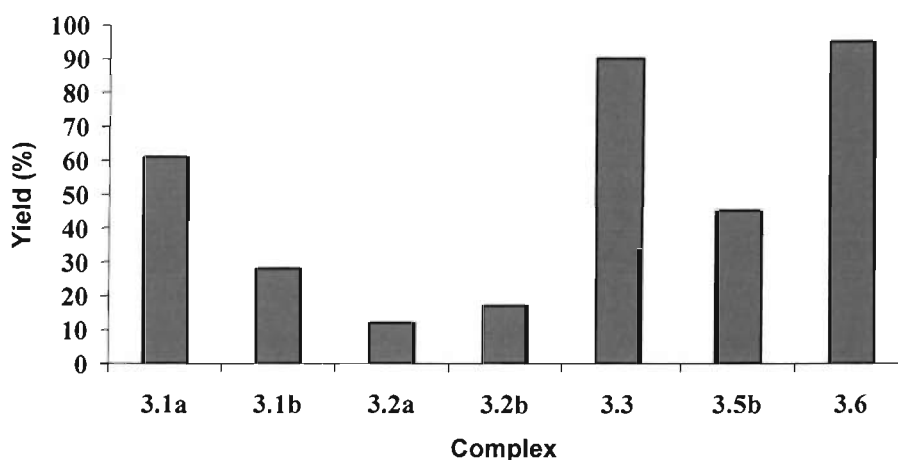

Figure 4.23: Graphic representation of the catalytic results given in the above table 4.14.

It is easily seen that changing the base from NEt_3 to Cs_2CO_3 has a dramatic influence in product yields. When NMP was the solvent these changes were not as profound. But when DMAC was used, these were increased. When complex **3.1a** was used as a catalyst under these conditions ($DMAC/Cs_2CO_3$) the product yields increased from 9.4% to 60.9%. The most remarkable increases were observed for complexes **3.3** (90% with $DMAC/Cs_2CO_3$ vs 17% with NMP/NEt_3) and **3.6** (95% with $DMAC/Cs_2CO_3$ vs 52% with NMP/NEt_3) where the conversion of the substrates was almost quantitative. In the latter case where **3.6** was used as a catalyst the product was isolated and it showed to have *trans* geometry around the double bond (as evidenced by ^{1}H-NMR spectroscopy $^3J_{HH}$ = 16.1 Hz for the olefinic protons). The reasons behind these huge differences in reactivity

are not clear. Figure 4.24 gives an illustrative representation of the above observations and from it can be easily deduced that the most active catalysts are either complex **3.3** or complex **3.6**, while complex **3.5b** is a moderate catalyst. Once again catalyst leaching was observed in the case of the phosphine functionalised NHC complexes, whereas no black precipitates were observed in the case of catalysts **3.5b** and **3.6**.
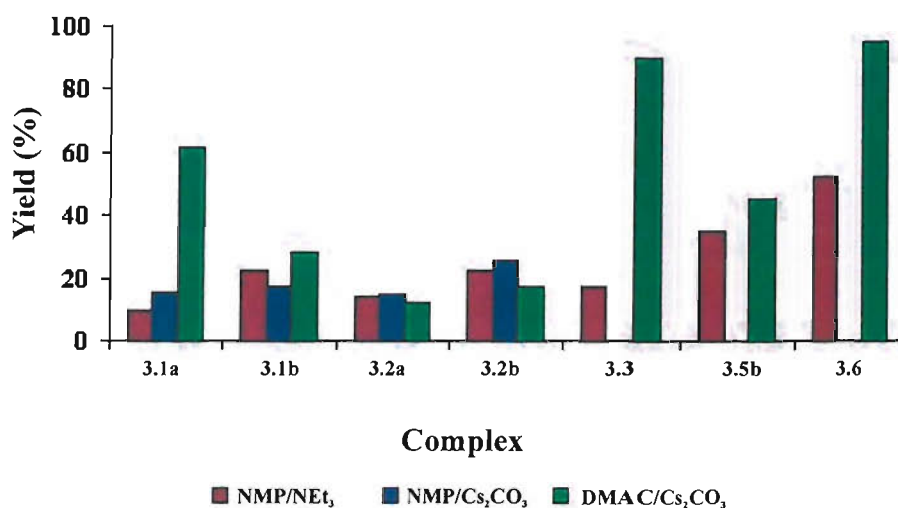
Figure 4.24: Graphic representation of the comparative study of Heck olefination of bromobenzene with methyl acrylate using neutral Pd(II) complexes as catalysts.

When aryl chlorides were tested as substrates for the Heck coupling using the above complexes, the results were quite disheartening. Little conversion is observed only with complexes **3.2a/b** (3% and 1.9% respectively) for the Heck olefination of p-chloroacetophenone, in NMP in the presence of $N_2H_4.H_2O$ and NEt$_3$ as a base. When NEt$_3$ was replaced by Cs_2CO_3 the neutral dimethyl complexes showed some reduced reactivity, which is summarised in table 4.15. Changing the solvent to DMAC did not improve catalytic conversions as only complexes **3.1a** and **3.1b** promoted the Heck olefination of p-chloroacetophenone to a 4.7% and 1.5% yield respectively. Increased catalyst loadings were also applied in an effort to improve yields, but they also met no success (*e.g.* 1% loading of **3.1a** in NMP/Cs$_2$CO$_3$ or NMP/NEt$_3$ gave 1.8% and 2.3% yield respectively for the olefination of p-chloroacetophenone with methyl acrylate).
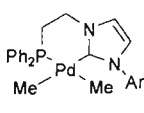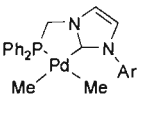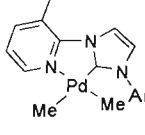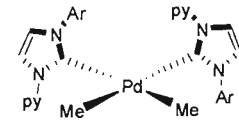
Complex	3.1a/b	3.3	3.5b	3.6
Yield (%)	2/4.5	0	3	2
T.O.N.	4/9	0	6	4

Table 4.15: Heck olefination of *p*-chloroacetophenone with methyl-acrylate. Conditions: NMP, 1mmol of aryl bromide, 1.4 eq. of alkene, 2 eq of Cs_2CO_3 at 120 °C for 6hrs, with 0.5% mole catalyst loading (Ar = 2,6-diisopropyl-phenyl (**a**), 2,4,6-trimethyl-phenyl (**b**). For **3.3**, **3.5b** and **3.6** Ar = 2,6-diisopropyl-phenyl throughout).

The use of NaOAc as a base in DMAC or NMP with complex **3.1a** as a catalyst was also considered. Different aryl bromides were tested, but the results confirm the inertness of the catalytic system under these conditions, even with activated aryl-bromides (Figure 4.25). When NMP was used as a solvent some limited reactivity was observed only for *p*-bromoacetophenone (39%).
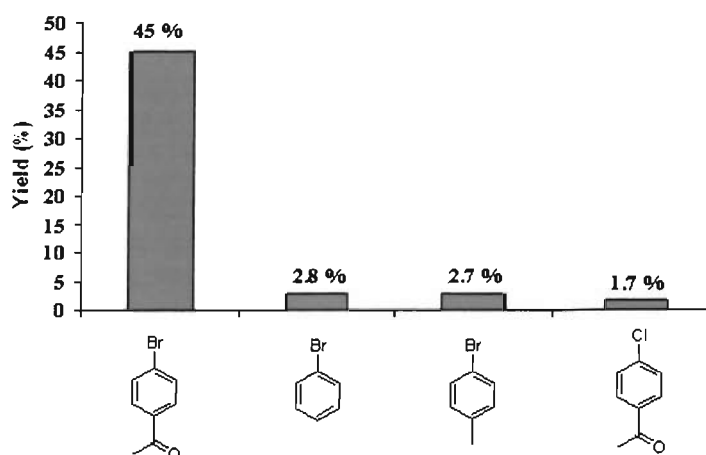
Figure 4.25: Heck olefination of aryl halides with methyl acrylate using catalyst **3.1a**. Conditions: Solvent is DMAC with NaOAc (2 mmol) as a base, 1 mmol aryl halide and 1.4 mmol of acrylate with 0.5% catalyst loading of **3.1a** at 120 °C for 6 hrs.

Lower catalyst loadings and longer reaction times accompanied by higher reaction

temperatures were also employed, with no significant influence in reactivity. In some cases one equivalent (to the catalyst **3.1a/b**) of norbonadiene (nbd) was added to the reaction mixture. This again had no effect on yields but no catalyst degradation was observed with the phosphine functionalized NHC complexes (a 0.01% catalyst loading of **3.1b** with 1 equivalent of nbd at 140°C for 12 hrs in NMP with NEt3 as a base catalysed the Heck coupling of bromobenzene with methyl acrylate to a 19.2% yield, while under the same catalytic condition the coupling of p-chloroacetophenone proceeded to a 7.7% yield).

Replacing methyl acrylate with n-butyl acrylate for the Heck olefination of bromobenzene in the presence of **3.1b** as a catalyst did not influence the observed yields. For a catalyst loading of 0.01% of complex **3.1b** in NMP with NEt3 as a base at 140 °C for 12 hrs, the yield for the Heck coupling of bromobenzene with n-butyl acrylate was 21.9% (compared to 19.2 % when methyl acrylate was used under identical conditions). Interestingly when nbd was added in the reaction mixture two products were isolated. These were identified by GC-CIMS to be n-butyl-cinnamate and n-butyl 3,3-diphenyl-propen-2-ate (65% and 35% from an overall 23.2% yield).

The reaction mixture of the Heck olefination of p-bromoacetophenone with methyl acrylate in the presence of **3.6** or **3.5b** as a catalyst was probed by ES^+. The mass spectrum in both cases showed the existence in solution of cations 2-[3-(2,6-diisopropyl-phenyl)-2-methyl-3H-imidazol-1-yl]-pyridine **3.6** and 2-[3-(2,6-diisopropyl-phenyl)-2-methyl-3H-imidazol-1-yl]-3-methyl-pyridine for **3.5b** in a100% abundance. Palladium cationic species were not observed. The formation of this species is probably due to reductive elimination of the carbene with one Pd-CH3 methyls. Similarly the Heck coupling reaction mixtures of **3.3** and **3.1a** were probed with mass spectrometry (ES^+) but the spectra acquired did not provide any information. The use of $^{31}P\{^1H\}$-NMR spectroscopy gave some insight in both cases, as it revealed that the major species in solution were the neutral dimethyl complexes (singlet at 32.7 ppm for **3.3** and 12.4 ppm for **3.1a**). These spectra also contained, among other resonances, signals located at 26.4 and 48.4 ppm when **3.1a** and **3.3** were used respectively as catalysts for the Heck olefination of p-bromoacetophenone with methyl acrylate. The last two signals compare with the resonances observed for the reactions of complexes **3.3** (49.4 ppm) and **3.1a** (26.9 ppm) with MeI. This in turn means that, as in the case of **3.5b**, **3.6**, when **3.1a** and **3.3** are used as catalysts reductive elimination, producing 2-methyl-imidazolium species, is a process that does occur during the catalytic run.

No catalytic conversion was observed with the neutral Pd(II)complexes described above when electron rich aryl-bromides (1-bromotoluene and 4-bromotoluene) were used as substrates. When complexes **4.3**, **4.4** and **4.6** were used as catalysts for the Heck coupling of chlorobenzene or *p*-bromoacetophenone with methyl acrylate, no conversion to the desired cinnamate was observed.

The phosphine functionalized NHC complexes **3.1a/b** and **3.2a/b** were also tested as catalysts for the Suzuki coupling and the hydroamination of aryl-halides with no success. The cationic species **4.3** and **4.4** reported above were also ineffective as catalysts for the Suzuki coupling or the hydroamination of aryl-halides.

It has been claimed that the imidazolium salt **2.4b** in the presence of $Pd(dba)_2$ (Scheme 4.10) and KO^tBu or Cs_2CO_3 is a higly active catalyst for the Heck coupling of aryl-bromides with acrylates.[36] Attempts to reproduce the reactivity reported in the literature under identical conditions met with limited success in our hands.

R = H, OMe, Me, C(O)Me, CHO, F, NO_2
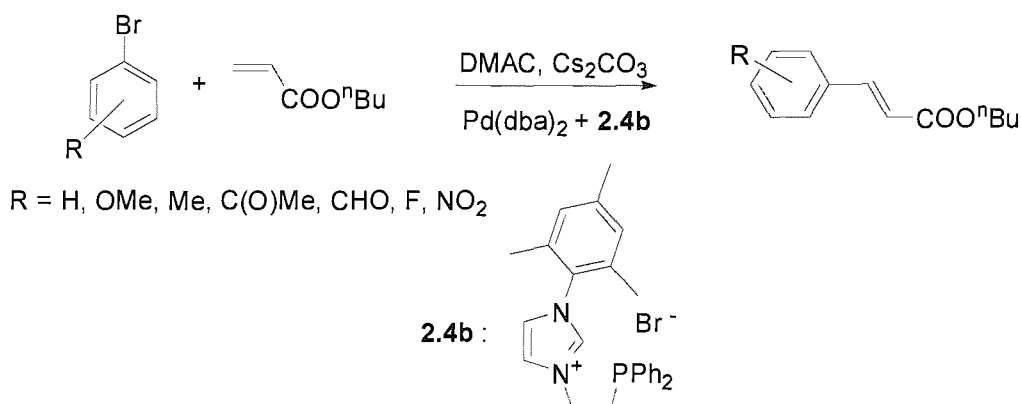
Scheme 4.10: Heck coupling of aryl bromides with $Pd(dba)_2$ and the imidazolium salt **2.4b**.

Following a similar catalysis protocol, instead of using imidazolium salt **2.4b**, we used its 2,6-diisopropylphenyl analog **2.4a** and the imidazolium salt **2.2a** (Scheme 4.10). The solvent in this case was NMP and the base was either NEt_3 or $NMeCy_2$. The investigation on whether such a catalytic protocol would be successful started with the Heck olefination of *p*-bromoacetophenone with n-butylacrylate. In both cases the coupling reaction did not proceed. Changing the solvent to DMAC and the base to Cs_2CO_3 did not yield the desired coupling product.

The phosphinoxide imidazolium salt **2.3a** (Scheme 4.11) was also used in the

catalytic Heck coupling of p-bromoacetophenone with n-butylacrylate following Nolan's protocol. Again, no conversion to the desired product was observed.

Using the imidazolium salts **2.2a** and **2.4a** in the presence of Pd(dba)$_2$, the catalytic coupling of phenylboronic acid with p-bromoacetophenone was attempted. Unfortunately, no coupling products were detected by means of GC. In all cases the solvent was NMP, while different bases, like KF, KHPO$_4$ and NEt$_3$, were tried. In the case where KF was used as a base, a catalytic run in the presence of 18-crown-6 was also undertaken, to ensure that the solubility of the inorganic base is not an issue. Nevertheless no conversion was observed.
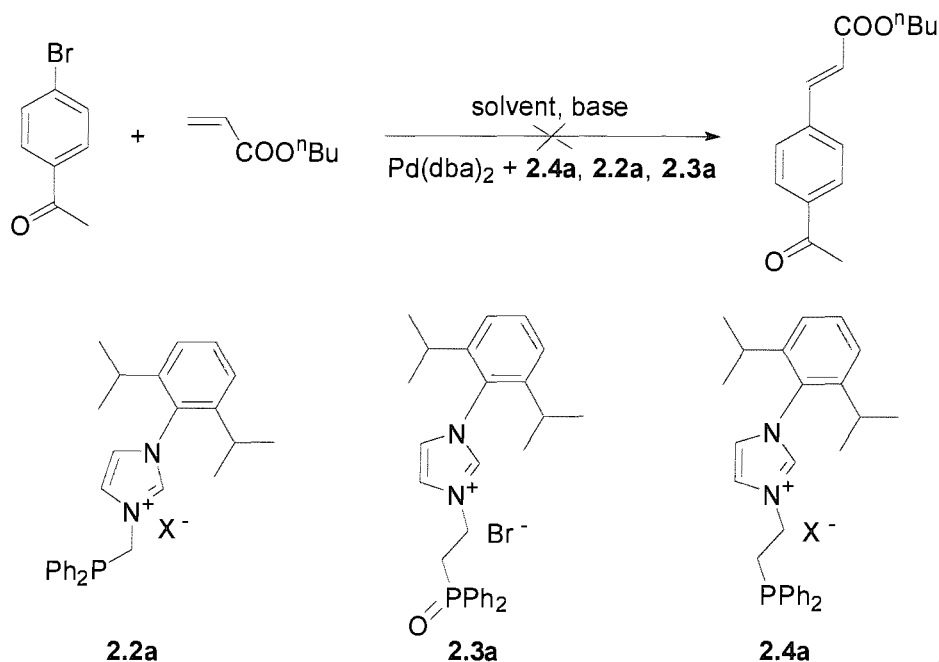
Scheme 4.11: Heck coupling using Nolan's protocol. Conditions: 0.5% Pd(dba)$_2$, 1 eq. of imidazolium salt/Pd, 1 mmol of p-bromoacetophenone/1.4 mmol n-butylacrylate. When solvent = NMP then base = NEt$_3$ or NMeCy$_2$. When solvent = DMAC then base = Cs$_2$CO$_3$. T = 120 °C for 6 hours.

Complex **3.8a** in the presence of sodium methylmalonate (Scheme 4.12) was also utilised as a catalyst for Suzuki and Heck couplings. It was hoped that this would generate *in situ* the Pd(0) complex that would be the active catalytic species. In the case of the Heck coupling of p-bromoacetophenone with n-butylacrylate no conversion was detected.

On the other hand the Suzuki coupling of this activated arylbromide with phenylboronic acid gave the desired product at an 82% yield. The product was isolated (65% yield) and was characterised by ^{1}H-NMR. When NaCH(COOMe)$_2$ was used as a base no product was detected. Finally un-activated aryl bromides (*i.e.* bromobenzene) yielded no coupling products.

3.8a
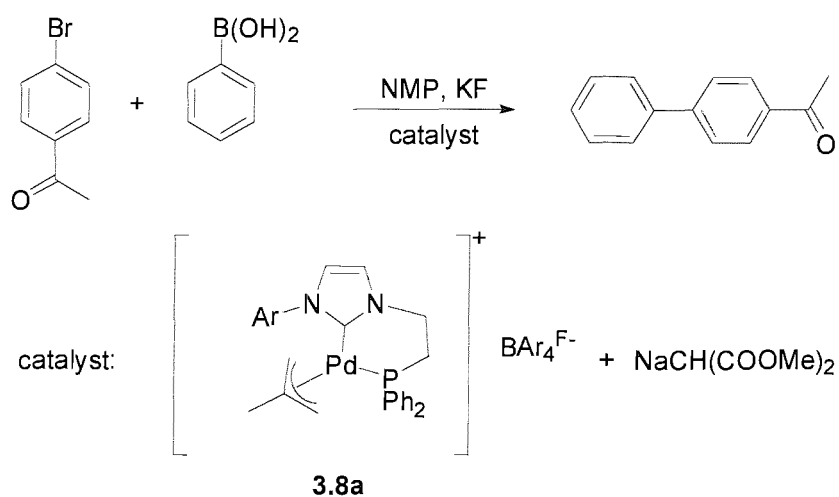
Scheme 4.12: Suzuki coupling using **3.8a** in the presence of NaCH(COOMe)$_2$ as a catalyst. Conditions: 0.5% catalyst loading generated by 1:1 reaction of **3.8a** with NaCH(COOMe)$_2$ in THF at -78 °C and warm to RT. 2 eq. of base, 1mmol arylbromide and 1.1 eq of PhB(OH)$_2$ at 120 °C for 6 hrs (Ar = 2,6-diisopropylphenyl, BAr$_4$$^{F-}$ = tetrakis-[3,5-bis(trifluoromethyl)phenyl]borate).

4.6.4 Polymerisation using *in-situ* generated cations

Cationic PdII) complexes incorporating diphosphines and diimines have been found to act as olefin polymerisation catalysts. Other ligands include nonsymmetric chelating ligands with N-O, P-P', P-N and P-O donor atoms.[38, 39] This fact prompted us to investigate whether mono-cationic Pd(II) species incorporating chelating phosphine functionalused NHC ligands generated *in situ* from the corresponding neutral dimethyl Pd(II) would promote polymerisation.

As discussed in previous sections of this chapter, Brookhart's acid reacts with **3.1a** to produce cationic Pd(II) species. When a mixture of **3.1a** and Brookhart's acid at –30 °C was pressurised with a 1:1 gas mixture of CO/C_2H_4, followed by warming to room temperature yielded poly-$(CO$-alt-$(CH_2)_2)$ after a 2 hrs period (Scheme 4.13). The white polymeric mass had a melting point of 218 °C and was identified by its ^1H, $^{13}C\{^1H\}$-NMR spectra and its IR spectrum. The yield of 69 mg corresponds to a catalytic turnover of 3.5 mg polymer × [(mmole catalyst) × bar × hr]$^{-1}$. Attempts to polymerise ethylene under identical conditions failed.
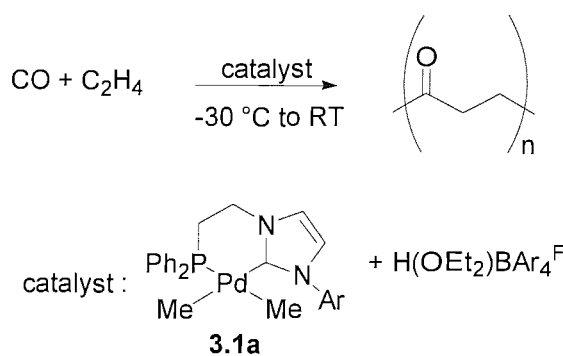
Scheme 4.13: Copolymerisation of CO/C_2H_4 using the generated *in-situ* cationic species from the interaction of Brookhart's acid with **3.1a** (Ar = 2,6-diisopropylphenyl; BAr_4^{F-} = tetrakis-[3,5-bis(trifluoromethyl)phenyl]borate).

4.7 Conclusions

The neutral Pd(II) dimethyl complexes described in the previous chapter have served as useful starting materials for the synthesis of cationic species by their reaction with Lewis acids containing noncoordinating anions. In all studied cases the electrophilic attack takes place stereospecifically, and only one isomer could be isolated. In the case of the pyridine functionalised NHC Pd(II) dimethyl complexes, the Pd-CH$_3$ bond trans to the carbene is attacked as expected. On the other hand the Pd-CH$_3$ bond cleavage occurs at the site trans to the phosphine moiety of the P-functionalised NHC Pd(II) dimethyl complexes. The reasons for this selectivity are not fully understood.

The oxidative addition of the thermally stable Pd(II) dimethyl complexes with MeI was also studied and revealed interesting results. The phosphine functionalised complexes **3.1a** and **3.3** undergo repeated oxidative addition and reductive eliminations to give methylimidazolium salts. The pyridine functionalised NHC complex **3.5b** oxidatively adds MeI and dichloromethane to give complexes **4.13** and **4.14**. The first was observed spectroscopically while the other coexists in the crystal structure of **4.13**.

Furthermore the neutral dimethyl complexes showed moderate catalytic activity in the Heck coupling of aryl bromides with acrylates. Our studies showed that the cut-off point in their reactivity is bromobenzene. Different conditions were applied but no improvement in yields or T.O.N.s was observed. Their activity is lower than that previously reported for systems generated *in situ* from Pd(dba)$_2$ and the (diphenylphosphino)ethyl imidazolium salts in the presence of Cs$_2$CO$_3$.

Our systems proved inactive for other C-C and C-X (X = heteroatom) coupling reactions, mainly Suzuki coupling and catalytic amination of aryl halides. Some success was achieved in the Suzuki coupling of activated aryl bromides by employing the cationic allyl complex **3.8a** in the presence of a nucleophile in order to generate in-situ Pd(0) species.

Finally the cationic species generated in-situ from interaction of **3.1a** with Brookhart's acid showed low to moderate activity in the co-polymerisation of CO/C$_2$H$_4$ under mild conditions.

4.8 Experimental:

General materials: Brookhart's acid ($H(OEt_2)\{B[(3,5-CF_3)_2C_6H_2]_4\}$) was prepared by a modification of a published procedure [40] using a 2 M HCl solution in Et_2O instead of gaseous HCl. Ph_3COTf [41] and $Ph_3CBAr_4^F$ [42] were prepared according to literature procedures. All aryl halides, MeI, $AgBF_4$, AgOTf and Cs_2CO_3 were purchased from Aldrich and were used as received (the last three were kept in the glovebox). $Pd(dba)_2$ [43] was prepared according to literature procedure or was given as a generous loan from Johnson-Matthey. $(CF_3)_2CHOH$ was bought from Fluorochem and was used as received. $NaCH(COOMe)_2$ was prepared from NaH and $CH_2(COOMe)_2$. Water was removed from N-methyl-2-pyrolidinone (NMP) by azeotropic distillation with benzene, followed by distillation under reduced pressure under an inert atmosphere (N_2) and was stored over molecular sieves 4 Å. N,N'-dimethyl-acetamide (DMAC) was dried by stirring with molecular sieves 4 Å overnight and distilled under reduced pressure under a N_2 atmosphere.

Thermolytic study of 3.1a: 15 mg (0.03 mmol) of complex **3.1a** were placed in the glovebox in a Young's tap NMR tube and were dissolved in dry-degassed d_8-THF. The proton spectra were recorded from room temperature up to 70 °C in 10 °C intervals.

Thermolytic study of 3.3: 16 mg (0.03 mmol) of complex **3.3** and 2 mg (0.01 mmol) of Cp_2Fe (as an internal standard) were charged in a Young's tap NMR tube in the glovebox, and were dissolved in degassed d_5-PhCl. The ^{1}H-NMR spectrum was acquired at room temperature. The sample was then placed in an oil bath thermostated at 50 °C. The ^{1}H-NMR spectra were recorded (1st:10 minutes, 2nd:20 minutes, 3rd:40 minutes, 4th:40 minutes).

VT-NMR studies of the reaction of 3.1a with $B(C_6F_5)_3$, $Ph_3CBAr_4^F$, Ph_3COTf: 20 mg (0.04 mmol) of complex **3.1a** and one equivalent of the appropriate scavenger were placed in an NMR tube. The tube was connected to a small vacuum line and deuterated solvent (CD_2Cl_2) was added by trap-to-trap distillation. The tube was kept in liquid N_2 and was sealed under vacuum. It was then warmed up to -78 °C and brought into a precooled at -78 °C NMR probe. The ^{1}H-NMR spectra were acquired up to 25 °C in 10 °C intervals. After reaching room temperature the $^{31}P\{^1H\}$-NMR spectrum of its reaction mixture was also recorded.

Reaction of 3.3 with $(CF_3)_2CHOH$ in d_5-pyridine(4.1): In the glove box 20 mg (0.034 mmol) of **3.3** was dissolved in d_5-pyridine in a NMR tube. This solution was cooled at -78

°C and 3-4 drops of $(CF_3)_2CHOH$ were added using a microlitre syringe. The contents of the NMR tube were brought to RT and the NMR spectra were acquired. ^1H-NMR $\delta(d_5\text{-}$py): 0.04 (3H, broad s, PdCH_3), 0.99 (6H, d, $^3J_{HH}$ = 6.5 Hz, CH(C$H_3)_2$), 1.09 (6H, d, $^3J_{HH}$ = 6.6 Hz, CH(C$H_3)_2$), 2.21 (2H, broad d, CH(CH$_3)_2$), 5.54 (3H, broad d, [PPh$_2$CH_2-ylidene]PdMe$^+$ and $(CF_3)_2$CHO^-), 7.01-8.03 (15H, m, aromatic), 10.11 (1H, $(CF_3)_2$CHOH); $^{13}C\{^1H\}$-NMR $\delta(d_5\text{-}$py): 2.1 (s, PdCH_3), 23.0 (s, CH(C$H_3)_2$), 24.7 (s, CH(C$H_3)_2$), 28.4 (s, CH(CH$_3)_2$), 52.5 (d, $^1J_{PC}$ = 53.6 Hz, [PPh$_2$CH_2-ylidene]PdMe$^+$), 70.9 (sept., $^2J_{FC}$ = 50.3 Hz, $(CF_3)_2$CHO^-), 120.9 (d, J_{PC} = 7.4 Hz, aromatic), 122.4 (s, aromatic), 124.1 (s, aromatic), 126.3 (s, aromatic), 129.6 (d, J_{PC} = 11.8 Hz, aromatic), 130.6 (s, aromatic), 132.4 (s, aromatic), 133.6 (d, J_{PC} = 12.5 Hz, aromatic), 145.3 (s, aromatic), 183.6 (s, aromatic), 194.1 (s, NCN) [signals due to CF_3 are obscured by the signals of the deuterated solvent]; $^{31}P\{^1H\}$-NMR $\delta(d_5\text{-}$py): 55.3 (s, [PPh$_2$CH$_2$-ylidene]PdMe$^+$); $^{19}F\{^1H\}$-NMR $\delta(d_5\text{-}$py): -74.1 (s, CF_3).

Reaction of 3.1a with $(CF_3)_2CHOH$ in d_5-py (4.2): In the glove 19 mg (0.032 mmol) of **3.1a** was dissolved in d_5-py. The solution was then cooled down to -78 °C and 3-4 drops of $(CF_3)_2CHOH$ were added using a microlitter syringe. The solution was brought to RT and the NMR spectra were acquired. ^1H-NMR $\delta(d_5\text{-}$py): 0.01 (6H, d, $^3J_{PH}$ = 2.7 Hz, PdCH_3), 0.20 (s, CH_4), 0.91 (6H, d, $^3J_{HH}$ = 6.7 Hz, CH(C$H_3)_2$), 1.12 (6H, d, $^3J_{HH}$ = 6.8 Hz, CH(C$H_3)_2$), 2.65 (2H, sept., $^3J_{HH}$ = 6.7 Hz, CH(CH$_3)_2$), 2.80 (2H, m, [PPh$_2$CH_2CH$_2$-ylidene]PdMe$^+$), 4.44 and 4.62 (1H each, m, [PPh$_2$CH$_2$CH_2-ylidene]PdMe$^+$), 5.44 (sept., $^3J_{FH}$ = 7.8 Hz, $(CF_3)_2$CHO^-), 6.98-7.77 (10H, m, aromatics), 7.87-8.12 (5H, m, aromatics); $^{13}C\{^1H\}$-NMR $\delta(d_5\text{-}$py): 8.0 (d, $^2J_{PC}$ = 4.6 Hz, PdCH_3), 23.7 (s, CH(C$H_3)_2$), 26.4 (s, CH(C$H_3)_2$), 29.4 (s, CH(CH$_3)_2$), 31.0 (d, $^1J_{PC}$ = 34.2 Hz, [PPh$_2$CH_2CH$_2$-ylidene]PdMe$^+$), 47.7 (s, [PPh$_2$CH$_2$CH_2-ylidene]PdMe$^+$), 71.7 (sept., $^2J_{FC}$ = 31.1 Hz), 123.8 (s, ylidene backbone), 124.8 (s, aromatic), 125.5 (s, aromatic), 130.3 (d, J_{PC} = 19.9 Hz), 131.4 (s, aromatic), 131.7 (s, aromatic), 132.6 (s, aromatic), 134.5 (d, J_{PC} = 9.8 Hz, aromatic), 139.9 (s, aromatic), 146.6 (s, aromatic), 180.3 (s, NCN) [the CF_3 signals and one more carbon signal of the compound are obscured by the peaks of d_5-py]; $^{31}P\{^1H\}$-NMR $\delta(d_5$-py): 35.2 (s, [PPh$_2$CH$_2$CH$_2$-ylidene]PdMe$^+$); $^{19}F\{^1H\}$-NMR $\delta(d_5\text{-}$py): 87.9 (s, CF_3).

Preparation of cationic species. General method: A solution of the appropriate neutral dimethyl Pd(II) complex in dichloromethane (20 mL) at −78 °C, was treated with a solution of H(OEt$_2$){B[(3,5-CF$_3)_2$C$_6$H$_2$]$_4$} (1 eq. in 20 mL of dichloromethane) cooled at −78 °C. The mixture was then allowed to warm up to between −40 and −50 °C, when 1 equivalent of donor L (L = pyridine, acetonitrile, benzonitrile, trimethylphosphine) was

added. The mixture was then allowed to reach room temperature, upon which time volatiles were removed under reduced pressure. The residue was washed three times with *ca.* 10 mL petroleum ether and dried under vacuum.

4.3: This was prepared according to the general method described above starting from 60 mg (0.10 mmol) of **3.1a**, 94 mg (1 eq.) of $H(OEt_2)\{B[(3,5-CF_3)_2C_6H_2]_4\}$ and 8 µL (1 eq.) of pyridine. Yield: 150 mg (96 %). ^{1}H-NMR $\delta(CD_2Cl_2)$: -0.33 (3H, d, $^3J_{PH}$ = 2.7 Hz, PdCH_3), 0.89 (6H, d, $^3J_{HH}$ = 6.8 Hz, CH(CH_3)$_2$), 1.02 (6H, d, $^3J_{HH}$ = 6.8 Hz, CH(CH_3)$_2$), 2.49 (4H, m, CH(CH$_3$)$_2$ and [PPh$_2$CH_2CH$_2$-ylidene]PdMe(py)$^+$), 4.33 and 4.39 (1H each, m, [PPh$_2$CH$_2$CH_2-ylidene]PdMe(py)$^+$), 6.91 (1H, s., ylidene backbone), 7.01-7.21 (4H, m, aromatics), 7.35 (2H, d, J_{HH} = 5.2 Hz, aromatic), 7.48-7.89 (m, 25H, aromatic); ^{13}C$\{^1$H$\}$-NMR $\delta(CD_2Cl_2)$: 7.6 (s, PdCH$_3$), 23.3 (s, CH(CH_3)$_2$), 26.1 (s, CH(CH_3)$_2$), 29.1 (s, CH(CH$_3$)$_2$), 32.0 (s, [PPh$_2$CH$_2$CH$_2$-ylidene]PdMe(py)$^+$), 47.9 (s, [PPh$_2$CH$_2$CH$_2$-ylidene]PdMe(py)$^+$), 121.0 (s, ylidene backbone) 122.5 (s, ylidene backbone), 123.7 (s, aromatic), 124.5 (s, aromatic), 125.5 (s, aromatic), 129.7 (d, J_{PC} = 9.0 Hz, aromatic), 130.3 (d., J_{PC} = 7.1 Hz, aromatic), 130.8 (s, aromatic), 132.6 (quartet, $^2J_{CF}$ = 29.9 Hz), 133.5 (s, aromatic) 134.7 (s, aromatic), 134.8 (d, J_{PC} = 5.1 Hz, aromatic), 141.3 (s, aromatic), 141.9 (s, aromatic), 142.3 (s, aromatic), 146.6 (s, aromatic), 162.6 (q., $^1J_{CF}$ = 45.8 Hz, CF$_3$), 180.3 (s, NCN); ^{31}P$\{^1$H$\}$-NMR $\delta(CD_2Cl_2)$: 34.8 (s, [PPh$_2$CH$_2$CH$_2$-ylidene]PdMe(py)$^+$); ^{19}F$\{^1$H$\}$-NMR $\delta(CD_2Cl_2)$: 100.2. Anal. Found: C, 51.77; H, 3.77; N, 2.49 %. Calcd for $C_{67}H_{54}BF_{24}N_3PPd.CH_2Cl_2$: C, 51.36; H, 3.55; N, 2.64 %. Colourless needles suitable for a single crystal X-ray diffraction study were grown by slow evaporation of an ether solution of **4.3** in air.

4.4: This was prepared according to the synthetic method described above starting from 60 mg (0.10 mmol) of **3.1a**, 94 mg (1 eq.) $H(OEt_2)\{B[(3,5-CF_3)_2C_6H_2]_4\}$ and 6 µL (1.1 eq.) of acetonitrile. Yield: 110 mg (75 %). ^{1}H-NMR $\delta(CD_2Cl_2)$: -0.10 (3H, d, $^3J_{PH}$ = 1.8 Hz, PdCH_3), 1.11 (6H, d, $^3J_{HH}$ = 6.4 Hz, CH(CH_3)$_2$), 1.19 (6H, d, $^3J_{HH}$ = 6.4 Hz, CH(CH_3)$_2$), 1.90 (3H, s, CH_3CN), 2.61 (4H, m, CH(CH$_3$)$_2$ and [PPh$_2$CH_2CH$_2$-ylidene]PdMe(MeCN)$^+$), 4.12 and 4.21 (1H each, m, [PPh$_2$CH$_2$CH_2-ylidene]PdMe(MeCN)$^+$), 6.91 (1H, s, ylidene backbone), 7.01 (1H, s, ylidene backbone), 7.34 (2H, d, J_{HH} = 4.9 Hz, aromatic), 7.41-7.59 (8H, m, aromatic), 7.68-7.90 (15H, m, aromatic); No ^{13}C$\{^1$H$\}$-NMR spectra are available due to sample decomposition during acquisition. ^{31}P$\{^1$H$\}$-NMR $\delta(CD_2Cl_2)$: 35.3 (s, [PPh$_2$CH$_2$CH$_2$-ylidene]PdMe(MeCN)$^+$); ^{19}F$\{^1$H$\}$-NMR $\delta(CD_2Cl_2)$: 100.2. Anal. Found: C, 49.76; H, 3.29; N, 4.26 %. Calcd for

$C_{64}H_{52}BF_{24}N_3PPd \cdot CH_2Cl_2 \cdot 2CH_3CN$: C, 50.74; H, 3.64; N, 4.29 %. Colourless crystals were grown by slow diffusion of PE in an ether solution of **4.4** at -30 °C.

4.5: This was prepared by following the above method from **3.1a** (60 mg, 0.10 mmol), $H(OEt_2)\{B[(3,5-CF_3)_2C_6H_2]_4\}$ (94 mg, 1 eq.) and benzonitrile (10 µL, 1 eq.). Yield: 140 mg (88 %). ^{1}H-NMR δ(CD_2Cl_2): 0.01 (3H, d, $^3J_{PH}$ = 2.7 Hz, PdCH_3), 1.11 (6H, d, $^3J_{HH}$ = 6.4 Hz, CH(CH_3)$_2$), 1.29 (6H, d, $^3J_{HH}$ = 6.4 Hz, CH(CH_3)$_2$), 2.71 (4H, m, CH(CH$_3$)$_2$ and [PPh$_2$CH_2CH$_2$-ylidene]PdMe(PhCN)$^+$), 4.12 and 4.21 (1H each, m, [PPh$_2$CH$_2$CH_2-ylidene]PdMe(PhCN)$^+$), 6.59 (1H, s, ylidene backbone), 7.11 (1H, s, ylidene backbone), 7.20 (4H, broad s, aromatics), 7.32 (3H, broad s, aromatic), 7.42 (2H, d, J_{HH} = 5.1 Hz, aromatic), 7.49-7.60 (9H. m, aromatic), 7.68-7.90 (12H, m, aromatic); ^{13}C$\{^1$H$\}$-NMR δ(CD_2Cl_2): 4.9 (s, PdCH_3), 24.4 (s, CH(CH_3)$_2$), 25.2 (s, CH(CH_3)$_2$), 29.3 (s, CH(CH$_3$)$_2$), 31.6 (d, $^1J_{PC}$ = 34.4 Hz, [PPh$_2$CH_2CH$_2$-ylidene]PdMe(PhCN)$^+$), 47.3 (s, [PPh$_2$CH$_2$CH_2-ylidene]PdMe(PhCN)$^+$), 117.5 (broad, aromatic), 118.2 (s, PhCN), 121.8 (s, ylidene backbone), 122.8 (s, ylidene backbone), 124.0 (s, aromatic), 124.2 (s, aromatic), 124.8 (s, aromatic), 126.7 (s, aromatic), 129.4 (s, aromatic), 129.9 (broad d., J = 11.0 Hz, aromatic of BARF), 131.5 (s, aromatic), 132.6 (s, aromatic), 133.2 (s, aromatic), 134.2 (d, J_{PC} = 11.1 Hz, aromatic), 135.5 (s, aromatic), 136.3 (s, aromatic), 139.7 (s, aromatic), 146.8 (s, aromatic), 162.7 (q, $^1J_{CF}$ = 48.6 Hz, CF$_3$); ^{31}P$\{^1$H$\}$-NMR δ(CD_2Cl_2): 36.5 (s, [PPh$_2$CH$_2$CH$_2$-ylidene]PdMe(PhCN)$^+$); ^{19}F$\{^1$H$\}$-NMR δ(CD_2Cl_2): 100.2.

4.6: This was prepared by following the above method from **3.1a** (60 mg, 0.10 mmol), $H(OEt_2)\{B[(3,5-CF_3)_2C_6H_2]_4\}$ (94 mg, 1 eq.) and PMe$_3$ (8 µL, 1.1 eq.). Yield: 140 mg (93 %). ^{1}H-NMR δ(CD_2Cl_2): 0.01 (3H, t., $^3J_{PH}$ = 7.3 Hz, PdCH_3), 0.93 (15H, m, PMe_3 and CH(CH_3)$_2$), 1.19 (6H, d, $^3J_{HH}$ = 7.3 Hz, CH(CH_3)$_2$), 2.40 (2H, m, [PPh$_2$CH_2CH$_2$-ylidene]PdMe(PMe$_3$)$^+$), 2.62 (2H, sept., $^3J_{HH}$ = 6.4 Hz, CH(CH$_3$)$_2$), 4.30 and 4.38 (1H each, m, [PPh$_2$CH$_2$CH_2-ylidene]PdMe(PMe$_3$)$^+$), 7.05 (1H, s, ylidene backbone), 7.15 (1H, s, ylidene backbone), 7.26 (2H, d, J_{HH} = 5.5 Hz, aromatic), 7.32-7.57 (16H, m, aromatic), 7.74 (7H, broad s, aromatic); No ^{13}C$\{^1$H$\}$-NMR data are available due to sample decomposition during acquisition; ^{31}P$\{^1$H$\}$-NMR δ(CD_2Cl_2): -15.8 (d, $^2J_{PP}$ = 32.8 Hz, [PPh$_2$CH$_2$CH_2-ylidene]PdMe(PMe$_3$)$^+$), 4.6 (d, $^2J_{PP}$ = 32.8 Hz, [PPh$_2$CH$_2$CH_2-ylidene]PdMe(PMe$_3$)$^+$); ^{19}F$\{^1$H$\}$-NMR δ(CD_2Cl_2): 100.2. Anal. Found: C, 52.41; H, 4.01; N, 1.99 %. Calcd for $C_{65}H_{57}BF_{24}N_2P_2Pd$: C, 52.00; H, 3.83; N, 1.87 %.

4.7: This was prepared by following the above general method from **3.3** (55 mg, 0.098 mmol), $H(OEt_2)\{B[(3,5-CF_3)_2C_6H_2]_4\}$ (92 mg, 1 eq.) and pyridine (8 µL, 1 eq.). ^{1}H-NMR δ(CD_2Cl_2): -0.09 (3H, d, $^3J_{PH}$ = 2.5 Hz, PdCH_3), 0.90 (6H, d, $^3J_{HH}$ = 6.6 Hz, CH(CH_3)$_2$),

0.99 (6H, d, $^3J_{HH}$ = 6.6 Hz, CH(CH_3)$_2$), 2.29 (2H, d, $^3J_{HH}$ = 6.6 Hz, CH(CH$_3$)$_2$), 4.92 (2H, d, $^2J_{PH}$ = 6.6 Hz, [PPh$_2$CH_2-ylidene]PdMe(py)$^+$), 6.89 (3H, m, aromatics), 7.09 (2H, m, aromatics), 7.31 (5H, m, aromatics), 7.50 (6H, m, aromatics), 7.81 (14H, m, aromatics), 7.99 (2H, m, aromatics); ^{13}C{^{1}H} δ(CD$_2$Cl$_2$): 1.8 (s, PdCH$_3$), 23.1 (s, CH(CH_3)$_2$), 24.9 (s, CH(CH_3)$_2$), 29.8 (s, CH(CH$_3$)$_2$), 53.7 (d, $^1J_{PC}$ = 48.4 Hz, [PPh$_2$CH$_2$-ylidene]PdMe(py)$^+$) peaks at the aromatic region are not assigned due to impurities giving rise to more peaks than expected; ^{31}P{^{1}H}-NMR δ(CD$_2$Cl$_2$): 54.0 (s, [PPh$_2$CH$_2$-ylidene]PdMe(py)$^+$); ^{19}F{^{1}H}-NMR δ(CD$_2$Cl$_2$): -63.1 (s, CF_3).

4.8: This was prepared by following the above general method from **3.3** (55 mg, 0.098 mmol), H(OEt$_2$){B[(3,5-CF$_3$)$_2$C$_6$H$_2$]$_4$} (92 mg, 1 eq.) and 4-$tert$-butylpyridine (9 µL, 1 eq.). Yield: 110 mg (68 %). ^{1}H-NMR δ(CD$_2$Cl$_2$): -0.09 (3H, d, $^3J_{PH}$ = 2.6 Hz, PdCH_3), 0.92 (6H, d, $^3J_{HH}$ = 6.8 Hz, CH(CH_3)$_2$), 1.01 (6H, d, $^3J_{HH}$ = 6.8 Hz, CH(CH_3)$_2$), 1.22 (9H, s, 4-$^t Bu$-pyridine), 2.30 (2H, sept., $^3J_{HH}$ = 6.7 Hz, CH(CH$_3$)$_2$), 4.93 (2H, d, $^2J_{PH}$ = 6.6 Hz, [PPh$_2$CH_2-ylidene]PdMe(4-tBu-py)$^+$), 7.01 (4H, m, aromatic), 7.33 (2H, m, aromatics), 7.46 (10H, m, aromatics), 7.79 (11H, m, aromatics), 8.01 (2H, d, J_{HH} = 4.5 Hz, aromatics); ^{13}C{^{1}H}-NMR δ(CD$_2$Cl$_2$): 1.9 (s, PdCH$_3$), 23.2 (s, CH(CH_3)$_2$), 25.1 (s, CH(CH_3)$_2$), 28.6 (s, 4-C(CH_3)$_3$-pyridine), 30.2 (s, CH(CH$_3$)$_2$), 53.6 (d, $^1J_{PC}$ = 48.9 Hz, [PPh$_2$CH$_2$-ylidene]PdMe(4-tBu-py)$^+$), 117.8 (s, ylidene backbone), 122.7 (s, ylidene backbone), 123.1 (s, aromatic), 124.3 (s, aromatic), 126.3 (s, aromatic), 126.8 (broad s, aromatic), 128.9 (s, aromatic), 129.2 (s, aromatic), 129.5 (s, aromatic), 129.8 (d, J_{PC} = 15.2 Hz, aromatic), 130.3 (s, aromatic), 130.9 (s, aromatic), 132.8 (s, aromatic), 133.5 (d, J_{PC} = 20.0 Hz, aromatic), 135.2 (s, aromatic), 145.6 (s, aromatic), 150.1 (s, aromatic), 163.1 (q, $^1J_{CF}$ = 49.9 Hz, CF_3 s); ^{31}P{^{1}H}-NMR δ(CD$_2$Cl$_2$): 53.8 (s, [PPh$_2$CH$_2$-ylidene]PdMe(4-tBu-py)$^+$); ^{19}F{^{1}H}-NMR δ(CD$_2$Cl$_2$): -63.1 (s, CF_3).

4.9: This was prepared according to the method described above starting from 80 mg (0.18 mmol) of **3.5b**, 165 mg (1 eq.) of H(OEt$_2$){B[(3,5-CF$_3$)$_2$C$_6$H$_2$]$_4$} and 15 µL (1.1 eq.) of pyridine. Yield: 200 mg (82 %). ^{1}H-NMR δ(CD$_2$Cl$_2$): -0.09 (3H, s., PdCH_3), 1.01 (6H, d, $^3J_{HH}$ = 6.9 Hz, CH(CH_3)$_2$), 1.09 (6H, d, $^3J_{HH}$ = 6.9 Hz, CH(CH_3)$_2$), 2.61 (2H, sept., $^3J_{HH}$ = 6.9 Hz, CH(CH$_3$)$_2$), 2.74 (3H, s, 3-CH_3 pyridine backbone), 7.13 (1H, d, $^3J_{HH}$ = 2.2 Hz, ylidene backbone), 7.20 (1H, m, aromatics), 7.33 (3H, m, aromatics), 7.53 (6H, broad s, aromatics), 7.71 (9H, broad s, aromatics), 7.86 (1H, dd, J_{HH} = 1.0 Hz, 7.7 Hz, aromatic), 7.91 (1H, broad s, aromatic), 8.07 (1H, d, $^3J_{HH}$ = 2.2 Hz, ylidene backbone), 8.54 (2H, dd, J_{HH} = 1.5 Hz, 6.2 Hz, aromatic); ^{13}C{^{1}H}-NMR δ(CD$_2$Cl$_2$): 7.7 (s, PdCH$_3$), 21.5 (s, CH(CH$_3$)$_2$), 23.8 (s, 3-CH$_3$ pyridine backbone), 25.2 (s, CH(CH_3)$_2$), 29.4 (s, CH(CH_3)$_2$),

118.2 (s, ylidene backbone), 119.8 (s, ylidene backbone),121.3 (s, aromatic), 124.0 (s, aromatic), 124.2 (s, aromatic), 124.6 (s, aromatic), 125.0 (s, aromatic), 126.7 (s, aromatic), 127.2 (s, aromatic), 129.8 (q., $^2J_{CF}$ = 30.2 Hz), 131.7 (s, aromatic), 135.1 (s, aromatic), 135.6 (s, aromatic), 139.8 (s, aromatic), 145.5 (s, aromatic), 145.8 (s, aromatic), 146.1 (s, aromatic), 151.8 (s, aromatic), 162.3 (q., $^1J_{CF}$ = 49.7 Hz, CF_3); $^{19}F\{^1H\}$-NMR $\delta(CD_2Cl_2)$: -62.8. Colourless crystals of **4.9** were grown by slow diffusion of PE in an ether solution of **4.9**.

Thermolytic study of 4.3: 12 mg (0.008 mmol) of **4.3** was charged in the glove box in an NMR tube fitted with a suba-seal cap and was dissolved in dry-degassed d_5-pyridine. The proton spectra were acquired from room temperature up to 90 °C in 10 °C intervals.

Thermolytic study of 4.4: This was performed as above in dry-degassed d_3-MeCN starting with 15 mg (0.01 mmol) of complex **4.4**. Proton spectra were recorded from room temperature up to 60 °C in 10 °C intervals.

VT-NMR study of the reaction of 3.1a with $(CF_3)_2CHOH$: 20 mg (0.04 mmol) of complex **3.1a** were dissolved in dry-degassed CD_2Cl_2 in an NMR tube in the glove box. The tube was fitted with a suba-seal cap and the tube was submerged in liquid N_2. The inert atmosphere in the NMR tube was maintained by attaching it to the N_2 manifold *via* a syringe needle and 3-4 drops of $(CF_3)_2CHOH$ were added by a micro-litter syringe as along with 1.1 eq. of dry-degassed pyridine and the tube was put in a -78 °C slush-bath. It was then placed in a NMR machine precooled to -78 °C. Proton spectra were acquired from -78 °C to 25 °C in 10 °C intervals.

Reaction of 3.1a with MeI (4.10): To a precooled solution (0 °C) of 80 mg (0.14 mmol) of complex **3.1a** in 20 mL dichloromethane was added *via* a microlitre syringe a three-fold excess of MeI (26 μL, 0.42 mmol). The solution was allowed to warm to room temperature and was stirred overnight. A colour change occurred within the first 30 min. of stirring at room temperature from pale yellow to deep orange. The solution was filtered through Celite and the volatiles were removed under vacuum. Repeated recrystallisation from dichloromethane/ether at 35 °C gave a small crop of the title compound as orange crystals.

VT-NMR study of the reaction of 3.1a with MeI: 20 mg (0.04 mmol) of complex **3.1a** was dissolved in dry-degassed CD_2Cl_2 in an NMR tube in the glove box. The tube was fitted with a suba-seal cap and the solution was cooled to -78 °C using a dry-ice-acetone slush bath. Three equivalents of MeI were added at this temperature by means of a microsyringe and the tube was placed in an NMR probe pre-cooled to -78 °C. The ^1H and

$^{31}P\{^1H\}$-NMR spectra were acquired up to 25 °C in 10 °C intervals. The ^1H and $^{31}P\{^1H\}$-NMR spectra were also acquired 20 minutes, 40 minutes, 2 hours and 12 hours after the sample reached room temperature (25 °C).

Reaction of 3.3 with MeI (4.12): 16 mg (0.03 mmol) of complex **3.3** were dissolved in dry-degassed CD_2Cl_2 in the glovebox and were transferred to a NMR tube with a suba-seal. To this solution was added at 0 °C 3 eq. of MeI by means of a microlitre syringe. The ^1H and $^{31}P\{^1H\}$ spectra were acquired immediately. Upon standing at room temperature overnight a black precipitate formed which, and was separated from the mother-liquor by filtration through Celite. The orange-yellow solution was then re-dissolved in CD_2Cl_2 and the spectra were re-acquired. The solution was layered in the NMR tube with Et_2O and was placed in the freezer (-30 °C). The microcrystalline bright yellow solid thus produced was collected by decanting the supernatant and the ^1H and $^{31}P\{^1H\}$-NMR spectra of the solid reacquired. A very small amount of the microcrystalline solid was dissolved in CH_3CN and the ES^+ mass spectrum was obtained. ES^+: (m/z) 473.

Reaction of 3.5b with MeI (4.13 & 4.14): In the glove box 20 mg (0.044 mmol) of **3.5b** were charged in an NMR tube and were dissolved in CD_2Cl_2. The NMR tube was connected to the N_2 manifold *via* a syringe needle and 15.3 µL (3 eq.) of MeI were added at room temperature and the NMR spectra were recorded. Upon addition the colour of the solution changed rapidly from pale to very bright yellow. Due to the excess of MeI the contents of the NMR tube were carried in a Schlenk tube and volatiles were removed under vacuum to give an orange-yellow solid that was dissolved in CD_2Cl_2 and the spectra were reacquired. ^1H-NMR $\delta(CD_2Cl_2)$: 0.29 (3H, s, PdCH_3), 1.11 (6H, d, $^3J_{HH}$ = 7.3 Hz, CH(CH_3)$_2$), 1.28 (6H, d, $^3J_{HH}$ = 7.3 Hz, CH(CH_3)$_2$), 2.70 (2H, sept., $^3J_{HH}$ = 7.3 Hz, CH(CH$_3$)$_2$), 2.79 (3H, s, 3-CH_3-pyridine), 6.98 (1H, s, ylidene backbone), 7.40 (3H, m, aromatic), 7.50 (1H, m, aromatic), 7.82 (1H, d, J_{HH} = 7.3 Hz, aromatic), 7.98 (1H, s, ylidene backbone), 9.55 (1H, d, J_{HH} = 5.9 Hz, aromatic); $^{13}C\{^1H\}$-NMR $\delta(CD_2Cl_2)$: 0.3 (s, PdCH$_3$), 19.4 (s, 3-CH$_3$-pyridine), 21.7 (s, CH(CH_3)$_2$), 22.7 (s, CH(CH$_3$)$_2$), 26.7 (s, CH(CH$_3$)$_2$), 116.8 (s, ylidene backbone), 119.9 (s, ylidene backbone), 121.5 (s, aromatic), 122.3 (s, aromatic), 122.5 (s, aromatic), 128.7 (s, aromatic), 141.4 (s, aromatic), 143.6 (s, aromatic), 144.2 (s, aromatic), 144.3 (s, aromatic), 147.8 (s, *ipso* carbon of the aryl group), 188.9 (s, NCN). Scarlet crystals of the mixed Cl, Me complex were grown by layering a DCM solution of (**4.13 & 4.14**) with ether.

Reaction of 3.2a with AgBF$_4$ (4.15): To a cold (0 °C) solution of 60 mg (0.085 mmol) of **3.2a** in 20 mL of acetonitrile were added by cannula a solution of 33 mg (0.17 mmol) of

AgBF$_4$ in 5 mL of acetonitrile. Upon addition a grey precipitate was formed which was separated from the mother liquor by filtration through Celite, at 0 °C. The resulting bright yellow solution was evaporated to dryness giving a yellow solid. ^{1}H-NMR δ(CD$_3$CN): 0.82 (6H, d, $^3J_{HH}$ = 6.9 Hz, CH(CH_3)$_2$), 0.90 (6H, d, $^3J_{HH}$ = 6.9 Hz, CH(CH_3)$_2$), 2.51 (2H, sept., $^3J_{HH}$ = 6.9 Hz, CH(CH$_3$)$_2$), 2.83 (2H, m, [PPh$_2$CH_2CH$_2$-ylidene]Pd(MeCN)$_2$$^{2+}$), 4.41 and 4.59 (1H each, m, [PPh$_2$CH$_2$CH_2-ylidene]Pd(MeCN)$_2$$^{2+}$), 7.11-8.03 (15H, m, aromatics and ylidene backbone); No ^{13}C{^{1}H}-NMR data are available due to rapid sample decomposition during acquisition; ^{31}P{^{1}H}-NMR δ(CD$_3$CN): 29.9 (s, [PPh$_2$CH$_2$CH$_2$-ylidene]Pd(MeCN)$_2$$^{2+}$).

Reaction of 3.2a with AgOTf (4.16): To a cold solution (-10 °C) of 80 mg (0.113 mmol) of **3.2a** in 20 mL of acetonitrile were added *via* cannula a solution of 29 mg (2 eq.) of AgOTf in 15 mL of acetonitrile. The solution was stirred for 10 min. at RT and was then filtered through Celite. The volatiles were removed *in vacuo* and the resulting yellow solid was dissolved in CH$_2$Cl$_2$ and filtered through a filter-cannula to remove black aggregates. The volume was reduced to about 1 mL and ether was added to facilitate the precipitation of the compound. The bright yellow solid was isolated from the mother liquor by filtration and was dried *in vacuo* for 5 minutes. The yellow solid is stable at low temperatures without any obvious decomposition. ^{1}H-NMR δ(CD$_2$Cl$_2$): 0.90 (6H, d, $^3J_{HH}$ = 6.9 Hz, CH(CH_3)$_2$), 1.12 (6H, d, $^3J_{HH}$ = 6.9 Hz, CH(CH_3)$_2$), 1.91 (6H, s, MeCN), 2.45 (2H, sept., $^3J_{HH}$ = 6.9 Hz, CH(CH$_3$)$_2$), 2.71 (2H, broad s, [PPh$_2$CH_2CH$_2$-ylidene]Pd(MeCN)$_2$$^{2+}$), 4.73 and 4.89 (1H each, broad s, [PPh$_2$CH$_2$CH_2-ylidene]Pd(MeCN)$_2$$^{2+}$), 6.99 (1H, s, ylidene backbone), 7.21 (2H, d, J_{HH} = 5.5 Hz, aromatics), 7.38 (2H, m, aromatics), 7.49-7.61 (4H, m, aromatics), 7.74 (3H, d, J_{HH} = 4.9 Hz, aromatics), 7.88 (4H, m, aromatics); No ^{13}C{^{1}H}-NMR data are available due to rapid sample decomposition during acquisition at RT; ^{31}P{^{1}H}-NMR δ(CD$_2$Cl$_2$): 28.9 (s, [PPh$_2$CH$_2$CH$_2$-ylidene]Pd(MeCN)$_2$$^{2+}$).

Heck Catalytic Studies: A 1 mmol portion of aryl halide, 1.4 equivalents of alkene (methyl or n-butyl acrylate), 2 equivalents of base (NEt$_3$ or dried Cs$_2$CO$_3$) and 0.3 equivalents of diethylene glycol-n-dibutyl ether (internal standard) were placed in a 50 mL Young's tap ampoule using a microlitre syringe. A 1 mL portion of N-methyl-2-pyrolidinone or N,N-dimethylacetamide was added to dissolve the organics. To these solutions was added 1 mL of a 5 × 10^{-3} M or 1 × 10^{-4} M pre-prepared solution of the catalyst in the appropriate solvent. The ampoule was then placed under partial vacuum and placed in a preheated oil bath. After the end of the catalytic run the ampoule was cooled to room temperature and water followed by dichloromethane were added to the reaction

mixture. The organic phase was separated, dried over MgSO$_4$ and subjected to analysis by GC. GC yields (average of two runs) were calculated using diethylene glycol-n-dibutyl ether as an internal standard. In the case of the isolated methyl cinnamate, the dichloromethane phase was pumped down and the oily residue was loaded on a chromatographic column (SiO$_2$) and was eluted with PE/Et$_2$O 4:1. In the case of the coupling of p-bromoacetophone with methyl acrylate the product methyl 3-(4-acetylphenyl)acrylic acid methyl ester precipitates from the solution of NMP upon addition of water as an off-white solid.

Heck and Suzuki catalytic studies using Nolan's protocol: In the glove box a 50 mL Young's tap ampoule was charged with Pd(dba)$_2$ and the appropriate imidazolium salt was added (1:1 salt/Pd) so that a catalyst loading of 0.5 % was obtained. The ampoule was then opened under an atmosphere of N$_2$ and dry-degassed solvent was added. This was followed by addition of the base (2 equivalents/ aryl halide) (base = dry-degassed NEt$_3$ or degassed NMeCy$_2$; when base = Cs$_2$CO$_3$, the addition took place in the glovebox). Aryl halide (1 mmol) and the acrylate were then added (1.4 equivalents), and the ampoule was placed under partial vacuum and placed in a thermostated oil bath. The work up of the reaction mixture was the same as in the case of the Heck reactions. In the case of Suzuki couplings the same conditions were applied. When KF was used as a base for the Suzuki coupling a 0.5% (to KF) of dried 18-crown-6 was added to the reaction mixture.

Suzuki coupling using 3.8a and NaCH(COOMe)$_2$: In the glove box a 20 mL Schlenk was charged with complex **3.8a** and NaCH(COOMe)$_2$ (1:1) so that a catalyst loading of 0.5% was obtained. The contents of the Schlenk were cooled to -78 °C and THF (5 mL) was added slowly in the reaction mixture. A 50 mL Young's tap ampoule was charged under an atmosphere of N$_2$ with p-bromoacetophenone (1 mmol), phenylboronic acid (1.1 mmol), dry-degassed NEt$_3$ (2 mmol), dry-degassed NMP (2 mL) and diethylene glycol-n-dibutyl ether (internal standard, 0.3 mmol), and was then cooled down at -30 °C. The THF solution of **3.8a** and NaCH(COOMe)$_2$ was added *via* cannula to the contents of the ampoule and the whole was left stirring at -30 °C for 5 minutes. The slash bath was removed, and the ampoule was placed under partial vacuum and then submerged in a thermostated oil bath. The work up of the reaction mixture is the same as above. The isolation of the coupling product was achieved by column chromatography (SiO$_2$) with PE/Et$_2$O (3:1) as eluent.

Copolymerisation of CO/C$_2$H$_4$: In a typical run 10 mg of complex **3.1a** (0.02 mmol) were dissolved in 10 mL of dichloromethane, the solution transferred to a glass pressure

reactor and cooled to -78 °C. To this solution was added 18 mg (1 eq.) of Brookhart's acid dissolved in 10 mL of dichloromethane and cooled to -78 °C. After the addition was complete the temperature was raised slowly to -30 °C and the apparatus was slowly pressurised with a 1:1 mixture of CO/C_2H_4 up to about 0.5 bar. The slush bath was then removed, and the reaction mixture was pressurised at 5 bar. After 30 minutes the solution became cloudy. The reaction was quenched after 2 hrs with 30 mL of methanol. The precipitated polymer was filtered and dried under vacuum to yield 69 mg of poly-(CO-block-(CH$_2$)$_2$). The polymer was dissolved in a 1:1 mixture of C_6D_6 and $(CF_3)_2CHOH$ and the NMR spectra were recorded. ^{1}H-NMR $\delta(C_6D_6)$: 2.40 (s, poly-(CO-alt-(CH_2)$_2$); ^{13}C{^{1}H}-NMR $\delta(C_6D_6)$: 35.9 (s, poly-(CO-alt-(CH_2)$_2$), 212.3 (s, poly-(CO-alt-(CH$_2$)$_2$); IR (KBr disk): 2906 cm^{-1} (ν_{CO} stretching).

Crystallographic data for 4.3, 4.4 and 4.9:

Complex	4.3	4.4	4.9
Chemical Formula	$C_{136}H_{111}B_2F_{48}N_6O_{0.50}P_2Pd_2$	$C_{64}H_{51}BF_{24}N_3PPd$	$C_{59}H_{45}BF_{24}N_4Pd$
Formula weight	3045.67	1466.26	1383.20
Crystal system	Triclinic	Triclinic	Monoclinic
Space group	P-1	P-1	$P\,2_1/n$
a / $\mathring{A}$	14.258(5)	10.2531(2)	24.5559(8)
b / $\mathring{A}$	17.042(5)	15.1598(5)	19.7453(7)
c / $\mathring{A}$	27.324(5)	22.1848(7)	25.285(8)
α / °	92.213(5)	74.158(2)	90
β / °	94.633(5)	80.735(2)	97.3400(10)
γ / °	91.360(5)	73.122(2)	90
Z	2	2	8
T/K	120(2)	120(2)	120(2)
μ / mm^{-1}	0.417	0.433	0.420
No. of data collected	60460	56165	120423
No. of unique data	18875	14437	27861
Goodness of fit on F^2	0.990	1.015	1.031
$R_{int.}$	0.1037	0.1028	0.1433
Final $R(|F|)$ for $F_0 > 2\sigma(F_0)$	0.0657	0.0561	0.0786
Final $R(F^2)$ for all data	0.1183	0.1117	0.1526

Crystallographic data for 4.10 and 4.13&4.14:

Complex	4.10	4.13&4.14
Chemical Formula	$C_{62}H_{76}Cl_6I_4N_4P_2Pd_2$	$C_{21.48}H_{26.43}Cl_{0.52}IN_3Pd$
Formula weight	1872.31	578.44
Crystal system	Monoclinic	Monoclinic
Space group	$I2/a$	$P\ 2_1/c$
a / $\mathring{A}$	18.5870(4)	10.6431(16)
b / $\mathring{A}$	14.5626(3)	12.314(2)
c / $\mathring{A}$	27.2787(6)	17.038(2)
α / °	90	90
β / °	108.7830(10)	99.799(13)
γ / °	90	90
Z	4	4
T/K	120(2)	120(2)
μ / mm^{-1}	2.596	2.321
No. of data collected	34896	24498
No. of unique data	7991	5028
Goodness of fit on F^2	1.049	1.058
$R_{int.}$	0.0484	0.0396
Final $R(|F|)$ for $F_0 > 2\sigma(F_0)$	0.0579	0.0408
Final $R(F^2)$ for all data	0.0879	0.0476

References:

1. Douthwaite, R. E.; Green, M. L. H.; Silcock, P. J.; Gomes, P. T. *J. Chem. Soc., Dalton Trans.* **2002**, 1386.
2. Ittel, S. D.; Johnson, L. K.; Brookhart, M. *Chem. Rev.* **2000**, *100*, 1169.
3. Gardiner, M. A.; Herrmann, W. A.; Reisinger, C. P.; Schwartz, J.; Speigler, M. *J. Organomet. Chem.* **1999**, *572*, 239.
4. a) Malinoski, J. M.; Brookhart, M. *Organometallics* **2003**, *22*, 5324.b) Morise, X.; Braunstein, P.; Welter, R. *Inorg. Chem.* **2003**, *42*, 7752.
5. Bernard, C.; Jacques D. *Anal. Chim. Acta* **1981**, *131*, 141
6. Estevan, F.; G.-Bernade, A.; Lahuerta, P.; Sanau, M.; Ubeda, M. A.; de Arellano, M. C. R. *Inorg. Chem.* **2000**, *39*, 5964.
7. McGuiness, D. S.; Saendig, N.; Yates, B. F.; Cavell, K. J. *J. Am. Chem. Soc.* **2001**, *123*, 4029.
8. Nielson, D. J.; Cavell, K. J.; Skelton, B. W.; White, A. H. *Inorg. Chim. Acta* **2002**, *325*, 116.
9. Zhao, D.; Fei, Z.; Scopelliti, R.; Dyson, P. J. *Inorg. Chem.* **2004**, *43*, 2197.
10. de Graaf, W.; Boersma, J.; Smeets, W. J. J.; Spek, A. L.; van Koten, G. *Organometallics* **1989**, *8*, 2907.
11. Canty, A. J., *Acc. Chem. Res.* **1992**, *25*, 83.
12. Gardiner, M. G.; Herrmann, W. A.; Reisinger, C.-P.; Spiegler, M. *J. Organomet. Chem.* **1999**, *572*, 239.
13. Negishi, E. -I. *Handbook of organopalladium chemistry for organic synthesis;* Wiley: New York, 2002.
14. Roncali, J., *Chem. Rev.* **1992**, *92*, 711.
15. Littke, A. F.; Dai, C.; Fu, G. C. *J. Am. Chem. Soc.* **2000**, *122*, 4020.
16. Hillier, A. C.; Nolan, S. P. *Platinum Metals Rev.* **2002**, *46*, 50.
17. Zapf, A.; Beller, M. *Chem. Eur. J.* **2001**, *7*, 2908.
18. Lappert, M. F., *J. Organomet. Chem.* **1988**, *358*, 185.
19. Caddick, S.; Cloke, F. G. N.; Clentsmith, G. K. B.; Hitchcock, P. B.; McKerrecher, D.; Titcomb, L. R.; Williams, M. R. V. *J. Organomet. Chem.* **2001**, *617-618*, 635.
20. Heck, R. F.; Nolley, J. P. *J. Org. Chem.* **1972**, *37*, 2320.
21. Whitcombe, N. J.; Hii, K. K. M.; Gibson, S. E. *Tetrahedron* **2001**, *57*, 7449
22. Bedford, R. B.; Cazin, C. S. J.; Hursthouse, M. B.; Light, M. E.; Scordia, V. J. M. *J. Chem. Soc., Dalton Trans.* **2004**, 3864.
23. M.-Morales, D.; Yung, C.; Jensen, C. M. *Chem. Commun.* **2000**, 1619.
24. Shaw, B. L., *New J. Chem.* **1998**, *22*, 77.
25. Rocaboy, C.; Gladysz, J. A. *New J. Chem.* **2003**, *27*, 39-49.
26. Littke, A. F.; Fu, G. C. *J. Org. Chem.* **1999**, *64*, 10.
27. Herrmann, W. A.; Bohm, V. P. W.; Reisinger, C. P. *J. Organomet. Chem.* **1999**, *576*, 1124.
28. Schwarz , J.; Bohm, V. P. W.; Gardiner, M. G.; Grosche, M.; Herrmann, W. A.; Hieringer, W.; R.-Sieber, G. *Chem. Eur. J.* **2000**, *6*, 1773.
29. Weskamp, T.; Bohm, V. P. W.; Herrmann, W. A. *J. Organomet. Chem.* **2001**, *585*, 348.
30. McGuiness, D. S.; Cavell, K. J.; Skelton, B. W.; White, A. H. *J. Organomet. Chem.* **1998**, *565*, 165.
31. McGuiness, D. S.; Cavell, K. J.; Skelton, B. W.; White, A. H. *Organometallics* **1999**, *18*, 1596.
32. McGuiness, D. S.; Cavell, K. J. *Organometallics* **2000**, *19*, 741.

33. Tulloch, A. A. D.; Danopoulos, A. A.; Tizzard, G. J.; Coles, S. J.; Hursthouse, M. B.; H.-Motherwell, R. S.; Motherwell, W. B. *Chem. Commun.* **2001**, 1270.

34. Danopoulos, A. A.; Tulloch, A. A. D.; Winston, S.; Eastham, G.; Hursthouse, M. B. *J. Chem. Soc., Dalton Trans.* **2003**, 1009.

35. Albert, K.; Gisdakis, P.; Rosch, N. *Organometallics* **1998**, *17*, 1608.

36. Yang, C.; Lee, H. M.; Nolan, S. P. *Org. Lett.* **2001**, *3*, 1511.

37. Lee, H. M.; Zeng, J. Y.; Hu, C.-H.; Lee, M.-T. *Inorg. Chem.* **2004**, *43*, 6822.

38. Liu, W.; Brookhart, M. *Organometallics* **2002**, *21*, 2836.

39. Bianchini, C.; Meli, A.; Oberhauser, W. *J. Chem. Soc., Dalton Trans.*, **2003**, 2627.

40. Brookhart, M.; Grant, B.; Volpe, A. F. *Organometallics* **1992**, *11*, 3920.

41. Strauss, D. A.; Zhang, C.; Tilley, T. D. *J. Organomet. Chem.* **1989**, *369*, C13.

42. Bahr, S. R.; Boudjouk, P. *J. Org. Chem.* **1992**, *57*, 5545.

43. Toshinao, U.; Kawazura, H.; Ishii, Y. *J. Organomet. Chem.* **1974**, *65*, 253.

Chapter 5: Synthesis and reactivity of pyridine and phosphine functionalised NHC complexes of Pt(II)

Chapter 5: Synthesis and reactivity of pyridine and phosphine functionalised NHC complexes of Pt(II)

5.1 Introduction

The use of palladium-catalysed reactions in organic syntheses has increased to such a stage over the last twenty years, that is common practice to witness a palladium catalysed reaction as the key step for the preparation of many complex organic products. [1,2] The use of platinum complexes as catalysts in organic reactions has been overlooked. Nevertheless over the past few years there has been an upsurge in the number of processes where platinum complexes are used as catalysts. Some examples are the hydrosilylation [3] and diboration [4] of alkenes, oxidation [5] of alkenes, hydroformylation, [6] hydration reactions, [7] functionalisation of cyclopropanes, [8] hydrophosphination [9] and allylic substitution. [10] In all the above cases the reactions are catalysed by phosphine platinum complexes. [11]

Although the use of NHCs as phosphine mimics has produced complexes of almost every transition metal, very few reports on the synthesis of platinum NHC complexes are known. Arduengo *et al.* have reported the synthesis of the Pt(IMes)$_2$ (**5.1**) complex, [12] while Cavell and co-workers have reported the synthesis of complexes of the type Pt(NHC)(η^2-alkene)$_2$ (NHC = IMes, SIMes, alkene = dimethyl *trans*-but-2-enedioate) (Scheme 5.1). [13] The latter complexes readily activate the C-H bond at the 2 position of imidazolium salts to give the Pt(II) complexes **5.4** and **5.5**. [13] The latter group have also utilised imidazolium salts to generate *in situ* platinum complexes that were used as catalysts for the hydrosilylation of styrene. [14]

In this chapter pyridine- and phosphine-functionalised NHCs are utilised to access novel neutral Pt(II) dimethyl complexes. These complexes are further reacted with various acids in an attempt to investigate the preference of the electrophilic attack on the two electronically different Pt-Me bonds. The oxidative addition of MeI to these complexes is also studied.
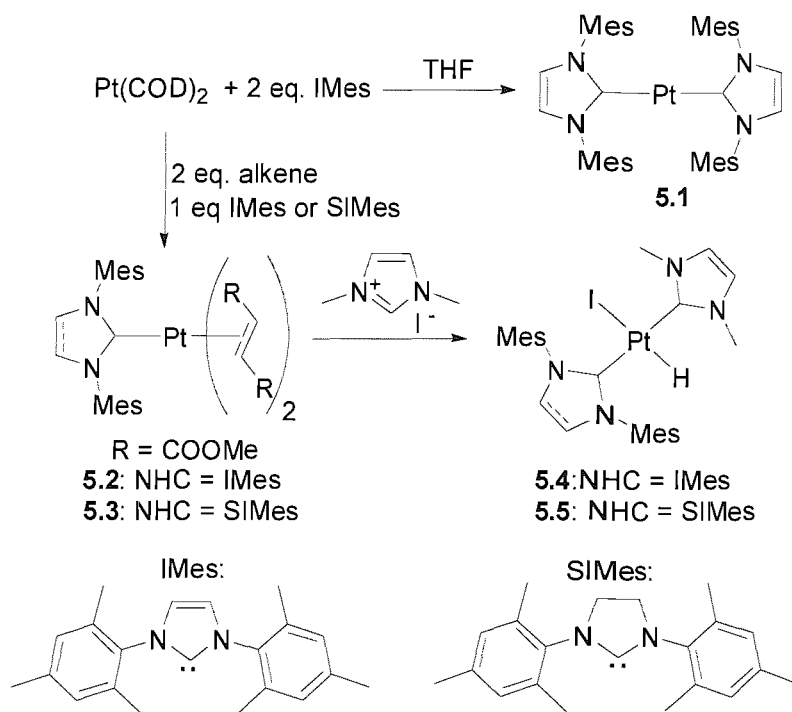
Scheme 5.1: Synthesis of Pt(0) and Pt(II) NHC complexes reported by Arduengo [11] (**5.1**) and Cavell [13] (**5.2-5.5**).

5.2 Results and discussion

5.2.1 Synthesis of pyridine and phosphine functionalized NHC neutral Pt(II) complexes

The synthesis of the novel neutral Pt(II) complexes incorporating the mixed donor NHC ligands, follows a synthetic protocol similar to the one described in Chapter 3 for the homologous Pd(II) complexes. This involves the substitution of a leaving ligand by either the isolated free carbene in the case of the pyridine functionalised NHC, or by the *in situ* generated carbene in the case of phosphine functionalised NHC ligand (Scheme 5.2).
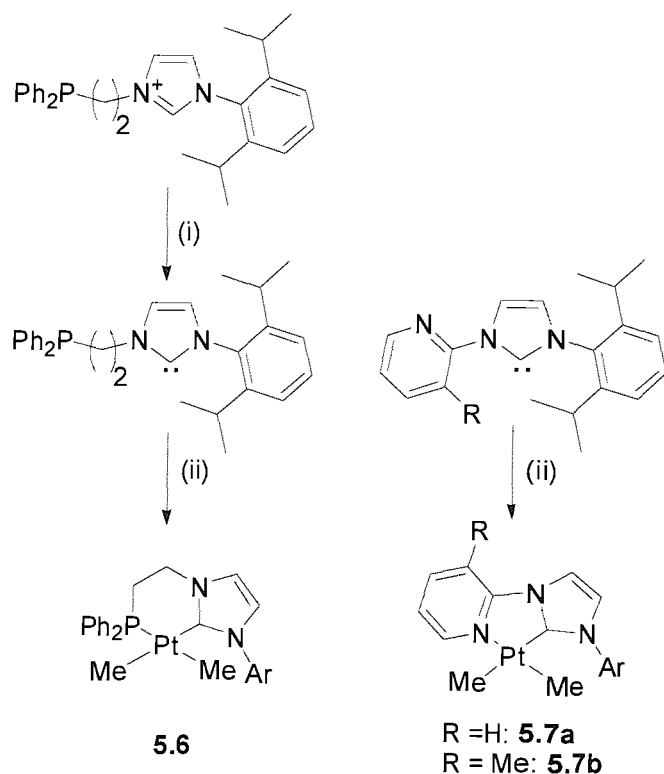
Scheme 5.2: Synthesis of phosphine and pyridine functionalised neutral Pt(II) complexes. Reagents and conditions: (i): 1.1 equiv. $KN(SiMe_3)_2$, THF -78 °C. (ii) 0.5 equiv. [Pt(μ-Me_2S)Me_2]$_2$ THF -78 °C to RT (Ar = 2,6-diisopropylphenyl).

The compounds described above are air-stable at room temperature. Complex **5.6** is colourless and is soluble in acetone, CH_2Cl_2 and THF. Prolonged exposure to dichloromethane leads to decomposition products and solutions of the complex in deuterated dichloromethane left standing at room temperature for 2-3 hours have been found to contain more than one species. The complex is also soluble in $CHCl_3$ but rapid decomposition to black aggregates occurs.

Complexes **5.7a** and **5.7b** are bright yellow air-stable solids exhibiting the same solubilities as above as well as the same decomposition behaviour to complex **5.6** in certain chlorinated solvents. They are also sparingly soluble in toluene. It is interesting to note that complex **5.7a** is cleanly isolated by interaction of the pyridine functionalised free carbene and [Pt(μ-Me_2S)Me_2]$_2$ in a 2:1 molar stoichiometry, unlike its analogue Pd(II) neutral complex **3.5a** where a 40% excess of the mixed pyridine donor NHC ligand had to be utilised to drive the reaction to completion. This difference can be explained by the better leaving group properties of dimethylsulfide (DMS) as compared to tmeda.

5.2.2 Characterisation of neutral complexes 5.6, 5.7a and 5.7b

5.2.2.1 NMR spectroscopy

The ^{1}H-NMR spectra of the above complexes concur with non-symmetric structures. This is evidenced by the appearance of the inequivalent Pt-CH_3 peaks as a pair of singlets in the case of 5.7a and 5.7b, and as a pair of doublets (due to P-H coupling) in the case of the 5.6. These Pt-*Me* resonances are in all cases accompanied by Pt satellite peaks due to Pt-H coupling. These satellites appear also as doublets in the case of compound 5.6. These features are outlined in Table 5.1. The Pt-CH_3 resonances are shifted upfield, in the case of 5.6, while they are isochronous, in the case of 5.7a and 5.7b, with complexes of the type [PtP$_2$Me$_2$] (P = tertiary phosphine).[15]

The relative upfield shift of the Pt-Me resonances in complex 5.6 compared to the observed peaks for 5.7a and 5.7b, suggests that the phosphine-NHC ligand architecture has a stronger overall σ-donating effect on the metal centre compared to the pyridine-NHC architecture. The same trend was observed for the analogous Pd(II) complexes. There also seems to be a correlation between the value of the Pt-H coupling constant ($^2J_{PtH}$) with the electron donating properties of the hybrid ligands. This is shown by the bigger $^2J_{PtH}$ coupling constants observed for the pyridine functionalised NHC Pt(II) dimethyl complexes 5.7a and 5.7b. Furthermore, a comparison of the M-CH_3 (M = Pd, Pt) ^{1}H-NMR chemical shifts shows that the Pt-*Me* protons resonate further downfield compared to their analogous Pd(II) complexes (-0.62 and –0.41 ppm for the analogous to 5.6 palladium complex, 0.01 and 0.12 ppm for the analogous to 5.7a palladium complex and 0.12 and 0.22 ppm for the analogous to 5.7b palladium complex).[16]
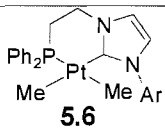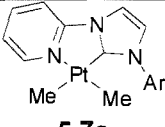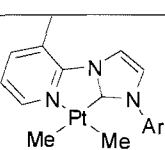
Complex	$\delta(^1H)$-PdCH_3	$^2J_{PtH}$ of satellites
5.6	-0.18 (d, $^3J_{PH}$ = 7.7 Hz) 0.03 (d, $^3J_{PH}$ = 6.9 Hz)	29.0 Hz 28.8 Hz
5.7a	0.29 (singlet) 0.45 (singlet)	46.6 Hz 31.2 Hz
5.7b	0.19 (singlet) 0.44 (singlet)	46.1 Hz 30.1 Hz

Table 5.1: Pt-CH_3 NMR chemical shifts (ppm) and their satellites.

The stronger electron donating character of the phosphine NHC hybrid ligand is also indicated by the upfield ^{195}Pt$\{^1H\}$ NMR shift in complex **5.6** (-4257.9 ppm, d, $^1J_{PtP}$ = 1822.5 Hz) compared to the observed ^{195}Pt$\{^1H\}$ shifts for compounds **5.7a** and **5.7b** (-3764.1 and –3763.9 ppm respectively).

The topology of the inequivalent Pt-CH$_3$ groups in complexes **5.7a** and **5.7b** was determined by NOESY experiments. In both cases they revealed a cross-peak between the methyls resonating downfield (0.44 and 0.45 ppm) and the α-CH hydrogen of the pyridine heterocycle. This means that this metal-alkyl bond is situated *trans* to the carbene moiety of the ligand.

The presence of a chelating ligand in **5.6** was further supported by the observed downfield shift in the ^{31}P$\{^1H\}$ spectrum compared to the mixed phosphine imidazolium salt precursor (-22.4 ppm) of the mixed carbene ligand. This consists of a singlet centred at 11.7 ppm with two Pt satellites with a $^1J_{PtP}$ coupling constant of 1822.5 Hz. This shift is very similar to the value of 12.4 ppm observed for the analogous palladium complex **3.1a**.

The formation of complexes **5.6** and **5.7a-b** was also evidenced by the appearance of certain peaks of diagnostic value in their ^{13}C$\{^1H\}$ spectra. These are attributed to the Pt-CH$_3$ and carbene (NCN) carbons. These shifts are summarised in Table 5.2.

Complex	$\delta(^{13}C\{^{1}H\})$-PdCH$_3$	$\delta(^{13}C\{^{1}H\})$-NCN
5.7a	-31.4 ($^{1}J_{PtC}$ = 401.9 Hz) -21.8 ($^{1}J_{PtC}$ = 397.8 Hz)	189.5 ($^{1}J_{PtC}$ = 441.9 Hz)
5.7b	-31.2 ($^{1}J_{PtC}$ = 402.6 Hz) -21.8 ($^{1}J_{PtC}$ = 397.5 Hz)	189.7 ($^{1}J_{PtC}$ = 442.7 Hz)

Table 5.2: Pd-CH$_3$ and carbene $^{13}C\{^{1}H\}$-NMR chemical shifts (ppm) for complexes **5.7a** and **5.7b**, along with the $^{1}J_{PtC}$ coupling constants for their Pt satellites in parenthesis.

Unfortunately, neither the carbene carbon, nor the Pt-CH$_3$ resonances were located in the case of complex **5.6**. Nevertheless the formation of the complex is substantiated by microanalysis results, which agree with the proposed structure, and by X-ray diffraction studies which confirm the structure unambiguously. It has to be noted that the spectra of crystals of compound **5.6** show the same resonances as spectra obtained by the bulk of the reaction mixture.

The Pt-Me carbon resonances in complexes **5.7a** and **5.7b** are significantly shifted upfield compared to their palladium analogues **3.5a** (-0.1 and 0.0 ppm) and **3.5b** (-0.2 and 0.0 ppm).

5.2.2.2 X-ray diffraction studies on complexes 5.6 and 5.7a

Complexes **5.6** and **5.7a** were also characterised by single crystal X-ray diffraction. X-ray quality crystals of **5.6** were obtained by layering a THF solution of the compound with ether. The structure of **5.6** as determined by single crystal X-ray diffraction studies is shown in Figure 5.1.

Figure 5.1: ORTEP representation of the structure of **5.6**, showing 50% probability ellipsoids. H atoms have been omitted for clarity. Selected bond lengths (Å) and angles (°): C(1)-Pt(1) = 2.031(4), C(30)-Pt(1) = 2.075(4), C(31)-Pt(1) = 2.085(4), P(1)-Pt(1) = 2.2491(12); C(1)-Pt(1)-C(30) = 176.91(16), C(1)-Pt(1)-C(31) = 95.15(16), C(30)-Pt(1)-C(31) = 84.60(16), C(1)-Pt(1)-P(1) = 90.93(12), C(30)-Pt(1)-P(1) = 89.53(12), C(31)-Pt(1)-P(1) = 172.93(11).

The geometry around the platinum centre is square planar with the ligand occupying two *cis* positions. The two Pt-CH$_3$ bond lengths, 2.075(4) and 2.085(4) Å, are equal within esds, a trend of suppressed *trans* influence observed in the homologous palladium complex **3.1a** described in Chapter 3. The corresponding Pd-CH$_3$ bond distances of 2.098(5) Å (*trans* to the NHC part of palladium complex **3.1a**) and 2.111(5) Å (*trans* to the phosphine part of palladium complex **3.1a**), compare with the ones observed above within esds. Table 5.3 below compares the M-C(carbene) and M-P (M = Pd, Pt) bond distances in complexes **3.1a** and **5.6**. The Pt-C(carbene) and Pt-P bond distances are shorter than the Pd-C(carbene) and Pd-P bonds respectively. One reason could be the soft-soft interactions between the Pt^{2+} metal centre and the phosphorous atom . Finally the six-membered chelate is puckered and the ligand bite angle is 90.93(12)°, which is the same within esds with the observed bite angle of 91.06(14)° in complex **3.1a**.

Bond distance (Å)	5.6 (M = Pt)	3.1a (M = Pd)
M-C(carbene)	2.031(4)	2.088(5)
M-P	2.2491(12)	2.2994(13)

Table 5.3: Comparison of M-NHC, M-P bond distances in complexes **5.6** and **3.1a**.

The formation of complex **5.7a** was also established by an X-ray diffraction study of single crystals obtained by slow diffusion of ether into a CH_2Cl_2 solution of **5.7a**. An ORTEP diagram of this crystal structure is shown at Figure 5.2.
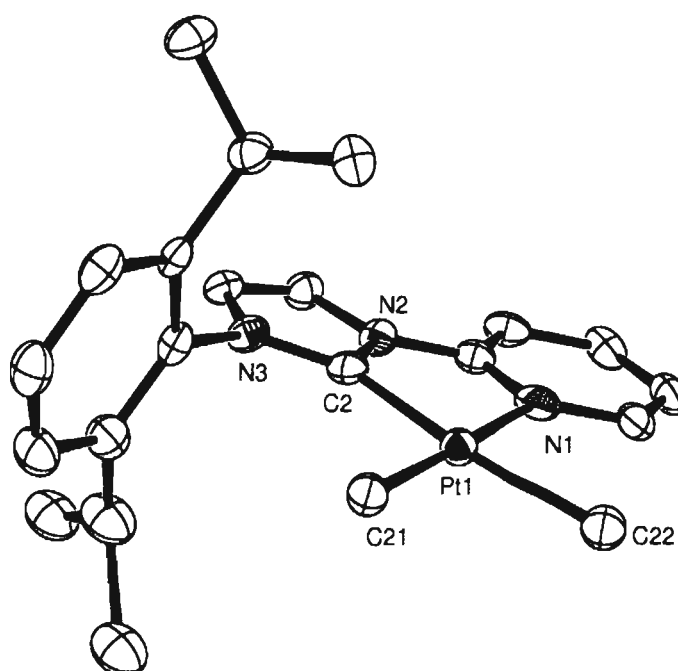
Figure 5.2: ORTEP representation of the structure of **5.7a**, showing 50% probability ellipsoids. H atoms have been omitted for clarity. Selected bond lengths (Å) and angles (°): C(2)-Pt(1) = 2.005(6), N(1)-Pt(1) = 2.128(4), C(22)-Pt(1) = 2.087(6), C(21)-Pt(1) = 2.044(5); C(2)-Pt(1)-C(21) = 98.0(2), C(2)-Pt(1)-C(22) = 171.9(2), C(21)-Pt(1)-C(22) = 90.1(2), C(2)-Pt(1)-N(1) = 78.2(2), C(21)-Pt(1)-N(1) = 175.7(2), C(22)-Pt(1)-N(1) = 93.7(2)

The geometry around the metal centre is approximately square planar with the bidentate ligand occupying two *cis* positions and forming a ligand bite angle of 78.2(2)°. The Pt-C(carbene) bond distance of 2.005(6) Å is the same, within esds, with the value of

164

2.031(4) Å observed for complex **5.6**, while the Pt-N(pyridine) bond length of 2.128(4) Å is significantly shorter than the Pt-P bond distance of 2.2491(12) Å found in complex **5.6**.

The NHC plane forms an angle of 2.97° with the pyridine plane. The NHC and pyridine plane form an angle with the plane defined by the two Pt-Me bonds of 5.44° and 4.23° respectively. Although the angle between the NHC plane and the metal centre coordination plane in **5.7a** is significantly smaller than the respective NHC-metal centre coordination plane angle of 43.70° in **5.6**, this should not be mistaken as an indication of possible π-backbonding. Such an effect would result in the shortening of the Pt-NHC bond distance in **5.7a** compared to **5.6**: this is not observed.

As the exactly analogous palladium complex has not been crystallographically characterised, a comparison similar to the one discussed in the case of **5.6** cannot be carried out. In an attempt to crystallise the platinum complex **5.7a** from CH_2Cl_2/Et_2O the undesired complex **5.8** was obtained (Scheme 5.3).

5.7b   **5.8**
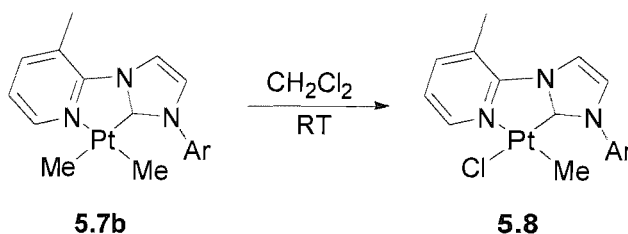
Scheme 5.3: Formation of **5.8** from prolonged exposure of **5.7b** to CH_2Cl_2 at room temperature.

A plausible mechanism for the formation of **5.8** involves oxidative addition of dichloromethane followed by reductive elimination of chloroethane, to yield the observed product. The formation of **5.8** accounts for the observation of extra resonances in NMR spectra obtained from CD_2Cl_2 solutions of either **5.7a** or **5.7b** left standing overnight at room temperature. Complex **5.8** was characterised only by a single crystal X-ray diffraction study, as this compound was not soluble in common organic solvents. Attempts to independently prepare **5.8** by reaction of **5.7b** with HCl (2M solution in ether) in CH_2Cl_2 led to decomposition products. An ORTEP diagram of the crystal structure of **5.8** is shown at Figure 5.3.
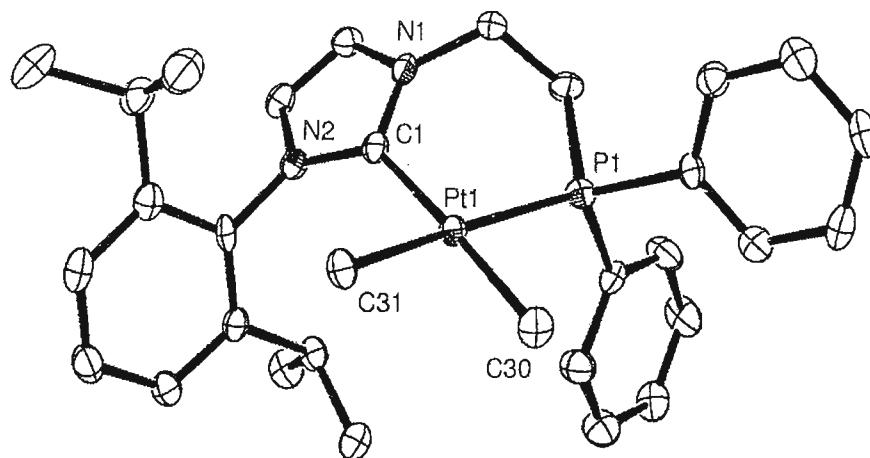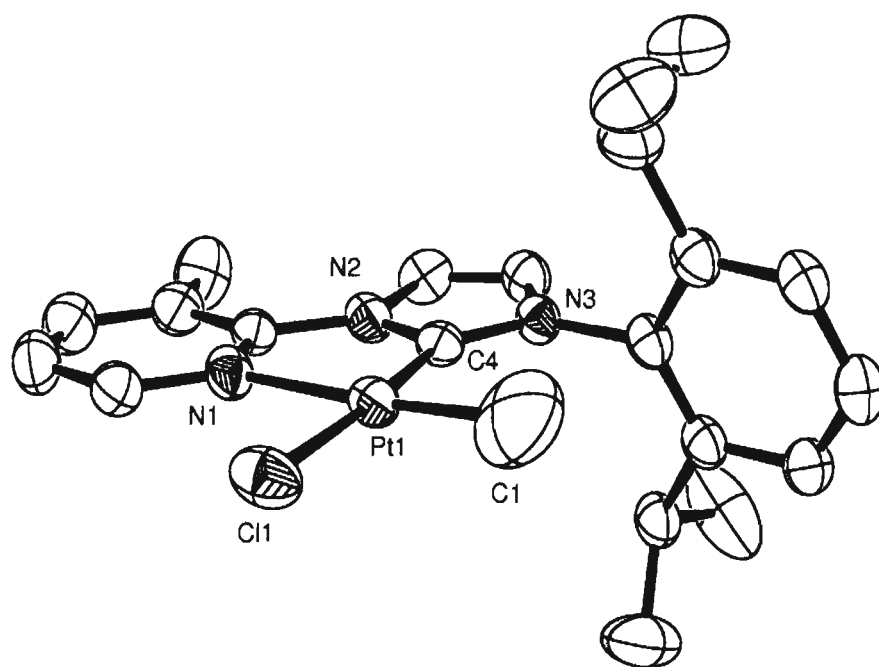
Figure 5.3: ORTEP representation of the structure of **5.8**, showing 50% probability ellipsoids. H atoms have been omitted for clarity. Selected bond lengths (Å) and angles (°): C(1)-Pt(1) = 2.044(13), N(1)-Pt(1) = 2.113(5), Pt(1)-Cl(1) = 2.3352(15), C(4)-Pt(1) = 1.935(6); C(4)-Pt(1)-C(1) = 103.4(4), C(4)-Pt(1)-N(1) = 78.3(2), C(1)-Pt(1)-N(1) = 174.8(3), C(4)-Pt(1)-Cl(1) = 174.92(18), C(1)-Pt(1)-Cl(1) = 81.6(3), N(1)-Pt(1)-Cl(1) = 96.67(14)

The geometry around the metal centre is square planar, with the coordination sphere comprising of two different metal carbon bonds, one nitrogen metal bond and one metal halogen bond. The Pt-C(carbene) and Pt-N(pyridine) bond distances are equal within esds with the ones (2.005(6) and 2.128(4) Å respectively) observed in **5.7a**. The Pt-Me bond length of 2.044(13) Å in **5.8** is virtually equal, within esds, with the Pt-Me bond distances of 2.044(5) Å (*trans* to the pyridine) and 2.087(6) Å (*trans* to the NHC) found in complex **5.7a**.

It is interesting to note that the oxidative addition of CH_2Cl_2 has been observed with the palladium complex **4.13** described in Chapter 4 (Scheme 5.4). In both cases the chloride occupies the site *trans* to the NHC part of the molecule, and as it has already been demonstrated in Chapter 4 and will be shown in this chapter as well, this is the site where the M-CH$_3$ bond is cleaved by an electrophile.
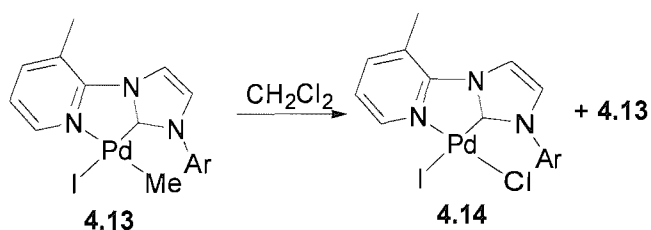
Scheme 5.4: Oxidative addition of CH_2Cl_2 into a palladium centre as described in Chapter 4.

5.2.3 Synthesis of cationic Pt(II) functionalised NHC complexes

Following the synthetic protocol described in Chapter 4, novel cationic Pt(II) functionalised NHC complexes were prepared. Interaction of either complex **5.7a** or **5.7b** with Brookhart's acid in the presence of a donor ligand led to the isolation of complexes **5.9-5.12** (Scheme 5.5).
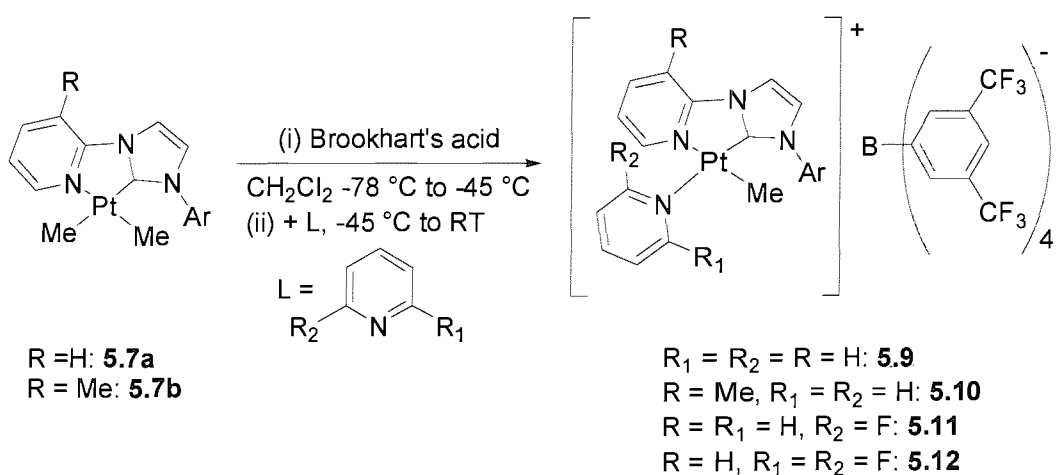
Scheme 5.5: Synthesis of cationic Pt(II) pyridine functionalised NHC complexes (Ar = 2,6-diisopropyl-phenyl).

5.2.4 Characterisation of complexes 5.9-5.12

5.2.4.1 NMR spectroscopy

The formation of complexes **5.9-5.12** was verified by NMR spectroscopy. The replacement of the two Pt-Me resonances by one signal at the metal alkyl region in their ^{1}H and ^{13}C{^{1}H} spectra was of significant diagnostic value (Table 5.4).
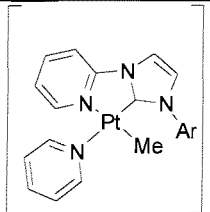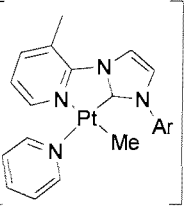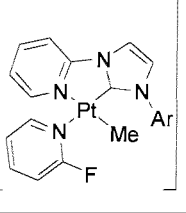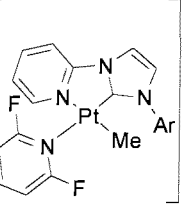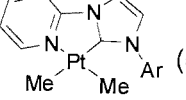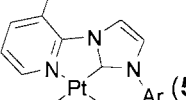
Complex	$\delta(^1H)$-PtCH_3	$\delta(^{13}C\{^1H\})$-PtCH$_3$
[structure] **5.9**	0.13 ($^2J_{PtH}$ = 40.9 Hz)	-16.8 ($^1J_{PtC}$ = 517.7 Hz)
[structure] **(5.10)**	0.14 ($^2J_{PtH}$ = 40.2 Hz)	-16.5 ($^1J_{PtC}$ = 519.9 Hz)
[structure] **(5.11)**	0.11 ($^2J_{PtH}$ = 39.5 Hz)	-3.2 ($^1J_{PtC}$ = 542.8 Hz)
[structure] **(5.12)**	0.13 ($^2J_{PtH}$ = 38.4 Hz)	-2.6 ($^1J_{PtC}$ = 518.1 Hz)
[structure] **(5.7a)**	0.29 ($^2J_{PtH}$ = 46.6 Hz) 0.45 ($^2J_{PtH}$ = 31.2 Hz)	-31.4 ($^1J_{PtC}$ = 401.9 Hz) -21.8 ($^1J_{PtC}$ = 397.8 Hz)
[structure] **(5.7b)**	0.19 ($^2J_{PtH}$ = 46.1 Hz) 0.44 ($^2J_{PtH}$ = 30.1 Hz)	-31.2 ($^1J_{PtC}$ = 402.6 Hz) -21.8 ($^1J_{PtC}$ = 397.5 Hz)

Table 5.4: ^{1}H and ^{13}C{^{1}H}-NMR Pt-Me shifts (ppm) in neutral and cationic Pt(II) species.

The existence of only one resonance in the ^{1}H and ^{13}C$\{^1$H$\}$ spectra of salts **5.9-5.12** attributed to the Pt-Me group shows that the electrophillic attack proceeds stereospecifically. It is worth noting the downfield shift of the Pt-CH$_3$ carbons, compared to the neutral parent complexes **5.7a** and **5.7b**, upon the formation of the cationic species. This downfield shift is even more profound when 2-fluoropyridine or 2,6-difluoropyridine were used to trap the 14 e$^-$ cationic species formed by the interaction of **5.7a** with Brookhart's acid. This is due to the electron-withdrawing properties of the fluorine atoms. Unfortunately the carbene carbon could not be observed in any of the above cations.

Another indication for the regiospecific formation of compounds **5.9** and **5.10** is their ^{195}Pt$\{^1$H$\}$ spectra. In both cases they consist of one peak shifted downfield relative to their neutral parent complexes **5.7a** and **5.7b**. These values are presented in Table 5.5.

Complex	δ-^{195}Pt$\{^1$H)
5.7a	-3764.1
5.9	-3495.8
5.7b	-3763.9
5.10	-3496.4.

Table 5.5: ^{195}Pt$\{^1$H$\}$-NMR chemical shifts of cationic and neutral Pt(II) complexes

The *o*-isopropyl methyls are diastereotopic and appear as a set of doublets in complexes **5.9-5.12**. One would expect that in the case of **5.11**, four different signals for these methyls should appear in its ^{1}H-NMR spectrum, since a conformation where the fluorine atom is situated either up or below the metal centre plane would destroy the plane of symmetry in the complex. The lack of this observation means that the 2-fluoropyridine occupying the position *trans* to the NHC moiety of the ligand either rotates around the Pt-N bond or occupies the two possible positions simultaneously, thus preserving the symmetry plane. This is further proved by the existence of only two signals for these methyls in the ^{13}C$\{^1$H$\}$ spectrum of the compound.

The formation of complexes **5.11** and **5.12** was also proved by their ^{19}F$\{^1$H$\}$ spectra. These contained peaks for the non-coordinating anion (-63.1 ppm) and a peak at -61.1 ppm for **5.11** and -60.3 ppm for **5.12**. Interestingly, the latter signal was

accompanied by Pt satellites, with a J_{PtF} coupling constant of 110.1 Hz. This shows some long range interaction between the platinum metal centre and the fluorine atoms.

Finally the geometry of the proposed structures was, in all cases, confirmed by NOESY experiments. These showed a long-range interaction between the Pt-Me proton and the methinic septet of the diisopropyl groups. This means that the remaining Pt-Me bond is situated *trans* to the pyridine part of the hybrid ligand.

5.2.4.2 X-ray diffraction studies on complexes 5.10 and 5.11

The stereospecific electrophilic attack on the Pt-CH$_3$ bond trans to the NHC moiety was further proved by single crystal X-ray diffraction studies on complexes **5.10** and **5.11**. Colorless crystals of **5.10** were obtained by layering an ether solution of the complex with petroleum ether. An ORTEP diagram of the cation in complex **5.10** is shown in Figure 5.4.
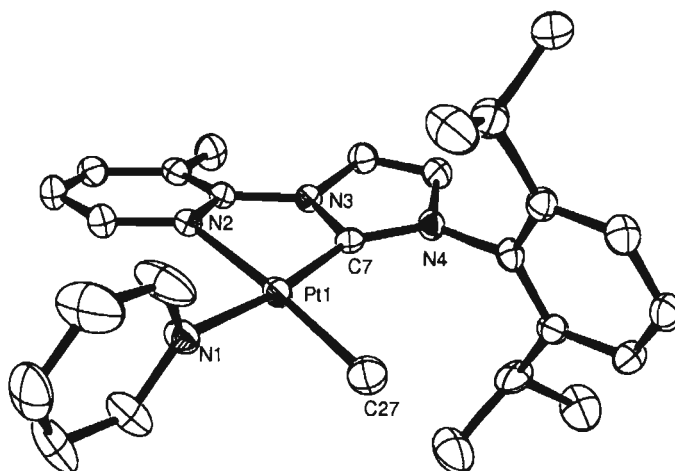
Figure 5.4: ORTEP representation of the cation in **5.10** showing 50% probability ellipsoids. The BAr$_4$$^{F-}$ anion and H atoms are omitted for clarity. Selected bond lengths (Å) and angles (°): C(7)-Pt(1) = 1.945(3), N(1)-Pt(1) = 2.069(3), N(2)-Pt(1) = 2.129(3), C(27)-Pt(1) = 2.050(4); C(7)-Pt(1)-C(27) = 101.35(15), C(7)-Pt(1)-N(1) = 172.53(12), C(27)-Pt(1)-N(1) = 85.29(14), C(7)-Pt(1)-N(2) = 78.11(12), C(27)-Pt(1)-N(2) = 174.20(14), N(1)-Pt(1)-N(2) = 95.63(11).

A comparison of the respective bond lengths in the analogous palladium complex **4.9** shows that they are equal within esds (Table 5.6).

Bond	**5.10** (M = Pt)	**4.9** (M = Pd)
M-C(carbene)	1.945(3) Å	1.964(5) Å
M-N(pyridine donor)	2.069(3) Å	2.084(4) Å
M-N(pyridine ligand)	2.129(3) Å	2.154(4) Å
M-CH$_3$	2.050(4) Å	2.021(5) Å

Table 5.6: Comparison of bond distances (Å) in **5.10** and **4.9**.

The geometry around the metal centre is essentially square planar with the chelating ligand occupying two cis positions, forming a bite angle of 78.11(12)°. One metal-alkyl bond and the pyridine donor molecule complete the coordination sphere. The donor pyridine plane is almost perpendicular to the metal centre plane as it forms an angle of 88.97°. The NHC and pyridine plane of the ligand form an angle of 17.18°, in order to accommodate the methyl in the 3 position of the pyridine heterocycle of the hybrid ligand.

X-ray quality crystals of complex **5.11** were grown by slow diffusion of pentane into an ether solution of the complex. An ORTEP diagram of the cation in complex **5.11** is given in Figure 5.5. The 2-fluoropyridine molecule is disordered over two positions, so that one fluorine atom is above the metal centre plane and the below. This is in agreement with the NMR spectroscopic data, suggesting that the metal centre symmetry plane is retained.
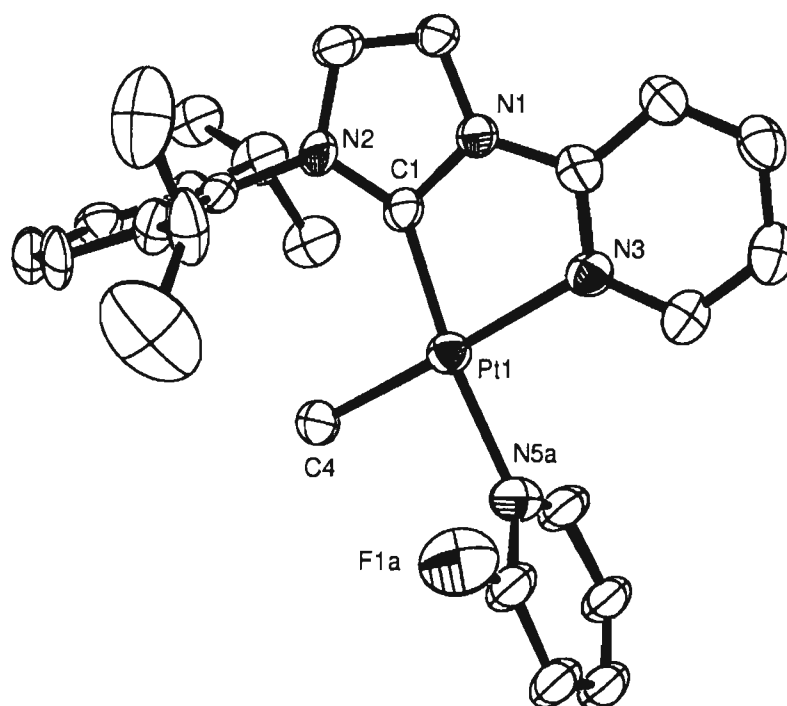
Figure 5.5: ORTEP representation of the cation in **5.11** showing 50% probability ellipsoids. The BAr_4^{F-} anion, one molecule of pentane, the H atoms and the 2-fluoropyridine molecule occupying the other position are omitted for clarity. Selected bond lengths (Å) and angles (°): C(1)-Pt(1) = 1.943(6), N(3)-Pt(1) = 2.134(5), Pt(1)-N(5A) = 2.095(7), C(4)-Pt(1) = 2.050(6); C(1)-Pt(1)-N(5A) = 172.8(5), C(4)-Pt(1)-N(5A) = 87.6(5), C(1)-Pt(1)-N(3) = 78.7(2), C(4)-Pt(1)-N(3) = 178.1(2), N(5A)-Pt(1)-N(3) = 94.3(5)

5.2.5 Reaction of 5.7a with Brookhart's acid in the presence of either CF₃CH₂OH (TFE) or styrene. Synthesis and characterisation of complex 5.13

Following the synthetic protocol described in Scheme 5.5 (page 160), the donor pyridine L was replaced by TFE or styrene, in an attempt to isolate complexes **5.14** and **5.15** (Figure 5.6).
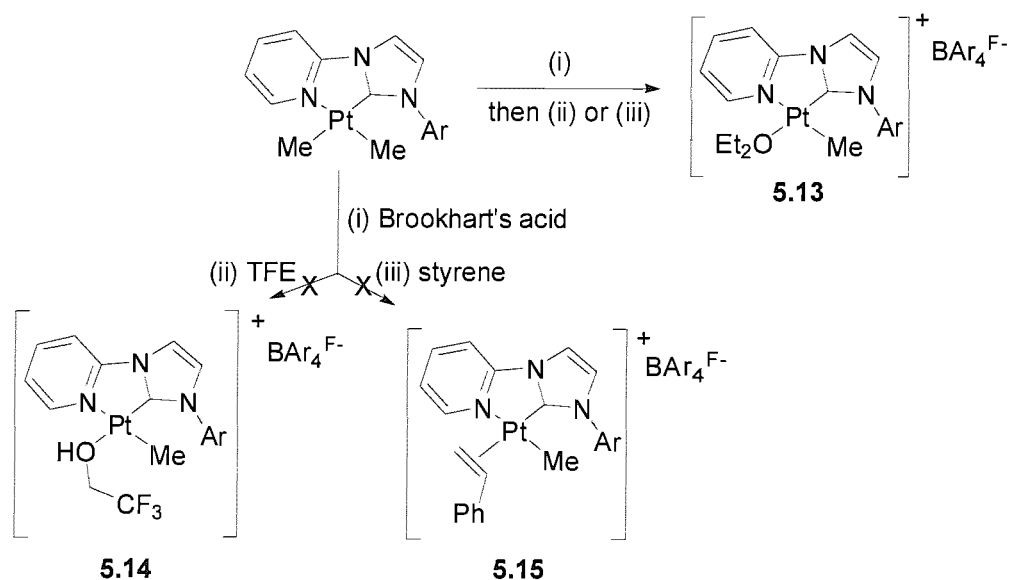
Scheme 5.6: Targeted complexes **5.14** and **5.15** from the reaction of **5.7a** with Brookhart's acid in the presence of TFE or styrene respectively and formation of **5.13** (Ar = 2,6-diisopropylphenyl).

These two complexes could not be identified in solution as the ^{1}H-NMR spectra were quite broad and even though they contained peaks assignable to the ligand and indeed showed the abstraction of one Pt-Me bond, peaks for the ligand L (L = TFE, styrene) could not be located. In the case where L = TFE, the ^{19}F{^{1}H}-NMR contained only the peak assigned to the non-coordinating anion BAr₄$^{F\,-}$. The reaction was repeated and after workup the solid residue was dissolved in Et₂O and was layered with petroleum ether, to afford in both cases crystals of complex **5.13**.

An ORTEP diagram of the cation in **5.13** is shown in Figure 5.7. The geometry around the metal centre is square planar. The ether donor molecule forms a dihedral angle of approximately 50.24° with the metal centre plane. The Pt-C(carbene), Pt-Me and Pt-N bond distances are similar within esds with the ones found in the cation of complex **5.11**.

The Pt-O(ether) (2.181(4) Å) bond length is longer than the Pt-N(2-fluoropyridine) (2.095(7) Å) one as expected.
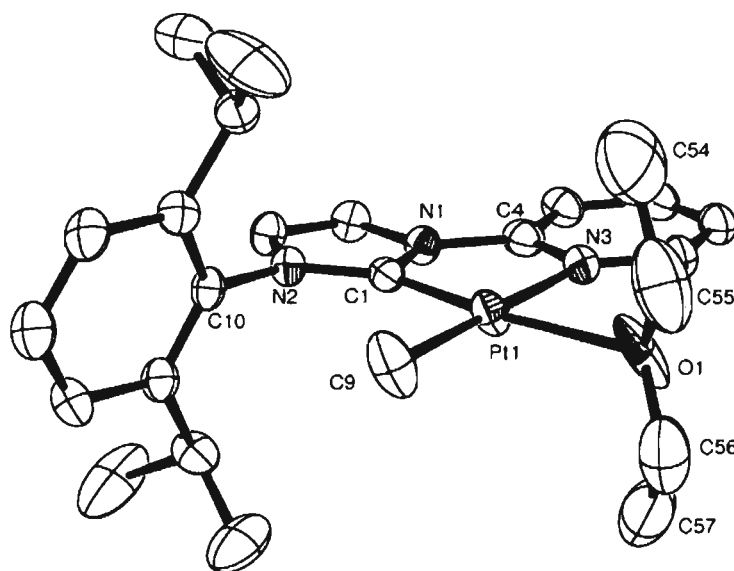
Figure 5.6: ORTEP representation of the cation in **5.13** showing 50% probability ellipsoids. The BAr_4^{F-} anion and H atoms are omitted for clarity. Selected bond lengths (Å) and angles (°): C(1)-Pt(1) = 1.935(5), N(3)-Pt(1) = 2.126(4), O(1)-Pt(1) = 2.181(4), C(9)-Pt(1) = 2.046(5); C(1)-Pt(1)-C(9) = 98.6(2), C(1)-Pt(1)-N(3) = 79.41(17), C(9)-Pt(1)-N(3) = 177.97(19), C(1)-Pt(1)-O(1) = 170.08(17), C(9)-Pt(1)-O(1) = 91.3(2), N(3)-Pt(1)-O(1) = 90.68(16).

The formation of **5.13** was also established by ^{1}H-NMR spectroscopy. The ^{1}H-NMR spectrum of crystals of **5.13** in d_5-PhCl showed that the crystal structure contains two molecules of ether in a 1:1 ratio. This is indicated by two quartets located at 3.40 and 3.53 ppm assigned to the methylenic protons of the ether molecules. The signal shifted downfield is assigned to the coordinated ether molecule. The spectrum also contained one singlet at 1.5 ppm and one singlet accompanied by platinum satellites ($^2J_{PtH}$ = 37.9 Hz) at 1.9 ppm, in a 1:1 ratio. The first one is water in C_5D_5Cl and the latter is coordinated water due to exchange between H_2O and Et_2O (Scheme 5.7). When the sample was shaken with

174

D$_2$O, the ratio of coordinated to uncoordinated water changed to 3:1, while the ratio of coordinated *versus* uncoordinated ether changed to 1:8. The sample was heated to 45 °C for 10 minutes, upon which time the coordinated/uncoordinated H$_2$O ratio increased to 4:1, while the two ether resonances collapsed into one quartet at 3.4 ppm, indicating that the equilibrium was completed shifted towards the water coordinated cationic species.
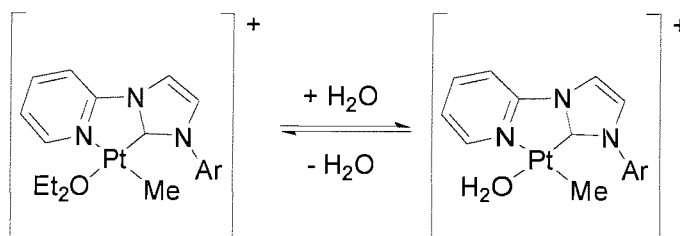
Scheme 5.7: Equilibrium between the ether coordinated and water coordinated cation.

The Pt-Me protons in **5.13** resonate at 0.22 ppm with a two bond scalar coupling to platinum of 35.1 Hz. These characteristic signal is shifted upfield in comparison to complexes of the type [(R$_2$PCH$_2$CH$_2$PR$_2$)PtMeOEt$_2$]BAr$_4$^{F} (R = Et, Cy).[17] Unlike the above chelating bisphosphine monocationic Pt(II) species, complex **5.13** is stable in the presence of water, and no bis-μ-OH products were observed, as such a transformation would result in the loss of the Pt-Me signal in the ^{1}H-NMR spectrum, which is not observed.

Due to the observed lability of ether, as well as literature reports that complexes of the type [(R$_2$PCH$_2$CH$_2$PR$_2$)PtMeOEt$_2$]BAr$_4$^{F} facilitate aromatic C-H activation,[17] a sample of the complex in dry d$_5$-PhCl was treated with one equivalent of benzene, in an attempt to check if C-H activation with this cationic complex could be achieved. Such a transformation could not be observed at ambient temperature. In fact no signs of aromatic C-H activation could be observed up to 60 °C. A further increase of temperature to 80 °C resulted in the formation of decomposition products.

5.2.6 Reaction of 5.6 with Brookhart's acid in the presence of pyridine

Unlike the pyridine functionalised NHC Pt(II) complexes, in which the Pt-Me bond is cleaved cleanly, the phosphine functionalised NHC Pt(II) dimethyl complex exhibits a different behaviour, upon interaction with Brookhart's acid in the presence of pyridine. The reaction protocol that was followed is identical to the one in Chapter 4

(Scheme 5.8).

Brookhart's acid
CH₂Cl₂ -78 °C to -45 °C
+ L, -45 °C to RT

species (A) and (B)

CD₂Cl₂

5.6

Brookhart's acid
Et₂O, -78 °C to -45 °C
+ L, -45 °C to RT

5.16
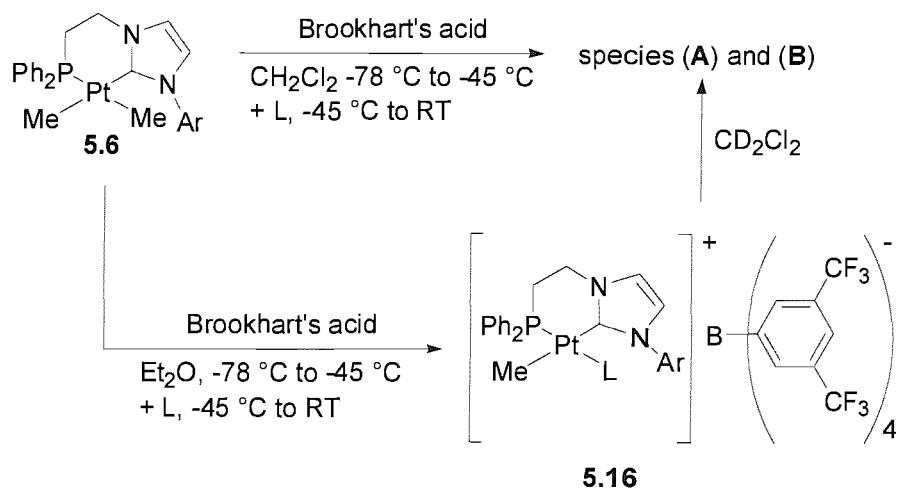
Scheme 5.8: Synthesis of cationic phosphine functionalised NHC Pt(II) complexes.

The ^{1}H-NMR spectrum of the reaction mixture after workup showed two species in a 2:1 ratio present in solution. The metal-alkyl region contained two distinct resonances for Pt-Me protons, and so did the alkyl region where four different o-isopropyl methyls were detected in a 2:2:1:1 ratio. Other characteristic features of the spectra were also doubled in an exact 2:1 ratio. This was at first considered as a sign of probably incomplete reaction between the complex and Brookhart's acid. When the ^{31}P{^{1}H} was obtained no starting material was observed (11.7 ppm $^1J_{PtP}$ = 1822.5 Hz). Instead the spectrum consisted of one peak at 10.1 ppm with two platinum satellites with a $^1J_{PtP}$ coupling constant of 746.0 Hz, and a peak at 8.7 ppm with a $^1J_{PtP}$ coupling constant of 1977.1 Hz (Figure 5.7).

The reaction was repeated using freshly prepared complex **5.6** using the same preparative method, but using ether instead of dichloromethane as the solvent. After the reaction was complete, the solution of the reaction mixture was layered with petroleum ether and afforded crystals of the target compound **5.16** (Scheme 5.8). An X-ray diffraction study revealed that the electrophilic attack had taken place again selectively at the site *trans* to the phosphine moiety of the ligand. Unfortunately the quality of the data was not good enough to produce a publishable model or an ORTEP diagram. The identity of the compound was further established by microanalysis. When crystals were dissolved in CD₂Cl₂ the two unidentified species described above were observed by ^{1}H and ^{31}P{^{1}H}-
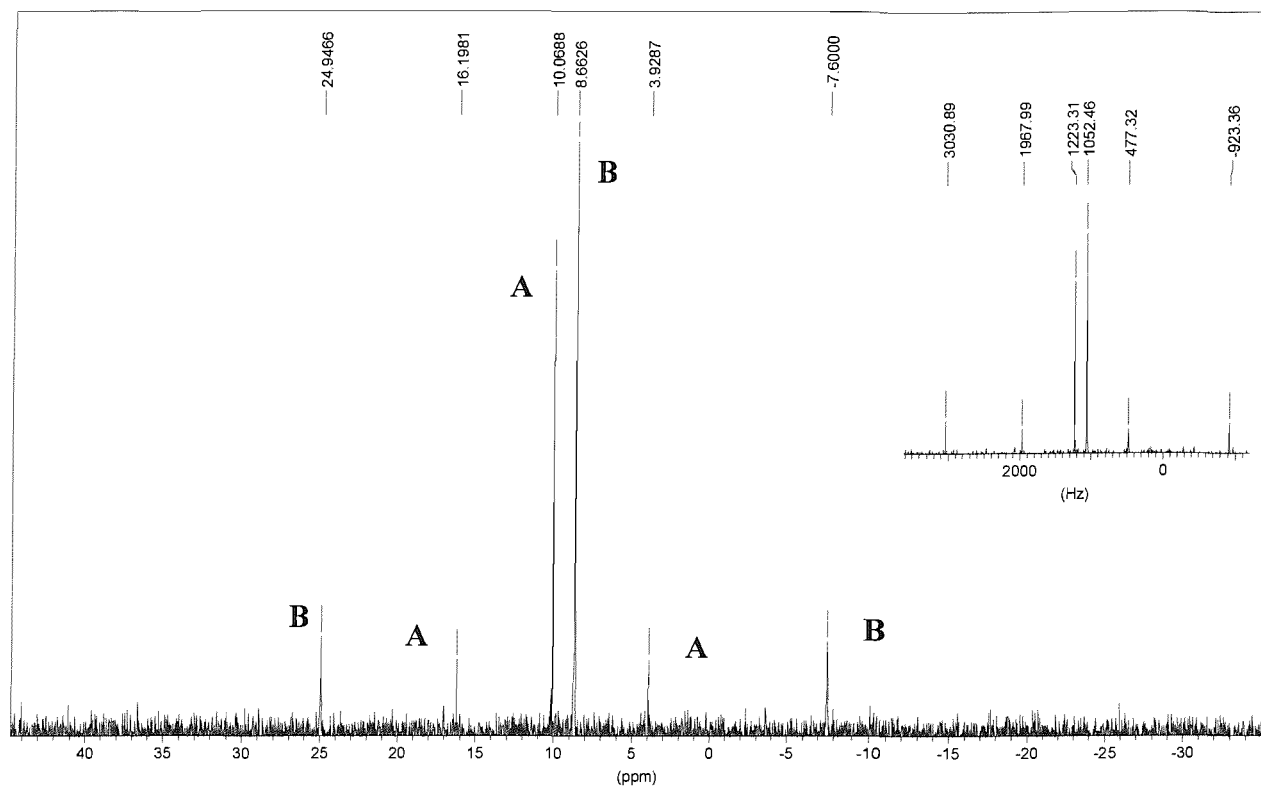
Figure 5.7: $^{31}P\{^1H\}$-NMR spectrum of the reaction mixture and of the crystals of compound **5.16** in CD_2Cl_2.

The appearance of two $^{31}P\{^1H\}$ signals and two species in the ^1H-NMR spectrum in solution could be due to flipping of the methylenic bridges giving rise to the λ and δ isomers. Nevertheless the upfield shift in the $^{31}P\{^1H\}$-NMR spectrum observed is inconsistent with $^{31}P\{^1H\}$ value of 34.8 ppm reported for the analogous cationic Pd(II) complex. Another explanation could be found in the non-innocence of dichloromethane as a solvent. The observed species could be a Pt(IV) cationic complexes. The only restriction is that they should have a plane of symmetry as the ^1H-NMR spectrum shows only two pairs of doublets for the o-isopropyl methyls. Attempts to clarify the situation by mass spectrometry resulted in no success. ES⁻ and $^{19}F\{^1H\}$ NMR showed the existence of the non-coordinating BAr_4^{F-} anion.

5.2.7 Reaction of 5.6 and 5.7a with other acids

In Chapter 4 we discussed the selective cleavage of the Pd-Me bond *trans* to the phosphine, resulting from the interaction of either **3.3** or **3.1a** with $(CF_3)_2CHOH$ (Scheme 5.9). Following the protocol described in Chapter 4, the neutral dimethyl Pt(II) complexes **5.6** and **5.7a** were reacted with $(CF_3)_2CHOH$. In both cases no reaction was observed even over long periods of time of the reaction mixtures standing at room temperature. This was established by the existence in both cases of two resonances for the Pt-Me protons in the ^{1}H-NMR spectra of the reaction mixtures and a broad singlet at 10.1 ppm assigned to unreacted $(CF_3)_2CHO$*H*. In the case of **5.6**, the absence of an electrophilic attack taking place was confirmed by the ^{31}P{^{1}H} spectrum which contained only one peak (with its platinum satellites) corresponding to the starting material **5.6** (11.7 ppm, $^1J_{PtP} = 1822.5$ Hz).
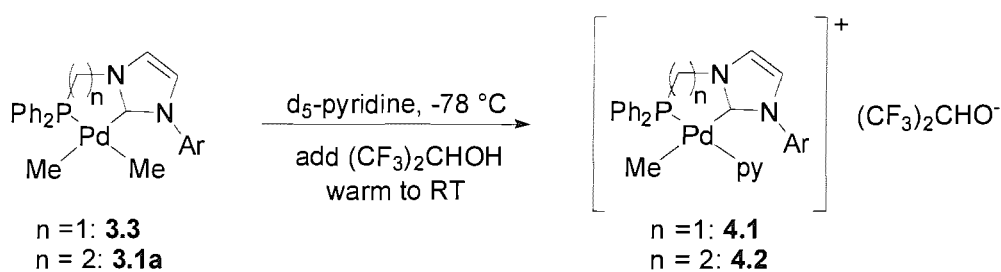
Scheme 5.9: Reaction of Pd(II) neutral complexes **3.3** and **3.1a** with $(CF_3)_2CHOH$ discussed in Chapter 4 (Ar = 2,6-diisopropylphenyl).

In an attempt to probe the selectivity of the electrophilic attack a more acidic reagent was sought. Therefore both **5.6** and **5.7a** were reacted with pentafluorophenol in CD_2Cl_2. Unfortunately once again no reaction took place at ambient temperature as confirmed by ^{1}H and where applicable ^{31}P{^{1}H}-NMR spectroscopy.

Complex **5.6** was further reacted with one equivalent of HBF_4 (ether solution) in the presence of pyridine or 1,1,1-trifluoroethanol or water in CH_2Cl_2. In all cases complex reaction mixtures were obtained by ^{1}H and ^{31}P{^{1}H} NMR. The ^{1}H-NMR spectra revealed that the abstraction of methyl had occurred, while the ^{31}P{^{1}H} spectra contained a myriad of peaks with a predominant one situated in the region of 15-16 ppm.

Interaction of **5.6** or **5.7a** with one equivalent trifluoroacetic acid (TFA) resulted in the cleavage of one Pt-Me bonds (Scheme 5.10). This was evidenced by the disappearance of one Pt-CH$_3$ resonance, in both cases, in their ^{1}H-NMR spectra. The protons of the remaining Pt-Me resonate at 0.08 ppm for **5.17** ($^2J_{PtH}$ = 35.5 Hz) and 0.17 ppm for **5.18** ($^2J_{PtH}$ = 38.4 Hz). Both signals are shifted upfield in comparison to [Pt(dmpe)MeO$_2$CCF$_3$] (dmpe = dimethylphosphine-ethane).[18] Furthermore in the case of complex **5.6**, the ^{31}P{^{1}H} NMR spectrum revealed a peak shifted downfield from 11.7 ppm in the neutral complex **5.6** to 19.6 ppm in complex **5.17** with platinum satellites and a $^1J_{PtP}$ coupling constant of 2017.8 Hz (Scheme 5.10). Based on the spectroscopic and structural data discussed in Chapter 4 for analogous Pd(II) cationic species, the Pt-Me bond *trans* to the phosphine moiety of the ligand seems to be cleaved.

^{31}P{^{1}H}: 11.7 ppm
$^1J_{PtP}$ = 1822.5 Hz

^{31}P{^{1}H}: 19.6 ppm
$^1J_{PtP}$ = 2017.8 Hz

δ–^{13}C{^{1}H} Pt-CH$_3$:
-31.4 ($^1J_{PtC}$ = 401.9 Hz)
-21.8 ($^1J_{PtC}$ = 397.8 Hz)

δ–^{13}C{^{1}H} Pt-CH$_3$:
-19.7 ($^1J_{PtC}$ = 266.3 Hz)
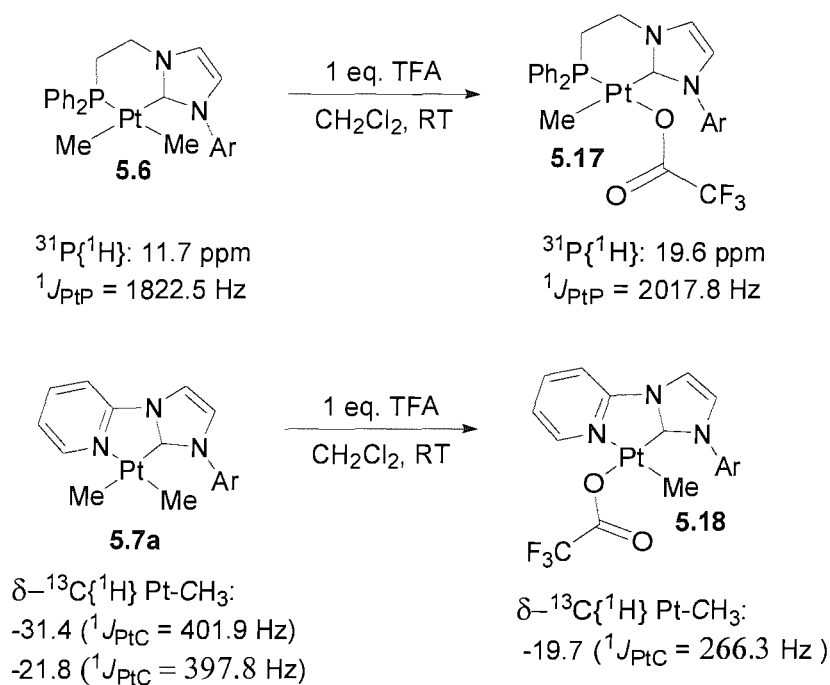
Scheme 5.10: Reaction of **5.6** and **5.7a** with TFA.

The ^{13}C{^{1}H} NMR spectrum of the reaction of **5.7a** with TFA also accounts for the formation of complex **5.18** as it contains one peak assigned to the Pt-CH$_3$ carbon at – 19.7 ppm. This is shifted downfield relative to the Pt-CH$_3$ resonances in complex **5.7a**. The carbene carbon was not observed (Scheme 5.10).

The geometry in complex **5.18** deriving from the reaction of **5.7a** with one equivalent of TFA, was established by a NOESY NMR experiment which revealed a long

range interaction between the remaining Pt-Me protons and the septet assigned to the *o*-isopropyl methinic protons. This suggests that this metal-alkyl bond is *trans* to the pyridine part of the ligand.

When **5.7a** was reacted with an excess of TFA, both Pt-Me bonds were cleaved. This was evidenced by the absence in the ^{1}H-NMR spectrum of Pt-CH_3 resonances as well as by the appearance in the ^{19}F{^{1}H} NMR spectrum of two peaks at –76.4 and –73.9 ppm (Scheme 5.11). The alternative geometry where the trifuoroacetic anion is bridging cannot be excluded.
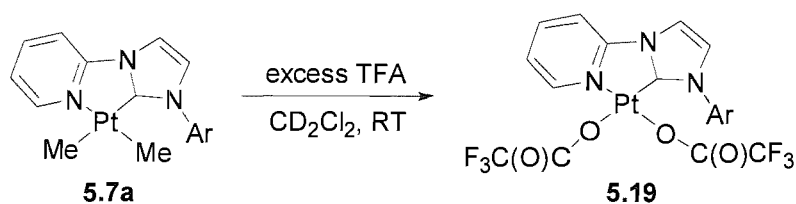
Scheme 5.11: Reaction of **5.6** with an excess of TFA.

Puddephatt *et al.* have reported that in the presence of water $B(C_6F_5)_3$ does not directly attack a Pt-Me bond but forms the adduct $H_2OB(C_6F_5)_3$ which acts as the acid $H[(OH)B(C_6F_5)_3]$. This in turn rapidly deprotonates a Pt-Me bond giving rise to intermediates of the type [(NN)PtMe]$^+$[OHB(C$_6$F$_5$)$_3$] $^-$ (NN = 4,4'-di-*tert*-butyl-2,2'-bypiridine = bu$_2$bpy). If a donor ligand is not present, the anion coordinates forming complex **5.21** (Scheme 5.12).[19] The formation of H[(OH)B(C$_6$F$_5$)$_3$] has been known to be facilitated by the addition of a nucleophile in the $H_2OB(C_6F_5)_3$ adduct. In this case the nucleophile is the Pt-Me bond, and upon protonolysis CH_4 is produced.

180
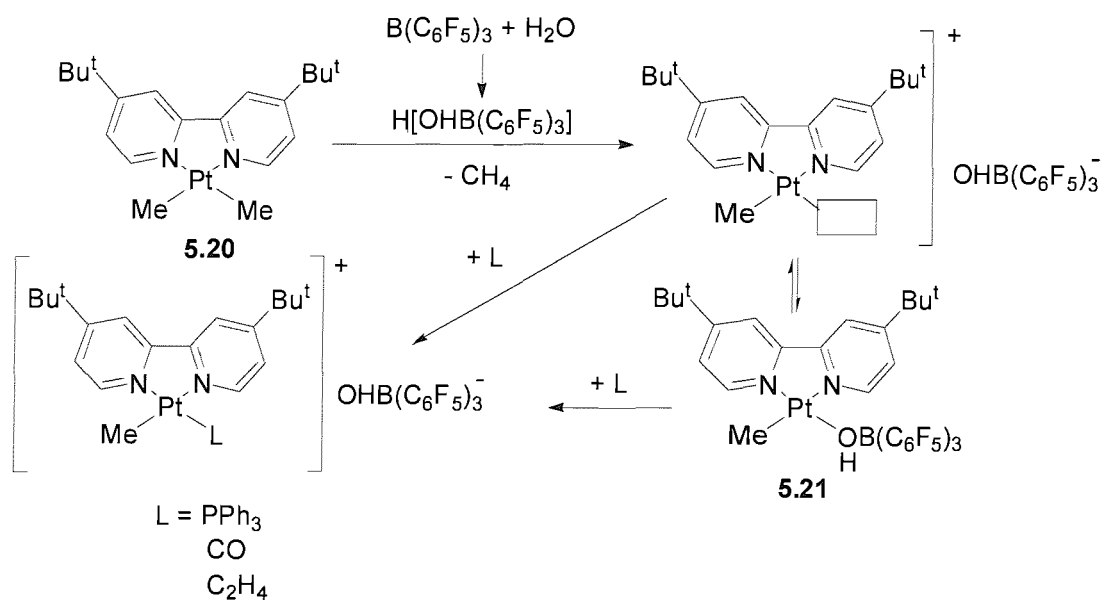
Scheme 5.12: Formation of the intermediate **5.21** isolated by Puddephatt *et al.*.

Since the Pt-Me protons in **5.7a** resonate at 0.29 and 0.45 ppm an indication of a more basic metal alkyl bond compared to **5.20** where the Pt-CH_3 signals appear at 0.71 ppm (*i.e.* the NHC-pyridine hybrid ligand is overall a stronger σ donor than bu$_2$bpy), the reaction of **5.7a** with one equivalent of B(C$_6$F$_5$)$_3$ in the presence of water was undertaken in the absence of a donor ligand (Scheme 5.13). This gave the product **5.22**. Its identity was established by spectroscopic methods. The ^{1}H-NMR spectrum had one peak at –0.01 ppm assigned to the Pt-Me protons. Platinum satellites with a $^2J_{PtH}$ coupling constant of 37.7 Hz accompanied this resonance. The existence of the OH was confirmed firstly by broad singlet at 2.93 ppm in the ^{1}H-NMR spectrum and secondly by a peak at 3599 cm^{-1} in the IR spectrum of the compound. The topology of the Pt-Me bond within the molecule was substantiated by a NOESY experiment that revealed that the Pt-Me bond *trans* to the NHC moiety is cleaved.
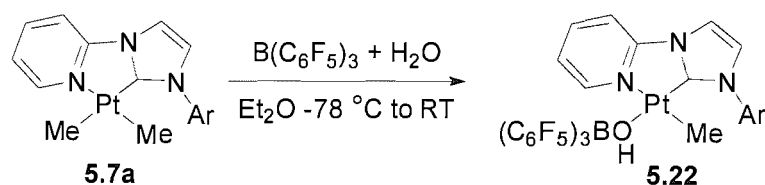
Scheme 5.13: Reaction of **5.7a** with B(C$_6$F$_5$)$_3$ in the presence of H$_2$O.

The structure of **5.22** was unambiguously established by an X-ray diffraction study on crystals obtained by layering an ether solution of **5.22** with petroleum ether. An ORTEP diagram of the crystal structure of **5.22** is shown on Figure 5.8.
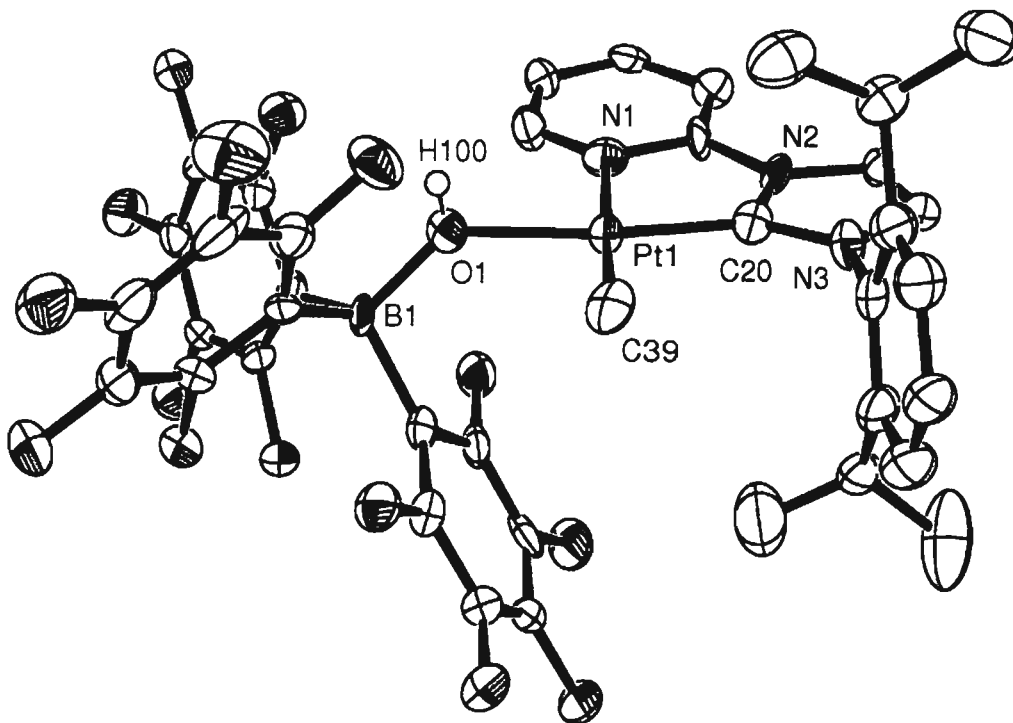
Figure 5.8: ORTEP representation of the structure of **5.22** showing 50% probability ellipsoids. Atom H100could not be located experimentally and was refined using a riding model. One distorted molecule of ether and H atoms (except H100) are omitted for clarity. Selected bond lengths (Å) and angles (°):C(20)-Pt(1) = 1.887(12), B(1)-O(1) = 1.535(16), N(1)-Pt(1) = 2.131(12), O(1)-Pt(1) = 2.106(9), O(1)-H(100) = 0.67(2), C(39)-Pt(1) = 1.994(15); C(20)-Pt(1)-C(39) = 98.3(6), C(20)-Pt(1)-O(1) = 170.9(5), C(39)-Pt(1)-O(1) = 90.6(5), C(20)-Pt(1)-N(1) = 80.3(5), C(39)-Pt(1)-N(1) = 177.4(5), O(1)-Pt(1)-N(1) = 90.8(4), B(1)-O(1)-H(100) = 118(10), Pt(1)-O(1)-H(100) = 101(10), B(1)-O(1)-Pt(1) = 134.5(7).

The geometry around the metal centre is square planar with the coordination sphere being comprised of the hybrid pyridine-NHC ligand (occupying two *cis* positions), one metal alkyl bond and the $HOB(C_6F_5)_3^-$ anion.. The ligand bite angle is 80.3(5)° and is slightly bigger than the bite angle of 78.7(2)° observed in the cation in **5.11**. The Pt-Me, Pt-C(carbene) and Pt-N(ligand) bond lengths in **5.22** compare within esds with the ones observed in the crystal structure of **5.11** (Table 5.7).

Bond	**5.22**	**5.11**
Pt-C(carbene)	1.887(12) Å	1.943(6) Å
Pt-Me	1.994(15) Å	2.050(6) Å
Pt-N(ligand)	2.131(12) Å	2.134(5) Å

Table 5.7: Comparison of bond lengths between **5.22** and **5.11**.

The Pt-O bond length (2.106(9) Å) in **5.22** is also the same within esds with the Pt-N(2-fluoropyridine) bond distance (2.095(7) Å) in **5.11**, and longer than the Pt-O bond length (2.062(2) Å) in **5.21**.

Bond	**5.22**	**5.21**
Pt-Me	1.994(15) Å	2.037(3) Å
Pt-O	2.106(9) Å	2.062(2) Å
Pt-N(ligand)	2.131(12) Å	2.097(2) Å
O-H	0.67 Å	0.67(4) Å

Table 5.8: Comparison of bond lengths in **5.22** and **5.21**. The Pt-N(ligand) refers to the bond distance between the metal centre and the pyridine nitrogen *trans* to the Pt-Me bond.

The crystal structure of **5.21** has been published [19] and Table 5.8 compares selected bond lengths between **5.21** and **5.22**. This table shows that all bond lengths, except the Pt-O one, are similar within esds. The longer Pt-O bond distance in **5.22** can be explained on the basis of the stronger *trans* influence of the NHC moiety exerted to this bond compared to the bu_2bpy ligand. The crystal structure of **5.21** also reveals intermolecular hydrogen bonding, within the $OHB(C_6F_5)_3^-$ anion, between fluorine atoms and the O*H* hydrogen.

Such an interaction was not observed in the case of **5.22** and it may account for the upfield shift of the O*H* hydrogen (2.93 ppm) in the ^{1}H-NMR spectrum of **5.22**, compared to the O*H* ^{1}H-NMR shift of 3.21 ppm reported for **5.21**.[19]

5.2.9 Reaction of 5.6 and 5.7a with MeI

The oxidative addition of MeI into complexes **5.6** and **5.7a** was investigated. In both cases the reaction takes place within seconds at room temperatures affording the Pt(IV) complexes *fac*-**5.23** and *fac*-**5.24** in good yields (Scheme 5.14).

5.6

^{31}P{^{1}H}: 11.7 ppm
$^1J_{PtP}$ = 1822.5 Hz

fac-**5.23**

^{31}P{^{1}H}: 10.8 ppm
$^1J_{PtP}$ = 799.6 Hz

5.7a

δ–^{13}C{^{1}H} Pt-CH$_3$:
-31.4 ($^1J_{PtC}$ = 401.9 Hz)
-21.8 ($^1J_{PtC}$ = 397.8 Hz)

fac-**5.24**

δ–^{13}C{^{1}H} Pt-CH$_3$:
-32.8 ($^1J_{PtC}$ = 328.5 Hz)
-20.5 ($^1J_{PtC}$ = 146.8 Hz)
-10.6 ($^1J_{PtC}$ = 330.4 Hz)
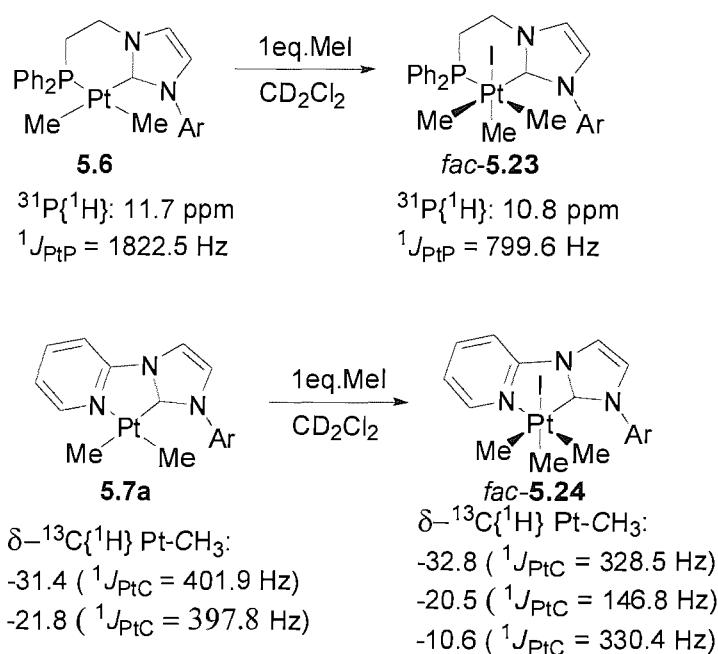
Scheme 5.14: Synthesis of Pt(IV) complexes *fac*-**5.23** and *fac*-**5.24** from oxidative addition of MeI to complexes **5.6** and **5.7a** respectively (Ar = 2,6-diisopropyl-phenyl).

The formation of complexes *fac*-**5.23** and *fac*-**5.24** was established by spectroscopic methods. The ^{1}H-NMR spectra of the compounds confirm the formation of non-symmetric structures. The two characteristic doublets assigned to the disatereotopic *o*-isopropyl methyls are split into four distinct doublets. Furthermore, two methinic septets of the *o*-isopropyl groups are observed in their ^{1}H-NMR spectra. The ^{1}H-NMR spectra of the compounds also have resonances for an extra Pt-Me bond. The latter shifts are summarized in Table 5.9.
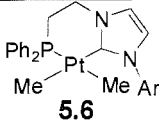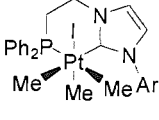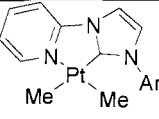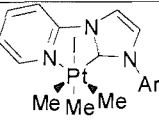
Complex	$\delta(^1H)$-PdCH_3	$^2J_{PtH}$ of satellites
Ph$_2$P, Pt, Me, Me, Ar **5.6**	-0.18 (d, $^3J_{PH}$ = 7.7 Hz) 0.03 (d, $^3J_{PH}$ = 6.9 Hz)	29.0 Hz 28.8 Hz
Ph$_2$P, Pt, Me, Me, Me, Ar *fac*-**5.23**	0.23 (d, $^3J_{PH}$ = 8.2 Hz) other resonances coincide with the CH(CH_3)$_2$ signals	36.3 Hz
N, Pt, Me, Me, Ar **5.7a**	0.29 (singlet) 0.45 (singlet)	46.6 Hz 31.2 Hz
N, Pt, Me, Me, Me, Ar *fac*-**5.24**	0.32 0.66 1.12	38.1 Hz 38.1 Hz 26.4 Hz

Table 5.9: Comparison of Pt-CH_3 ^{1}H-NMR chemical shifts (ppm) in Pt(II) and Pt(IV) species.

As it can be easily seen from the above table, that once the oxidative addition has occured the Pt-CH_3 resonate further downfield compared to their Pt(II) parent complexes. In the case of **5.24** the same is observed with the ^{13}C{^{1}H} Pt-CH_3 shifts.

The Pt-Me proton resonances in *fac*-**5.23** and *fac*-**5.24** are isochronous with systems of the type *fac*-[(PP)PtMe$_3$X] (X = I, OTf, PP = chelating phosphine).[20]

The ^{31}P{^{1}H}-NMR shift in *fac*-**5.23** is shifted upfield in comparison to the Pt(II) complex **5.6**. This trend has been observed during the oxidative addition of MeI and MeOTf to the Pt(II) complex [(dppe)PtMe$_2$] (dppe = diphenylphosphinoethane).[21]

5.2.10 X-ray diffraction study on 5.24

The structure of *fac*-**5.24** was determined by a single crystal X-ray diffraction study run on crystals grown by slow diffusion of ether in a dichloromethane solution of *fac*-**5.24**. An ORTEP representation of the structure of **5.24** is shown at Figure 5.9.
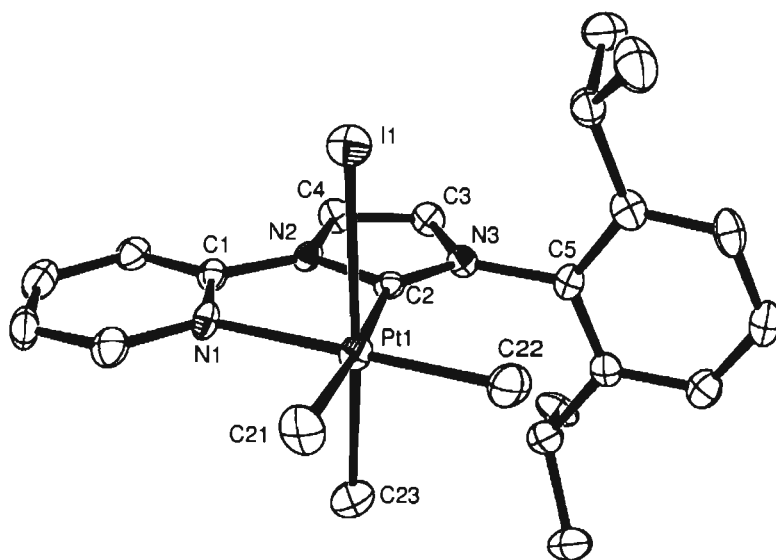
Figure 5.9: ORTEP representation of the structure of *fac*-**5.24** showing 50% probability ellipsoids. H atoms are omitted for clarity. Selected bond lengths (Å) and angles (°):C(2)-Pt(1) = 2.079(4), C(21)-Pt(1) = 2.089(4), C(22)-Pt(1) = 2.061(5), C(23)-Pt(1) = 2.079(5), I(1)-Pt(1) = 2.7902(4), N(1)-Pt(1) = 2.178(4); C(22)-Pt(1)-C(2) = 99.49(18), C(22)-Pt(1)-C(23) = 88.8(2), C(2)-Pt(1)-C(23) = 90.40(18), C(22)-Pt(1)-C(21) = 85.8(2), C(2)-Pt(1)-C(21) = 174.56(19), C(23)-Pt(1)-C(21) = 88.7(2), C(22)-Pt(1)-N(1), 176.17(16), C(2)-Pt(1)-N(1) = 77.09(15), C(23)-Pt(1)-N(1) = 89.51(18), C(21)-Pt(1)-N(1) = 97.54(17), C(22)-Pt(1)-I(1) = 93.59(15), C(2)-Pt(1)-I(1) = 91.29(12), C(23)-Pt(1)-I(1) = 176.82(15), C(21)-Pt(1)-I(1) = 89.37(15), N(1)-Pt(1)-I(1) = 88.24(10).

The geometry around the metal centre is octahedral, with the ligand occupying two *cis* positions and a bite angle of 77.09(15)°. The Pt-Me bond distances are the same within esds and they compare with the Pt-Me bond lengths found in the crystal structure of the

Pt(II) parent complex **5.7a** (Table 5.10).

Bond	*fac*-**5.24**	**5.7a**
Pt-C(carbene)	2.079(4) Å	2.005(6) Å
Pt-Me (*trans* to NHC)	2.089(4) Å	2.087(6) Å
Pt-Me (*trans* to pyridine)	2.061(5) Å	2.044(5) Å
Pt-N	2.178(4) Å	2.128(4) Å

Table 5.10: Comparison of bond distances in complexes **5.7a** and *fac*-**5.24**.

The Pt-Me bond distances remain unaffected from the two electron oxidation from the Pt(II) complex **5.7a** to the Pt(IV) complex *fac*-**5.24**. On the other hand the Pt-C(carbene) and Pt-N bond lengths are longer in complex *fac*-**5.24**. This could be due to hard acid-hard base interactions, meaning that the Pt(IV) metal centre is a too hard Lewis acid for the ligand. Another explanation could be lying in the fact that the δ^- in the dipole along the Pt-I bond is on the metal centre as platinum is more electronegative than iodine.

5.2.11 Thermolysis of *fac*-**5.24**

It has been established that Pt(IV) complexes of the type [Pt(LL)Me$_3$X] (LL = dppe, bu$_2$bpy, tmeda, imines; X = OTf, H$_2$O), when heated, reductively eliminate ethane going through a five coordinate intermediate of the type [Pt(LL)Me$_3$]$^+$.[20] In order to investigate if *fac*-5.24 follows a similar reaction pathway at elevated temperatures or prefers the reductive elimination of MeI or imidazolium salt, it was heated in d_8-toluene. Upon dissolving in d$_8$-toluene the Pt-Me proton, the *o*-isopropyl methyls and methines were shifted significantly. The solution was then heated in a thermostat at 40 °C for 40 minutes and no significant change was observed in the ^{1}H-NMR spectrum. No changes were observed even during prolonged heating at the same temperature for 48 hours. The temperature was increased in 10 °C steps up to 80 °C, but again the only observed species in solution was complex *fac*-**5.24**, for an approximate 24 hours of heating at each stage of the thermolysis. The temperature was increased to 125 °C and the ^{1}H-NMR spectrum acquired after 4 hours showed extended decomposition, which was also evidenced by the formation of black aggregates in the NMR tube. One minute peak at 0.83 ppm was

0.83 ppm was observed (C_2H_6 protons resonate at 0.86 ppm in $CDCl_3$) that could be ethane. Interestingly imidazolium proton peaks appeared in the ^{1}H-NMR spectrum in the region of 10.5 ppm as well as one peak at 2.16 ppm, almost coinciding with the solvent's residual proton signals that could be assigned to CH_3I.

5.2.12 Further reactivity of 5.6 and 5.7a

Both complexes **5.6** and **5.7a** were reacted with $SiHEt_3$ and C_6F_5H in CD_2Cl_2. In both cases no reaction was observed by means of ^{1}H-NMR, even though in the case of $SiHEt_3$ a rapid colour change occurred. The lack of reactivity in the case of $SiHEt_3$ was somewhat expected as it is known that Pt(II) dimethyl complexes with strong σ-donor ligands do not easily undergo oxidative addition of Si-H bond.[22]

5.3 Conclusions

The synthesis of novel Pt(II) complexes bearing phosphine and pyridine functionalized NHC ligands has been achieved. The new neutral dimethyl complexes **5.6** and **5.7a** were successfully synthesized by substitution of dimethyl sulfide with the generated in-situ phosphine functionalized NHC and the isolated pyridine functionalized NHC ligands respectively. To the best of our knowledge these are the first examples of Pt(II) complexes incorporating these types of ligand architectures. Both complexes show similar structural trends to their analogue Pd(II) dimethyl complexes described in Chapter 3.

The susceptibility of the unequal Pt-Me bonds towards electrophilic attack from acids was scrutinized and it revealed differences and similarities to their palladium analogues. Unlike its palladium analogue, complex **5.6** is resilient towards protonation of the Pt-Me bond from $(CF_3)_2CHOH$ or even from the more acidic C_6F_5OH. On the other hand, both complexes react with Brookhart's acid in the presence of a donor ligand L (L = py (complexes **5.15**, **5.9**, **5.10** from complexes **5.6**, **5.7a**, **5.7b** respectively), L = 2-F-py (complex **5.11** from complex **5.7a**), L = 2,6-F_2-py (complex **5.12** from complex **5.7a**), L = Et_2O (complex **5.13** from complex **5.7a**)) to afford cationic species, in which the electophilic cleavage of the Pt-Me is stereospecific and concurs with the behaviour of their Pd(II) analogues, discussed in Chapter 4. In the case of **5.6** the protonation yields two species in solution. Single crystal X-ray diffraction revealed that the Pt-Me bond cleaved

is situated *trans* to the phosphorus part of the ligand and the formation of the cationic species **5.16** was further confirmed by microanalysis results. The Pt-Me cleaved upon interaction of either complex **5.7a** or **5.7b** with Brookhart's acid is situated trans to the NHC moiety of the ligand. Structural motifs of some of these complexes resemble their Pd(II) analogues.

When L = Et$_2$O complex **5.13** was isolated which exchanges the coordinated ether molecule with water. This lability prompted us to investigate if aromatic C-H activation could be achieved. Unfortunately such a process was not observed.

The reactivity of both **5.6** and **5.7a** with other acidic reagents was also studied and it showed that the electrophilic attack is indeed stereospecific, following the selectivity of Pt-Me bond cleavage when Brookhart's acid is used, regardless of the acid used. Interaction of **5.6** and **5.7a** with one equivalent of TFA resulted in the formation of complexes **5.17** and **5.18** respectively, while interaction of **5.7a** with B(C$_6$F$_5$)$_3$ in the presence of water formed the zwitterion **5.22**.

Finally complexes **5.6** and **5.7a** readily undergo oxidative addition with MeI to form complexes *fac*-**5.23** and *fac*-**5.24** respectively.

5.4 Experimental:

General materials: [Pt(μ-Me$_2$S)Me$_2$]$_2$ [23] was prepared according to literature procedure. The preparation of Brookhart's acid is described in Chapter 4. Pentafluorobenzene, pentafluorophenol and hexafluoroisopropanol were purchased from Fluorochem and were used as received. Iodomethane, dimethylsulfide, trifluoroacetic acid, styrene, 1,1,1-trifluoroethanol, 2-fluoropyridine and 2,6-difluoropyridine, HBF$_4$ (2M solution in ether) were from Aldrich and were used as received.

5.6: In the glove box a Schlenk tube was charged with 80 mg (0.14 mmol) of [Pt(μ-Me$_2$S)Me$_2$]$_2$. A second Schlenk was charged with 146 mg (1 equiv.) of imidazolium salt **2.4a**, while a third Schleck was charged with 62 mg (1.1 equiv.) of KN(SiMe$_3$)$_2$. [Pt(μ-Me$_2$S)Me$_2$]$_2$ and KN(SiMe$_3$)$_2$ were dissolved in 10 mL THF while the imidazolium salt was suspended in 15 mL of the same solvent. The contents of the three Schlenks were then cooled at -78 °C using a dry ice-acetone slush bath. The solution of the base (KN(SiMe$_3$)$_2$) was added to the suspension of the imidazolium salt and the mixture was allowed to warm up to $-$ 50 °C. The *in situ* generated free carbene was then transferred by cannula to the solution of [Pt(μ-Me$_2$S)Me$_2$]$_2$. The slush baths were removed and the reaction mixture was left stirring at room temperature for 2 hours. Volatiles were then removed under vacuum and the resulting solid was extracted with CH$_2$Cl$_2$ (15 mL) and filtered through Celite. The Celite pad was washed with CH$_2$Cl$_2$ (3 × 10mL). Volatiles were then removed under reduced pressure and the residue was washed with Et$_2$O (10 mL) and PE (2 × 10 mL), and dried under vacuum to give the title compound as an off-white solid soluble in chlorinated solvents (CH$_2$Cl$_2$, CHCl$_3$ (decomposition), chlorobenzene) and THF. Prolonged exposure to CH$_2$Cl$_2$ leads to decomposition. Yield: 150 mg (81 %). Crystals of **5.6** were grown by layering a THF solution of **5.6** with PE. ^{1}H-NMR δ(CD$_2$Cl$_2$): -0.18 (3H, d, $^3J_{PH}$ = 7.7 Hz, PtCH_3, satellites appear as dd with $^3J_{PH}$ = 7.7 Hz and $^2J_{PtH}$ = 29.0 Hz), -0.03 (3H, d, $^3J_{PH}$ = 7.7 Hz, PtCH_3, satellites appear as dd with $^3J_{PH}$ = 7.7 Hz and $^2J_{PtH}$ = 29.0 Hz), 0.93 (6H, d, $^3J_{HH}$ = 6.9 Hz, CH(CH_3)$_2$), 1.14 (6H, d, $^3J_{HH}$ = 6.9 Hz, CH(CH_3)$_2$), 2.30 (2H, m, [PPh$_2$CH_2CH$_2$-ylidene]PtMe$_2$), 2.82 (2H, sept. $^3J_{HH}$ = 6.9 Hz, CH(CH$_3$)$_2$), 4.21 and 4.27 (1H each, m, [PPh$_2$CH$_2$CH_2-ylidene]PtMe$_2$), 6.76 (1H, m, aromatic), 7.01 (1H, m, aromatic), 7.15 (2H, distorted d, aromatic), 7.37 (7H, m, aromatic), 7.64 (4H, m, aromatic); ^{13}C{^{1}H}-NMR δ(CD$_2$Cl$_2$): no PtCH_3 resonances observed, 21.8 (s, CH(CH_3)$_2$), 24.4 (s, CH(CH_3)$_2$), 26.9 (d, $^1J_{PC}$ = 14.2 Hz, [PPh$_2$CH$_2$CH$_2$-

ylidene]PtMe$_2$), 27.5 (s, CH(CH$_3$)$_2$), 48.4 (d, $^2J_{PC}$ = 10.4 Hz, [PPh$_2$CH$_2$CH_2-

ylidene]PtMe$_2$), 118.6 (s, aromatic), 122.6 (s, aromatic), 122.9 (s, aromatic), 127.2 (d, J_{PC}

= 3.1 Hz, aromatic), 128.1 (s, aromatic), 128.8 (s, aromatic), 132.3 (d, J_{PC} = 5.0 Hz,

aromatic), 132.9 (d, J_{PC} = 11.4 Hz, aromatic), 136.1 (s, aromatic), 145.0 (s, aromatic);

^{31}P{^{1}H}-NMR δ(CD$_2$Cl$_2$): 11.7 (s, [PPh$_2$CH$_2$CH$_2$-ylidene]PtMe$_2$, $^1J_{PtP}$ = 1822.5 Hz);

^{195}Pt{^{1}H}-NMR δ(CD$_2$Cl$_2$): -4257.9 (d, $^1J_{PtP}$ = 1822.5 Hz, [PPh$_2$CH$_2$CH$_2$-ylidene]PtMe$_2$);

Anal. Found: C, 55.49; H, 5.79; N, 4.21 %. Calcd for C$_{31}$H$_{39}$N$_2$PPt: C, 55.93; H, 5.90; N,

4.21 %.

5.7b: In the glove box a Schlenk tube was charged with 80 mg (0.14 mmol) of [Pt(μ-

Me$_2$S)Me$_2$]$_2$. A second Schlenk was charged with 90 mg (2 equiv.) of 2-[3-(2,6-

diisopropylphenyl)imidazol-2-ylidine]-3-methyl-pyridine (**2.9d**). The contents of the two

Schlenks were dissolved in THF and cooled down to −78 °C. The solution of the free

carbene was transferred by means of cannula to the solution of [Pt(μ-Me$_2$S)Me$_2$]$_2$ and the

reaction mixture was stirred at room temperature for two hours. Volatiles were then

removed and the resulting yellow solid was washed with Et$_2$O (10 mL) and PE (2 ×

10mL) and was dried *in vacuo* to yield 110 mgr (72 %) of the title compound as a bright

yellow air-stable solid soluble in CH$_2$Cl$_2$, CHCl$_3$ (decomposition), chlorobenzene and

slightly soluble in toluene. Prolonged exposure to CH$_2$Cl$_2$ leads to decomposition and

product **5.8**. ^{1}H-NMR δ(CD$_2$Cl$_2$): 0.19 (3H, s, PtCH_3 *trans* to carbene, $^2J_{PtH}$= 46.1 Hz),

0.44 (3H, s, PtCH_3 *trans* to pyridine, $^2J_{PtH}$= 31.0 Hz), 1.11 (6H, d, $^3J_{HH}$= 6.9 Hz,

CH(CH_3)$_2$), 1.37 (6H, d, $^3J_{HH}$= 6.9 Hz, CH(CH_3)$_2$), 2.73 (2H, sept, $^3J_{HH}$= 6.9 Hz,

CH(CH$_3$)$_2$), 2.76 (3H, s, 3-CH_3-pyridine), 6.90 (1H, d, $^3J_{HH}$= 2.2 Hz, ylidene backbone),

7.22 (1H, distorted dd, J_{HH}= 5.7 Hz, 5.4 Hz and 7.6 Hz, pyridine), 7.35 (2H, d, $^3J_{HH}$= 7.9

Hz, aromatic), 7.50 (1H, t, $^3J_{HH}$= 7.9 Hz), 7.90 (1H, distorted dd, J_{HH}= 1.0 Hz, 0.7 Hz and

8.1 Hz, pyridine), 8.04 (1H, d, $^3J_{HH}$= 2.2 Hz, ylidene backbone), 9.18 (1H, broad dt,

pyridine); ^{13}C{^{1}H}-NMR δ(CD$_2$Cl$_2$): -31.2 (s, PtCH$_3$, $^1J_{PtC}$ = 402.6 Hz), -21.8 (s, PtCH$_3$,

$^1J_{PtC}$ = 397.5 Hz), 19.1 (s, CH(CH$_3$)$_2$), 20.3 (s, CH(CH$_3$)$_2$), 20.9 (s, CH(CH$_3$)$_2$), 23.5 (s,

CH(CH$_3$)$_2$), 27.5 (s, py-CH$_3$), 116.5 (s, ylidene backbone), 120.9 (s, ylidene backbone),

121.6 (s, aromatic), 122.7 (s, aromatic), 122.9 (s, aromatic), 129.0 (s, aromatic), 135.1 (s,

aromatic), 141.3 (s, aromatic), 144.2 (s, aromatic), 151.4 (s, aromatic), 189.7 (s, NCN,

$^1J_{PtC}$ = 442.7 Hz); ^{195}Pt{^{1}H}-NMR δ(D$_2$O): -3763.9.

5.7a: This was prepared in a way similar to above starting from 80 mg of [Pt(μ-

Me$_2$S)Me$_2$]$_2$ (0.14 mmol) and 85 mg (2 equiv.) of free carbene **2.9c** to give the title

compound as a bright yellow air-stable solid soluble in chlorinated solvents (CH_2Cl_2, $CHCl_3$ (decomposition), chlorobenzene) and slightly soluble in toluene. Yield: 115 mg (78 %). ^{1}H-NMR $\delta(CD_2Cl_2)$: 0.29 (3H, s, PdCH_3, $^2J_{PtH}$ = 46.6 Hz), 0.45 (3H, s, $^2J_{PtH}$ = 31.2 Hz), 1.09 (6H, d, $^3J_{HH}$ = 6.9 Hz, CH(CH_3)$_2$), 1.34 (6H, d, $^3J_{HH}$ = 6.9 Hz, CH(CH_3)$_2$), 2.75 (2H, sept. $^3J_{HH}$ = 6.9 Hz, CH(CH$_3$)$_2$), 6.58 (1H, d, $^3J_{HH}$ = 2.0 Hz), 7.28 (3H, m, aromatic), 7.45 (2H, t, $^3J_{HH}$ = 7.9 Hz, aromatic pyridine), 7.63 (1H, d, $^3J_{HH}$ = 2.0 Hz, ylidene backbone), 8.09 (1H, ddt, J_{HH} = 0.7 Hz, 1.5 Hz, 7.4 Hz, aromatic pyridine), 9.07 (1H, s, m, aromatic pyridine); ^{13}C{^{1}H}-NMR $\delta(CD_2Cl_2)$: -31.4 (s, PtCH_3, $^1J_{PtC}$ = 401.9 Hz), -21.8 (s, PtCH_3, $^1J_{PtC}$ = 397.8 Hz), 22.2 (s, CH(CH$_3$)$_2$), 23.4 (s, CH(CH_3)$_2$), 27.6 (s, CH(CH$_3$)$_2$), 109.4 (s, ylidene backbone), 113.5 (s, ylidene backbone), 121.8 (s, aromatic), 122.9 (s, aromatic), 124.1 (s, aromatic), 129.1 (s, aromatic), 134.9 (s, aromatic), 137.7 (s, aromatic), 144.9 (s, aromatic), 146.2 (s, aromatic), 152.6 (s, aromatic), 189.5 (s, NCN, $^1J_{PtC}$ = 441.9 Hz); ^{195}Pt{^{1}H}-NMR $\delta(D_2O)$: -3764.1. Anal. Found: C, 50.45; H, 5.38; N, 7.93 %. Calcd for $C_{22}H_{29}N_3Pt$: C, 49.80; H, 5.51; N, 7.92 %. Crystals were grown by slow diffusion of Et_2O into a CH_2Cl_2 solution of **5.7a**.

5.10: In the glove box a Schlenk tube was charged with 50 mg (0.09 mmol) of **5.7b**. A second Schlenk was charged with 85 mg (1 equiv.) of H(OEt$_2$){B[(3,5-CF$_3$)$_2$C$_6$H$_2$]$_4$}. The two Schlenk tubes were connected on the Schlenk line and their contents were dissolved in 10 mL CH_2Cl_2. The two solutions were cooled at -78 °C using a dry ice-acetone slush bath, upon which time the Brookhart's acid solution was transferred to the solution of the complex by means of cannula. Upon addition the colour of the solution of the complex changed from bright yellow to almost colourless. The mixture was allowed to warm up to –40 °C and 8 μL (1.1 equiv.) of dry-degassed pyridine were added using a microsyringe. The reaction mixture was allowed to reach room temperature and was stirred for an additional 30 minutes. Volatiles were removed under reduced pressure and the residue was washed with PE (3x10 mL). The solid was then dried under vacuum to give the title compound as an off-white fluffy solid. Yield: 118 mg (89 %). ^{1}H-NMR $\delta(CD_2Cl_2)$: 0.14 (3H, s, PtCH_3, $^2J_{PtH}$ = 40.2 Hz), 1.15 (6H, d, $^3J_{HH}$ = 6.4 Hz, CH(CH_3)$_2$), 1.33 (6H, d, $^3J_{HH}$ = 6.4 Hz, CH(CH_3)$_2$), 2.65 (2H, $^3J_{HH}$ = 6.4 Hz, CH(CH$_3$)$_2$), 2.81 (3H, s, 3-CH_3-pyridine), 7.05 (1H, m, ylidene backbone), 7.21 (1H, m, aromatic), 7.33 (2H, distorted d, aromatic), 7.53 (6H, broad s, aromatic), 7.74 (10H, broad s, aromatic), 7.92 (2H, m, aromatic), 8.10 (1H, d, J_{HH} = 2.7 Hz, aromatic), 8.52 (2H, m, aromatic); ^{13}C{^{1}H}-NMR $\delta(CD_2Cl_2)$: -16.5 (s, PtCH_3, $^1J_{PtC}$ = 519.9 Hz), 19.8 (s, CH(CH_3)$_2$), 22.2 (s, CH(CH_3)$_2$), 23.6 (s, CH(CH_3)$_2$), 27.8 (s, py-CH_3), 116.7 (s, ylidene backbone), 118.1 (ylidene backbone), 119.8 (s,

aromatic), 122.5 (s, aromatic), 123.2 (s, aromatic), 123.6 (s, aromatic), 125.0 (s, aromatic), 125.2 (s, aromatic), 126.3 (s, aromatic), 128.1 (q, $^2J_{FC}$ = 28.8 Hz, aromatic), 130.2 (s, aromatic), 134.0 (s, aromatic), 138.4 (s, aromatic), 143.3 (s, aromatic), 144.1 (s, aromatic), 144.3 (s, aromatic), 150.4 (s, aromatic), 160.9 (q, $^1J_{FC}$ = 43.9 Hz, CF_3); ^{19}F{^{1}H} $\delta(CD_2Cl_2)$: -63.1 (s, CF_3); ^{195}Pt{^{1}H}-NMR $\delta(CD_2Cl_2)$: -3496.4. Colourless crystals appropriate for single crystal X-ray diffraction were grown by slow diffusion of PE into an Et_2O solution of **5.10**.

5.11: This was prepared as above starting from 50 mg (0.09 mmol) of complex **5.7a**, 88 mg (1 equiv.) of H(OEt$_2$){B[(3,5-CF$_3$)$_2$C$_6$H$_2$]$_4$} and 6 μL (1.1 equiv.) of 2-fluoropyridine. Yield: 105 mg (77 %). ^{1}H-NMR $\delta(CD_2Cl_2)$: 0.11 (3H, s, PtCH_3, $^2J_{PtH}$ = 39.5 Hz), 1.17 (6H, d, $^3J_{HH}$ = 7.3 Hz, CH(CH_3)$_2$), 1.25 (6H, d, $^3J_{HH}$ = 7.3 Hz, CH(CH_3)$_2$), 2.67 (2H, sept., $^3J_{HH}$ = 7.3 Hz, CH(CH$_3$)$_2$), 7.03 (1H, d, $^3J_{HH}$ = 2.2 Hz, ylidene backbone), 7.30 (3H, q, $^3J_{HH}$ = 7.3 Hz, aromatic), 7.42 (1H, t, $^3J_{HH}$ = 6.6 Hz, aromatic), 7.55 (5H, broad s, aromatic), 7.68 (1H, d, J_{HH} = 8.0 Hz, aromatic), 7.84 (11H, broad s, aromatic), 7.89 (1H, d, $^3J_{HH}$ = 2.2 Hz, ylidene backbone), 8.16 (1H, dt, J_{HH} = 1.5 Hz, 8.0 Hz, aromatic), 8.32 (2H, m, aromatic); ^{13}C{^{1}H}-NMR $\delta(CD_2Cl_2)$: -3.2 (s, PtCH_3, $^1J_{PtC}$ = 542.8 Hz), 18.4 (s, CH(CH_3)$_2$), 23.6 (s, CH(CH_3)$_2$), 27.9 (s, CH(CH$_3$)$_2$, 116.7 (s, ylidene backbone), 117.3 (s, ylidene backbone), 119.7 (s, aromatic), 122.5 (s, ylidene backbone), 122.9 (s, aromatic), 123.7 (s, aromatic), 125.2 (s, aromatic), 125.9 (s, aromatic), 128.0 (q, $^2J_{FC}$ = 28.5 Hz, aromatic), 130.4 (s, aromatic), 132.1 (s, aromatic), 134.0 (s, aromatic), 136.2 (d, $^2J_{FC}$ = 18.3 Hz, 2-F-pyridine), 140.3 (d, $^1J_{FC}$ = 33.1 Hz, 2-F-pyridine carbon), 141.1 (s, aromatic), 145.6 (s, aromatic), 148.3 (s, aromatic), 160.7 (q, $^1J_{FC}$ = 43.6 Hz, CF_3); ^{19}F{^{1}H} $\delta(CD_2Cl_2)$: -63.1 (s, CF_3), -61.1 (s, 2-F-pyridine). Colourless crystals were grown by layering an ether solution of **5.11** with pentane.

5.12: This was prepared as above from 50 mg (0.09 mmol) of complex **5.7a**, 88 mg (1 equiv.) of H(OEt$_2$){B[(3,5-CF$_3$)$_2$C$_6$H$_2$]$_4$} and 6 μL (1.3 equiv.) of 2,6-difluoropyridine. Yield: 105 mg (76 %). ^{1}H-NMR $\delta(CD_2Cl_2)$: 0.13 (3H, s, PtCH_3, $^2J_{PtH}$ = 38.4 Hz), 1.11 (6H, d, $^3J_{HH}$ = 6.9 Hz, CH(CH_3)$_2$), 1.30 (6H, d, $^3J_{HH}$ = 6.9 Hz, CH(CH_3)$_2$), 2.65 (2H, sept., $^3J_{HH}$ = 6.9 Hz, CH(CH$_3$)$_2$), 7.08 (1H, d, $^3J_{HH}$ = 2.2 Hz, ylidene backbone), 7.21 (1H, d $^3J_{HH}$ = 8.2 Hz, aromatic), 7.33 (3H, m, aromatic), 7.53 (4H, broad s, aromatic), 7.63 (1H, d, $^3J_{HH}$ = 8.5 Hz, aromatic), 7.70 (8H, broad s, aromatic), 7.77 (3H, m, aromatic), 8.19 (2H, m, aromatic); ^{13}C{^{1}H}-NMR $\delta(CD_2Cl_2)$: -2.6 (s, PtCH_3, $^1J_{PtC}$ = 518.1 Hz), 19.8 (s, CH(CH3)$_2$), 22.6 (s, CH(CH_3)$_2$), 24.1 (s, CH(CH3)$_2$), 116.9 (s, ylidene backbone), 117.9 (ylidene backbone), 119.8 (s, aromatic), 122.5 (s, aromatic), 123.2 (s, aromatic), 123.6 (s,

aromatic), 125.0 (s, aromatic), 125.2 (s, aromatic), 126.3 (s, aromatic), 128.1 (q, $^2J_{FC}$ = 28.8 Hz, aromatic), 130.2 (s, aromatic), 134.0 (s, aromatic), 138.4 (d, $^2J_{FC}$ = 19.0 Hz, 2,6-F_2-pyridine), 143.3 (s, aromatic), 144.1 (d, $^1J_{FC}$ = 32.9 Hz, 2,6-F_2-pyridine carbon), 144.3 (s, aromatic), 150.4 (s, aromatic), 160.9 (q, $^1J_{FC}$ = 43.9 Hz, CF_3 's); $^{19}F\{^1H\}$ $\delta(CD_2Cl_2)$: -63.1 (s, CF_3 's), -60.3 (s, 2,6-F_2-pyridine, J_{PtF} = 110.1 Hz). Colourless crystals were grown by layering an ether solution of **5.12** with PE.

5.13: This was prepared as above starting from 50 mg (0.09 mmol) of complex **5.7a**, 88 mg (1 equiv.) of $H(OEt_2)\{B[(3,5-CF_3)_2C_6H_2]_4\}$ and 7 μL of styrene or 5 μL of 2-trifluoroethanol (1 equiv. in both cases. The volatiles were removed and the solid residue was dissolved in Et_2O and was layered with PE to give colourless crystals of **5.13**. Yield: 25 mg (18 %). ^1H-NMR $\delta(d_5$-PhCl): 0.22 (s, PtCH_3, $^2J_{PtH}$ = 35.1 Hz), 1.13 (6H, d, $^3J_{HH}$ = 6.9 Hz, CH(CH_3)$_2$), 1.21 (12H, m, coordinated and uncoordinated (CH_3CH$_2$)$_2$O), 1.32 (6H, d, $^3J_{HH}$ = 6.9 Hz, CH(CH_3)$_2$), 2.59 (2H, d, $^3J_{HH}$ = 6.9 Hz, CH(CH$_3$)$_2$), 3.40 (4H, q, $^3J_{HH}$ = 6.9 Hz, uncoordinated (CH$_3$CH_2)$_2$O), 3.53 (4H, broad q, $^3J_{HH}$ = 7.1 Hz, coordinated (CH$_3$CH_2)$_2$O), 6.70 Hz (1H, d, $^3J_{HH}$ = 2.2 Hz, ylidene backbone), 6.78 (1H, d, $^3J_{HH}$ = 8.5 Hz, aromatic), 7.09 (6H, m, aromatic), 7.23 (7H, m, aromatic), 7.48 (4H, m, aromatic), 8.23 (1H, m, aromatic), 8.46 (1H, m, aromatic); $^{19}F\{^1H\}$ $\delta(d_5$-PhCl): -63.6 (s, CF_3 s); $^{195}Pt\{^1H\}$ $\delta(d_5$-PhCl): -3703.

Reaction of 5.6 with Brookhart's acid and synthesis of 5.16: This was prepared as above from 80 mg (0.12 mmol) of complex **5.6** and 113 mg (1 equiv.) of Brookhart's acid. ^1H-NMR $\delta(CD_2Cl_2)$: -0.22 (3H, d, Pt-CH_3, $^3J_{PH}$ = 3.2 Hz, $^2J_{PtH}$ = 49.9 Hz), 0.80 (6H, $^3J_{HH}$ = 6.4 Hz CH(C$H3$)$_2$, species B), 0.93 (6H, $^3J_{HH}$ = 7.0 Hz CH(CH_3)$_2$, species A), 1.00 (3H, $^3J_{HH}$ = 7.0 Hz, CH(CH_3)$_2$), 1.32 (3H, $^3J_{HH}$ = 6.4 Hz, CH(CH_3)$_2$), 2.5 (5H, m, CH(CH$_3$)$_2$ and ([PPh$_2$CH_2CH$_2$-ylidene]PtMe)$^+$ of two species), 2.84 (1H, sept., $^3J_{HH}$ = 7.0 Hz, CH(CH$_3$)$_2$), 4.38 (2H, m, ([PPh$_2$CH$_2$CH_2-ylidene]PtMe)$^+$), 4.65 (1H, m, ([PPh$_2$CH$_2$CH_2-ylidene]PtMe)$^+$), 6.89-7.88 (48H, m, aromatics); $^{31}P\{^1H\}$ $\delta(CD_2Cl_2)$: 8.7 (s, $^1J_{PtP}$ = 1977.1 Hz), 10.1 (s, $^1J_{PtP}$ = 746.0 Hz); $^{19}F\{^1H\}$ $\delta(CD_2Cl_2)$: -63.1 (s, CF_3). The reaction was repeated using Et_2O as solvent starting from 50 mg (0.075 mmol) of **5.6** and 70 mg (1 equiv.) of Brookhart's acid. Yield after crystallisation: 35 mg (29 %). Anal.Found: C, 50.81; H, 3.42; N, 2.59 %. Calcd for $C_{67}H_{53}BF_{24}N_3PPt$: C, 50.52; H, 3.35; N, 2.64 %. Colourless needles were obtained by layering an Et_2O solution of **5.16** with PE.

5.17: An NMR tube was charged with 15 mg (0.03 mmol) of complex **5.7a** in the glovebox and its contents were dissolved in CD_2Cl_2. The NMR tube was capped with a sure-seal lid and was connected to the nitrogen supply of a Schlenk line. To this bright

yellow solution 3 μL (1.1 equiv.) of CF_3COOH were added by means of a microsyringe at room temperature. Upon addition the colour of the solution turned from bright yellow to almost colourless. ^{1}H-NMR δ(CD_2Cl_2): 0.17 (3H, s, PtCH_3, $^2J_{PtH}$ = 38.6 Hz), 1.12 (6H, d, $^3J_{HH}$ = 6.8 Hz, CH(CH_3)$_2$), 1.29 (6H, d, $^3J_{HH}$ = 6.8 Hz, CH(CH_3)$_2$), 2.50 (2H, sept., $^3J_{HH}$ = 6.8 Hz, CH(CH$_3$)$_2$), 6.94 (1H, d, $^3J_{HH}$ = 2.3 Hz, ylidene backbone), 7.29 (2H, d, $^3J_{HH}$ = 7.8 Hz, aromatic), 7.51 (3H, m, aromatic), 7.66 (1H, d, $^3J_{HH}$ = 2.3 Hz, ylidene backbone), 8.14 (1H, ddd, J_{HH} = 1.6Hz, 7.5Hz, 9.8 Hz, aromatic), 8.59 (1H, ddd, J_{HH} = 0.9 Hz, 1.6 Hz, 4.6 Hz, aromatic); ^{13}C{^{1}H}-NMR δ(CD_2Cl_2): -19.7 (s, PtCH_3, $^1J_{PtC}$ = 266.3 Hz), 23.5 (s, CH(CH_3)$_2$)., 25.0 (s, CH(CH_3)$_2$), 29.1 (s, CH(CH$_3$)$_2$), 110.8 (s, ylidene backbone), 115.6 (s, ylidene backbone), 124.2 (s, aromatic), 124.7 (s, aromatic), 126.3 (s, aromatic), 131.2 (s, aromatic), 135.3 (s, aromatic), 141.0 (s, aromatic), 145.9 (s, aromatic), 147.6 (s, aromatic), 150.8 (s, aromatic); ^{19}F{^{1}H} δ(CD_2Cl_2): -75.4 (s, CF_3COO$^-$).

5.18: This was done as above starting from 20 mg (0.030 mmol) of compound **5.6** and 3 μL of TFA. ^{1}H-NMR δ(CD_2Cl_2): 0.08 (3H, d, $^3J_{PH}$ = 2.9 Hz, $^2J_{PtH}$ = 35.5 Hz, Pt-CH_3), 0.99 (6H, d, $^3J_{HH}$ = 6.9 Hz, CH(CH_3)$_2$), 1.12 (6H, d, $^3J_{HH}$ = 6.9 Hz, CH(CH_3)$_2$), 2.39 (4H, m, CH(CH$_3$)$_2$ and [PPh$_2$CH_2CH$_2$-ylidene]PtMeO$_2$CCF$_3$), 4.4 (2H, m, [PPh$_2$CH$_2$CH_2-ylidene]PtMeO$_2$CCF$_3$), 6.88 (1H, d, $^3J_{HH}$ = 1.9 Hz, ylidene backbone), 7.19 (2H, distorted t, aromatic), 7.22 (6H, broad s, aromatic), 7.33 (1H, d, $^3J_{HH}$ = 1.8 Hz, ylidene backbone), 7.77 (5H, m, aromatic); ^{31}P{^{1}H} δ(CD_2Cl_2): 19.6 (s, [PPh$_2$CH$_2$CH$_2$-ylidene]PtMeO$_2$CCF$_3$, $^1J_{PtH}$ = 2017.8 Hz); ^{19}F{^{1}H} δ(CD_2Cl_2): -74.4 (s, [PPh$_2$CH$_2$CH$_2$-ylidene]PtMeO$_2$CCF_3).

5.19: An NMR tube was charged with 15 mg (0.03 mmol) of complex **5.7a** in the glovebox and its contents were dissolved in CD_2Cl_2. The NMR tube was capped with a sure-seal lid and was connected to the nitrogen supply of a Schlenk line. To this bright yellow solution 8 μL (3 equiv.) of CF_3COOH were added by means of a microsyringe at room temperature. Upon addition the colour of the solution turned from bright to pale yellow. ^{1}H-NMR δ(CD_2Cl_2): 1.08 (6H, d, $^3J_{HH}$ = 6.6 Hz, CH(CH_3)$_2$), 1.31 (6H, d, $^3J_{HH}$ = 6.6 Hz, CH(CH_3)$_2$), 2.67 (2H, broad sept., $^3J_{HH}$ = 6.6 Hz, CH(CH$_3$)$_2$), 7.11 (1H, s, ylidene backbone), 7.26 (2H, d, $^3J_{HH}$ = 8.2 Hz, aromatic), 7.5 (2H, m, aromatic), 7.65 (1H, broad d, $^3J_{HH}$ = 8.2 Hz, aromatic), 7.69 (1H, s, ylidene backbone), 8.29 (1H, t, $^3J_{HH}$ = 7.4 Hz, aromatic), 8.51 (1H, broad s, aromatic), 10.42 (s, free CF$_3$COOH); ^{19}F{^{1}H} δ(CD_2Cl_2): -76.4, -73.9 (s, CF_3COO$^-$).

5.22: Two flame dried Schlenk tubes were charged in the glove-box with 60 mg (0.12 mmol) of **5.7a** and 61 mg (1 equiv.) of B(C$_6$F$_5$)$_3$ respectively. To the contents of the two Schlenks ether was added (15 mL). To the solution of B(C$_6$F$_5$)$_3$ two drops of H$_2$O were

added *via* a Pasteur pipette at room temperature and the solution was immediately cooled down to -78 °C using a dry ice-acetone slush bath. The suspension of the complex in ether was also cooled down at the same temperature and the solution of $H\{OHB(C_6F_5)_3\}$ generated *in situ*, as described above, was transferred to the suspension of the complex *via* cannula. Upon addition the slush baths were removed and the mixture was allowed to equilibrate up to room temperature and was left stirring overnight. Volatiles were removed and the resulting off-white solid was dried under vacuum, washed with PE and dried under reduced pressure. Yield: 50 mg (40 %). ^{1}H-NMR $\delta(CD_2Cl_2)$: -0.01 (3H, s, PtCH_3 $^2J_{PtH}$ = 37.7 Hz), 1.06 (6H, d, $^3J_{HH}$ = 6.8 Hz, CH(CH_3)$_2$), 1.15 (6H, d, $^3J_{HH}$ = 6.8 Hz, CH(CH_3)$_2$), 2.49 (2H, sept., $^3J_{HH}$ = 6.8 Hz, CH(CH$_3$)$_2$), 2.93 (1H, broad s, OH(B(C$_6$F$_5$)$_3$), 6.89 (1H, $^3J_{HH}$ = 2.4 Hz, ylidene backbone), 7.21 (2H, $^3J_{HH}$ = 7.9 Hz, aromatic), 7.45 (3H, m, aromatic), 7.53 (1H, d, $^3J_{HH}$ = 2.4 Hz, ylidene backbone), 8.12 (1H, dt, J_{HH} = 1.7 Hz, 8.1 Hz, aromatic), 8.56 (1H, broad d., $^3J_{HH}$ = 5.5 Hz, aromatic); ^{19}F$\{^1$H$\}$ $\delta(CD_2Cl_2)$: -165.9 (d, $^2J_{FF}$ = 19.3 Hz, o-F of B(C$_6$$F_5$)$_3$), -161.0 (t, $^2J_{FF}$ = 19.3 Hz, m-F of B(C$_6$$F_5$)$_3$), -134.5 (m, p-F of B(C$_6$$F_5$)$_3$); IR(Nujol, cm^{-1}): 3599 (s, ν_{OH}). Colourless crystals of compound **5.22** were grown by slow diffusion of PE into an Et$_2$O solution of **5.22**.

fac-**5.23**: 20 mg (0.030 mmol) of **5.6** were charged in a NMR tube in the glove box and were dissolved in CD$_2$Cl$_2$. To this solution 4 μL of MeI were added at room temperature under a N$_2$ atmosphere, and the NMR spectra were recorded. ^{1}H-NMR $\delta(CD_2Cl_2)$: 0.23 (3H, d, $^3J_{PH}$ = 8.2 Hz, Pt-CH_3, $^2J_{PtH}$ = 36.3 Hz), 0.74, 0.83, 0.98, 1.10, 1.25, 1.39 (18H, overlapping d, remaining Pt-CH_3 and CH(CH_3)$_2$), 2.38 (1H, sept. $^3J_{HH}$ = 6.8 Hz, CH(CH$_3$)$_2$), 2.53 (1H, m, [PPh$_2$CH_2CH$_2$-ylidene]PtMe$_3$I), 2.78 (1H, sept. $^3J_{HH}$ = 6.9 Hz, CH(CH$_3$)$_2$), 2.95 (1H, m, [PPh$_2$CH_2CH$_2$-ylidene]PtMe$_3$I), 4.31 (1H, m, [PPh$_2$CH$_2$CH_2-ylidene]PtMe$_3$I), 5.64 (1H, m, [PPh$_2$CH$_2$CH_2-ylidene]PtMe$_3$I), 6.79 (1H, broad s, ylidene backbone), 7.15 (4H, m, aromatic), 7.33 (3H, broad s, aromatic), 7.42 (5H, broad s, aromatic), 8.11 (2H, m, aromatic); ^{31}P$\{^1$H$\}$ $\delta(CD_2Cl_2)$: 10.8 (s, [PPh$_2$CH$_2$CH$_2$-ylidene]PtMe$_3$I, $^1J_{PtP}$ = 799.6 Hz).

fac-**5.24**: 55 mg (0.10 mmol) of **5.7a** (0.10 mmol) were charged in a Schlenk tube. The complex was dissolved in 15 mL of DCM and 9 μL (1.1 equiv.) of MeI were added *via* a micro-syringe through a septum under a N$_2$ atmosphere. The reaction mixture was stirred at room temperature for 30 min. upon which time the colour of the reaction mixture changed from bright to pale yellow. Volatiles were removed under reduced pressure and the resulting pale yellow solid was washed with PE (2 × 10 mL) to yield 62 mg of the title compound (89 %). ^{1}H-NMR $\delta(CD_2Cl_2)$: 0.32-1.12 (6H, three singlets with their Pt

satellites, $^2J_{PtH}$= 38.1 Hz, 38.1 Hz and 26.4 Hz Pt(CN)Me_3I), 1.22 (6H, app. t, CH(CH_3)$_2$), 1.25 (3H, d, $^3J_{HH}$= 7.3 Hz, CH(CH_3)$_2$), 1.30 (3H, d, $^3J_{HH}$= 7.3 Hz, CH(CH_3)$_2$), 2.55 (sept., 1H, $^3J_{HH}$= 7.3 Hz, CH(CH$_3$)$_2$), 3.41 (sept., 1H, $^3J_{HH}$= 7.3 Hz, CH(CH$_3$)$_2$), 6.93 (s, 1H, ylidene backbone), 7.22 (1H, d, $^3J_{HH}$= 7.3 Hz, aromatic), 7.28 (1H, d, $^3J_{HH}$= 7.3 Hz, aromatic), 7.38 (1H, t, $^3J_{HH}$= 7.3 Hz, aromatic), 7.41(1H, t, $^3J_{HH}$= 8.8 Hz, py-H_4), 7.59 (1H, d, $^3J_{HH}$= 8.8 Hz, py-H_3), 7.77 (1H, s, ylidene backbone), 8.05 (1H, t, $^3J_{HH}$= 8.8 Hz, py-H_5), 8.61 (1H, d, $^3J_{H-H}$= 8.8 Hz, py-H_6); ^{13}C{^{1}H}-NMR δ(CD$_2$Cl$_2$): -32.8 (s, with one Pt satellite, ^{1}J$_{PtC}$= 328.5 Hz, Pt(CN)Me_3I), -20.5 (s, $^1J_{PtC}$= 146.8 Hz, Pt(CN)Me_3I), -10.6 (s, $^1J_{PtC}$= 330.4 Hz, Pt(CN)Me_3I), 20.7, 21.8, 24.1, 24.3, 26.5, 26.6 > (s, CH(CH$_3$)$_2$), 110.2 (s, aromatic), 114.2 (s, aromatic), 121.4 (s, aromatic), 121.8 (s, aromatic), 122.6 (s, aromatic), 124.8 (s, aromatic), 128.8 (s, aromatic), 132.3 (s, aromatic), 138.9 (s, aromatic), 143.9 (s, aromatic), 145.1 (s, aromatic), 145.2 (s, aromatic), 149.8 (s, aromatic), 183.4 (s, NCN, $^1J_{PtC}$= 421.8 Hz). Yellow crystals of fac-5.24 were obtained by layering a CH$_2$Cl$_2$ solution of fac-5.24 with PE.

Crystalographic data for 5.6, 5.7a, 5.8 and 5.9

Complex	5.6	5.7a	5.8	5.9
Chemical Formula	$C_{31}H_{39}N_2PPt$	$C_{22}H_{29}N_3Pt$	$C_{22}H_{28}ClN_3Pt$	$C_{59}H_{45}BF_{24}N_4Pt$
Formula weight	665.70	530.57	565.01	1471.89
Crystal system	Monoclinic	Monoclinic	Monoclinic	Triclinic
Space group	$P2_1/n$	$P\,2_1/n$	$P\,2_1/n$	$P\,-1$
a / $\mathring{A}$	12.5675(19)	8.7905(7)	9.0112(8)	13.4405(7)
b / $\mathring{A}$	15.1164(10)	18.482(2)	17.2104(16)	15.1552(6)
c / $\mathring{A}$	15.212(3)	12.4068(10)	13.1379(12)	15.4886(10)
α / °	90	90	90	76.778(5)
β / °	110.368(14)	98.768(7)	93.787(2)	84.170(5)
γ / °	90	90	90	72.930(4)
Z	4	4	4	2
T/K	120(2)	120(2)	120(2)	120(2)
μ / mm^{-1}	5.260	7.054	7.045	2.510
No. of data collected	32044	39241	24137	41301
No. of unique data	6307	4620	4669	13520
Goodness of fit on F^2	1.004	1.039	1.046	1.023
$R_{int.}$	0.0721	0.0951	0.1018	0.0820
Final $R(|F|)$ for $F_0 > 2\sigma(F_0)$	0.0317	0.0362	0.0419	0.0368
Final $R(F^2)$ for all data	0.0539	0.0618	0.0570	0.0438

Crystallographic data for 5.11, 5.13, 5.22 and *fac*-5.24

Complex	5.11	5.13	5.22	*fac*-5.24
Chemical Formula	$C_{63}H_{54}BF_{25}N_4Pt$	$C_{57}H_{48}BF_{24}N_3OPt$	$C_{43}H_{37}BF_{15}N_3O_2Pt$	$C_{23}H_{32}IN_3Pt$
Formula weight	1548.00	1452.88	1118.66	672.51
Crystal system	Triclinic	Triclinic	Triclinic	Monoclinic
Space group	*P-1*	*P-1*	*P-1*	*P 2_1/n*
a / $\overset{\circ}{A}$	14.1039(11)	14.2846(16)	10.734(6)	8.5894(6)
b / $\overset{\circ}{A}$	15.1745(8)	14.3239(14)	11.247(8)	29.989(4)
c / $\overset{\circ}{A}$	15.2310(11)	15.6445(12)	19.611(16)	9.6329(14)
α / °	92.894(6)	97.346(7)	81.61(7)	90
β / °	96.530(6)	96.952(9)	79.13(5)	103.388(9)
γ / °	99.627(4)	97.259(9)	71.43(4)	90
Z	2	2	2	4
T/K	120(2)	120(2)	120(2)	120(2)
μ / mm^{-1}	2.319	2.361	3.301	7.104
No. of data collected	58202	61790	29558	23820
No. of unique data	14459	14423	7699	5495
Goodness of fit on F^2	1.028	1.053	1.050	1.040
$R_{int.}$	0.1104	0.0554	0.1070	0.0617
Final $R(|F|)$ for $F_0 > 2\sigma(F_0)$	0.0608	0.0531	0.0842	0.0320
Final $R(F^2)$ for all data	0.1338	0.0725	0.1144	0.0502

References:

1. Littke, A. F.; Fu, G. C. *Angew. Chem. Int. Ed. Engl.* **2002**, *41*, 4176.

2. Clique, B.; Fabritius, C.-H.; Coutirier, C. N.; Balme, G. *Chem. Commun.* **2003**, 272.

3. Green, M.; Spencer, J. L.; Stone, F. G. A. *J. Chem. Soc. Dalton Trans.* **1977**, 1519.

4. Ishiyama, T.; Matsuda, N.; Miyaura, N.; Suzuki, A. *J. Am. Chem. Soc.* **1993**, *115*, 11018.

5. Frisone, M. D. T.; Pinna, F.; Strukul, G. *Organometallics* **1993**, *12*, 148.

6. Haelg, P.; Consiglio, G.; Pino, P. *J. Organomet. Chem.* **1985**, *296*, 281.

7. Yoshida, T.; Matsudi, M.; Okano, T.; Kitani, T.; Otsuka, S. *J. Am. Chem. Soc.* **1979**, *101*, 2027.

8. Ikura, K.; Ryu, I.; Kambe, N.; Sonoda, N. *J. Am. Chem. Soc.* **1992**, *114*, 1520.

9. Wicht, D. K.; Kourine, I. V.; Lew, B. M.; Ntenge, J. M.; Glueck, D. S. *J. Am. Chem. Soc.* **1997**, *119*, 5039.

10. Kurosawa, H. *J. Chem. Soc., Dalton Trans.* **1979**, 939.

11. Clarke, M.L. *Polyhedron* **2001**, *20*, 151.

12. Arduengo III, A. J.; Gamber, S. F.; Calabrese, J. C.; Davidson, F. *J. Am. Chem. Soc.* **1994**, *116*, 4391.

13. Duin, M. A.; Clement, N. C.; Cavell, K. J.; Elsevier, C. J. *Chem. Commun.* **2003**, 400.

14. Sprengers, J. W.; Mars, M. J.; Duin, M. A.; Cavell, K. J.; Elsevier, C. J.; *J. Organomet. Chem.* **2003**, *679*, (2), 149.

15. Haar, C. M.; Nolan, S. P.; Marshall, W. J.; Moloy, K. G.; Prock, A.; Giering, W. P. *Organometallics* **1999**, *18*, 474.

16. Tsoureas, N.; Danopoulos, A. A.; Tulloch, A. A. D.; Light, M. E. *Organometallics* **2003**, *22*, 4750.

17. Konze, W. V.; Scott, B. L.; Kubas, G. J. *J. Am. Chem. Soc.* **2002**, *124*, 2786.

18. Peters, R. G.; White, S.; Roddick, D. M. *Organometallics* **1998**, *17*, 4493.

19. Hill, G. S.; Muir, L. M.; Muir, K. W.; Puddephatt, R. J. *Organometallics* **1997**, *16*, 525.

20. Hill, G. S.; Yap, G. P. A.; Puddephatt, R. J. *Organometallics* **1999**, *18*, 1408.

21. Bregel, C.; Dawn, M.; Goldberg, K. I. *J. Am. Chem. Soc.* **2003**, *125*, 9442.

22. Thomson, S. M.; Stoehr, F.; Sturmayr, D.; Kickelbbick, G.; Schubert, U. *J. Organomet. Chem.* **2003**, *686*, (1-2), 183.

23. Hill, G. S.; Irwin, M. J.; Louis, M.; Puddephatt, R. J. *Inorganic Synthesis* **1998**, *32*, 149.

Chapter 6: Phosphine functionalised NHC complexes of Rh(I) and Ir(I)

6.1 Introduction

The coordination chemistry of NHCs with group 9 transition metals (mainly Rh and Ir) has attracted much interest due to the involvement of these metals in a number of very important homogeneous catalytic transformations such as hydrogenation,[1] hydroformylation,[2] hydroboration[3] and hydrosilylation[4] of olefins. It is hoped that NHCs will complement the phosphines that are still the useful ligands for performing catalysis with rhodium and iridium.[5] For this reason Nolan and co-workers have prepared iridium NHC complexes[6] analogous to Crabtree's catalyst[7] and rhodium complexes analogous to Wilkinson's catalyst, where a PPh_3 ligand has been replaced by a NHC.[8] Examples of chiral NHC complexes of rhodium have also been reported.[9] Oxazoline,[10, 11] pyridine,[12] phosphine[13, 14] and thioether[13] functionalised NHC complexes of rhodium and iridium have been reported and some examples are given in Figure 6.1.

Ar = 2,4,6-trimethyl-phenyl: **6.1**

Ar = 2,6-diisopropyl-phenyl: **6.2**
Ar = 2,4,6-trimethyl-phenyl: **6.3**
Ar = phenyl: **6.4**

Ar = 2,6-diisopropyl-phenyl: **6.5**

Ar = 2,6-diisopropyl-phenyl: **6.6**

6.7

R = Me, R' = Pr^i: **6.8**
R = Bu^t, R' = Bz: **6.9**
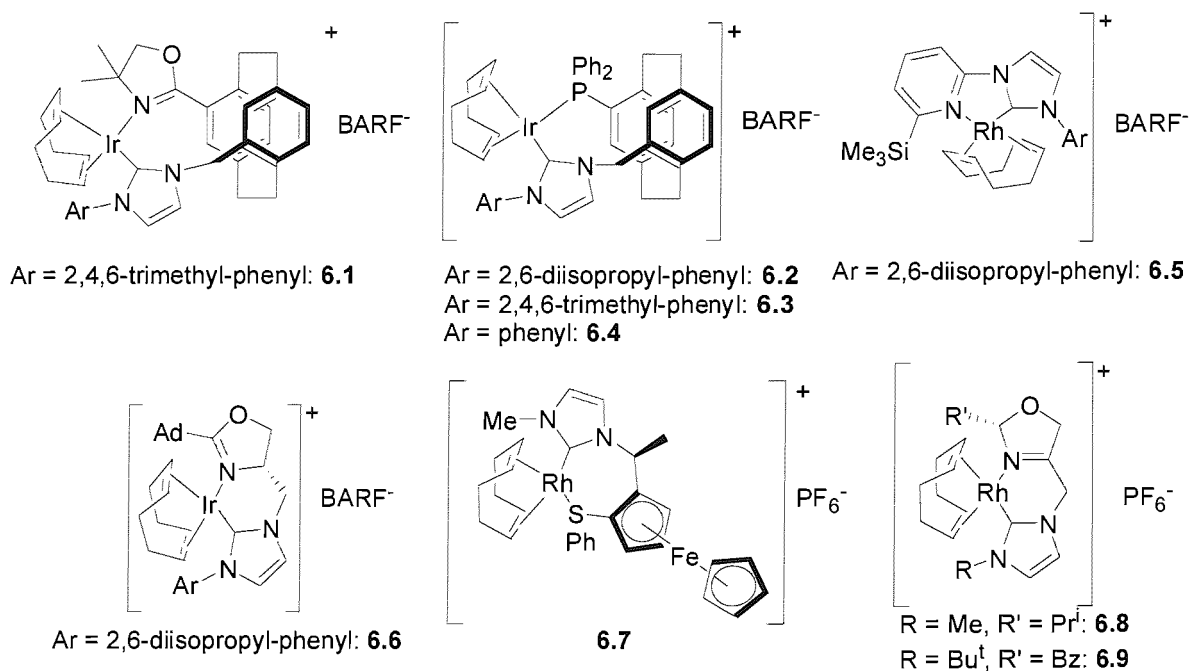
Figure 6.1: Functionalised NHC complexes of Rh(I) and Ir(I) (BARF$^-$ = [{3,5-(CF$_3$)$_2$-C$_6$H$_3$}$_4$B]$^-$).

In this chapter attempts to synthesise novel phosphine functionalised NHC complexes Rh(I) and Ir(I) are described. These have met various degrees of success and in certain case unexpected complexes have emerged.

6.2 Synthesis and characterisation of rhodium(I) complexes

6.2.1 Synthesis of Rh(I) complexes

The synthesis of novel phosphine-functionalised NHC complexes of group 10 transition metals (Pd, Pt) was achieved through simple ligand substitution reactions. In all cases the phosphine NHC hybrid ligand was generated *in situ* and was reacted with an appropriate metal precursor. Attempts towards accessing phosphine-functionalised NHC Rh(I) complexes, by reaction of the *in situ* generated free carbene with $[Rh(COD)(\mu\text{-Cl})]_2$ under various reaction conditions met with no success. In all cases complex reaction mixtures were obtained as evidenced by ^1H and $^{31}P\{^1H\}$-NMR spectroscopy and attempts to separate the various components by column chromatography or recrystallisation were unsuccessful. Despite this, the problem was solved, in various degrees, by choosing some alternative Rh(I) precursors. The synthesis of the novel Rh(I) complexes is outlined in Scheme 6.1. The method of generating the functionalised NHC *in situ*, followed by its immediate interaction with an appropriate metal precursor, was used to prepare complexes **6.12-6.15** in moderate to low yields.

When the imidazolium salts **2.2a** or **2.4a** were reacted with $[Rh(COD)(\mu\text{-OMe})]_2$ in the absence of a base, complex reaction mixtures were acquired. Nevertheless the ^1H-NMR spectra of these reaction mixtures revealed the absence of the acidic imidazolium protons. This synthetic methodology was chosen as it is known that the introduction of NHCs onto Rh(I) metal centres can be achieved by deprotonation, under mild conditions, of their corresponding imidazolium salts by basic metal precursors of the type $[Rh(COD)(\mu\text{-OR})]_2$ (R = Me, Et).[15] The failure of this preparative method in the case of our system prompted us to use $KN(SiMe_3)_2$ in conjunction with the basic metal precursor. Therefore, the imidazolium salt and $[Rh(COD)(\mu\text{-OMe})]_2$ were mixed in a 2:1 ratio and to this mixture a solution of the base was added at low tempearure (−78 °C). This led to the formation of complexes **6.10** (n = 1) and **6.11** (n = 2).
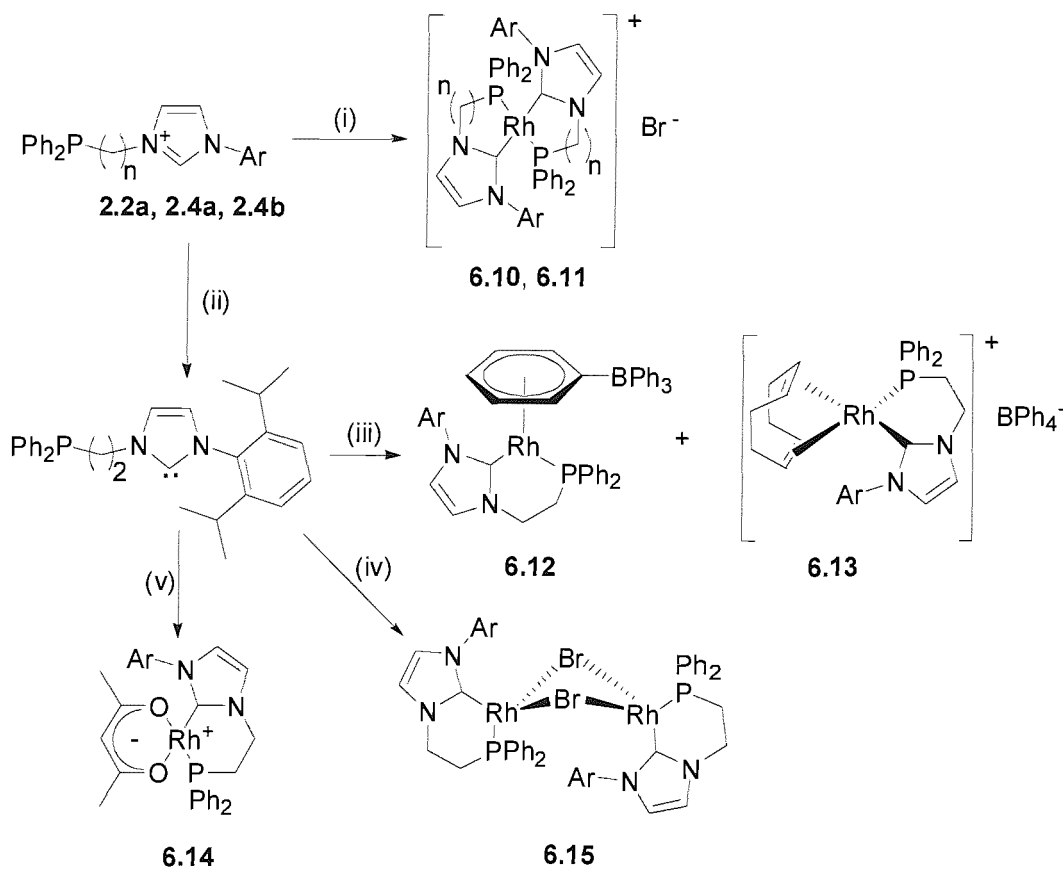
Scheme 6.1: Synthesis of new Rh(I) functionalised NHC complexes. Reagents and conditions: n =1, 2, Ar = 2,4,6-trimethyl-phenyl: **2.2a**, **2.4b** respectively; n = 2, Ar = 2,6-diisopropyl-phenyl: **2.4a**; n = 1, 2, Ar = 2,4,6-trimethylphenyl: **6.10** and **6.11** respectively; for **6.12**, **6.13**, **6.14** and **6.15** Ar = 2,6-diisopropylphenyl. (i) 0.5 equiv. [Rh(COD)(μ-OMe)]$_2$ and then KN(SiMe$_3$)$_2$ (ii) KN(SiMe$_3$)$_2$, THF -78 °C to -50 °C (iii) 1 equiv. [Rh(COD)(py)$_2$]$^+$BPh$_4^-$ (iv) 1 equiv. [Rh(COD)(PPh$_3$)$_2$]BF$_4^-$ (v) 1 equiv. [Rh(COE)$_2$acac].

Interaction of the *in situ* generated free carbene with [Rh(COD)py$_2$]BPh$_4$ resulted in the formation of a complex reaction mixture. Purification *via* crystallisation gave complexes **6.12** and **6.13** in a 1:1 ratio as judged by ^{1}H-NMR spectroscopy. The formation of **6.12** was unexpected as substitution of the pyridine ligands should lead to the formation of complex **6.13**. In an attempt to synthesise **6.12** selectively the free carbene was reacted with [{η^6-Ph-(BPh$_3$)}Rh(py)$_2$], but unfortunately the formation of a complex reaction mixture hindered further characterisation. On the other hand an alternative route for the selective preparation of cationic species of the type [Rh(COD)(PPh$_2$CH$_2$CH$_2$-ylidene)]$^+$ was sought. Therefore the free carbene was reacted with [Rh(COD)(PPh$_3$)$_2$]BF$_4$. This reaction afforded a complex reaction mixture, from which only compound **6.15** was

203

isolated by crystallisation in 11.4% yield. The isolation of yet another unexpected product, prompted us to try to prepare it by choosing a different metal precursor. For this reason, the free carbene was reacted with $[Rh(COE)_2(\mu\text{-}Cl)]_2$. Unfortunately this reaction yielded an intractable reaction mixture from which complex **6.15** could not be isolated.

Finally complex **6.14** was prepared by substitution of two cyclooctene molecules by the *in situ* generated free carbene, by interaction of the latter with one equivalent of $[Rh(COE)_2acac]$. The compound **6.14** was isolated in a moderate 30% yield by cooling a petroleum spirit solution of the reaction mixture to -30 °C. This resulted in the formation of a yellow crystalline material, which was proved to be the **6.14** by spectroscopic methods. This moderate yield is probably due to side reactions occurring as evidenced by the crystals' mother liquor ^1H and $^{31}P\{^1H\}$-NMR spectra that showed the existence of more than one species in solution.

6.2.2 Characterisation of Rh(I) complexes

6.2.2.1 NMR spectroscopy

Spectroscopic methods and microanalysis accounted for the formation of **6.10**. The absence of signals for 1,5-cyclooctadiene in the ^1H-NMR spectrum of the compound, as well as the existence of only one secondary carbon, shifted at 52.8 ppm with a $^1J_{PC}$ coupling constant of 11.8 Hz, in the $^{13}C\{^1H\}$-NMR spectrum, demonstrated that the Rh(I) centre was flanked by two ligands. The $^{31}P\{^1H\}$-NMR spectrum consisted of one doublet centred at 53.2 ppm with a $^1J_{RhP}$ coupling constant of 167.7 Hz, proving that the ligand is chelating. The speculation that the coordination sphere is occupied by two ligands was further confirmed by ES^+ mass spectrometry that showed the existence of the $[(PPh_2CH_2\text{-}ylidene)_2Rh + MeOH]$ cation. The above observations show that the Rh(I) centre is connected to two ligands that adopt a chelating mode. This raises the question of the geometry around the metal centre, as it is easily seen that two alternative configurations could exist: one where the complex adopts a D_{2h} symmetry with the carbene moieties (and subsequently the phosphine moieties) *trans* to each other, and a second one where the carbene moieties are *cis* to each other (C_{2v} symmetry). A geometry giving rise to a C_{2v} symmetry would mean that the NHC carbon of one ligand is situated *trans* to the phosphine moiety of the other ligand. This would mean that the NHC carbons should appear as a doublet of doublets due to coupling with rhodium and phosphorus. This is not

observed in the $^{13}C\{^1H\}$-NMR spectrum where the NHC carbon is located at 179.9 ppm and is only split into a doublet due to coupling to rhodium with a $^1J_{RhC}$ coupling constant of 48.9 Hz. Finally it is interesting to note that the mesityl methyls appear as a three distinct singlets.

Unlike complex **6.10**, its analogue **6.11** is not formed without concurrent contamination of other side products. The ^1H-NMR spectrum revealed a complex reaction mixture, but the $^{31}P\{^1H\}$-NMR had only one doublet centred at 10.7 ppm ($^1J_{RhP}$ = 164.8 Hz) while the ES^+ mass spectrum showed the parent cation $[Rh(PPh_2CH_2CH_2\text{-ylid})_2]^+$. The geometry around the metal centre is speculated to resemble the one of the analogous complex **6.10**.

The isolation of the two complexes **6.12** and **6.13** from the reaction of the *in situ* generated free carbene with $[Rh(COD)py_2]BPh_4$ (Scheme 6.1) was achieved by crystallisation. This produced yellow crystals appropriate for X-ray diffraction studies as well as a yellow amorphous solid. The crystals proved to be the zwitterion **6.12** while the existence of **6.13** was based on NMR spectroscopic evidence. The ^1H-NMR spectrum of the solids from the crystallisation contained broad peaks assignable to signals from COD Furthermore the $^{31}P\{^1H\}$ NMR contained two doublets centred at 19.1 and 38.8 ppm with $^1J_{RhP}$ coupling constants of 155.4 and 219.6 Hz respectively. The first one is attributed to zwitterion **6.12** while the second one is assignable to the cationic species **6.13**.

The identity and the butterfly like conformation (Scheme 6.1) of complex **6.15** were initially confirmed by an X-ray diffraction study. Further evidence for its formation was found in the ^1H and the $^{31}P\{^1H\}$-NMR spectra of the compound. The first consisted of broad peaks, probably due to the fluxional behaviour of the dimmer, while the latter showed only one doublet centred at 19.5 ppm with a $^1J_{RhP}$ coupling constant of 150.2 Hz.

The identity of complex **6.14** was verified by NMR spectroscopy as well as an X-ray diffraction study. The formation of the compound was evidenced, firstly by the appearance of two CH_3 singlets, at 1.38 and 1.65 ppm in the ^1H-NMR spectrum, assignable to the backbone methyls of acac and secondly to the downfield shift in the $^{31}P\{^1H\}$- NMR spectrum of the compound (46.9 ppm, $^1J_{RhP}$ = 205.7 Hz) compared to the shift of –22.4 ppm in the $^{31}P\{^1H\}$-NMR spectrum of the imidazolium NHC precursor **2.4b**. The $^{13}C\{^1H\}$-NMR spectrum was also of significant diagnostic value as it contained doublets centred at 180.1 ($^2J_{RhC}$ = 22.5 Hz), 181.5 ($^2J_{RhC}$ = 18.9 Hz), and 183.4 ppm ($^1J_{RhC}$ = 50.8 Hz) assignable to the quartenary acac carbons (180.1 amd 181.5 ppm) and the

carbene carbon. These features are attributed to the electronic asymmetry imposed by the phosphine-NHC hybrid ligand.

6.2.2.2 X-ray diffraction studies on 6.10, 6.12, 6.14 and 6.15

The geometry proposed for complex **6.10** based on spectroscopic evidence was unambiguously established by an X-ray diffraction study on crystals obtained by layering a CH_2Cl_2 solution of **6.10** with Et_2O. An ORTEP diagram of the cation in the crystal structure of **6.10** is shown in Figure 6.2.
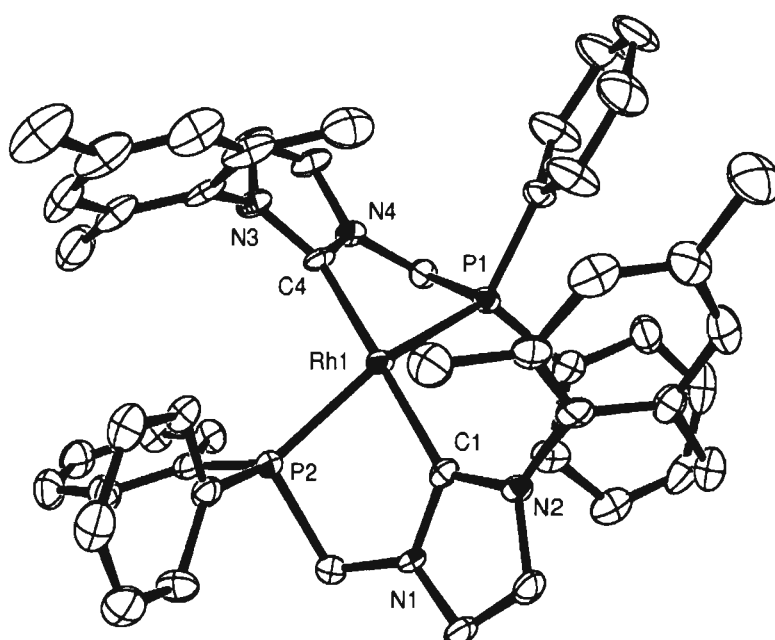
Figure 6.2: ORTEP representation of the cation in **6.10** showing 50 % probability ellipsoids. The bromide anion, two molecules of solvent (CH_2Cl_2), and H atoms are omitted for clarity. Selected bond lengths (Å) and angles (°): C(1)-Rh(1) = 2.044(6), C(4)-Rh(1) = 2.058(6), P(1)-Rh(1) = 2.2693(16), P(2)-Rh(1) = 2.2539(16); C(1)-Rh(1)-C(4) = 176.8(2), C(1)-Rh(1)-P(2) = 79.09(17), C(4)-Rh(1)-P(2) = 100.41(18), C(1)-Rh(1)-P(1) = 100.27(17), C(4)-Rh(1)-P(1) = 78.64(18), P(2)-Rh(1)-P(1) = 151.60(6).

The geometry around the metal centre is square planar with the rhodium centre being flanked by two ligands each occupying *cis* positions. The Rh(I)-C(carbene) are not unusual and are equivalent within esds. The Rh(I)-P bond distances are also equal within

esds. The two ligands form a bite angle of 79.09(17)° and 78.64(18)°. This deviation from an idealised 90° conformation is adopted probably due to the steric requirements imposed by the fact that the coordination sphere is comprised by two ligands. This is also reflected in the angle formed by the carbene carbon of one ligand with the metal centre and the phosphine moiety of the second ligand. The need to accommodate this steric requirements is also reflected on the almost perpendicular to each other arrangement of the two NHC planes.

Compound **6.12** was characterised by an X-ray diffraction study on crystals obtained by slow diffusion of PE into a benzene solution of **6.12**. An ORTEP diagram of the cation in the crystal structure of **6.12** is shown in Figure 6.3. The Rh(I) metal centre is eight coordinate with the ligand occupying two *cis* positions and one phenyl ring of the BPh_4^- counter anion bonded to the metal centre in an η^6 mode. The Rh-C(carbene) bond length is shorter than the the Rh-P one while the Rh-C(η^6-phenyl) bond lengths are different. This is probably due to the different *trans* influences imposed by the asymmetric ligand architecture. The formation of this complex can be rationalised either by contamination of the starting material $[Rh(COD)(py)_2]BPh_4$ by the zwiterrion $[\{\eta^6\text{-Ph-}BPh_3\}Rh(py)_2]$ or by displacement of the 1,5-COD ligand after the formation of **6.13**. Complexes of the type $[Rh\{\eta^6\text{-Ph-}BPh_3\}(PP)]$ (PP= DPPE, DiPPE) have been synthesised,[16] but no crystallographic data have been reported. To the best of our knowledge this is the first compound of this type of complexes bearing a hybrid NHC-phosphine system.
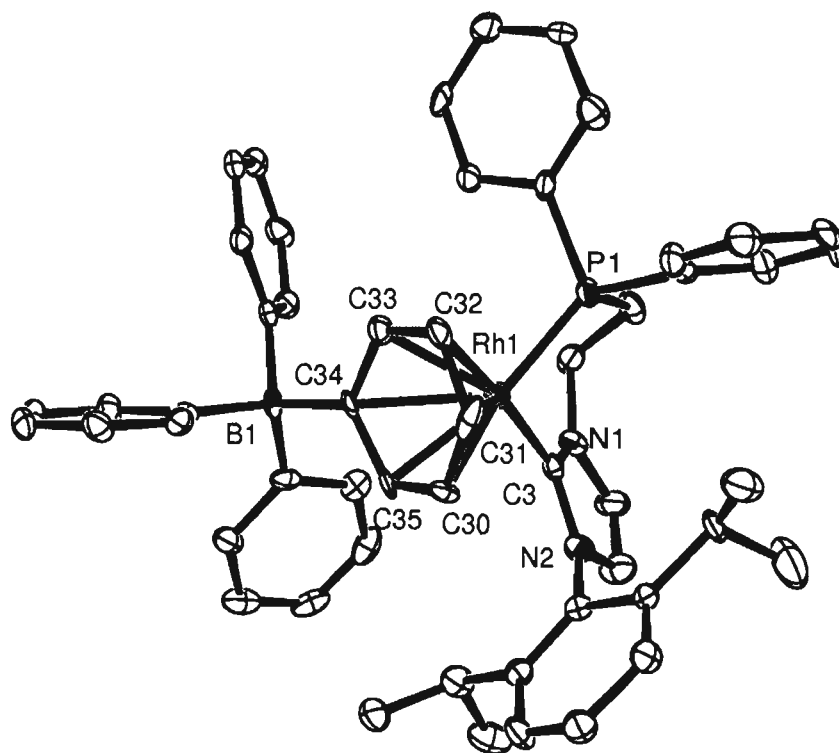
Figure 6.3: ORTEP representation of the zwitterion **6.12** showing 50 % probability ellipsoids. Two molecules of solvent (C_6H_6), and H atoms are omitted for clarity. Selected bond lengths (Å) and angles (°):C(3)-Rh(1) = 1.968(6), C(30)-Rh(1) = 2.305(6), C(32)-Rh(1) = 2.246(7), C(33)-Rh(1) = 2.276(6), C(34)-Rh(1) = 2.407(5), C(35)-Rh(1) = 2.283(6), C(31)-Rh(1) = 2.318(6), P(1)-Rh(1) = 2.197(2); C(3)-Rh(1)-P(1) = 87.85(18), C(3)-Rh(1)-C(32) = 167.9(2), P(1)-Rh(1)-C(32) = 100.06(18), C(3)-Rh(1)-C(33) = 149.4(2), P(1)-Rh(1)-C(33) = 107.23(17), C(32)-Rh(1)-C(33) = 36.1(2), C(3)-Rh(1)-C(35) = 99.6(3), P(1)-Rh(1)-C(35) = 168.22(16), C(32)-Rh(1)-C(35) = 74.2(2), C(33)-Rh(1)-C(35) = 62.0(2), C(3)-Rh(1)-C(30) = 106.2(2), P(1)-Rh(1)-C(30) = 150.04(16), C(32)-Rh(1)-C(30) = 62.6(2), C(33)-Rh(1)-C(30) = 73.9(2) = C(35)-Rh(1)-C(30) = 35.7(2), C(3)-Rh(1)-C(31) = 131.9(2), P(1)-Rh(1)-C(31) = 118.6(2), C(32)-Rh(1)-C(31) = 36.0(2), C(33)-Rh(1)-C(31) = 64.1(2), C(35)-Rh(1)-C(31) = 62.5(3), C(30)-Rh(1)-C(31) = 33.7(2), C(3)-Rh(1)-C(34) = 116.8(2), P(1)-Rh(1)-C(34) = 133.32(16), C(32)-Rh(1)-C(34) = 63.9(2), C(33)-Rh(1)-C(34) = 34.7(2), C(35)-Rh(1)-C(34) = 34.9(2)

An X-ray diffraction study on crystals obtained by slow diffusion of PE into a toluene solution of **6.15** revealed that in the solid state the complex adopts a butterfly conformation. An ORTEP diagram of this crystal structure is given in Figure 6.4. Unfortunately the quality of the data was low and does not allow the accurate calculation

of bond lengths and angles. The picture is given only to demonstrate connectivity.
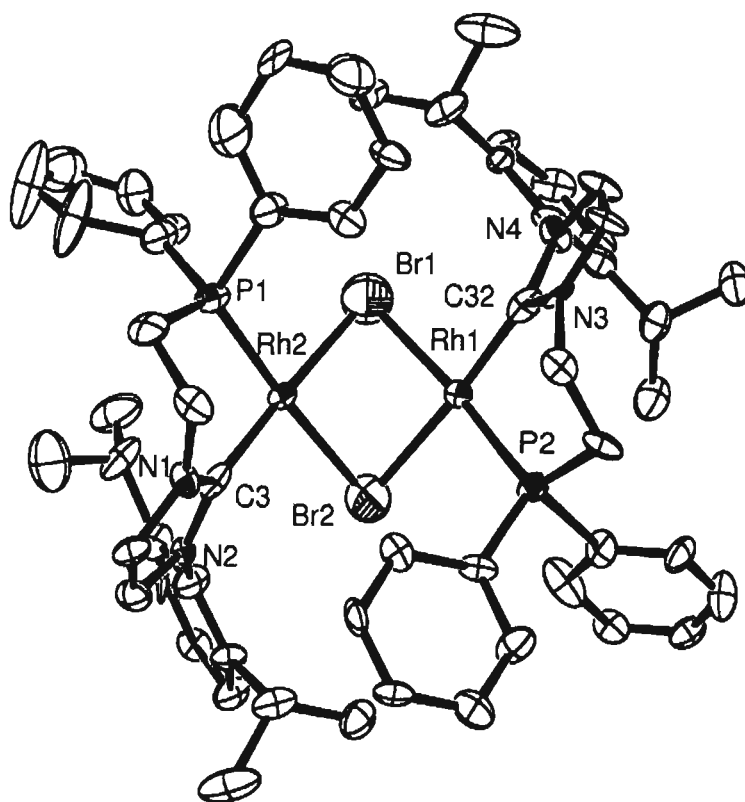
Figure 6.4: ORTEP representation of the crystal structure of **6.15**. H atoms are omitted for clarity.

The formation of complex **6.14** was unambiguously confirmed by an X-ray diffraction study on crystals obtained by cooling a PE solution of **6.14** at -30 °C. An ORTEP diagram of this crystal structure is given in Figure 6.5.
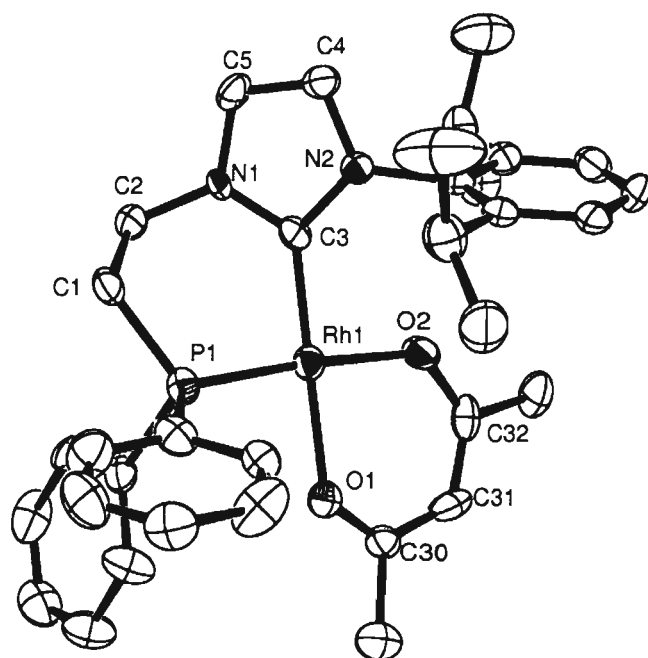
Figure 6.5: ORTEP representation of **6.14** showing 50 % probability ellipsoids. H atoms have been omitted for clarity. Selected bond lengths (Å) and angles (°): C(3)-Rh(1) = 1.951(7), O(1)-Rh(1) = 2.058(5), O(2)-Rh(1) = 2.097(5), P(1)-Rh(1) = 2.160(2); C(3)-Rh(1)-O(1) = 175.2(3), C(3)-Rh(1)-O(2) = 93.2(3), O(1)-Rh(1)-O(2) = 89.0(2), C(3)-Rh(1)-P(1) = 91.5(2), O(1)-Rh(1)-P(1) = 86.68(16), O(2)-Rh(1)-P(1) = 172.40(14).

The geometry around the metal centre is square planar with the ligand occupying two *cis* positions, and a bite angle of 91.5(2)°. The two Rh-O bond lengths are equal within esds, showing the same trend of suppressed *trans* influence as observed in the palladium complexes described in Chapter 3. The Rh-C(carbene) and the Rh-P bond lengths in **6.14** are shorter than the ones observed in complex **6.10** (Table 6.1). Although the ligand is quite different, one would expect that a five-member chelate would exert shorter bonds. The reason may lie in the steric congestion by the saturation of the coordination sphere with two ligands.

Bond	6.14	6.10
Rh-C(carbene)	1.951(7) Å	2.044(6) Å
Rh-P	2.160(2) Å	2.2693(16) Å

Table 6.1: Comparison of bond lengths between 6.14 and 6.10.

6.3 Synthesis and characterisation of Ir(I) complexes

6.3.1 Synthesis of Ir(I) complexes

The synthesis of Ir complexes was also attempted following the synthetic protocol described above. When the *in situ* generated free carbene was reacted with [Ir(COD)(μ-Cl)]$_2$, intractable reaction mixtures were obtained that could not be purified. For that reason the imidazolium salt 2.4b was reacted with [Ir(COD)(μ-Cl)]$_2$ to give complex 6.16 where the phosphine has coordinated (Scheme 6.2). When this complex was further reacted with NaOAc or KN(SiMe$_3$)$_2$, formation of complex reaction mixtures occurred. Interaction of the *in situ* generated free carbene with [Ir(COD)(μ-Cl)$_2$(μ-H)]$_2$ gave a complex reaction mixture from which complex 6.17 was isolated by crystallisation (Scheme 6.2).
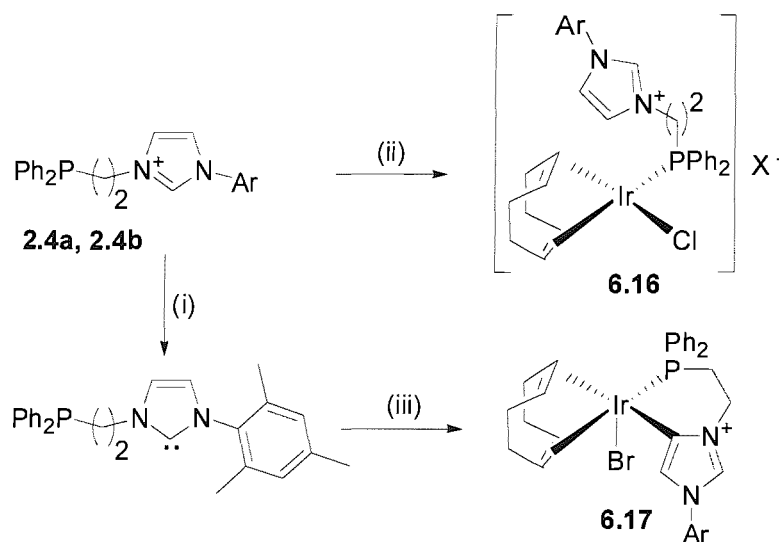
Scheme 6.2: Formation of complexes 6.17 and 6.16. Reagents and conditions: (i) KN(SiMe$_3$)$_2$, THF −78 °C to −50 °C, (ii) 0.5 equiv. [Ir(COD)(μ-Cl)]$_2$ (iii) 0.5 equiv. [Ir(COD)(μ-Cl)$_2$(μ-H)]$_2$ (X =Cl, Br, Ar = 2,6-diisopropylphenyl: 2.4b and 6.16; Ar = 2,4,6-trimethyl-phenyl: 2.4a and 6.17).

The formation of **6.17** was unexpected, but it has been reported in the literature that pyridine functionalised imidazolium salts react with [IrH₃(PPh₃)₂] to yield Ir(III) complexes where one of the imidazolium backbone carbons is connected to the metal centre.[17] A plausible mechanism for the formation of **6.17** is given in Scheme 6.3.
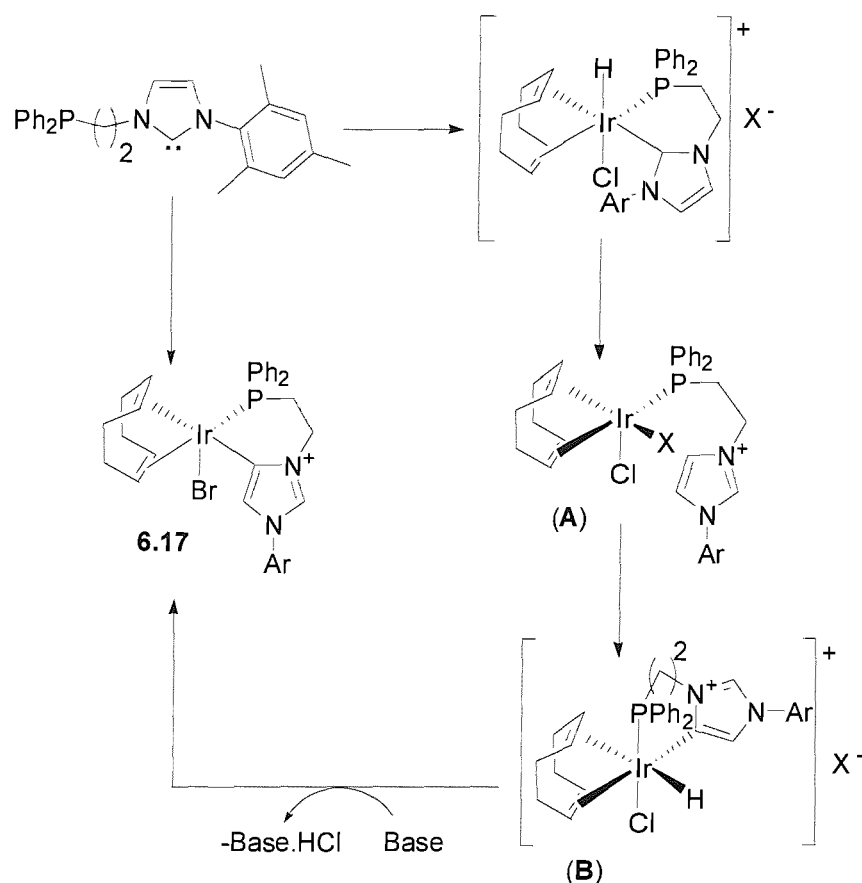
Scheme 6.3: Possible mechanism for the formation of **6.17** (X = Cl, Br).

This mechanism involves in the first place coordination of the ligand in a bidentate mode with the carbene carbon coordinated to the Ir(III) centre. Reductive elimination of imidazolium salt gives rise to intermediate (**A**). The Ir(I) metal centre activates the olefinic C-H of the imidazolium backbone, resulting in the formation of Ir(III) complex (**B**), which in the presence of base gives complex **6.17**. The base comes from the small excess of the KN(SiMe₃)₂ used to generate the free carbene.

In an attempt to synthesise the analogous Ir complexes of **6.10** and **6.14**, [Ir(COD)(μ-OMe)]₂ and [Ir(COE)₂acac] were reacted under similar conditions as the ones

described for the preparation of complexes **6.10** and **6.14**, but unfortunately intractable reaction mixtures were produced.

6.3.2 Characterisation of 6.16 and 6.17

6.3.2.1 NMR spectroscopy

The formation of **6.16** was verified by ^{1}H and ^{31}P$\{^1$H$\}$-NMR spectroscopy. The ^{1}H-NMR spectrum contained signals for 1,5-cyclooctadiene, while the existence of the imidazolium proton at 10.13 ppm suggested that deprotonation had not occurred through another route, i.e. oxidative addition of this acidic C-H bond. The fact that the phosphine has coordinated is shown by the shift of 0.3 ppm observed in the ^{31}P$\{^1$H$\}$-NMR spectrum (-22.4 ppm for the imidazolium salt **2.4b**). The ES$^+$ mass spectrum agrees with the formulation given in Scheme 6.2, while the ES$^-$ mass spectrum shows that it is a 1:1 chloride/bromide salt. The bromide anion originates from **2.4b**, as it is isolated as mixed 1:1 bromide/chloride salt.

The identity of complex **6.17** was verified by the ^{1}H and ^{31}P$\{$1H$\}$-NMR spectra of the isolated crystals. The ^{1}H-NMR showed the existence of the imidazolium proton from a peak located at 9.8 ppm as well as peaks indicative of 1,5-cyclooctadiene. It also revealed that only one imidazolium backbone proton was present. Finally the ^{31}P$\{^1$H$\}$-NMR shift of 23.2 ppm revealed that the phosphine had coordinated.

6.3.2.2 X-ray diffraction studies on 6.17

The identity of **6.17** was established without doubt by an X-ray diffraction study on crystals obtained by slow diffusion of Et$_2$O into a CH$_2$Cl$_2$ solution of **6.17** at -30 °C. An ORTEP diagram of the crystal structure of **6.17** is shown in Figure 6.6. The geometry around the metal centre is square pyramidal with the base of the pyramid being defined by the η^4-COD, one metal-alkyl bond and the metal-phosphine bond. Five coordinate Ir(I) complexes incorporating pyridine functionalised NHC are known.[18] The Ir-C(2) bond distance is not unusual and is shorter than one reported for the Ir(III) complexes where pyridine functionalised "NHCs" adopt this abnormal bonding to the metal centre.[19] The ligand is occupying two *cis* positions with a bite angle of 88.9(3)°. The Ir(1)-C(27) and Ir(1)-C(28) bond distances are equal within esds but shorter than the Ir(1)- C(31) and

Ir(1)-C(32) ones. This is probably due to the stronger *trans* influence imposed by the Ir(1)-C(2) bond to the latter η^2 bond.
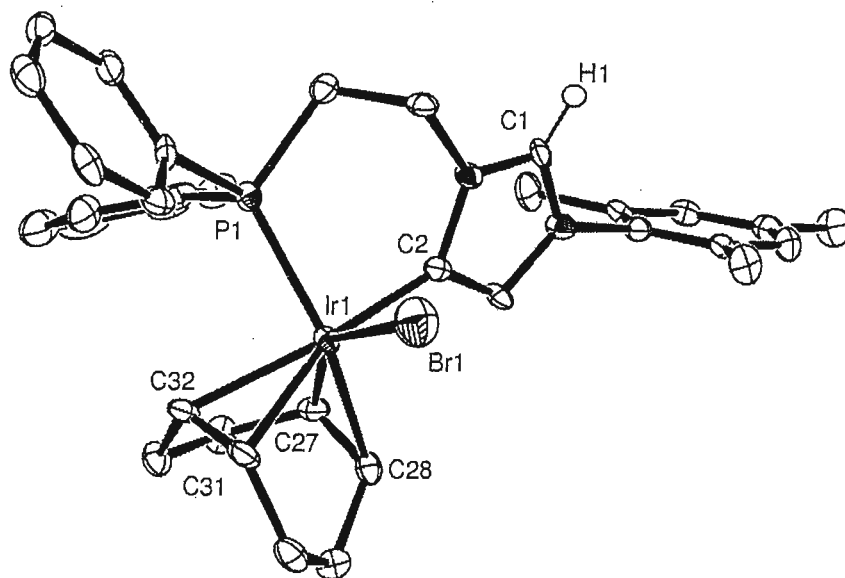
Figure 6.6: ORTEP representation of **6.17** showing 50 % probability ellipsoids. H atoms (except for the imidazolium proton H1) and one molecule of solvent (CH_2Cl_2) have been omitted for clarity. Selected bond lengths (Å) and angles (°):C(2)-Ir(1) = 2.018(9), C(27)-Ir(1) = 2.089(8), C(28)-Ir(1) = 2.139(9), C(31)-Ir(1) = 2.217(9) = C(32)-Ir(1) = 2.235(10), P(1)-Ir(1) = 2.283(2), Ir(1)-Br(1) = 2.6865(11); C(2)-Ir(1)-C(27) = 87.9(4), C(2)-Ir(1)-C(28) = 89.5(4), C(27)-Ir(1)-C(28) = 39.5(3), C(2)-Ir(1)-C(31) = 158.6(4), C(27)-Ir(1)-C(31) = 95.4(4), C(28)-Ir(1)-C(31) = 79.9(4), C(2)-Ir(1)-C(32) = 162.5(3), C(27)-Ir(1)-C(32)= 79.2(4), C(28)-Ir(1)-C(32) = 87.9(4), C(31)-Ir(1)-C(32) = 36.6(3), C(2)-Ir(1)-P(1) = 88.9(3), C(27)-Ir(1)-P(1) = 112.6(3), C(28)-Ir(1)-P(1) = 152.1(2), C(31)-Ir(1)-P(1) = 109.0(3), C(32)-Ir(1)-P(1) = 85.3(3), C(2)-Ir(1)-Br(1) = 86.6(2), C(27)-Ir(1)-Br(1) = 148.8(3), C(28)-Ir(1)-Br(1) = 109.7(2), C(31)-Ir(1)-Br(1) = 79.7(3), C(32)-Ir(1)-Br(1) = 110.5(2), P(1)-Ir(1)-Br(1) = 97.93(6).

6.4 Reactivity of Rh(I) complex 6.14

Complex **6.14** reacts with CO and syn-gas at ambient temperature to give complexes **6.18** and **6.19** respectively (Scheme 6.4).

6.19   1 atm. syn-gas   RT   **6.14**   1 atm. CO   RT   **6.18**
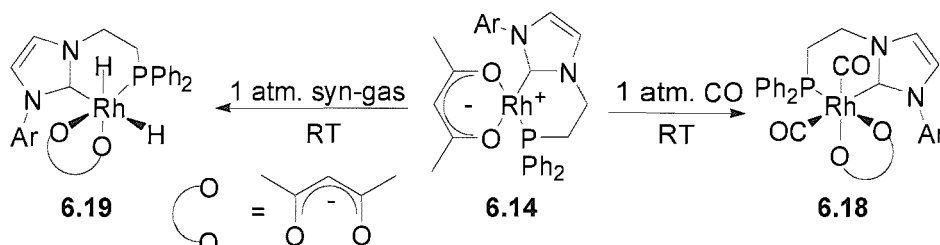
Scheme 6.4: Synthesis of complexes **6.18** and **6.19** by reaction of **6.14** with CO and syn-gas respectively (Ar = 2,6-diisopropyl-phenyl).

The reactions were carried out in Young's NMR tubes that were pressurised at atmospheric pressure with the appropriate gas. When CO was used, the colour of the solution turned immediately from yellow to bright red, indicating that a reaction had happened. Complex **6.19** was characterised by ^{1}H, ^{31}P$\{^1$H$\}$ and IR spectroscopy. The first showed that the two diastereotopic o-isopropyl doublets were split to four doublets, an indication that the symmetry was perturbed. This excludes a structure where the CO molecules occupy equatorial sites. The fact that two CO molecules connected to the metal centre are present was also demonstrated by the IR spectrum of the solution in C_6D_6, which showed two resonances at 1977.4 and 1887.4 cm^{-1} that correspond to terminal bonded CO molecules. The ^{31}P$\{^1$H$\}$ NMR spectrum showed an upfield shift to 22.4 ppm ($^1J_{RhP}$ = 109.9 Hz) from 46.9 ppm ($^1J_{RhP}$ = 205.7 Hz) in complex **6.14**. This indicates that only one isomer is present in solution and that the formation of a cationic species where the CO molecules have displaced that acac is unlikely (this is also confirmed by the ^{1}H-NMR spectrum since such a structure would be symmetric). The formation of which isomer could be easily confirmed by the ^{13}C$\{^1$H$\}$-NMR spectrum of the reaction mixture since a topology where the CO molecule is *trans* to the phosphine moiety of the ligand would generate different coupling constants than the geometry proposed in Scheme 6.4. Unfortunately the compound decomposed during acquisition and the CO, and NHC carbons in the recorded ^{13}C$\{^1$H$\}$-NMR spectrum could not be located. Nevertheless the

spectrum contained nine different peaks in the alkyl region, suggesting the geometry proposed in Scheme 6.4.

When **6.14** was reacted with syn-gas (1:1 mixture H_2/CO) in a similar manner, the same colour change described above occurred. Again the ^{1}H-NMR spectrum showed the characteristic signals of a distorted octahedral lacking symmetry. It also revealed a distorted triplet at –9.88 ppm, which is better assigned as two overlapping doublets ($^1J_{RhH}$ = 9.1 Hz, $^1J_{RhH}$ = 11.0 Hz) and which integrates for two protons. The ^{31}P{^{1}H}-NMR was shifted upfield (25.1, $^1J_{RhP}$ = 134.1 Hz) relative to complex **6.14**. Alternative geometries cannot be excluded since sample decomposition hindered further characterisation. It is interesting to notice though that under similar reaction conditions complex **6.14** is completely inert towards H_2. It could be that the formation of the Rh(III) complex **6.19** proceeds through complex **6.18**.

In addition, it was found that complex **6.14** catalyses the insertion of arylboronic acids into aldehydes in moderate yields at ambient temperature (Scheme 6.5).
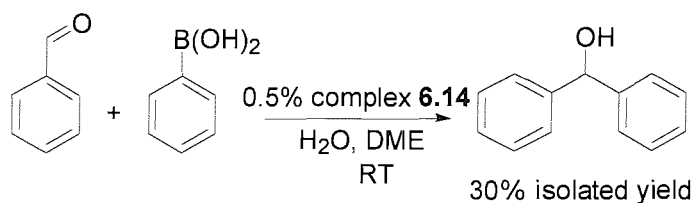
Scheme 6.5: Catalytic insertion of phenylboronic acid into benzaldehyde using **6.14**.

6.5 Conclusions

In this chapter the preparation of some novel Rh(I) and Ir(I) complexes bearing phosphine-NHC hybrid ligand architectures has been demonstrated. The synthesis of these complexes has not been straightforward and in most cases it has yielded unexpected products. Of particular mention is the Ir(I) complex **6.17** where the "NHC" functionality adopts an abnormal binding to the metal centre.

The only compound that has been prepared in a moderate yield is **6.14,** which acts as moderate catalyst for the insertion of phenylboronic acid into benzaldehyde at ambient temperature. It also reacts with syn-gas to give rise to Rh(III) bis-hydride species. This reactivity suggests that this compound could potentially act as a hydroformylation catalyst.

6.6 Experimental

General materials: [Rh(COD)(μ-Cl)]$_2$,[20] [Rh(COE)$_2$(μ-Cl)]$_2$,[21] [Rh(COD)(μ-OMe)]$_2$,[22] [Ir(COD)(μ-OMe)]$_2$,[22] [Rh(COE)$_2$(acac)],[23] [Ir(COE)$_2$(acac)],[24] [Rh(COD)(py)$_2$]BPh$_4$,[25] [{η^6-Ph-BPh$_3$}Rh(py)$_2$],[26] [Rh(COD)(PPh$_3$)$_2$]BF$_4$[27] and [Ir(COD)(μ-H)(μ-Cl)$_2$]$_2$[7] were prepared according to literature procedures. [Ir(COD)(μ-Cl)]$_2$[28] was prepared according to literature procedure or was given as a generous loan from Johnson-Matthey.

6.10: In the glove box a Schlenk tube was charged with 60 mg (0.12 mmol) of [Rh(COD)(μ-OMe)]$_2$ and 155 mg (2 equiv.) of the phosphine functionalised imidazolium salt **2.3a**. A second Schlenk was charged with 48 mg (1.1 equiv. to imidazolium salt) of KN(SiMe$_3$)$_2$. Approximately 20 mL of THF were added to the Schlenk containing the imidazolium salt and [Rh(COD)(μ-OMe)]$_2$, while the base was dissolved in approximately 10 mL of THF. The two were immediately cooled down to -78 °C using a dry ice-acetone slush bath. The THF solution of the base was then added *via* cannula to the suspention of the metal precursor and imidazolium salt. Upon addition the colour of the suspention changed from yellow to orange and after the addition was complete the resulting homogeneous orange solution was left to warm to room temperature overnight under stirring. The solvent was then removed under vacuum and non-volatiles were dissolved in CH$_2$Cl$_2$ and filtered through a Celite pad. The volatiles were removed at reduced pressure and the yellow solid was washed with Et$_2$O and PE to afford the title compound. Yield: 70 mg (58 %). Crystals were grown by layering a CH$_2$Cl$_2$ solution of the compound with Et$_2$O. ^{1}H-NMR δ(CD$_2$Cl$_2$): 1.05 (6H, s, C*H$_3$*), 2.00 (6H, s, C*H$_3$*), 2.33 (6H, s, C*H$_3$*), 4.42 (2H, br. s, [Rh(PPh$_2$C*H$_2$*-ylid)$_2$]$^+$), 4.71 (2H, br. s, [Rh(PPh$_2$C*H$_2$*-ylid)$_2$]$^+$), 6.66 (4H, br. s, aromatic), 6.73 (8H, m, aromatic), 7.33 (16H, m, aromatic); ^{13}C{^{1}H}-NMR δ(CD$_2$Cl$_2$): 18.8 (s, C*H$_3$*), 19.1 (s, C*H$_3$*),, 20.5 (s, C*H$_3$*), 52.8 (d, $^1J_{PC}$ = 23.7 Hz, [Rh(PPh$_2$C*H$_2$*-ylid)$_2$]$^+$), 117.8 (s, ylidene backbone), 119.2 (s, ylidene backbone), 121.9 (s, aromatic), 124.4 (s, aromatic), 125.1 (d, J_{PC} = 7.1 Hz), 125.9 (s, aromatic), 128.6 (d, J_{PC} = 11.8 Hz, aromatic), 131.3 (s, aromatic), 137.5 (d, J_{PC} = 2.2 Hz), 147.1 (s, aromatic), 179.9 (d, $^1J_{RhC}$ = 48.9 Hz, NC*N*); ^{31}P{^{1}H}-NMR δ(CD$_2$Cl$_2$): 53.2 (d, $^1J_{RhP}$ = 167.7 Hz, [Rh(*P*Ph$_2$CH$_2$-ylid)$_2$]$^+$); ES$^+$: 903 [M+MeOH]$^+$; Anal. Found: C, 46.47; H, 4.07; N, 3.93 %. Calcd for C$_{50}$H$_{50}$BrN$_4$P$_2$Rh.6CH$_2$Cl$_2$: C, 46.03; H, 4.28; N, 3.83 %.

6.11: This was prepared as above starting from 60 mg (0.12 mmol) of [Rh(COD)(μ-OMe)]$_2$, 125 mg of imidazolium salt **2.4a** (2 equiv.) and 52 mg of KN(SiMe$_3$)$_2$ (1.1 equiv. to imidazolium salt). The ^{1}H-NMR spectrum in CD$_2$Cl$_2$ is not informative and does not

account for the formation of the title compound. $^{31}P\{^1H\}$-NMR δ(CD_2Cl_2): 10.7 (d, $^1J_{RhP}$ = 164.8 Hz), [Rh(*P*Ph$_2$CH$_2$CH2-ylid)$_2$]$^+$); ES$^+$: 984 [Rh(PPh$_2$CH$_2$CH$_2$-ylid)$_2$]$^+$.

6.12 and **6.13**: In the glove box 100 mg (0.14 mmol) of [Rh(COD)py$_2$]BPh$_4$ were placed into a Schlenk tube. A second Schlenk was charged with 73 mg (1 equiv.) of the phosphine functionalised imidazolium salt **2.4b**, while a third Schlenk was charged with 31 mg (1.1 equiv.) of KN(SiMe$_3$)$_2$. The contents of the three Schlenks were cooled at -78 °C using a dry ice-acetone slush bath. The imidazolium salt was then suspended in approximately 20 mL THF and the base was dissolved in approximately 10 mL THF and they were left to equilibrate to the temperature of the slush bath. The solution of KN(SiMe$_3$)$_2$ was then transferred to the suspention of the imidazolium salt by means of cannula and after the addition was complete, a pale yellow solution was formed which was left to warm up to -50 °C. [Rh(COD)py$_2$]BPh$_4$ was dissolved in approximately 10 mL of THF and was cooled down to -78 °C. The solution of the free carbene was then transferred by means of cannula to the solution of [Rh(COD)py$_2$]BPh$_4$, and the slush baths were removed and the reaction mixture was left stirring at room temperature overnight. The volatiles were removed under reduced pressure and the resulting bright yellow solid was extracted with toluene (3 × 15 mL) and filtered through a Celite pad. The solvent was removed under vacuum and non-volatiles were washed with petroleum ether and dried under reduced pressure. The ^1H and $^{31}P\{^1H\}$-NMR spectra of the resulting solid in d$_8$-toluene were impure, and purification via crystallisation was achieved by layering a benzene solution of the reaction mixture with PE. Yellow crystals and a yellow amorphous solid were obtained. ^1H-NMR δ(CD_2Cl_2): 0.88 (12H, br. s, CH(C*H$_3$*)$_2$), 0.95 (6H, d, $^3J_{HH}$ = 6.7 Hz, CH(C*H$_3$*)$_2$), 1.21 (6H, d, $^3J_{HH}$ = 6.7 Hz, CH(C*H$_3$*)$_2$), 2.01 (12H, m, [(PPh$_2$C*H$_2$*CH$_2$-ylidene)Rh(COD)]$^+$, C*H*(CH$_3$)$_2$ and COD-C*H$_2$*s), 2.35 (2H, m, [(PPh$_2$C*H$_2$*CH$_2$-ylidene)Rh(η^6-Ph-(BPh$_3$))], 2.54 (2H, sept., $^3J_{HH}$ = 6.7 Hz, C*H*(CH$_3$)$_2$), 4.07 (2H, br. s, olefinic COD-C*H*), 4.39 and 4.42 (1H each, m, [(PPh$_2$CH$_2$C*H$_2$*-ylidene) moiety), 4.62 (2H, m, [(PPh$_2$CH$_2$C*H$_2$*-ylidene) moiety), 5.45 (2H, br. s, olefinic COD-C*H*), 6.62 (1H, distorted t, aromatic), 6.71 (1H, s, ylidene backbone), 6.86 (5H, distorted t, [(PPh$_2$CH$_2$CH$_2$-ylidene)Rh(η^6-C$_6$*H$_5$*-(BPh$_3$))], 7.01 (21H, m, aromatic), 7.30 (32H, m, aromatic), 7.48 (10H, m, aromatic); $^{31}P\{^1H\}$-NMR δ(CD_2Cl_2): 19.1 (d, $^1J_{RhP}$ = 155.4 Hz, [(*P*Ph$_2$CH$_2$CH$_2$-ylidene)Rh(η^6-Ph-(BPh$_3$))], 38.8 (d, $^1J_{RhP}$ = 219.6 Hz, [(*P*Ph$_2$CH$_2$CH$_2$-ylidene)Rh(COD)]$^+$). Further analysis was hindered due to sample decomposition.

6.14: In the glove box 100 mg (0.22 mmol) of Rh(COE)$_2$(acac) were charged in a Schlenk tube. A second Schlenk was charged with 115 mg (1 equiv.) of the phosphine

functionalised imidazolium salt **2.4b**. A third Schlenk was charged with 48 mg of KN(SiMe$_3$)$_2$. The contents of the three Schlenks were cooled at -78 °C using a dry ice-acetone slush bath. The imidazolium salt was then suspended in approximately 20 mL THF and the base was dissolved in approximately 10 mL THF and they were left to equilibrate to the temperature of the slush bath. The solution of KN(SiMe$_3$)$_2$ was then transferred to the suspention of the imidazolium salt by means of cannula and after the addition was complete, a pale yellow solution was formed which was left to warm up to – 50 °C. Rh(COE)$_2$acac was dissolved in approximately 10 mL of THF and was cooled down to -78 °C. The solution of the free carbene was then transferred by means of cannula to the solution of Rh(COE)$_2$(acac), and the slush baths were removed and the reaction mixture was left stirring at room temperature overnight. The volatiles were removed at reduced pressure and the yellow solid was extracted with petroleum ether 60-80 (4 × 25 mL) and filtered through a Celite pad. The Celite pad was washed with petroleum ether 40-60 (3 × 10 mL) and the volume of the filtrate was reduced to about 15 mL and it was placed at -30 °C under nitrogen to yield crystals of the title compound. Yield: 43 mg (30 %) [The extraction of the compound with petroleum spirits was assisted by gentle heating with a heat-gun]. ^{1}H-NMR δ(C$_6$D$_6$): 1.10 (6H, d, $^3J_{HH}$ = 7.0 Hz, CH(C*H$_3$*)$_2$), 1.38 (3H, s, (O)C(CH$_3$)CHC(C*H$_3$*)(O)), 1.42 (6H, d, $^3J_{HH}$ = 7.0 Hz, CH(C*H$_3$*)$_2$), 1.65 (3H, s, (O)C(C*H$_3$*)CHC(CH$_3$)(O)), 1.78 (2H, broad m, [PPh$_2$CH$_2$C*H$_2$*-ylidene]Rh(acac)), 3.60 (4H, m, C*H*(CH$_3$)$_2$ and [PPh$_2$C*H$_2$*CH$_2$-ylidene]Rh(acac)), 5.17 (1H, s, C(O)C(CH$_3$)C*H*C(CH$_3$)C(O)), 6.12 (1H, d, $^3J_{HH}$ = 1.5 Hz, ylidene backbone), 6.27 (1H, d, $^3J_{HH}$ = 1.5 Hz, ylidene backbone), 7.19 (9H, m, aromatics), 8.05 (4H, m, aromatics); ^{13}C{^{1}H}-NMR δ(C$_6$D$_6$): 22.7 (s, (O)C(CH$_3$)CHC(*C*H$_3$)(O)), 24.0 (s, CH(*C*H$_3$)$_2$), 24.8 (s, CH(*C*H$_3$)$_2$), 26.6 (d, $^1J_{PC}$ = 25.1 Hz, [PPh$_2$*C*H$_2$CH$_2$-ylidene]Rh(acac)), 27.5 (s, (O)C(*C*H$_3$)CHC(CH$_3$)(O)), 29.0 (s, *C*H(CH$_3$)$_2$), 45.8 (s, [PPh$_2$CH$_2$*C*H$_2$-ylidene]Rh(acac)), 98.1 (s, (O)C(CH$_3$)*C*HC(CH$_3$)(O)), 118.9 (s, ylidene backbone), 122.8 (s, ylidene backbone), 123.7 (s, aromatic), 127.6 (d, J_{PC} = 2.2 Hz, aromatic), 128.2 (s, aromatic), 128.6 (s, aromatic), 129.1 (s, aromatic), 133.6 (d, J_{PC} = 9.8 Hz, aromatic), 137.8 (d, J_{PC} = 15.7 Hz, aromatic), 144.9 (s, aromatic), 180.1 (d, $^2J_{RhC}$ = 22.5 Hz, (O)C(CH$_3$)CH*C*(CH$_3$)(O)), 181.5 (d, $^2J_{RhC}$ = 18.9 Hz, (O)*C*(CH$_3$)CHC(CH$_3$)(O)), 183.4 (d, $^1J_{RhC}$ = 50.8 Hz, N*C*N); ^{31}P{^{1}H}-NMR δ(C$_6$D$_6$): 46.9 (d, $^1J_{RhP}$ = 205.7 Hz, [*P*Ph$_2$CH$_2$CH$_2$-ylidene]Rh(acac)).

6.15: In the glove box 60 mg (0.07 mmol) of [Rh(COD)(PPh$_3$)$_2$]BF$_4$ were charged into a Schlenk tube. A second Schlenk was charged with 37 mg (1 equiv.) of the phosphine

219

functionalised imidazolium salt **2.4b**, while a third Schlenk was charged with 15 mg (1.1 equiv.) of $KN(SiMe_3)_2$. The contents of the three Schlenks were cooled at -78 °C using a dry ice-acetone slush bath. The imidazolium salt was then suspended in approximately 10 mL THF and the base was dissolved in approximately 5 mL THF and the two were left to equilibrate to the temperature of the slush bath. The solution of $KN(SiMe_3)_2$ was then transferred to the suspention of the imidazolium salt by means of cannula and after the addition was complete, a pale yellow solution was formed which was left to warm up to -50 °C. $[Rh(COD)(PPh_3)_2]BF_4$ was dissolved in approximately 10 mL of THF and was cooled down to -78 °C. The solution of the free carbene was then transferred by means of cannula to the solution of $[Rh(COD)(PPh_3)_2]BF_4$, and the slush baths were removed and the reaction mixture was left stirring at room temperature for 3 hours. The volatiles were removed under reduced pressure and the remaining solid was extracted with toluene (3 × 10 mL) and filtered through a Celite pad. Volatiles were removed under reduced pressure and the resulting brick-red solid was washed (2 × 10 mL) with petroleum ether and dried under vacuum. The remaining solid was dissolved in toluene and was layered with PE to afford brick-red crystals of the title compound. Yield: 5 mg (11.4 %). ^{1}H-NMR $\delta(CD_2Cl_2)$: 0.81 (24H, m, CH(CH_3)$_2$), 1.22 (4H, m, CH(CH$_3$)$_2$), 2.13 (4H, br. s, [(PPh$_2$CH$_2$CH_2-ylidene)Rh(μ-Br)]$_2$), 4.57 (4H, br. s, [(PPh$_2$CH_2CH$_2$-ylidene)Rh(μ-Br)]$_2$), 6.59 (2H, br. s, ylidene backbone), 6.99 (5H, m, aromatics), 7.20 (15H, br. s, aromatics), 7.48 (4H, m, aromatics), 8.18 (4H, br. s, aromatics); ^{31}P{^{1}H}-NMR $\delta(CD_2Cl_2)$: 19.5 (d, $^1J_{RhP}$ = 150.2 Hz, [(*P*Ph$_2$CH$_2$CH$_2$-ylidene)Rh(μ-Br)]$_2$). Further analysis was hindered due to sample decomposition.

6.16: In the glove box 60 mg (0.08 mmol) of $[Ir(COD)(\mu$-Cl)]$_2$ were charged in a Schlenk. A second Schlenk was charged with 83 mg (2 equiv.) of the phosphine functionalised imidazolium salt **2.4b**. The contents of the two Schlenks were cooled at -78 °C and the two solids were suspended in THF (approximately 10 mL each). The suspension of the imidazolium salt was transferred by means of a cannula to the suspension of $[Ir(COD)(\mu$-Cl)]$_2$ and the slush baths were removed. The two were left stirring for two hours at room temperature upon which time a dark red solution had formed. The solvent was then removed *in vacuo* and the resulting dark red solid was extracted with toluene (3 × 15 mL) and filtered through a Celite pad. The volatiles were removed at reduced pressure and the remaining solid was washed thrice with PE (3 × 10 mL). ^{1}H-NMR $\delta(C_6D_6)$: 1.20 (6H, d, $^3J_{HH}$ = 6.8 Hz, CH(CH_3)$_2$), 1.63 (6H, d, $^3J_{HH}$ = 6.8 Hz, CH(CH_3)$_2$), 1.93 (6H, br. s, COD-CH_2s and [Ir(COD)Cl(PPh$_2$CH_2CH$_2$-imidazolium)]$^+$), 2.22 (4H, br. s, COD-CH_2s), 2.24

(2H, distorted sept., CH(CH$_3$)$_2$), 2.80 (2H, br. s, COD-CHs), 3.91 (2H, br. s, COD-CHs),

5.33 (2H, m, [Ir(COD)Cl(PPh$_2$CH$_2$CH_2-imidazolium)]$^+$), 6.72 (1H, s, imidazolium

backbone), 7.11 (2H, m, aromatic), 7.39 (8H, m, aromatic), 7.90 (4H, m, aromatic), 10.1?

(1H, s, imidazolium proton); ^{31}P{^{1}H}-NMR δ(C$_6$D$_6$): 0.3 (s, [Ir(COD)Cl(PPh$_2$CH$_2$CH$_2$-

imidazolium)]$^+$)).; ES$^+$:765 [[Ph$_2$PCH$_2$CH_2-imidazolium]Ir(COD)Cl)]$^+$; ES$^-$: 35 (Cl$^-$), 79

(Br$^-$).

6.17: In the glove box 50 mg (0.07 mmol) of [Ir(COD)(μ-H)(μ-Cl)$_2$]$_2$ were placed into a

Schlenk. A second Schlenk was charged with 67 mg (2 equiv.) of the phosphine

functionalised imidazolium salt **2.4a** and 31 mg (1.1 equiv. to imidazolium salt) of

KN(SiMe$_3$)$_2$. The contents of the two Schlenks were cooled to -78 °C using a dry ice-

acetone slush bath. To the Schlenk containing the imdazolium salt and the base precooled

at -78 °C THF (approximately 20 mL) was added, *via* cannula, under vigorous stirring.

Upon addition a yellow solution was formed which was left stirring until it reached -50

°C. [Ir(COD)(μ-H)(μ-Cl)$_2$]$_2$ was suspended in 10 mL THF and was left to equilibrate to

the temperature of the slush bath. The solution of the free carbene was then transferred to

the suspention of [Ir(COD)(μ-H)$_2$(μ-Cl)]$_2$ by cannula, the slush baths were removed and

the whole was left stirring overnight at room temperature. The solvent was removed under

vacuum and the solid was dissolved in CH$_2$Cl$_2$ and filtered though Celite. The volatiles

were then removed at reduced pressure and the remaining solid was washed with Et$_2$O (10

mL) and PE (10 mL) and was dried under vacuum. The red solid was dissolved in CH$_2$Cl$_2$

and was layered with Et$_2$O and placed at -30 °C to yield orange crystals of the title

compound. ^{1}H-NMR δ(CD$_2$Cl$_2$): 1.44 (4H, br. s, COD-CH_2s), 1.65 (4H, br. s, COD-

CH_2s), 1.91 (6H, s, CH_3), 2.42 (3H, s, CH_3), 2.8 (2H, br. s, COD-CHs), 3.42 (2H, br. s,

COD-CHs), 4.8 (2H, broad s., [Ph$_2$PCH_2CH$_2$-imidazolium]Ir(COD)Br), 4.93 and 5.02 (1H

each, distorted t, , $^3J_{HH}$=5.85 Hz, [Ph$_2$PCH$_2$CH_2-imidazolium]Ir(COD)Br), 6.66 (1H, s,

imidazolium backbone), 6.97 (2H, s, aromatics), 7.44 (5H, m, aromatics), 7.68 (5H, m,

aromatics), 9.82 (1H, s, imidazolium proton); ^{31}P{^{1}H}-NMR δ(CD$_2$Cl$_2$): 23.2 (s,

[Ph$_2$PCH$_2$CH$_2$-imidazolium]Ir(COD)Br).

6.19: A Young's NMR tube was charged in the glove box with 15 mg (0.02 mmol) of **6.14**

which were dissolved in approximately 0.6 mL of C$_6$D$_6$. The NMR tube was connected to

a double manifold Schlenk line at which the N$_2$ inlet was replaced with a syn-gas cylinder

(1:1 H$_2$/CO). The pressure was regulated by means of an oil bubbler. The solution of **6.14**

was opened carefully in the syn-gas inlet, and an immediate colour change occurred from

yellow to red. ^{1}H-NMR δ(C$_6$D$_6$): -9.88 (2H, two overlapping broad doublets $^1J_{RhH}$ = 9.1

Hz, $^1J_{RhH}$ = 11.0 Hz, Rh-H), 0.94 (3H, d, $^3J_{HH}$ = 6.4 Hz, CH(CH_3)$_2$), 1.05 (3H, d, $^3J_{HH}$ = 6.4 Hz, CH(CH_3)$_2$), 1.12 (3H, d, $^3J_{HH}$ = 6.4 Hz, CH(CH_3)$_2$), 1.43 (3H, d, $^3J_{HH}$ = 6.4 Hz, CH(CH_3)$_2$), 1.50 (3H, d, $^3J_{HH}$ = 6.4 Hz, CH(CH_3)$_2$), 1.61 (6H, two overlapping singlets, (O)C(CH_3)CHC(CH_3)(O)), 1.94 (5H, m, [PPh$_2$CH_2CH$_2$-ylidene]Rh(acac)(H)$_2$, CH(CH$_3$)$_2$), 2.71 (1H, distorted septet., CH(CH$_3$)$_2$), 3.78 (4H, broad m, [PPh$_2$CH$_2$CH_2-ylidene]Rh(acac)(H)$_2$), 5.17 (1H, s, (O)C(CH$_3$)CHC(CH$_3$)(O)), 6.55 (3H, m, aromatic), 7.22 (5H, m, aromatic), 7.82 (3H, m, aromatic), 8.11 (4H, br. s, aromatic); ^{31}P{^{1}H}-NMR δ(C$_6$D$_6$): 25.1 (d, $^1J_{RhP}$ = 134.1 Hz, [PPh$_2$CH$_2$CH$_2$-ylidene]Rh(acac)(H)$_2$). Further analysis was hindered due to sample decomposition at room temperature.

6.18: This reaction took place as above using a CO instead of a CO/H$_2$ cylinder. ^{1}H-NMR δ(C$_6$D$_6$): 0.92 (3H, d, $^3J_{HH}$ = 6.4 Hz, CH(CH_3)$_2$), 1.18 (3H, d, $^3J_{HH}$ = 6.4 Hz, CH(CH_3)$_2$), 1.50 (3H, d, $^3J_{HH}$ = 6.4 Hz, CH(CH_3)$_2$), 1.71 (9H, br. s, CH(CH_3)$_2$ and (O)C(CH_3)CHC(CH_3)(O)), 2.18 (2H, m, [PPh$_2$CH_2CH$_2$-ylidene]Rh(acac)(CO)$_2$), 3.52 (2H, br. s, [PPh$_2$CH$_2$CH_2-ylidene]Rh(acac)(CO)$_2$ and CH(CH$_3$)$_2$), 3.99 (2H, br. s, [PPh$_2$CH$_2$CH_2-ylidene]Rh(acac)(CO)$_2$ and CH(CH$_3$)$_2$), 5.40 (1H, s, (O)C(CH$_3$)CHC(CH$_3$)(O)), 6.31 (1H, ylidene backbone), 6.44 (1H, ylidene backbone), 7.22 (8H, m, aromatic), 7.53 (1H, m, aromatic), 8.08 (4H, broad s., aromatic); ^{31}P{^{1}H}-NMR δ(C$_6$D$_6$): 22.4 (d, $^1J_{RhP}$ = 109.9 Hz, [PPh$_2$CH$_2$CH$_2$-ylidene]Rh(acac)(CO)$_2$); IR (solution in C$_6$D$_6$): 2280.0 cm^{-1} (ν C(O) from acac), 1977.4 cm^{-1}, 1887.4 cm^{-1} (ν_{CO}). The ^{13}C{^{1}H} NMR in C$_6$D$_6$ was also acquired but decomposition occurred during acquisition. It showed 9 resonances in the alkyl region at the following shifts (ppm): 19.6, 21.7, 22.7, 23.7, 25.4, 26.6, 27.4, 28.9 and 29.4 (4 CH(CH_3)$_2$, 2 CH(CH$_3$)$_2$, 2 (O)C(CH_3)CHC(CH_3)(O), 1 [PPh$_2$CH_2CH$_2$-ylidene]Rh(acac)(CO)$_2$) and resonances at 47.6 ppm ([PPh$_2$CH$_2$CH_2-ylidene]Rh(acac)(CO)$_2$) and 99.8 ppm ((O)C(CH$_3$)CHC(CH$_3$)(O)).

Insertion of Ph(BOH)$_2$ into PhCHO using 6.14 as catalyst: The set up of the reaction is similar to the one reported in the literature.[29] After overnight stirring at room temperature the solvent was removed in a rotary evaporator and the solid residue was dissolved in CH$_2$Cl$_2$, filtered through a short silica plug, then through a Celite pad and the organic phase was dried with MgSO$_4$. Volatiles were removed and the pale yellow solid was washed with PE and dried under vacuum to give 1,1-bisphenyl-methanol in 30% yield as an off-white solid.

Crystallographic data for 6.10, 6.12, 6.14 and 6.17

| Complex	6.10	6.12	6.14	6.17
Chemical Formula	$C_{52}H_{54}BrCl_4N_4P_2Rh$	$C_{65}H_{65}BN_2PRh$	$C_{34}H_{40}N_2O_2PRh$	$C_{35}H_{41}BrCl_2IrN$
Formula weight	1121.55	1018.88	642.56	863.68
Crystal system	Monoclinic	Triclinic	Monoclinic	Triclinic
Space group	$P\,2_1/n$	$P\text{-}1$	$P\,2_1/n$	$P\text{-}1$
a / $\mathring{A}$	16.6386(8)	13.501(3)	17.762(4)	10.7061(3)
b / $\mathring{A}$	13.1204(5)	13.987(3)	23.507(5)	12.0453(2)
c / $\mathring{A}$	24.8390(12)	14.889(3)	17.809(4)	14.7376(4)
α / °	90	108.45(3)	90	66.472(2)
β / °	105.4980(10)	105.43(3)	98.77(3)	89.2960(10)
γ / °	90	97.03(3)	90	73.5670(10)
Z	4	2	8	2
T/K	120(2)	120(2)	120(2)	150(2)
μ / mm^{-1}	1.396	0.418	0.536	5.461
No. of data collected	54316	12658	27877	23915
No. of unique data	11909	8540	13688	7430
Goodness of fit on F^2	1.026	0.976	0.965	1.057
$R_{int.}$	0.1188	0.0713	0.1184	0.1913
Final $R(|F|)$ for $F_0 >$ $2\sigma(F_0)$	0.0830	0.0667	0.0843	0.0658
Final $R(F^2)$ for all data	0.1162	0.1205	0.1602	0.0997

References:

1. Osborn, J. A.; Jardine, F. H.; Young, J. F.; Wilkinson, G. *J. Chem. Soc. A* **1966**, 1711.
2. van Rooy, A.; Kamer, P. C. J.; van Leeuwen G.; Fraanje, J.; Veldman, N.; Spek, A. L. *Organometallics* **1996**, *15*, 835.
3. Evans, D. A.; Fu, G. C.; Hoveyda, A. H. *J. Am. Chem. Soc.* **1992**, *114*, 6671.
4. Haszeldine, R. N.; Parish, R. V.; Parry, D. J. *J. Organomet. Chem.* **1967**, *9*, 13.
5. Parshall, G. W.; Ittel, S. D. *Homogeneous Catalysis.* ; John Wiley & Sons, Inc.: New York, 1992.
6. Lee, H. M.; Smith, D. C.; He, Z.; Stevens, E. D.; Yi, C. S.; Nolan, S. P. *Organometallics* **2001**, *20*, 794.
7. Crabtree, R. H.; Morris, G. E. *J. Organomet. Chem.* **1977**, *135*, 395.
8. Grasa, G. A.; Moore, Z.; Martin, K. L.; Stevens, E. D.; Nolan, S. P.; Paquet, V.; Lebel, H. *J. Organomet. Chem.* **2002**, *678*, 1.
9. Herrmann, W. A.; Goosen, L. J.; Artus, G. R. J.; Kocher, C. *Organometallics* **1997**, *16*, 2472.
10. Perry, M. C.; Cui, X.; Powell, M. T.; Hou, D. R.; Reibenspiess, J. H.; Burgess, K. *J. Am. Chem. Soc.* **2003**, *125*, 113.
11. Bolm, C.; Fochen, T.; Raabe, G. *Tetrahedron: Asymmetry* **2003**, *14*, 1733.
12. Danopoulos, A. A.; Winston, S.; Hursthouse, M. B. *J. Chem. Soc., Dalton Trans.* **2002**, 3090.
13. Seo, H.; Park, H.-J.; Kim, B.Y.; Lee, J. H.; Son, S. U.; Chung, Y. K. *Organometallics* **2003**, *22*, 618.
14. Fochen, T.; Raabe, G.; Bolm, C. *Tetrahedron: Asymmetry* **2004**, *15*, 1693.
15. Koscher, C.; Hermann, W. A. *J. Organomet. Chem.* **1997**, *532*, 261.
16. Westcott, S. A.; Blom, H. P.; Marder, T. B.; Baker, R. T. *J. Am. Chem. Soc.* **1992**, *114*, 8863.
17. Crabtree, R. H. *J. Chem. Soc., Dalton Trans.* **2003**, 3985.
18. Personal communication with Dr. A. A. Danopoulos.
19. Grundemann, S.; Kovasevic, A.; Albrecht, M.; Faller, J. W.; Crabtree, R. H. *Chem. Commun.* **2001**, 2274.
20. Giordano, G.; Crabtree, R. H. *Inorg. Synth.* **1979**, *19*, 218.
21. van der Ent, A.; Onderlinden, A. L.; *Inorg. Synth.* **1973**, *14*, 92.
22. Sakurai, F.; Suzuki, H.; Morooka, Y.; Ikaua, T. *J. Am. Chem. Soc.* **1980**, *102*, 1749.
23. Burke, J. M.; Coapes, R. B.; Goeta, A. E.; Howard, J. A. K.; Marder, T. B.; Robins, E. G.; Westcott, S. A. *J. Organomet. Chem.* **2002**, *649*, 199.
24. Diversi, D.; Ingroso, G.; Porzio, W.; Zocchi, M. *J. Organomet. Chem.* **1977**, *125*, 253.
25. Garralda, M. A.; Ibarlucea, L. *Polyhedron* **1982**, *1*, 339.
26. Oro, L. A.; Pinilla, E.; Tenajas, M. L. *J. Organomet. Chem.* **1978**, *148*, 81.
27. Albers, J.; Dinjus, E.; Pitter, S.; Walter, O. *J. Molecular Catalysis A: Chemical* **2004**, *219*, 41.
28. Renate, F.; Kirchner, S.; Walter, R.. U.S. patent 2001/0020107 A1, Sep. 6, 2001, 2001.
29. Ueda, M.; Miyaura, N. *J. Org. Chem.* **2000**, *65*, 4450.

Chapter 7: Towards bulky-alkyl phosphine functionalised NHC imidazolium precursors

Chapter 7: Towards bulky-alkyl phosphine functionalised NHC imidazolium precursors

7.1 Introduction

Bulky alkyl phosphines have been successfully used as ligands in various palladium-mediated catalytic transformations.[1] The catalytic activity of palladium(II) complexes incorporating novel phosphine-NHC hybrid ligand as catalysts for Heck couplings was discussed in Chapter 4, and our investigation concluded that these novel complexes exhibited good reactivity with activated aryl bromides but gave low activity with more challenging substrates such as aryl chlorides. We hoped that a ligand architecture combining a bulky alkyl phosphine with a NHC moiety would circumvent this problem. Due to the increased σ-donating ability of these ligands (Scheme 7.1) in comparison to the already discussed mixed phosphine-NHC architectures, stabilisation of possible electronically unsaturated under-ligated species formed during the catalytic cycle could occur, which in turn would account for better catalysts.

(I)
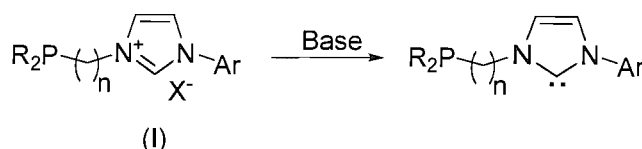
Scheme 7.1: Novel NHC architecture with phosphine tether containing bulky alkyl groups and its imidazolium precursor of type (I) (R = Ad, ^{t}Bu, Cy; Ar = 2,6-diisopropylphenyl; n = 0,1; X = halogen).

In this chapter, routes towards the synthesis of phosphine functionalised imidazolium salts of type (I) (Scheme 7.1) are described. These salts would act as precursors for the synthesis of the corresponding NHCs. Our synthetic approaches met various degrees of success but during our endeavour some interesting synthones were prepared.

7.2 Results and discussion

7.2.1 Synthetic approaches towards ^tBu and Ad phosphine functionalised imidazolium salts

The synthetic strategy employed for the preparation of the phosphine functionalised imidazolium salts described in Chapter 2, *i.e.* reduction of the phosphinoxide azolium salt with SiHCl₃, cannot be utilised in the case where the phosphine substituents are bulky alkyls. For this reason different synthetic approaches to the target compounds had to be sought.
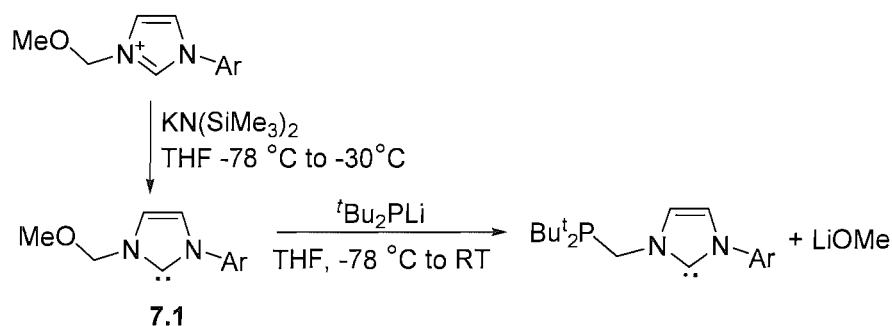
Scheme 7.2: Attempted synthesis of alkyl-phosphine functionalised NHC.

The first approach is based on the nucleophilic substitution of the methoxy group in the functionalised ylidene **7.1** by a lithium phosphide (Scheme 7.2). The reaction mixture afforded, after workup, pale yellow crystals, which were subjected to single X-ray analysis. Unfortunately the crystals proved to be those of the free carbene **7.1**. This isolated functionalised free carbene was unfortunately too thermally unstable for further characterisation. An ORTEP diagram of carbene **7.1** is shown in Figure 7.1. Bond lengths and angles are typical of other isolated free carbenes by Danopoulos and co-workers.[2]
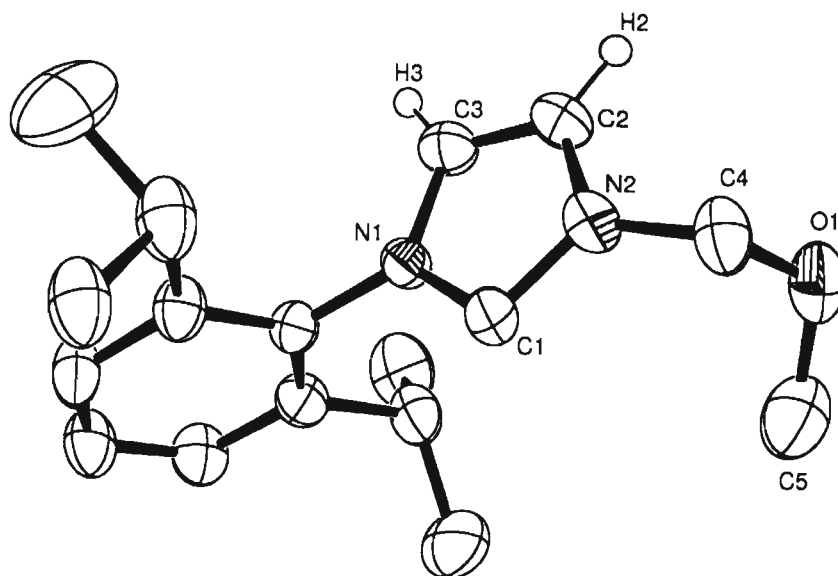
Figure 7.1: ORTEP representation of **7.1** showing 50 % probability ellipsoids. H atoms (except for the ylidene backbone ones) have been omitted for clarity.

A different synthetic approach to tackling the problem is summarised in Scheme 7.3. Test reactions were carried out using Ph_2PCl, as this material is readily available from commercial sources. The aim was to move to other substrates of the general type R_2PCl (with R = ^tBu, Ad) once the method had been perfected.
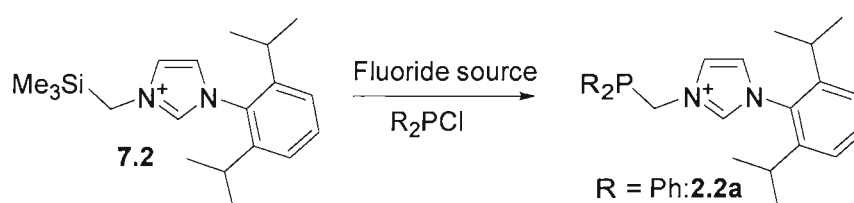
Scheme 7.3: Alternative approach for the synthesis of phosphine functionalised imidazolium salts.

The first reaction was performed in refluxing 1,4-dioxane in the presence of CsF. $^{31}P\{^1H\}$-NMR spectroscopy showed that after overnight heating the major constituent of the reaction mixture was Ph_2PCl (85 ppm), while there were also two set of doublets, one centred at 35.2 ppm (J = 225.1 Hz) and the other at 16.9 ppm (J = 222.4 ppm). One minor peak at 9.0 ppm was also observed. The reaction was repeated under the same conditions with the difference that the fluoride source was this time $N(n-Bu)_4F$. Surprisingly all of the

Ph$_2$PCl had been consumed. Unfortunately the spectrum consisted of a multitude of peaks with a minor one located at -10.0 ppm which is in agreement with the value reported for an authentic sample of the phosphine functionalised imidazolium salt **2.2a** (Scheme 7.3) prepared with the method described in Chapter 2. When the reaction was repeated in dichloromethane with N(n-Bu)$_4$F as the fluoride source, total consumption of Ph$_2$PCl was once again observed by means of ^{31}P{^{1}H}-NMR spectroscopy. Unfortunately no signals attributed to **2.2a** could be found in the ^{31}P{^{1}H}-NMR spectrum which consisted of peaks assignable to unidentified phosphorus containing species (a doublet of doublets centred at 7.4 ppm (J = 227.9 Hz, J = 580.5 Hz), and a singlet at 22.0 ppm)

The removal of the SiMe$_3$ functionality has been documented to occur by reaction with dry KF in the presence of dry 18-crown-6.[3] Once again, almost full conversion of Ph$_2$PCl (a minute peak at 82 ppm) was observed as well as formation of unidentified phosphorus species: a doublet centred at 163.7 ppm (J_{PF} = 877.0 Hz), a doublet centred at 36.7 ppm (J_{PF} = 227.4 Hz), three singlets at 29.0, 22.0 and −14.0 ppm and finally one triplet at -59.0 ppm (J_{PF} = 625.6 Hz).

These phosphorus species probably correspond to compounds containing P-F bonds. These are probably generated by substitution of chloride by fluoride in Ph$_2$PCl. Furthermore one must take into consideration that the experiments carried out in the presence of N(n-Bu)$_4$F have the inherent problem of moisture in N(n-Bu)$_4$F (anhydrous N(n-Bu)$_4$F has been recently prepared, during the preparation of this manuscript[4]). This could lead to the formation of oxo and hydroxo bridged species in solution.

In the light of these observations, it was clear that a new synthetic strategy had to be applied in order to access the target compounds. A simple route to the formation of the target imidazolium salt **7.5** is illustrated in Scheme 7.4. This synthetic approach presents as key reactants the imidazolium salt **7.3** and ^{t}Bu$_2$PH. Nucleophilic attack of the secondary phosphine on the secondary carbon attached to the halogen would generate the phosphonium salt **7.4** that, when treated with a base, would afford the target compound **7.5**.
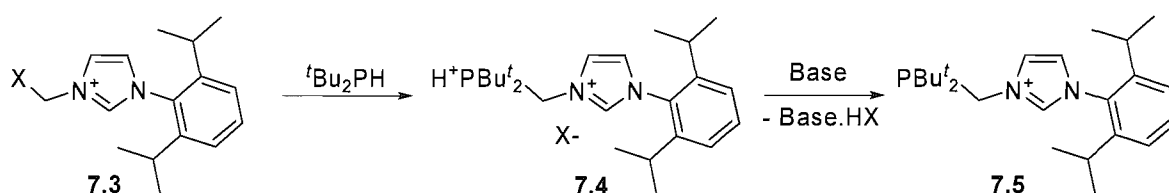
Scheme 7.4: Synthesis of phosphine functionalised imidazolium salts (X = halogen).

The synthesis of imidazolium salt **7.3** was attempted by reacting 3-(2,6-diisopropylphenyl)imidazole with dibromomethane in a microwave reactor. A 2:1 molar ratio of CH_2Br_2/3-(2,6-diisopropylphenyl)imidazole in toluene or acetonitrile gave a 1:1 mixture of the target imidazolium salt **7.6** and the imidazolium salt **7.7** (Scheme 7.5). When the reaction was performed in neat CH_2Br_2 (approximately 10:1 molar ratio of CH_2Br_2/3-(2,6-diisopropylphenyl)imidazole), the formation of the bis-imidazolium salt **7.7** was somewhat suppressed but not completely eliminated.
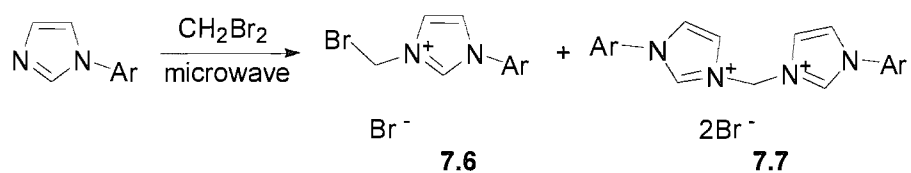
Scheme 7.5: Reaction of 3-(2,6-diisopropylphenyl)imidazole with CH_2Br_2 (Ar = 2,6-diisopropylphenyl).

In order to access the key imidazolium salt of type **7.3**, 1-(2,6-diisopropylphenyl)-imidazole was reacted with bromochloromethane (CH_2ClBr) to yield the imidazolium salt **7.8**. This was then converted to the imidazolium salt **7.9** by reaction with two equivalents of NaI in a 3:1 (v/v) mixture of $(CH_3)_2CO/CH_2Cl_2$ (Scheme 7.6).
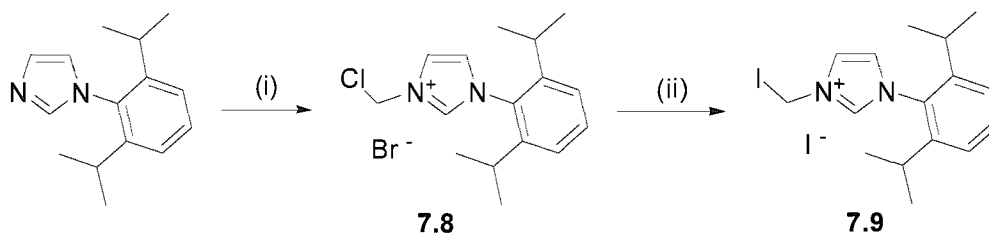
Scheme 7.6: Synthesis of imidazolium salts **7.8** and **7.9**. Reagents and conditions: (i): 10 equiv. CH_2ClBr, microwave at 110 °C for 10 min. (ii): 2 equiv. NaI in 3:1 (v/v) $(CH_3)_2CO/CH_2Cl_2$ at RT overnight.

The use of CH_2ClBr forms the imidazolium salt **7.8** selectively. This is probably due to the stronger C-Cl bond that hinders further nucleophilic attack by 1-(2,6-diisopropylphenyl)imidazole. The imidazolium salt **7.9** is easily derived from **7.8** by simple exchange of chloride with iodide. The formation of both imidazolium salts was established by ^{1}H-NMR and ^{13}C$\{^1$H$\}$-NMR spectroscopy as well as mass spectrometry. The latter was quite valuable in order to exclude the formation of mixed salts. In the case of **7.8** the ES$^+$ mass spectrum consisted of a peak at 277.1 Da with an isotopic envelope agreeing with the existence of a chloride atom in the parent cation. The ES$^-$ showed only the bromide anion. The same observations were made in the case of **7.9** where the ES$^+$ spectrum had only one peak at 369.1 Da, while the ES$^-$ spectrum showed the iodide anion at 126.9 Da.

Having synthesised the imidazolium salt **7.9**, its reaction with ^{t}Bu$_2$PH in ethanol was undertaken. After overnight stirring at room temperature, the reaction was quenched with NEt$_3$ or dry KOH. Unfortunately in both cases the ^{31}P$\{^1$H$\}$-NMR spectrum showed the existence of only ^{t}Bu$_2$PH (22.0 ppm). The failure of this reaction may be due to the fact that the formation of the intermediate phosphonium imidazolium salt **7.4** (Scheme 7.4) is disfavoured due to electrostatic repulsion.

Using the synthetic approach described above, we attempted to prepare the phosphine functionalised imidazolium salt **7.10** (Scheme 7.7).

X = OTf: **7.11**
X = Br: **7.12**

7.10
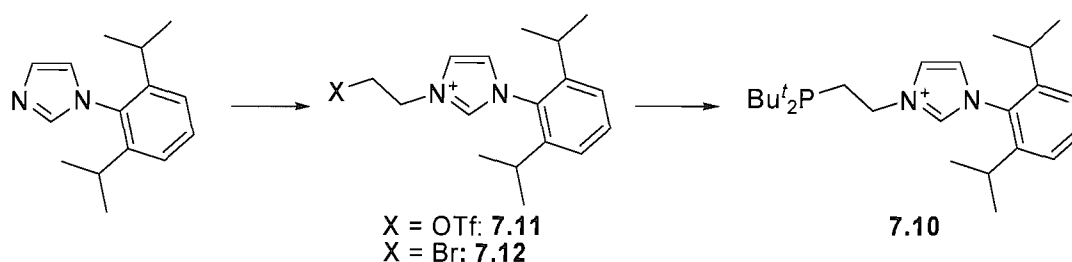
Scheme 7.7: Synthetic approach for the preparation of **7.10** (X = OTf (**7.11**), Br (**7.12**))

The key intermediates for this synthetic strategy are the imidazolium salts **7.11** and **7.12**. The first can be prepared by reaction of 3-(2,6-diisopropylphenyl)-1-(2-hydroxy-ethyl)-3H-imidazol-1-ium (**7.13**) with Tf$_2$O. Imidazolium salt **7.13** was prepared conventionally by reacting 1-(2,6-diisopropylphenyl)imidazole and 2-bromoethanol in refluxing 1,4-dioxane in a Young's ampoule. This method gave the desired imidazolium

salt in a very poor yield (28%). The formation of this imidazolium salt was forced to almost completion when the quarternisation took place under microwave irradiation (Scheme 7.8).
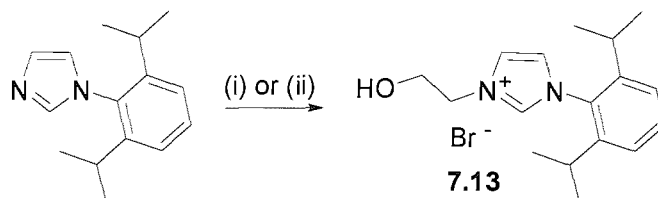
Scheme 7.8: Synthesis of imidazolium salt **7.13**.Reagents and conditions: (i): 3-(2,6-diisopropylphenyl)imidazole, 2-bromoethanol (1.2:1) in refluxing dioxane, (ii): 3-(2,6-diisopropyl-phenyl)-imidazole + 2-bromoethanol (1.1:1) microwave 120 °C for 10 minutes.

When the imidazolium salt was reacted with Tf$_2$O, a complex reaction mixture was formed as judged by ^{1}H-NMR spectroscopy. The most interesting feature of this spectrum was the existence of two imidazolium proton peaks in a 1:1 ratio. Mass spectrometry shed light on the identity of the mixture, which consisted of unreacted **7.13** and the imidazolium salt **7.12**, as evidenced by the isotopic pattern. This in turn means that the triflate being a good leaving group facilitates the exchange between bromide and triflate as counter anions. The hydroxyl functionalised imidazolium **7.13** was also reacted with TsCl in the presence of NEt$_3$ in DCM. Once again the tosylation was incomplete as evidenced by ^{1}H-NMR spectroscopy and the two imidazolium salts of the mixture could not be separated by column chromatography. Mass spectrometry provided some insight as it revealed that the two imidazolium proton peaks found in the ^{1}H-NMR spectrum can be attributed to **7.13** and the expected tosylated product.

The unexpected formation of **7.12** from the reaction of **7.13** with Tf$_2$O, led us to utilise it as key intermediate towards the synthesis of the target phosphine functionalised imidazolium salt **7.10** (Scheme 7.7). Nolan and co-workers have reported the synthesis of a similar to imidazolium salt **7.12** where the aryl functionality is 2,4,6-trimethylphenyl,[5] but the yield is unattractive.

Inspired by the almost quantitative preparative method described for **7.13** (Scheme 7.8), 1-(2,6-diisopropylphenyl)imidazole was dissolved in 1,2-dibromoethane (1:11 molar

ratio) and was heated in a microwave synthesizer at 120 °C for 15 minutes. This gave the desired imidazolium salt **7.12** (Scheme 7.9) in excellent yield (91%).
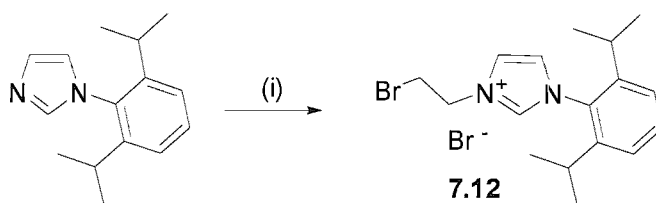
Scheme 7.9: Synthesis of imidazolium salt **7.12**. Reagents and conditions: (i): 1-(2,6-diisopropylphenyl)imidazole/Br(CH₂)₂Br (1:11), microwave radiation 120 °C for 15 minutes.

The imidazolium salt **7.12** was then reacted with ^{t}Bu₂PH in an attempt to access the desired phosphine functionalised imidazolium salt **7.10**. The reaction was attempted in EtOH, MeOH and DMSO. Unfortunately after work-up of the reaction mixture with a base (NEt₃ or KOH), ^{1}H-NMR spectroscopy revealed that two products coexisted. The major one proved to be unreacted imidazolium salt **7.12**, while the minor proved to be the vinyl functionalised imidazolium **7.15** (Scheme 7.10). Two plausible mechanisms for the formation of **7.15** are shown in Scheme 7.10.
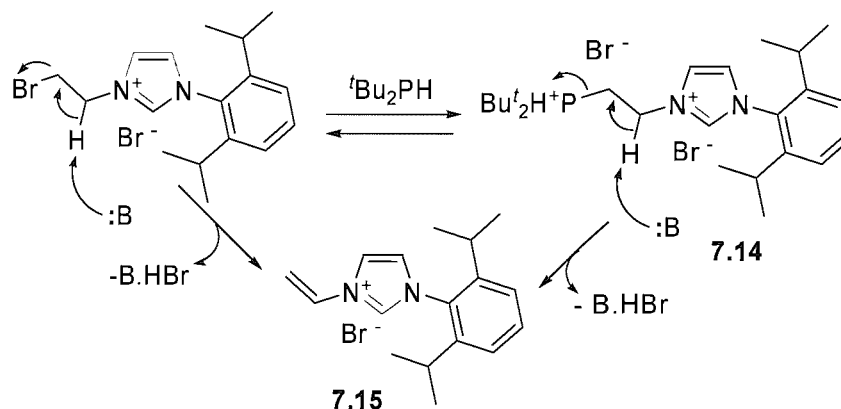
Scheme 7.10: Mechanisms for the formation of imidazolium salt **7.13** (Base = NEt₃, KOH).

After the formation of phosphonium salt **7.14**, addition of base produces **7.15** with concurrent release of ^{t}Bu₂PH. It could also be the case that **7.14** does not form at all due to electrostatic repulsion, and **7.15** is formed immediately upon interaction of **7.12** with the base.

In an other attempt to reach the target compound **7.10** (Scheme 7.7), the imidazolium salt **7.12** was reacted with two equivalents of $^tBu_2PLi$ or $^tBu_2P(BH_3)Li$ in either THF or DMSO. In all cases complex reaction mixtures were obtained. This could be due to the fact that the phosphides can act as bases deprotonating the imidazolium salt **7.12**. The $^{31}P\{^1H\}$-NMR spectra from aliquots of the reaction mixtures contained a myriad of peaks but showed the existence of $^tBu_2PH$ or $^tBu_2P(BH_3)H$ (48.3 ppm) as the major components of the reaction mixtures.

A fourth approach to achieving the synthesis of **7.10** could be found by reaction of the imidazolium salt **7.12** with $^tBu_2PSiMe_3$. The driving force is the formation of $SiMe_3Br$. Unfortunately the reaction led to the production of the vinyl functionalised imidazolium salt **7.15** and $^tBu_2PH$. The formation of the secondary phosphine was evidenced by the $^{31}P\{^1H\}$-NMR spectrum of an aliquot of the reaction mixture. The formation of **7.15** was substantiated by ES^+ mass spectrometry. A plausible mechanism for the formation of **7.15** is given in Scheme 7.11.
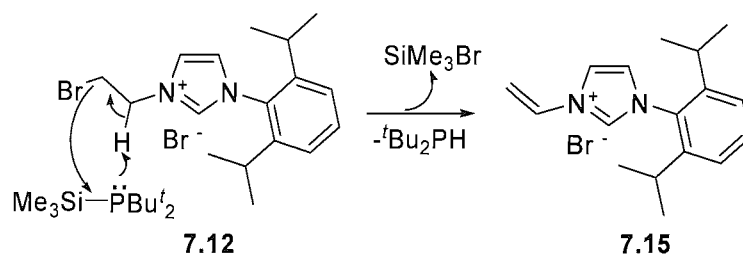
Scheme 7.11: Mechanism for the formation of **7.15** from the reaction of **7.12** with $^tBu_2PSiMe_3$.

In the light of this observation the reaction was repeated using $^tBu_2P(BH_3)SiMe_3$. The borane-protected phosphine could not facilitate the formation of **7.15** due to the unavailability of the electron lone pair. In this case the reaction would form the borane adduct of the desired phosphine functionalised imidazolium salt **7.10**, which could be converted to the target compound by deprotection with a mild base, *e.g.* NEt_3. The reaction took place using identical conditions as above but the $^{31}P\{^1H\}$-NMR spectrum of the reaction mixture showed after 12 hours that no reaction had taken place, since only $^tBu_2P(BH_3)SiMe_3$ (10.1 ppm) could be detected. Prolonged reaction times led to the formation of predominantly $^tBu_2P(BH_3)H$ through hydrolysis of $^tBu_2P(BH_3)SiMe_3$, and other unspecified phosphorus containing species. The ES^+ mass spectrum showed only the characteristic isotopic pattern for the imidazolium salt **7.12**.

233

Since the formation of the vinyl functionalised imidazolium salt **7.15** is so facile, it could be used as synthone towards the desired imidazolium salts. In an attempt to prepare an authentic sample, the imidazolium salt **7.12** was reacted with NEt_3 or DBU or pyridine in chlorobenzene. In all cases the formation of the imidazolium salt **7.15** was complete as judged by ^{1}H-NMR, but the samples were contaminated by Base·HBr salts that could not be separated by aqueous work-up. Nevertheless, salt **7.15** was prepared cleanly by reaction of **7.12** with KOH in refluxing THF. Having a reliable synthetic route for **7.15**, this was reacted with $^tBu_2PH$, in THF, in the presence of a radical initiator (AIBN) under photolysis conditions. This unfortunately produced intractable reaction mixtures. This radical mediated reaction was repeated thermally in refluxing chlorobenzene, without AIBN, but once again the reaction mixture contained as major constituents unreacted starting materials.

In view of the above failed attempts it was clear that different synthetic strategies had to be explored. Two different approaches are outlined in Scheme 7.12.
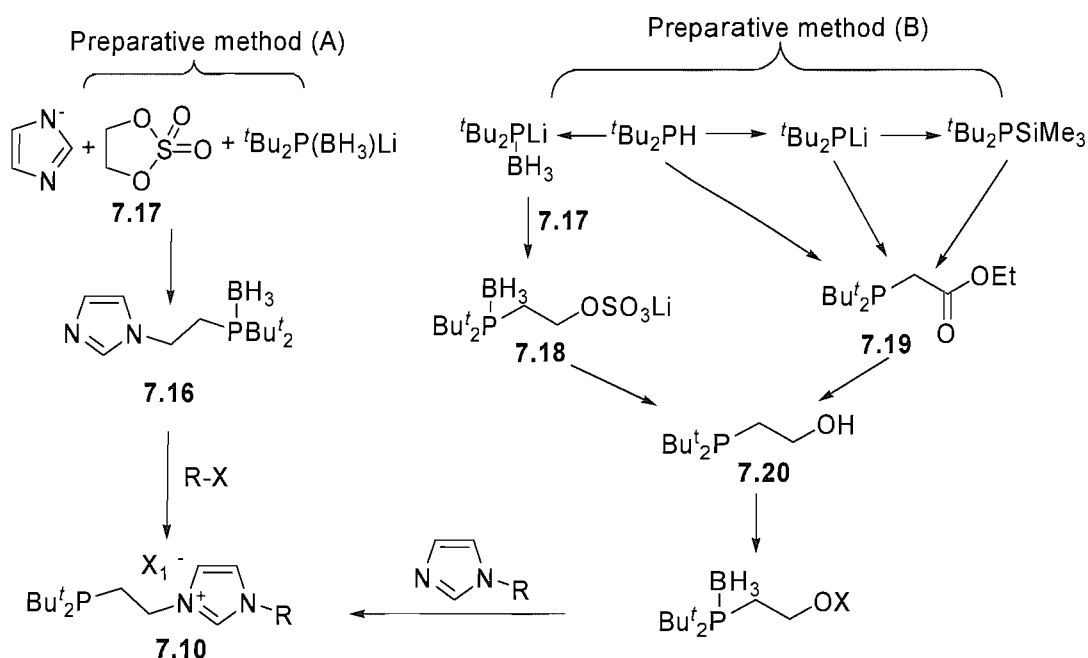
Scheme 7.12: Methods for accessing the target imidazolium salts (X_1 = halide, OTs, OTf; X = Ts, Tf).

The disadvantage of preparative method (A) is that it allows access only to phosphine functionalised imidazolium salts where R is an alkyl. The key intermediate of

this synthetic strategy is the phosphine functionalised imidazole **7.16**. Preparation of this was attempted by reacting $^tBu_2P(BH_3)Li$ with the cyclic sulphate **7.17** in THF followed by addition of potassium imidazolide. This reaction yielded a product soluble only in water, whose $^{31}P\{^1H\}$-NMR spectrum had one quartet centred at 38.7 ppm ($^1J_{PB}$ = 32.1 Hz). The ^1H-NMR spectrum presented the right number of peaks but the integration did not account for the formation of **7.16**. Analysis of this reaction mixture by mass spectrometry did not unravel the mystery.

Attempts to ring open **7.17** by using potassium imidazolide in either THF or DMF were not successful. The ^1H-NMR spectrum did not account for the formation of the desired product **7.21** (Scheme 7.13). Nevertheless ES$^-$ mass spectrometry showed the existence of the parent anion in 10% intensity.
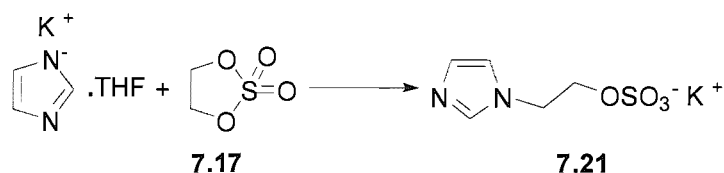
Scheme 7.13: Synthesis of **7.21** by ring opening of cyclic sulphate **7.17** with potassium imidazolide.

Unlike the synthetic strategy (A) outlined above, the preparative approach (B) allows access to imidazolium salts where R can be either an aryl or an alkyl. The key target compound is the 2-(alkylphosphino)ethanol **7.20**. Transformation of this alcohol to the tosylate or the triflate analogue, followed by protection of the phosphine with BH_3 and subsequent quarternisation with a bulky imidazole would lead to the desired imidazolium salts. Protection of the phosphine is essential, since bulky alkyl phosphines act as nucleophiles, removing the tosyl or triflic ester and yielding phosphonium salts. Another problem that might occur during the quarternisation is the removal of BH_3 from the phosphine by the free imidazole. In order to probe this, 1-(*tert*-butyl)-imidazole, 1-(2,4,6-trimethylphenyl)imidazole and 1-(2,6-diisopropylphenyl)imidazole were each mixed in an NMR tube with $^tBu_2P(BH_3)H$ in $CDCl_3$ and the $^{31}P\{^1H\}$ spectra were collected. Only in the case of 1-(*tert*-butyl)-imidazole was any deprotection observed; this was at a minimal level after two weeks.

The key phosphino alcohol **7.20** was prepared in moderate yield (46%) by reduction of phosphino ester **7.19** with LiAlH$_4$. Alternative routes (Scheme 7.12) were also investigated: the ring opening of the cyclic sulphate **7.17** with ^{t}Bu$_2$P(BH$_3$)Li followed by hydrolysis under acidic conditions yielded **7.20** in a 2% yield, while a more direct approach to **7.20** by reaction of ^{t}Bu$_2$PLi with *in situ* generated oxyrane, following a similar method described in the literature for the preparation of Cy$_2$P(CH$_2$)$_2$OH (Cy = cyclohexyl) [6], had no success.

Ester **7.19** has been reported in the literature and can be prepared by either elimination of SiMe$_3$Cl from the reaction between ^{t}Bu$_2$PSiMe$_3$ and ethyl chloroacetate[7] or from neutralisation of the phosphonium salt [^{t}Bu$_2$P$^+$(H)CH$_2$C(O)OEt]Br $^-$ with base.[8] The first preparative method did work but the yield was substantially lower than the one reported. Following an NMR scale reaction, in deuterated benzene, by ^{31}P$\{^1$H$\}$-NMR spectroscopy showed that after two hours at room temperature only ^{t}Bu$_2$PSiMe$_3$ could be detected. Upon standing at room temperature over the weekend, a myriad of peaks appeared in the ^{31}P$\{^1$H$\}$-NMR spectrum. Heating the benzene solution to boiling did not improve the appearance of the spectrum. Nevertheless a peak at 30.0 ppm could be detected which coincides with the reported value.[5] The reaction was repeated using n-octane and followed by ^{31}P$\{^1$H$\}$-NMR spectroscopy. Complete consumption of ^{t}Bu$_2$PSiMe$_3$ was evident after 16 hours at 100 °C. The spectrum showed a peak at 22.0 ppm corresponding to ^{t}Bu$_2$PH. The existence of the secondary phosphine can be rationalised from hydrolysis of ^{t}Bu$_2$PSiMe$_3$. The latter method yielded the phosphino ester **7.19** in 20% yield.

The preparative method (A) outlined in Scheme 7.12 was also utilised in an attempt to prepare phosphine functionalised imidazolium salts where the bulky alkyl is adamantyl (Ad) instead of *tert*-butyl. Bis-adamantyl-silyl phosphine was prepared by a method analogous for ^{t}Bu$_2$PSiMe$_3$, but unfortunately could not be isolated free of Ad$_2$PH.

The second method reported in the literature is based on the synthesis of a phosphonium salt, which is then neutralised with base to give the phosphino ester **7.19**. This literature method was unsuccessful in our hands.[6] The use of ethanol instead of acetone as solvent and triethylamine instead of NaOH$_{(aq.)}$ as base yielded the desired ester in 50% yield. The yield of the reaction was not amenable to scale up: doubling the scale of the reaction resulted in a decrease of yield by four times. This decrease in yield was observed both in the case of ^{t}Bu$_2$PH and Ad$_2$PH, with the adamantyl phosphine yielding no ester at all. The only major product that could be identified was the phosphonium salt

$[Ad_2P\{CH_2C(O)OEt\}]^+Br^-$ (**7.22**). The existence of the *tert*-butyl phosphonium salt analogue **7.23** was evident when $^tBu_2PH$ was used and was the major product upon scaling the reaction up. The rational behind this formation is outlined in Scheme 7.14.

R = Ad: **7.22**
R = ^{t}Bu: **7.23**
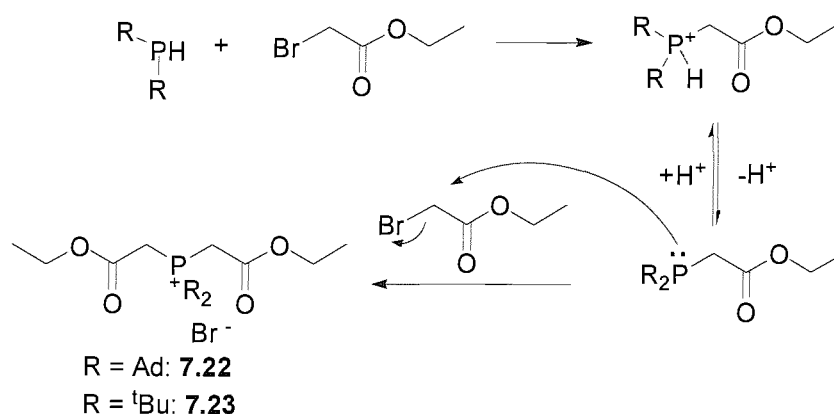
Scheme 7.14: Plausible mechanism for the formation of phosphonium salts **7.22** and **7.23**.

The first step, *i.e.* the quarternisation of the phosphine, is not quantitative. The phosphonium salt that is created is in equilibrium with the phosphino ester, which nucleophilically attacks the unreacted ethyl bromoacetate yielding the bis-ester phosphonium salts **7.22** and **7.23**. The driving force behind this transformation is the fact that the phosphonium salts are the energy sinks of the whole pathway.

In order to suppress the formation of the bis-ester phosphonium salt **7.23**, the reaction was repeated in neat $^tBu_2PH$. Removal of the excess secondary phosphine under vacuum yielded a white solid, which proved to be a mixture of mainly the mono-ester phosphonium salt (37.0 ppm) and minute traces of the bis-ester phosphonium salt **7.23** (46.7 ppm) as proved by $^{31}P\{^1H\}$-NMR spectroscopy. When this mixture was reacted with one equivalent of $KN(SiMe_3)_2$ in THF the phosphino ester **7.19** was formed as the sole product as determined by $^{31}P\{^1H\}$-NMR spectroscopy. Subsequent reduction of **7.19** with $LiAlH_4$ yielded the phosphino alcohol **7.20** in 50% yield.

A more direct method for accessing ester **7.19** was sought by reacting the BH_3 protected or unprotected di-*tert*-butylphosphide with ethyl bromoacetate, thus eliminating LiBr. Unfortunately the reaction did not work as expected. This failure was, to some extent, expected since it is well documented that reaction of alkyl halides with lithium alkyl phosphides leads to exchange between lithium and halide on the phosphorus centre, resulting subsequently in the formation of P_2R_4 species.[9]

Finally reaction of $^tBu_2P(BH_3)Li$ with ethylene bicarbonate in THF at room temperature (-78 °C to RT) or under more forcing conditions (-78 °C to RT and then to reflux) followed by hydrolysis, did not yield the desired phosphino alcohol **7.20**.

Nevertheless a reproducible method to preparing the novel phosphino alcohol **7.20** was devised, and the next step of our synthetic stratagem, *i.e.* the protection of the alcohol was undertaken. This step is essential since the protection of the phosphine part of the molecule with BH_3 would not work in the presence of a free OH functionality. Unfortunately conversion of **7.20** to either the tosylate or triflic ester did not work as evidenced by $^{31}P\{^1H\}$-NMR spectroscopy, which revealed in the reaction mixture unreacted **7.20** (16.1 ppm) and unidentified phosphorus species.

7.2.2 Synthetic approaches towards Cy phosphine functionalised imidazolium salts

Unlike the *tert*-butyl or adamantyl phosphine functionalised imidazolium salts, the cyclohexyl phosphine imidazolium salts **7.25** could be synthesised by reduction of the corresponding phosphine-oxide imidazolium salts **7.24** using $SiHCl_3$ (Scheme 7.15). It has been reported in literature that phosphinoxide $Cy_2P(O)(CH_2)_2P(O)Cy_2$ can be reduced to the corresponding bis-phosphine with $SiHCl_3$ under the same conditions used for the preparation of the phenyl phosphine functionalised imidazolium salts prepared in Chapter 2.[10]
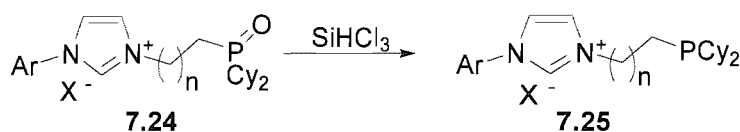
Scheme 7.15: Preparation of cyclohexyl functionalised imidazolium salts (X = halide, n = 0,1; Our investigation into the preparation of these imidazolium salts was limited only to those where n =1).

The synthesis of **7.24** could be achieved by quarternisation of the appropriate 3-aryl imidazole with (ω-bromoethyl)dicyclohexylphosphine oxide. The latter could be prepared by an Arbuzov reaction (Scheme 7.16). When the Arbuzov reaction was carried

out in the same way as for the synthesis of (ω-bromoethyl)diphenylphosphine oxide, the only product that could be isolated was $Cy_2P(O)(CH_2)_2P(O)Cy_2$.

Cy₂P(O)(CH₂)₂Br ←(–EtBr)— Cy₂POEt —(–EtBr)→ O=P(Cy₂)(CH₂)₂P(Cy₂)=O

with 1,2-dibromoethane (BrCH₂CH₂Br) reagents
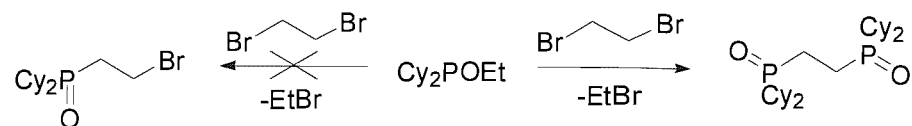
Scheme 7.16: Arbuzov reaction leading to the formation of $Cy_2P(O)(CH_2)_2P(O)Cy_2$.

To tackle this unexpected drawback, we decided to use $Cy_2PO^{i}Pr$ instead of Cy_2POEt, in order to hinder the reversibility of the Arbuzov reaction. The preparation of $Cy_2PO^{i}Pr$ has been achieved by reaction of Cy_2PCl with isopropanol, [11] but the isolated yield was significantly lower (50%) than the one reported. This problem was solved by reacting Cy_2PCl with LiOiPr in benzene giving the desired phosphite in quantitative yield.

When the Arbuzov reaction between $Cy_2PO^{i}Pr$ and 1,2-dibromoethane (1,2-DBE) was carried out as above it produced a mixture of the desired (ω-bromoethyl)dicyclo-hexylphosphine oxide and $Cy_2P(O)(CH_2)_2P(O)Cy_2$, with the latter being the predominant species. The formation of $Cy_2P(O)(CH_2)_2P(O)Cy_2$ could be due to the very fast rate of addition of $Cy_2PO^{i}Pr$ to the twenty fold excess of 1,2-DBE. In an attempt to suppress its formation, the reaction was carried out by controlling the addition of $Cy_2PO^{i}Pr$ using a mechanical syringe programmed to deliver the phosphite continuously over a period of 12 hours. Unfortunately the reaction mixture consisted of more than one phosphorus species as evidenced by $^{31}P\{^{1}H\}$-NMR spectroscopy and ES^{+} mass spectrometry (Scheme 7.17), and separation by column chromatography was unsuccessful.

Cy₂POPrⁱ —(BrCH₂CH₂Br, –ⁱPrBr)→ O=P(Cy₂)(CH₂)₂P(Cy₂)=O + Cy₂P(O)(CH₂)₂Br + Cy₂P(O)(allyl)
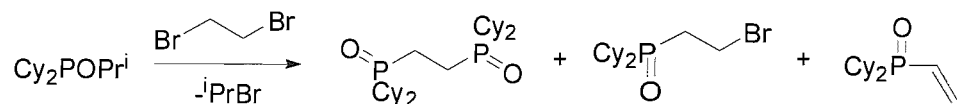
Scheme 7.17 Arbuzov reaction with $Cy_2PO^{i}Pr$, under slow addition conditions.

239

In an attempt to synthesise (ω-bromoethyl)dicyclohexylphosphine oxide, $Cy_2P(O)K$, prepared from $Cy_2P(O)H$ and $KN(SiMe_3)_2$, was reacted with 1,2-DBE. Unfortunately the $^{31}P\{^1H\}$-NMR of the reaction showed the presence of mainly $Cy_2P(O)H$ and other unidentified phosphorus species.

A more direct pathway to the phosphinoxide functionalised imidazolium salt **7.24** could be achieved by reacting $Cy_2P(O)K$ with the 2-bromoethyl-imidazolium salt **7.12**. The reaction was carried out in DMSO and after work up the ^1H-NMR spectrum showed largely unreacted imidazolium salt **7.12** and the vinyl functionalised imidazolium salt **7.15**. The existence of the latter was also confirmed by ES^+ mass spectrometry.

7.3 Conclusions

This chapter described attempts to tackle the synthesis of some challenging phosphine functionalised imidazolium salt NHC precursors. The troublesome synthesis of key intermediates, as well as the formation of by-products hindered the completion of the synthesis of our target compounds. Nevertheless our attempts to access these imidazolium salts through alternative synthetic pathways has led to the preparation of the novel functionalised imidazolium salts **7.8**, **7.9**, **7.12**, **7.13** and **7.15** as well as to the synthesis of the novel 2-(di-*tert*-butyl-phosphino)-ethanol. The most interesting feature of the synthesis of the above imidazolium salts (except **7.15** and **7.9**) is the utilisation of microwave radiation to successfully complete the quarternisation reaction cleanly, in high yields and with reduced reaction times, even with 3-aryl-imidazoles that are not as reactive as their alkyl analogues. This new synthetic approach could be applied in the preparation of novel ionic liquids.

7.4 Experimental

General materials: $^tBu_2PSiMe_3$,[5] Ad_2PH,[11] $Cy_2P(O)H$,[9] $^tBu_2P(BH_3)H$,[12] $^tBu_2PLi$,[13] $^tBu_2P(BH_3)Li$[14] and [1,3,2]-dioxothiolane-2,2-dioxane [15] (**7.17**) were prepared following literature procedures. Cy_2PCl was bought from Aldrich and was used as received. Imidazolium salt **7.2** was prepared by heating imidazole with bromomethyl-trimethyl-silane in 1,4-dioxane, while the imidazolium precursor of **7.1** was prepared according to literature procedures.[16] Carbene **7.1** was generated *in situ* by reacting its azolium precursor with one equivalent of $KN(SiMe_3)_2$ in THF. The microwave synthesizer was a Smith Synthesiser from Personal Chemistry.

Procedure for the synthesis of $^tBu_2PH$: A three L three-neck flask left in a 100 °C oven for 12 hours was equipped with a mechanical stirrer, a double jacketed condenser and a 100 mL pressure equalising funnel and was charged with 28 g (1.15 gr-at) of Mg turnings. The mechanical stirrer was set in motion and the apparatus was degassed by passing a stream of N_2 for at least 30 minutes. Approximately 400 mL of freshly distilled and degassed Et_2O were added and the Mg turnings were activated by adding 1 mL of 1,2-dibromopropane. More Et_2O was added until an approximate volume of 1.3 L The pale grey solution was brought to 0 °C and 5 mL of ^tBuCl was added. The solution was brought to room temperature and gently heated until Et_2O started to reflux. The rest of the 93 g (1.0 mol) of ^tBuCl was added in such a rate that reflux was maintained over a period of three hours. After the addition was completed the Grignard solution was refluxed for one more hour to complete the reaction. The mixture was then cooled to -15 °C using a salt-ice slush bath and 15 mL (0.30 mol) of PCl_3 in 50 mL of Et_2O was added dropwise. Precipitation occurred immediately and after the addition was complete the suspension was left stirring overnight at room temperature under a N_2 atmosphere. The contents of the flask were then transferred to a three-neck 5 L flask by means of a 3 cm diameter Teflon tube and more Et_2O was added (approximately 1 L). The new flask was equipped with a mechanical stirrer and a 50 mL pressure equalising funnel. The solution was cooled down to 0 °C and a suspension of 10 g (4 equiv.) of $LiAlH_4$ in 100 mL of Et_2O cooled at 0 °C was added slowly over a period of 40 minutes to the contents of the 5 L flask. Upon addition the suspension became very viscous and stirring was hindered. The addition at this point of 50 mL of THF circumvented the problem. The mixture was stirred overnight at room temperature under a N_2 atmosphere. It was then cooled down to 0 °C and approximately 40 mL of dry-degassed MeOH were added very carefully over a period of

241

one hour. After completing the addition of MeOH, approximately 500 mL of degassed

saturated $NH_4Cl_{(aq.)}$ solution were added slowly. 10 % (v/v) of degassed $HCl_{(aq.)}$ was added

until the pH of the water phase was around 4 and the two layers were separated. The

aqueous phase was extract twice with 1 L of Et_2O and the organic layers were combined,

dried over $MgSO_4$ and filtered through Celite. Et_2O was removed by distillation through a

fractionating column at atmospheric pressure. During this procedure a white precipitate

formed, which was separated from the mother liquor by vacuum distillation after addition

of 250 mL of PE to the latter. Distillation of the remaining solvents at atmospheric

pressure gave an almost colourless oil, from which $^tBu_2PH$ was distilled under reduced

pressure (60 °C at 40 mmHg) under a static vacuum into a Schlenk tube cooled at liquid

N_2 temperature. Yield: 11.2 g (65 %). ^1H and $^{31}P\{^1H\}$ data agree with reported values.[17]

$^tBu_2P(BH_3)SiMe_3$: 522 mg (2.4 mmol) of $^tBu_2PSiMe_3$ were charged into a Schlenk tube

and were dissolved in approximately 20 mL of PE. To this solution 0.4 mL of $BH_3.DMS$

(6.2M solution in THF) were added at room temperature and the reaction mixture was

stirred overnight. The solvent was removed under reduced pressure to give 555 mg (99 %)

of $^tBu_2P(BH_3)SiMe_3$ as a white solid. ^1H-NMR $\delta(C_6D_6)$: 0.09 (9H, d, $^3J_{PH}$ = 3.6 Hz,

$^tBu_2P(BH_3)SiMe_3$), 1.12 (18H, d, $^3J_{PH}$ = 12.8 Hz, $((CH_3)_3C)_2P(BH_3)SiMe_3$); $^{13}C\{^1H\}$-

NMR $\delta(C_6D_6)$: -0.1 (d, $^2J_{PH}$ = 15.6 Hz, $^tBu_2P(BH_3)Si(CH_3)_3$), 28.2 (s,

$((CH_3)_3C)_2P(BH_3)SiMe_3$), 31.5 (d, $^1J_{PH}$ = 19.3 Hz, $((CH_3)_3C)_2P(BH_3)SiMe_3$); $^{31}P\{^1H\}$-

NMR $\delta(C_6D_6)$: 10.1 (q, $^1J_{PB}$ = 40.9 Hz, $^tBu_2P(BH_3)SiMe_3$).

Ad_2PSiMe_3: In the glove box a Schlenk tube was charged with 500 mg (1.7 mmol) of

Ad_2PH. This was dissolved in 20 mL of THF and the solution was cooled down to -40 °C

using a dry-ice/acetone slush bath. To this solution 1.5 equivalents of n-BuLi (0.66 mL,

2.5 M solution in hexanes) were added and the reaction mixture was slowly warmed up to

room temperature and stirred for another hour, upon which time a yellow solid

precipitated. This was filtered, washed with toluene and dried under vacuum. This solid

was suspended in 10 mL of THF, cooled down to -40 °C using a dry-ice/acetone slush

bath and 210 μL (1 equiv. assuming full conversion to Ad_2PLi) of freshly dry-distilled

$SiMe_3Cl$ were added. The colour of the suspension changed immediately from yellow to

white and upon stirring at -40 °C the solids dissolved. Warming to room temperature,

stirring for another hour, followed by removal of the volatiles, extraction in benzene,

filtration and removal of the solvent gave a white solid. ^1H-NMR $\delta(C_6D_6)$: 0.12 (9H, d,

$^3J_{PH}$ = 8.9 Hz, $Ad_2PSi(CH_3)_3$), 1.08–2.10 (30H, m, Ad_2PSiMe_3); $^{31}P\{^1H\}$-NMR $\delta(C_6D_6)$:

0.31 (s, Ad_2PSiMe_3), 18.7 (s, Ad_2PH). The product was contaminated with Ad_2PH.

Attempts to prepare Ad₂PCH₂C(O)OEt from Ad₂PSiMe₃ and ethyl chloroacetate using a similar method to the one described for the *tert*-butyl analogue did not meet any success in our hands.

Cy₂POEt: A three-neck 100 mL round bottom flask equipped with condenser, pressure equalising addition funnel and nitrogen inlet was charged with 1 mL (1054 mg, 4.5 mmol) of Cy₂PCl. This was dissolved in approximately 25 mL of Et₂O. To this 630 μL of dry-degassed NEt₃ were added. 61 μL of EtOH in 2 mL of Et₂O were slowly added over 10 minutes. After the addition was completed a white precipitate formed, and the reaction mixture was left stirring overnight at room temperature. It was then filtered and the precipitate was washed with Et₂O (3 × 10 mL). The solvent was removed from the filtrate to leave an almost colourless oil which was bridge to bridge distilled to give 545 mg (50 %) of Cy₂POEt. ^{1}H-NMR δ(C₆D₆): 0.92-2.12 (27H, m, $Cy_2POCH_2CH_3$); ^{13}C{^{1}H}-NMR δ(C₆D₆): 26.4 (s, Cy₂POCH₂CH₃), 26.7 (d, J_{PC} = 6.7 Hz, CH₂ of (C_6H₁₁)₂POEt), 27.0 (d, J_{PC} = 12.7 Hz, CH₂ of (C_6H₁₁)₂POEt), 27.3 (d, J_{PC} = 7.7 Hz, CH₂ of (C_6H₁₁)₂POEt), 28.4 (d, $^2J_{PC}$ = 18.1 Hz, Cy₂POCH₂CH₃), 38.4 (d, $^1J_{PC}$ = 32.0 Hz, CH of (C_6H₁₁)₂POEt); ^{31}P{^{1}H}-NMR δ(C₆D₆): 45.5 (s, Cy₂POCH₂CH₃).

Cy₂PO^{i}Pr improved procedure:1 mL (1054 mg, 4.5 mmol) of Cy₂PCl was transferred into a Schlenk tube and 25 mL of dry-degassed benzene were added. To this solution 223 mg (1.1 equiv.) of LiO^{i}Pr in 15 mL of benzene were slowly added by means of a cannula and the mixture was left stirring at room temperature overnight under nitrogen. It was then filtered through Celite and the solvent was removed under reduced pressure (care should be taken as benzene freezes at 5 °C) to leave a colourless oil. This was trap-to-trap distilled to separate any excess of LiO^{i}Pr to give the title compound as a colourless oil. Yield: 1218 mg (>99 %). Spectroscopic data agree with the ones reported in literature.[9] LiO^{i}Pr was prepared by reaction of freshly dried and distilled under nitrogen ^{i}PrOH with n-BuLi (1:1 molar ratio) in hexanes.

Cy₂P(O)K: A Schlenk tube was charged with 500 mg (2.3 mmol) of Cy₂P(O)H. The apparatus was degassed and the phosphine oxide was dissolved in 20 mL of THF. The solution was cooled down to -30 °C and to this a solution of 458 mg (1 equiv.) of KN(SiMe₃)₂ in approximately 15 mL of THF was added *via* cannula. Upon addition a white precipitate formed. The reaction mixture was left stirring at room temperature for two hours, and volatiles were removed under reduced pressure to give the title compound as a white solid. Yield: 578 mg (>99 %). Anal. Found: C, 56.99; H, 8.78 %. Calcd for:

$C_{12}H_{22}KOP$: C, 57.11; H, 8.79 %. Further characterisation was hindered due to insolubility in common organic solvents.

7.8: A quartz vial was charged with 1000 mg (4.4 mmol) of 3-(2,6-diisopropylphenyl)-imidazole and 3 mL (11 equiv.) of CH_2BrCl. The imidazole was dissolved by stirring and the vial was sealed with a septum cap. The contents were then heated at 125 °C for 10 minutes in a microwave synthesiser. The volatiles were removed at reduced pressure, and the pale yellow oily residue was triturated with ether to give a white solid. This was left in contact with ether for 2 hours and after decantation of ether it was dried under vacuum to give 1.25 g (80 %) of the title compound. ^{1}H-NMR $\delta(CDCl_3)$: 1.13 (6H, d, $^3J_{HH}$ = 6.4 Hz, $CH(CH_3)_2$), 1.22 (6H, d, $^3J_{HH}$ = 7.3 Hz, $CH(CH_3)_2$), 2.17 (2H, two overlapping septets with $^3J_{HH}$ = 6.4 Hz and $^3J_{HH}$ = 7.3 Hz, $CH(CH_3)_2$), 7.01 (1H, s, imidazolium backbone), 7.12 (2H, d, $^3J_{HH}$ = 7.3 Hz, aromatic), 7.54 (1H, t, $^3J_{HH}$ = 7.3 Hz, aromatic), 8.04 (2H, s, imidazolium-CH_2Cl), 9.97 (1H, s, imidazolium backbone), 11.4 (1H, s, NC(H)N); $^{13}C\{^1H\}$-NMR $\delta(CDCl_3)$: 24.6 (s, $CH(CH_3)_2$), 24.8 (s, $CH(CH_3)_2$), 29.1 (s, $CH(CH_3)_2$), 29.3 (s, $CH(CH_3)_2$), 56.9 (s, imidazolium-CH_2Cl), 125.3 (s, imidazolium backbone), 125.4 (s, imidazolium backbone), 130.1 (s, aromatic), 132.5 (s, aromatic), 132.8 (s, aromatic), 139.4 (s, aromatic), 145.7 (s, NC(H)N); ES+: 277 [imidazolium-$CH_2Cl]^+$, 321 [imidazolium-$CH_2Cl+MeCN]^+$; ES⁻: 79 [Br]⁻.

7.9: 250 mg (0.7 mmol) of **7.8** were charged in a 50 mL round bottom flask and were dissolved in 5 mL of DCM at room temperature. To this was added 15 mL of acetone and 231 mg (2.2 equiv.) of NaI with vigorous stirring. Stirring at room temperature was continued overnight. The volatiles were removed on a rotary evaporator and DCM was added to the solid residue (20 mL). The solution was filtered through Celite and the solvent was removed to leave a pale yellow solid, which was washed with ether and dried under vacuum. Yield: 340 mg (98 %). ES⁺: 496 [imidazolium-$CH_2I]^+$; ES⁻: 127 [I]⁻. Anal.Found: C, 38.82; H, 4.39; N, 5.21 %. Calcd for $C_{16}H_{22}N_2I_2$: C, 38.73; H, 4.47; N, 5.65 %.

7.12: A quartz vial was charged with 1000 mg (4.4 mmol) of 3-(2,6-diisopropylphenyl)-imidazole and 4 mL (11 fold excess) of 1,2-dibromoethane. The imidazole was dissolved in DBE and the vial was sealed with a septum cap, placed in a microwave synthesiser and heated at 125 °C for 10 minutes. The volatiles were removed on a rotary evaporator to leave a yellow sticky solid. This was washed first with Et_2O (20 mL) and then with PE (20 mL). It was then dissolved in the minimum amount of THF and was precipitated by adding a 1:1 (v/v) mixture of Et_2O/PE to give the title compound as a white solid, which

244

was dried under vacuum overnight. Yield: 1650 mg (91 %). ^{1}H-NMR δ(CDCl$_3$): 1.09 (6H, d, $^3J_{HH}$ = 6.4 Hz, CH(C*H$_3$*)$_2$), 1.16 (6H, d, $^3J_{HH}$ = 6.4 Hz, CH(C*H$_3$*)$_2$), 2.20 (2H, sept., $^3J_{HH}$ = 6.4 Hz, C*H*(CH$_3$)$_2$), 3.95 (2H, t, $^3J_{HH}$ = 4.5 Hz, BrC*H$_2$*CH$_2$-imidazolium), 5.19 (2H, t, $^3J_{HH}$ = 4.5 Hz, BrCH$_2$C*H$_2$*-imidazolium), 6.98 (1H, s, imidazolium backbone), 7.11 (2H, d, $^3J_{HH}$ = 7.3 Hz, aromatic), 7.37 (1H, t, $^3J_{HH}$ = 7.3 Hz, aromatic), 8.72 (1H, s, imidazolium backbone), 10.1 (1H, s, NC(*H*)N); ES$^+$: 335 [BrCH$_2$CH$_2$-imidazolium]$^+$.

7.13 Method A: A 50 mL ROTAFLO ampoule was charged with 1.00 g (4.4 mmol) of 3-(2,6-diisopropylphenyl)imidazole and degassed. The ampoule was opened under a stream of nitrogen and 15 mL of dry-degassed 1,4-dioxane were added. The suspension was then stirred until all imidazole dissolved and 550 mg (0.9 equiv.) of 2-bromoethanol were added. The ampoule was sealed under partial vacuum and heated overnight at 100 °C. The volatiles were removed by rotary evaporator and the yellow oily product was left standing in contact with Et$_2$O overnight. During this time a white solid formed. Th ether was decanted and the solid was dried under vacuum to yield 434 mg (28 %) of the title compound as a white foamy solid. ^{1}H-NMR δ(CDCl$_3$): 1.11 (6H, d, $^3J_{HH}$ = 7.3 Hz, CH(C*H$_3$*)$_2$), 1.28 (6H, d, $^3J_{HH}$ = 7.3 Hz, CH(C*H$_3$*)$_2$), 2.31 (2H, sept., $^3J_{HH}$ = 7.3 Hz, C*H*(CH$_3$)$_2$), 4.07 (2H, t, $^3J_{HH}$ = 4.2 Hz, OHCH$_2$C*H$_2$*-imidazolium), 4.88 (2H, t, $^3J_{HH}$ = 4.2 Hz, OHC*H$_2$*CH$_2$-imidazolium), 7.00 (1H, s, imidazolium backbone), 7.11 (2H, d, $^3J_{HH}$ = 7.3 Hz, aromatic), 7.44 (1H, t, $^3J_{HH}$ = 7.3 Hz, aromatic), 8.07 (1H, s, imidazolium backbone), 9.83 (1H, s, NC(*H*)N); ^{13}C{^{1}H}-NMR δ(CDCl$_3$): 24.2 (s, CH(CH$_3$)$_2$), 24.5 (s, CH(CH$_3$)$_2$), 28.7 (s, *C*H(CH$_3$)$_2$), 52.3 (s, OHCH$_2$*C*H$_2$-imidazolium), 60.4 (s, OH*C*H$_2$CH$_2$-imidazolium), 123.9 (s, imidazolium backbone), 124.5 (s, imidazolium backbone), 124.7 (s, aromatic), 130.2 (s, aromatic), 132.1 (s, aromatic), 138.3 (s, aromatic), 145.6 (N*C*(H)N); ES$^+$: 273 [imidazolium-CH$_2$CH$_2$OH]$^+$.

7.13 Method B: A quartz vial was charged with 800 mg (3.5 mmol) of 3-(2,6-diisopropyl-phenyl)imidazole, 440 mg (0.9 equiv.) of 2-bromoethanol was slowly added so that the imidazole was moisturised by the 2-bromoethanol. The vial was then sealed with a septum cap and was heated at 120 °C for 10 minutes in a microwave synthesiser. The beige solid was dissolved in DCM (10 mL) and volatiles were removed by rotary evaporation, yielding a brown oily product. This was washed with ether and redissolved in DCM. The volatiles were removed to give 1177 mg (95 %) of the title compound as foamy beige solid. ^{1}H-NMR and ES$^+$ are identical with the ones reported in method A above.

7.15: 500 mg (1.2 mmol) of **7.12** were charged in a 100 mL round bottom flask and were dissolved under vigorous stirring in approximately 25 mL of THF. To this solution 68 mg

(1 equiv.) of ground KOH were added in one portion. The flask was equipped with a condenser and the reaction mixture was refluxed for two hours, upon which time the reaction was complete as determined by ES^+ spectrometry. The volatiles were removed at reduced pressre and DCM was added. The solution was filtered through Celite, the solvent was removed and the remaining solid was washed with ether and dried under vacuum. Yield: 350 mg (87 %). ^{1}H-NMR $\delta(CDCl_3)$: 1.08 (6H, d, $^3J_{HH}$ = 6.7 Hz, CH(CH_3)$_2$), 1.19 (6H, d, $^3J_{HH}$ = 6.7 Hz, CH(CH_3)$_2$), 2.27 (2H sept., $^3J_{HH}$ = 6.7 Hz, CH(CH$_3$)$_2$), 5.39 (1H, dd, $^2J_{HH}$ = 2.7 Hz, $^3J_{HH}$ = 8.7 Hz, terminal vinyl *cis* to the CH vinyl proton of the carbon attached to the imidazolium moiety), 6.04 (1H, dd, $^2J_{HH}$ = 2.7 Hz, $^3J_{HH}$ = 15.6 Hz, terminal vinyl *trans* to the CH vinyl proton of the carbon attached to the imidazolium moiety), 7.20 (1H, br. s, imidazolium backbone), 7.26 (2H, d, $^3J_{HH}$ = 7.7 Hz, aromatic), 7.48 (1H, t, $^3J_{HH}$ = 7.7 Hz, aromatic), 8.20 (1H, dd, $^3J_{HH}$ = 8.7 Hz, $^3J_{HH}$ = 15.6 Hz, vinyl CH), 8.34 (1H, br. s, imidazolium backbone), 10.9? (1H, s, NC(H)N); $^{13}C\{^1H\}$-NMR $\delta(CDCl_3)$: 24.4 (s, CH(CH$_3$)$_2$), 24.5 (s, CH(CH$_3$)$_2$), 28.9 (s, CH(CH$_3$)$_2$), 46.1 (s, terminal vinyl CH$_2$), 109.7 (s, vinyl CH), 119.4 (s, imidazolium backbone), 124.9 (s, imidazolium backbone), 129.3 (s, aromatic), 130.2 (s, aromatic), 132.2 (s, aromatic), 138.5 (s, aromatic), 145.5 (s, NC(H)N); ES^+: 255.

7.18: In the glove box 500 mg (3.0 mmol) of $^tBu_2P(BH_3)Li$ were placed in a Schlenk tube, and cooled down to -78 °C using a dry-ice/acetone slush bath, and 20 mL THF were slowly added to give a yellow solution. A second Schlenk was charged with 373 mg (1 equiv.) of cyclic sulphate **7.17**, degassed, cooled down to -78 °C and dissolved in 10 mL of THF. The solution of $^tBu_2P(BH_3)Li$ was slowly transferred by cannula to the solution of the cyclic sulphate, and the resulting reaction mixture was allowed to equilibrate at ambient temperature and then stirred for an extra two hours. Removal of volatiles under reduced pressure left a white solid, which was washed with PE (2 × 10 mL) and dried under vacuum. Yield: 800 mg (92 %). ^{1}H-NMR $\delta(CD_2Cl_2)$: 1.08 (3H, br. s, $^tBu_2P(BH_3)CH_2CH_2SO_3Li$), 1.18 (18H, d, $^3J_{PH}$ = 12.5 Hz, ((CH_3)$_3C$)$_2$P(BH$_3$)CH$_2$CH$_2$SO$_3$Li), 2,72 (2H, m, $^tBu_2P(BH_3)CH_2CH_2SO_3Li$), 4.86 (2H, m, $^tBu_2P(BH_3)CH_2CH_2SO_3Li$); $^{31}P\{^1H\}$-NMR $\delta(CD_2Cl_2)$: 39.4 (q, $^1J_{PB}$ = 25.6 Hz, $^tBu_2P(BH_3)CH_2CH_2SO_3Li$).

7.19 and 7.23 Method A: This was prepared using a modification of a published procedure.[18] 811 mg (5.5 mmol) of $^tBu_2PH$ was dissolved in 15 mL dry-degassed EtOH and the solution was cooled down to 0 °C. To this solution 928 mg (1 equiv.) of ethyl bromoacetate were added and the solution was stirred overnight at room temperature.

Ether was then added (50 mL) and after that NEt$_3$ (approx. 5 mL). The solution was filtered and washed with Et$_2$O (3 × 20 mL). Removal of volatiles produced a white oily solid, which was washed with PE (3 × 10 mL) and then filtered. PE was removed from the supernatant under reduced pressure to yield a yellow oil which upon bridge distillation gave 645 mg (50 % yield) of the phosphino ester **7.19**. Spectroscopic data agree with the ones reported in the literature.[5] The white solid insoluble in PE was the phosphonium salt [^{t}Bu$_2$P{CH$_2$C(O)OEt]$_2$]$^+$Br $^-$ (**7.23**). Spectroscopic data for **7.23**: ^{1}H-NMR δ(CDCl$_3$): 1.11 (6H, t, $^3J_{HH}$ = 7.3 Hz, salt [^{t}Bu$_2$P{CH$_2$C(O)OCH$_2$CH_3}$_2$]$^+$), 1.59 (18H, d, $^2J_{PH}$ = 16.4 Hz, [((CH_3)$_3$C)$_2$P{CH$_2$C(O)OCH$_2$CH$_3$}$_2$]$^+$), 4.01 (4H, d, $^2J_{PH}$ = 12.8 Hz, [^{t}Bu$_2$P{CH_2C(O)OCH$_2$CH$_3$}$_2$]$^+$), 4.20 (4H, q, $^3J_{HH}$ = 7.3 Hz, [^{t}Bu$_2$P{CH$_2$C(O)OCH_2CH$_3$}$_2$]$^+$); ^{13}C{^{1}H}-NMR δ(CDCl$_3$): 14.0 (s, [^{t}Bu$_2$P{CH$_2$C(O)OCH$_2$$CH_3$}$_2$]$^+$), 24.5 (d, $^1J_{PC}$ = 44.1 Hz, [^{t}Bu$_2$P{CH$_2$C(O)OCH$_2$CH$_3$}$_2$]$^+$), 27.8 (s, [((CH$_3$)$_3$C)$_2$P{CH$_2$C(O)OCH$_2$CH$_3$}$_2$]$^+$), 36.5 (d, $^1J_{PC}$ = 34.3 Hz, [((CH$_3$)$_3$$C$)$_2$P{CH$_2$C(O)OCH$_2CH_3$}$_2$]$^+$), 62.9 (s, [^{t}Bu$_2$P{CH$_2$C(O)O$CH_2CH_3$}$_2$]$^+$), 165.5 (d, $^2J_{PC}$ = 3.5 Hz, [^{t}Bu$_2$P{CH$_2$$C$(O)OCH$_2CH_3$}$_2$]$^+$); ^{31}P{^{1}H}-NMR δ(CDCl$_3$): 46.7 (s, [^{t}Bu$_2$$P${CH$_2$C(O)OCH$_2CH_3$}$_2$]$^+$); ES$^+$: 333 [^{t}Bu$_2$P{CH$_2$C(O)OCH$_2CH_3$}$_2$]$^+$.

7.19 Method B: A 100 mL two neck round bottom flask equipped with a nitrogen inlet was charged with 1.3 g (5.9 mmol) of ^{t}Bu$_2$PSiMe$_3$ and 638 μL (1 equiv.) of ethyl chloroacetate in 50 mL of n-octane. The apparatus was equipped with a Dean-Stark trap and heated in an oil bath at 100 °C for 16 hours. Filtration of the solution and removal of the solvent under reduced pressure followed by trap-to-trap distillation of the oily remnant yielded 360 mg (20 %) of the desired phosphino ester **7.19**.

7.19 Method C: A 25 mL ROTAFLO ampoule was charged with 850 mg (5.8 mmol) of ^{t}Bu$_2$PH and 130 μL of degassed ethyl bromoacetate (0.2 equiv.). The solution was stirred overnight at room temperature upon which time a white precipitate formed. The excess of ^{t}Bu$_2$PH was removed by vacuum distillation. The ^{31}P{^{1}H}-NMR spectrum of this solid in CDCl$_3$ showed the existence of the phosphonium salt [^{t}Bu$_2$PHCH$_2$C(O)OEt]$^+$Br $^-$ (37.0 ppm) and minute traces of [^{t}Bu$_2$P{CH$_2$C(O)OEt}$_2$]$^+$Br $^-$ (46.7 ppm). Reaction of this mixture with one equivalent of KN(SiMe$_3$)$_2$ (231 mg) in THF from-78 °C to RT gave the phosphino ester **7.19** quantitatively as evidenced by ^{31}P{^{1}H}-NMR spectroscopy.

7.20 Method A: A solution of 645 mg (2.8 mmol) of the phosphino ester dissolved in 15 mL of THF was cooled down to 0 °C, and slowly added by cannula to a suspension of 212 mg (2 equiv.) of LiAlH$_4$ in 20 mL of THF cooled at the same temperature. The mixture was stirred at 0 °C for one hour and at room temperature for 4 hours. After cooling down

to -10 °C using an ice-salt slush bath, dry-degassed MeOH (approx. 2 mL) was added until H_2 evolution ceased. Degassed water and Et_2O were then added (30 mL and 20 mL respectively), the layers were separated and the water phase was washed with Et_2O (3 × 15 mL). The organic layers were combined and dried over $MgSO_4$. Removal of the volatiles under reduced pressure gave 245 mg (46 %) of the title compound as a pyrophoric, low melting, crystalline white solid. ^1H-NMR $\delta(C_6D_6)$: 1.08 (18H, d, $^3J_{PH}$ = 11.0 Hz, ((CH_3)$_3C$)$_2PCH_2CH_2OH$), 1.65 (2H, dt, $^2J_{PH}$ = 3.5 Hz, $^3J_{HH}$ = 7.5 Hz, $^tBu_2PCH_2CH_2OH$), 2.11 (1H, br. s, $^tBu_2PCH_2CH_2OH$), 3.90 (2H, m, $^tBu_2PCH_2CH_2OH$); $^{13}C\{^1H\}$-NMR $\delta(C_6D_6)$: 23.3 (d, $^1J_{PC}$ = 20.4 Hz, $^tBu_2PCH_2CH_2OH$), 28.1 (d, $^2J_{PC}$ = 13.6 Hz, ((CH_3)$_3C$)$_2PCH_2CH_2OH$), 29.5 (d, $^1J_{PC}$ = 20.4 Hz, ((CH_3)$_3C$)$_2PCH_2CH_2OH$), 61.0 (d, $^2J_{PC}$ = 34.0 Hz, $^tBu_2PCH_2CH_2OH$); $^{31}P\{^1H\}$-NMR $\delta(C_6D_6)$: 16.1 (s, $^tBu_2PCH_2CH_2OH$).

7.20 Method B: 500 mg (1.7 mmol) of $^tBu_2P(BH_3)(CH_2)_2SO_3Li.1/4$ THF were dissolved in 20 mL of DCM and cooled down to -20 °C using an acetone/CO_2 slush bath. To this solution a five fold excess of HBF_4 (2M in Et_2O) was slowly added. The reaction mixture was warmed to room temperature, stirred for 30 minutes and then refluxed for two hours. After cooling to 0 °C degassed 10 % (w/v) $NaOH_{(aq.)}$ was added until the pH was alkaline. The two phases were separated and the water phase was extracted with DCM (3 × 10 mL). The combined organic phases were dried over $MgSO_4$ and filtered. Removal of the volatiles gave a colourless oil which after bridge to bridge distillation yielded 7 mg (2 %) of the title compound as a colourless viscous oil. ^1H and $^{31}P\{^1H\}$-NMR spectra agreed with the ones reported above.

7.22: This was the only product isolated from an attempt to prepare $Ad_2PCH_2C(O)OEt$. The synthesis follows the same protocol as for the one described for the analogous $^tBu_2PCH_2C(O)OEt$, starting from 1660 mg (5.5 mmol) of Ad_2PH and 928 mg (1 equiv.) of ethyl bromoacetate. THF or DCM were added to dissolve Ad_2PH in EtOH. The only product isolated in almost quantitative yield was the phosphonium salt $[Ad_2P\{CH_2C(O)OEt\}_2]^+Br^-$. ^1H-NMR $\delta(CD_3CN)$: 0.93 (6H, t, $^3J_{HH}$ = 7.0 Hz, $[Ad_2P\{CH_2C(O)OCH_2CH_3\}_2]^+$), 1.51–2.09 (30H, m, $[Ad_2P\{CH_2C(O)OCH_2CH_3\}_2]^+$), 3.37 (2H, q, $^3J_{HH}$ = 7.0 Hz, $[Ad_2P\{CH_2C(O)OCH_2CH_3\}_2]^+$), 3.62 (4H, d, $^2J_{PH}$ = 12.1 Hz, $[Ad_2P\{CH_2C(O)OCH_2CH_3\}_2]^+$), 4.04 (2H, q, $^3J_{HH}$ = 7.0 Hz, $[Ad_2P\{CH_2C(O)OCH_2CH_3\}_2]^+$); $^{31}P\{^1H\}$-NMR $\delta(CD_3CN)$: 34.0 (s, $[Ad_2P\{CH_2C(O)OCH_2CH_3\}_2]^+$; ES$^+$: 475 $[Ad_2P\{CH_2C(O)OCH_2CH_3\}_2]^+$.

<u>**Crystallographic data for 7.1:**</u> Chemical Formula: $C_{17}H_{24}N_2O$; Formula Weight: 272.38; Crystal System: Triclinic; Space Group: *P-1*; Unit Cell Dimensions: a = 5.7140(5)Å, b =

10.7417(11)Å, c = 13.7242(13)Å; α = 96.648(5)°, β = 94.774(5)°, γ = 92.057(6)°; T(K): 120(2); μ (mm^{-1}): 0.068; Data collected/unique: 8262/2737; Goodness of fit on F^2: 0.944; $R_{int.}$: 0.0605; Final $R(|F|)$ for $F_0 > 2\sigma(F_0)$: 0.0599; Final $R(F^2)$ for all data: 0.1000; Extinction coefficient: 0.073(14).

References:

1. A.F. Littke, G. C. F., *Angew. Chem. Int. Ed.* **2002**, 41, 4176.
2. A.A. Danopoulos, T. G., M.B. Hursthouse, S. Winston, *Chem. Commun.* **2002**, 482.
3. H. Takaku, M. K., S. Ishikawa, *J. Org. Chem.* **1981**, 46, 4062.
4. H. Sun, S. G. D., *J. Am. Chem. Soc.* **2005**, 127, 2050.
5. C. Yang, S. P. N., *Org. Lett* **2001**, 3, 1511.
6. K. Issleib, H.-M. M., *Chem. Ber.* **1962**, 102.
7. W. Werner, W. B., S. Bauer, A. Hampp, J. Wolf, H. Werner, *Zeitschrift fur Naturforchung* **1994**, 1659.
8. H. Empsall, E. M. H., D. Pawson, S.L. Bernard, *J. Chem. Soc. Dalton Transactions* **1977**, 1292.
9. J. Stefan, H. W., *J. Chem. Soc. Dalton Transactions* **2002**, 318.
10. L.C. Baldwin, M. J. F., *J. Organomet. Chem.* **2002**, 646, 230.
11. J.R. Goerlich, R. S., *Phosphorous, Silicon and related elements* **1992**, 211.
12. Landis, M. S., *J. Organomet. Chem.* **2002**, 646, 239.
13. R.A. Bartlett, M. M. O., P.P. Power, *Inorg. Chem.* **1986**, 25, 1243.
14. K. Bourumeau, A.-C. G., J.-M. Denis, *J. Organomet. Chem.* **1997**, 529, 205.
15. Y. Gao, K. B. S., *J. Am. Chem. Soc.* **1988**, 110, 7538.
16. A.A. Danopoulos, A. A. D. T., S. Winston, M.B. Hursthouse, G. Eastham, *J. Chem. Soc., Dalton Transactions* **2003**, 699.
17. O.T. Beachley, M. R. C., C.H. Lake, *Organometallics* **1993**, 12, 3992.
18. M. Gutpa, C. H., W.C. Kaska, C.E. Roger, C.M. Jensen, *J. Am. Chem. Soc.* **1997**, 119, 840.

Chapter 8: Conclusions

Chapter 8: Conclusions

The preparation of novel ligand architectures combining the spectator ligand properties of NHCs with "classical" donor functionalities has been accomplished. The preparation of novel phosphine and pyridine functionalised imidazolium salts is outlined in Scheme 8.1. The phosphine functionalised imidazolium salts are prepared in two steps. The first step is the quaternisation of ω-(bromoalkyl)diphenylphosphine oxides with the appropriate imidazole, and the second step is the reduction of the phosphine oxide imidazolium salt to the corresponding phosphine. This modular synthetic approach allows access to a variety of new ligands. The pyridine functionalised imidazolium salts are prepared by a quaternisation reaction between 3-R-2-bromopyridine and the appropriate imidazole. Deprotonation of the pyridine imidazolium salts with $K(NSiMe_3)_2$ produces the corresponding 'bottle-able' functionalized NHCs as crystalline materials and in good yields. When Ar = $3,5$-$(CF_3)_2$-C_6H_3 (**2.7**) the free carbene could not be isolated. An X-ray diffraction study on the latter imidazolium salt revealed intermolecular interactions between azolium molecules.
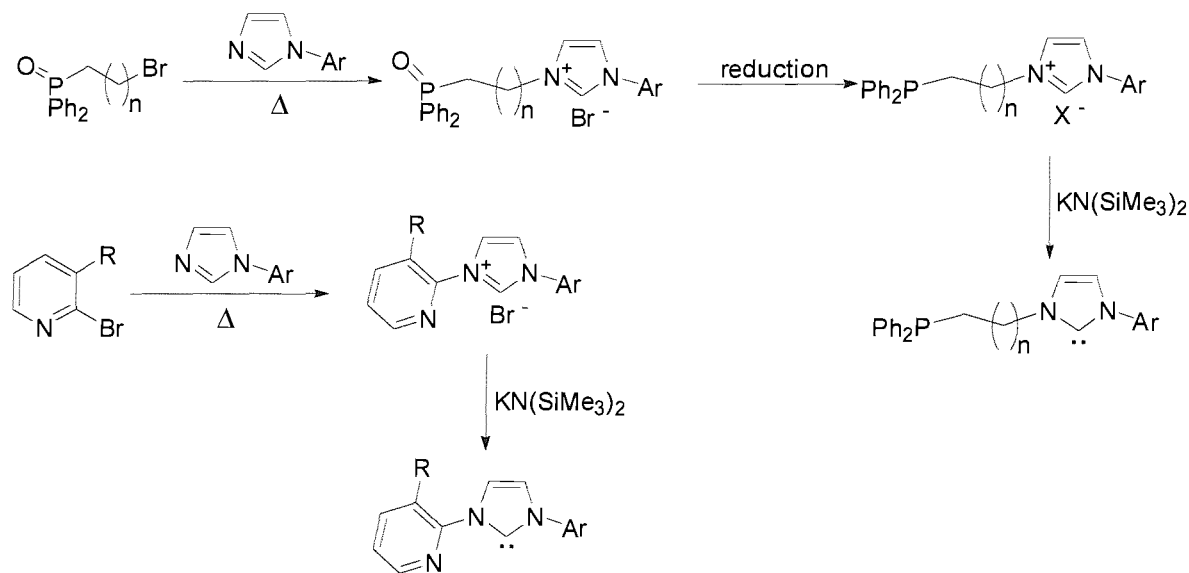
Scheme 8.1: Preparation of phosphine and pyridine functionalised imidazolium salts and NHCs (Ar = $2,6$-$(^iPr)_2$-C_6H_3 (n = 0, 1) and $2,4,6$-Me_3-C_6H_2 (n = 0, 1, 2) for the phosphine functionalised imidazolium salts and NHCs; Ar = $2,6$-$(^iPr)_2$-C_6H_3 (R = H, Me) and Ar = $3,5$-$(CF_3)_2$-C_6H_3 (R = H) for the pyridine functionalised imidazolium salts and NHCs).

Even though the isolation of phosphine functionalised NHCs has been communicated,[1] their isolation in good yields was hindered by their thermal instability. For this reason the NHCs were prepared *in-situ* and were reacted with appropriate palladium starting materials (Pd(COD)Br$_2$, Pd(tmeda)Me$_2$ and [Pd(η^3-methallyl)(μ-Cl)]$_2$) to yield novel Pd(II) neutral and cationic complexes that incorporate the ligand in bidentate mode as evidenced by spectroscopic and structural data.

The substitution of tmeda from the isolated pyridine functionalised NHCs led to the formation of the neutral Pd(II) dimethyl complexes incorporating the ligand in bidentate mode. Interaction of free carbene **2.9c** (Ar = 2,6-(^{i}Pr)$_2$-C$_6$H$_3$, R = H) with Pd(tmeda)Me$_2$ in a 2:1 molar stoichiometry, led to the isolation of a C_2 symmetrical Pd(II) complex (**3.6**) where only the two NHC moieties of **2.9c** are coordinated while the pyridine functionalities are not participating in the metal coordination sphere. The cationic Pd(II) complex **3.7** prepared by interaction of **2.9c** with [Pd(η^3-methallyl)(μ-Cl)]$_2$ followed by addition of NaBPh$_4$ was also isolated.

Structural studies on these complexes revealed some interesting structural features with the most important being the suppressed *trans*-influence the bidentate ligands exert on the Pd-Me bonds.

The thermal decomposition of the dimethyl complexes **3.1a** and **3.3** (Scheme 8.2) was investigated. In the case of **3.1a** it occurs *via* formation of 2-methyl-imidazolium salts, while in the case of **3.3** α-hydrogen elimination to produce methane seems to be the main decomposition pathway. This difference, although unclear, seems to be connected to the different chelate sizes of the ligands.

The thermally stable dimethyl complexes **3.1a**, **3.3** and **3.5b** (Scheme 8.2) served as useful starting materials for the synthesis of cationic species by their reaction with Lewis acids containing non-coordinating anions. In all studied cases, only one cationic isomer is spectroscopically observed and isolated. When **3.1a** or **3.3** are reacted with Brookhart's acid or (CF$_3$)$_2$CHOH in the presence of a donor (e.g. pyridine), the electrophilic attack happens stereospecifically at the Pd-Me bond *trans* to the phosphine moiety of the ligand. On the other hand, when **3.5b** is reacted with Brookhart's acid in the presence of pyridine, the Pd-Me *trans* to the NHC moiety of the ligand is cleaved.
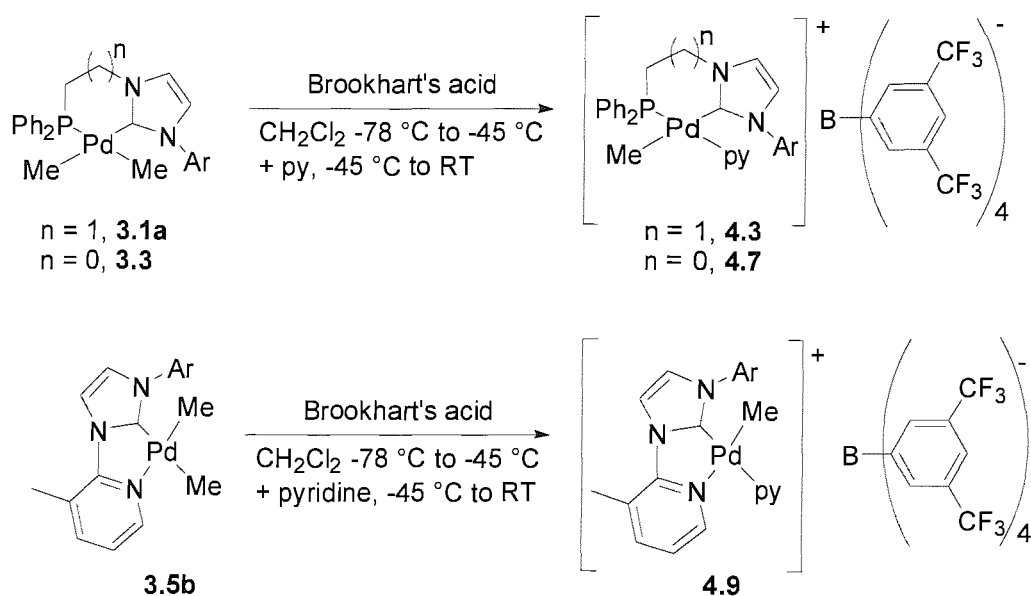
Scheme 8.2: Stereospecific electrophilic attack by acids on the electronically asymmetric Pd-Me bonds (Ar = 2,6-(^{i}Pr)$_2$-C$_6$H$_3$).

The formation of phosphine functionalised 2-methyl-imidazolium salts was found to be very facile when complexes **3.1a** and **3.3** were reacted with MeI at room temperature. On the other hand, such a process did not occur in the case of **3.5b** upon its reaction with MeI. In this case, oxidative addition of MeI was followed by reductive elimination of ethane to give complex **4.13** (Scheme 8.3) that was spectroscopically observed. The latter complex reacts with CH$_2$Cl$_2$ to produce complex **4.14**. It is interesting to note that the iodide occupies the site *trans* to the NHC moiety.
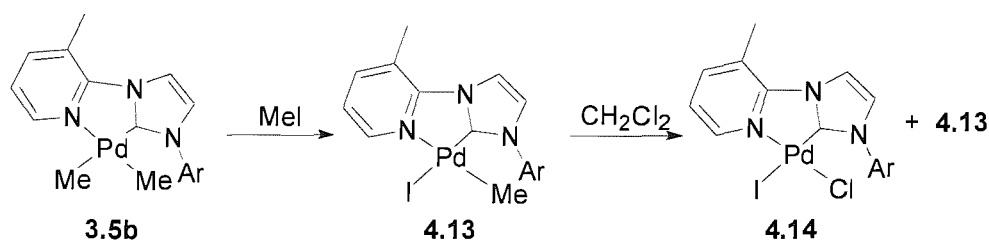
Scheme 8.3: Reaction of MeI with **3.5b** (Ar = 2,6-(^{i}Pr)$_2$-C$_6$H$_3$).

The use of the neutral dimethyl complexes **3.1a-b**, **3.3**, **3.5b** and **3.6** as well as the neutral dibromide complexes **3.2a-b** as catalysts for Heck olefinations was then studied. Our results reveal that the catalytic activity is dependant on the solvent and the base. All

complexes acted as very good catalysts in the case of activated substrates, but their reactivity was reduced when unactivated aryl bromides were used. The only exceptions seemed to be complexes **3.5b** and **3.6**. It is also interesting to note that the reductive elimination of 2-methyl-imidazolium salts is a process that seems to occur during the catalytic cycle when the neutral dimethyl complexes are used as catalysts. This could be the reason behind their reduced catalytic activity.

The phosphine and pyridine functionalised NHCs were used as ligands for the preparation of neutral Pt(II) dimethyl complexes. These were synthesised using the same protocol for the preparation of the analogous Pd(II) complexes. The reactivity of the new Pt(II) complexes towards electrophiles was then investigated, and our studies revealed that the stereoselectivity of the Pt-Me bond cleavage follows the same trend to the one observed for their Pd(II) homologues. Furthermore, we have demonstrated that the selectivity of the electrophilic attack is independent of the acid used. The new cationic Pt(II) complexes were unfortunately inert towards aromatic C-H activation.

Other aspects of the reactivity of the Pt(II) dimethyl complexes were also studied. Oxidative addition of MeI happens very readily and leads to the formation of *fac*-Pt(IV) complexes. These are thermally stable and a thermolytic study on *fac*-**5.24** (Figure 8.1) showed that reductive elimination of 2-methyl-imidazolium salt does not occur. Moreover the Pt(II) dimethyl complex are inert towards the insertion of Si-H bonds in ambient conditions.
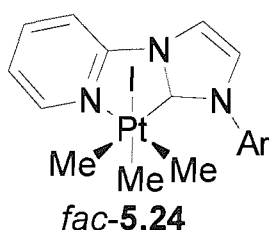

fac-**5.24**

Figure 8.1: Complex *fac*-**5.24** (Ar = 2,6-(^{i}Pr)$_2$-C$_6$H$_3$).

The coordination chemistry of the phosphine functionalised NHCs with other platinum group metals (rhodium and iridium) was also investigated. The synthesis of the Rh(I) and Ir(I) complexes proved troublesome, since the synthetic protocol based on the substitution of the leaving groups by the NHC-phosphine ligands led to the formation of complex reaction mixtures. The isolation of some unexpected products was never the less

achieved. The most interesting of them is the five coordinate Ir(I) complex **6.17** (Scheme 8.4) where the *NHC* moiety of the ligand adopts an abnormal bonding mode.
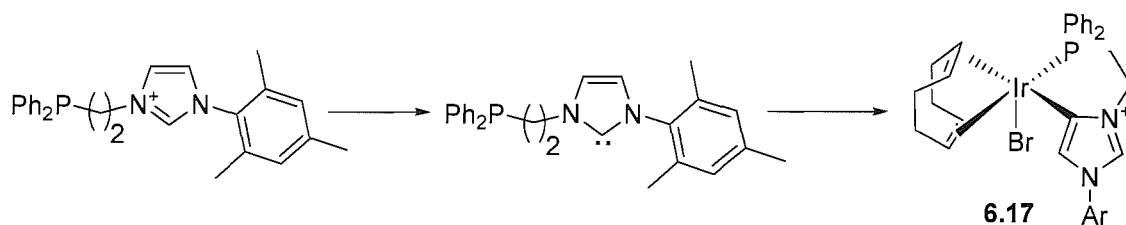
Scheme 8.4: Formation of **6.17**.

Interaction of the *in-situ* generated phosphine-NHC ligand with [Rh(COE)₂(acac)] led to the isolation of complex **6.14** (Scheme 8.5). This acts as a moderate catalyst for the insertion of aryl-boronic acids into aldehydes at ambient temperature. Furthermore, its reactivity with syn-gas suggests that it can act as a catalyst for hydroformylation reactions.
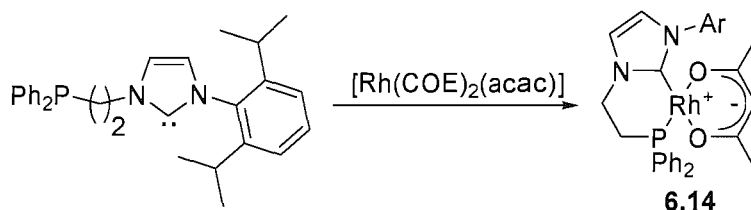
Scheme 8.5: Preparation of **6.14**.

In the last chapter we described attempts to prepare bulky alkyl phosphine functionalised imidazolium salts to act as precursors for the synthesis of the corresponding NHCs. Although our synthetic approaches were unsuccessful, our endeavour led to the isolation of novel imidazolium salts and phosphines. We have also highlighted the use of microwave irradiation as an efficient method to promote the synthesis of certain imidazolium salts cleanly, quickly and in high yield.

References

1. Danopoulos, A. A.; Gelbrich, T.; Hursthouse, M. B.; Winston, S. *Chem. Commun.* **2002**, 482.

Appendix

Appendix

General Considerations: All manipulations were carried under nitrogen in a Braun glovebox or by using standard Schlenk techniques unless otherwise stated. Solvents used were dried using standard techniques (THF, Et_2O, C_6H_6, dioxane and petroleum ether spirits over sodium-ketyl; toluene over Na; CH_2Cl_2 over CaH_2; C_6H_5Cl and CH_3CN over P_2O_5; pyridine over K; DMF over $MgSO_4$) and distilled under nitrogen prior to use or stored in Youngs ampoules over molecular sieves (4Å) under a nitrogen atmosphere. Petroleum ether had a boiling point 40-60 °C throughout unless otherwise stated. $SiMe_3Cl$ was dried over Na and was distilled under a nitrogen atmosphere and kept in a Youngs ampoule under nitrogen. $BH_3.DMS$, n-BuLi (2.5 M in hexanes) and MeLi (3 M in diethyl ether) were purchased from Aldrich and were stored in a Youngs ampoule at 5 °C under a nitrogen atmosphere. $KN(SiMe_3)_2$ was prepared by reacting KH and $NH(SiMe_3)_2$ in refluxing toluene under nitrogen and was kept in the glovebox.

Deuterated solvents were degassed by three freeze-thaw-pump cycles and were dried as follows: d_8-THF, C_6D_6 and d_8-toluene over Na/K, d_5-py over K, CD_2Cl_2 and CD_3CN over CaH_2, $CDCl_3$ was stirred overnight over molecular sieves (4Å), d_5-PhCl over P_2O_5. The solvents were separated from the drying agent by vacuum distillation under a static vacuum and were stored in the glovebox in Youngs ampoules over molecular sieves (4Å). Elemental analyses were carried by the University College, London microanalytical laboratory.

Instrumentation: ^1H-NMR spectra were recorded on Bruker AM-300 or Bruker AV-300 spectrometers. $^{13}C\{^1H\}$-NMR spectra were recorded on a Bruker AC-300 or Bruker AV-300 or Bruker DPX-400 spectrometers. Correlation experiments, variable temperature ^1H-NMR and $^{31}P\{^1H\}$-NMR experiments as well as $^{195}Pt\{^1H\}$-NMR spectra were recorded on a Bruker DPX-400 spectrometer. $^{31}P\{^1H\}$-NMR and $^{19}F\{^1H\}$-NMR spectra were recorded on a Bruker AC-300 or Bruker AV-300 spectrometer. ^1H-NMR and $^{13}C\{^1H\}$-NMR spectra were referenced internally from the residual protio solvent (^1H) or the signals of the solvent (^{13}C). $^{31}P\{^1H\}$-NMR were referenced externally relative to 85% H_3PO_4 in D_2O. $^{19}F\{^1H\}$-NMR spectra were referenced externally relative to either C_6F_6 (positive δ values in this manuscript) or $CFCl_3$ (negative δ values in this manuscript). $^{195}Pt\{^1H\}$-NMR spectra were referenced externally relative to K_2PtCN_6 in D_2O. Mass spectra were

on electrospray mode (positive or negative), unless otherwise stated, on a VG Biotech Platform. Gas chromatographs were obtained from a Varian 3400GC equipped with a flame ionisation detector and linked to a Hewlett-Packard 3396 Series 2 integrator.

X-ray Crystallography: All data sets were collected on a Enraf-Nonius Kappa CCD area detector diffractometer with an FR591 rotating anode (Mo/Ka radiation) and an Oxford Cryosystems low temperature device operating in ω scanning mode with ψ and ω scans to fill the Ewald sphere. The programs used for control and integration were Collect, Scalepack, and Denzo.[1] The crystals were mounted on a glass fiber with silicon grease, from Fomblin vacuum oil. All solutions and refinements were performed using the WinGX package [2] and all software packages within. All non-hydrogen atoms were refined using anisotropic thermal parameters, and hydrogens were added using a riding model. The data set for **6.12** was collected on a Bruker SMART 1K CCD diffractometer (synchrotron radiation) operating at narrow flame /ω scans.

In the case of **6.14** half a toluene molecule per moiety was present in the structure but could not be successfully modelled. In the case of **3.7** three highly distorted hexane molecules could be identified in the asymmetric unit but could not be successfully modelled. Finally in the case of **5.13** a molecule of diethyl ether was present in the asymmetric unit that could not be properly modelled. All the above disorders were treated by SQUEEZE.[3] Other crystallographic data are presented in tables in the experimental part of each chapter.

References

1.Hooft, R. COLLECT; Nonius BV, 1997-2000. Otwinowski, Z.; Minor, W. SCALEPACK, DENZO. *Methods Enzymol.* **1997**, *276*, 307.
2. Farrugia, L. J. *J. Appl. Crystallogr.* **1999**, *32*, 83.
3. Spek, A. L. *J. Appl. Cryst.* **2003**, *36*, 7-13.